



Kent Academic Repository

Sage, Elizabeth Ann (2004) *The functional competence of animal cells in culture: the NSO cell proteome*. Doctor of Philosophy (PhD) thesis, University of Kent.

Downloaded from

<https://kar.kent.ac.uk/94632/> The University of Kent's Academic Repository KAR

The version of record is available from

<https://doi.org/10.22024/UniKent/01.02.94632>

This document version

UNSPECIFIED

DOI for this version

Licence for this version

CC BY-NC-ND (Attribution-NonCommercial-NoDerivatives)

Additional information

This thesis has been digitised by EThOS, the British Library digitisation service, for purposes of preservation and dissemination. It was uploaded to KAR on 25 April 2022 in order to hold its content and record within University of Kent systems. It is available Open Access using a Creative Commons Attribution, Non-commercial, No Derivatives (<https://creativecommons.org/licenses/by-nc-nd/4.0/>) licence so that the thesis and its author, can benefit from opportunities for increased readership and citation. This was done in line with University of Kent policies (<https://www.kent.ac.uk/is/strategy/docs/Kent%20Open%20Access%20policy.pdf>). If you ...

Versions of research works

Versions of Record

If this version is the version of record, it is the same as the published version available on the publisher's web site. Cite as the published version.

Author Accepted Manuscripts

If this document is identified as the Author Accepted Manuscript it is the version after peer review but before type setting, copy editing or publisher branding. Cite as Surname, Initial. (Year) 'Title of article'. To be published in *Title of Journal*, Volume and issue numbers [peer-reviewed accepted version]. Available at: DOI or URL (Accessed: date).

Enquiries

If you have questions about this document contact ResearchSupport@kent.ac.uk. Please include the URL of the record in KAR. If you believe that your, or a third party's rights have been compromised through this document please see our [Take Down policy](https://www.kent.ac.uk/guides/kar-the-kent-academic-repository#policies) (available from <https://www.kent.ac.uk/guides/kar-the-kent-academic-repository#policies>).

**The Functional Competence of Animal Cells in Culture.
The NS0 Cell Proteome.**

ELIZABETH ANN SAGE

2004

A thesis submitted to the University of Kent for the degree of

DOCTOR OF PHILOSOPHY

**In the Faculty of Science, Technology and Medical Studies, The Research School of
Biosciences, University of Kent, Canterbury, Kent, CT2 7NJ UK.**

F185439



No part of this thesis has been submitted in support of an application for any degree or other qualification of the University of Kent, or any other University or Institution of learning.



E. A. SAGE

January 2004

Abstract

Mammalian cells are routinely utilised in industry for the production of therapeutic proteins. However, the adaptations that enable enhanced cellular productivity are poorly understood and improvements to date have been largely achieved by empirical optimisation of the cell culture environment and the use of enhanced expression systems. We have utilised an optimised proteomic platform, specifically two-dimensional gel electrophoresis (2-D PAGE) to investigate the alterations in functional gene expression that enable murine myeloma NS0 cells in culture to maintain high-level recombinant monoclonal antibody production. We have addressed the following fundamental questions; (1) when do cells in bioreactor culture perceive stress and how do associated changes in the pattern of protein synthesis during batch culture relate to secretory productivity and cell viability *in vitro*? and (2) are there conserved changes in gene expression which permit higher specific monoclonal antibody production (qMAb)? The protein complement of NS0 cells harvested at lag, exponential and death phase of batch culture was separated by high-resolution large format 2-D PAGE. Nascent polypeptide synthesis was also concurrently assessed by labelling with [³⁵S] methionine followed by 2-D PAGE. Analysis of the resultant digital images confirmed that although many proteins were constitutively expressed (and were therefore critical for the growth and survival of NS0 cells throughout culture), approximately 50% of the total proteins detected exhibited a change in the level of protein and polypeptide expression during batch culture. Changes in the level of polypeptide synthesis preceded a change in the level of protein expression. Proteins of interest were identified by mass spectrometry in order to characterise proteins (or groups of proteins) exhibiting alterations in expression causally related to changes in cellular activity during culture. The identified proteins could be separated into three major groups of proteins; (1) chaperones, (2) glycolytic proteins and (3) structural proteins. Closer analysis identified conserved, 'time specific' and productivity related changes in protein expression. These results suggest that although it is difficult to pinpoint exactly when NS0 cells in culture perceive stress it appears that NS0 cells recognised stress early in exponential phase. However, changes in the pattern of protein expression could not be directly attributable to the stress response or rIgG accumulation even though changes in protein expression correlated with the production of rIgG by GS-NS0 cells.

A series of NS0 cell transfectants expressing differing levels of antibody B72.3 productivity were also prepared. The cell lines were sequentially weaned off serum-containing media into 1% serum. A selection of the resulting cell lines were cultured under controlled conditions and extracted at mid-exponential phase for whole NS0 cell proteome analysis. During 4 L bioreactor culture the cell lines lost productivity and were therefore used to investigate clonal variation between a series of essentially non-producing cell lines derived from the same parental NS0 cell host. The results clearly show that many cell line specific changes in the global NS0 cell proteome were apparent at exponential phase. This cell specific 'bias' implies that engineering strategies which involve the overexpression of one or two proteins will not unlock the full potential of engineering cells for desired functional phenotypes.

Acknowledgements

I would like to extend thanks to my supervisors Dr. Mark Smales, Dr. David James and Dr. Peter Klappa, without whose help and advice over the past three years, the production of this thesis would not have been possible. In particular I would like to thank Dr. Mark Smales for his additional support during the writing of this thesis. I would also like to acknowledge my industrial supervisor at GlaxoSmithKline, Dr. Carol Marshall together with Hella Bosteels and Steve McGowan (previously of GlaxoSmithKline) particularly for their help regarding the fermentation work undertaken during my industrial placement at GlaxoSmithKline. I would also like to express my appreciation to the BBSRC and GlaxoSmithKline for honouring their commitment to the Special CASE Studentship.

I also wish to express my thanks to the members of the ex-David James group. In particular I would like to thank Mark Weeks, Mark Smales and Dan Alete for their uplifting spirits. Furthermore, I would like to thank Michèle Underhill, Clare Coley and Anna Hills for their friendship and enthusiasm.

Finally I wish to thank my family, friends and my partner Rob, without whose support I would not be where I am today.

Table of Contents

Abstract	ii
Acknowledgements	iv
Table of Contents	v
List of Figures	xii
List of Tables	xv
List of Schemes	xvii
Abbreviations	xviii

Chapter 1 Introduction

1.1 Cell Engineering	1
1.1.1 Recombinant Therapeutic Protein Production	1
1.1.2 Mammalian Cell Systems	2
1.1.2.1 NS0 Cell History	3
1.1.3 Strategies for Improved Cell Performance	4
1.1.3.1 Cell Culture Media	5
1.1.3.2 Bioreactor Design	6
1.1.3.3 Gene Amplification Systems	7
1.1.3.4 The Glutamine Synthetase (GS) System	8
1.1.4 Metabolic Engineering Strategies for Improved Cell Specific Productivity	10
1.1.4.1 Control of Apoptosis to Improve Cell Specific Productivity	10
1.1.4.2 Cell-Cycle Arrest Strategies to Increase Cell Specific Productivity	14
1.1.4.3 Glycosylation Engineering	18
1.1.4.4 Current Limitations of Metabolic Engineering	19
1.1.5 Inverse Metabolic Engineering	20
1.2 Introduction to Proteomics and the Post-Genome Revolution	23
1.2.1 Proteome Analysis - Current Technologies	23
1.2.1.1 Sample Preparation and Extraction	26
1.2.1.2 Two-Dimensional Gel Electrophoresis	27
1.2.1.3 First Dimension: Isoelectric Focussing	27
1.2.1.4 Second Dimension: SDS-PAGE	28
1.2.1.5 Protein Visualisation	28
1.2.1.6 Protein Identification and Characterisation	30
1.3 Complementary Technologies to 2-D PAGE	32
1.4 Aims of this Study	34

Chapter 2 Materials and Methods

2.1	Chemicals	36
2.2	Cell Culture	36
2.2.1	NS0 Cell Line	36
2.2.2	NS0 Cell Culture	36
2.2.2.1	<i>Growth Conditions for GS-NS0 Cells Secreting anti-CD38 Antibody</i>	37
2.2.2.2	<i>Growth Conditions for GS-NS0 Cells Secreting B72.3</i>	37
2.2.3	Transfection Procedure	37
2.2.4	Determination of Viable NS0 Cells	38
2.2.5	Creation of Master and Working Cell Banks	38
2.2.6	Resuscitation of Frozen Cell Lines	39
2.2.7	Adaptation of NS0 Cells Expressing B72.3 Antibody to 1% Serum in Characterised Protein-Free Medium	39
2.2.8	Bioreactor Culture	40
2.2.8.1	<i>3 L Bioreactor Preparation</i>	40
2.2.8.2	<i>Control and Operation of NS0 Cell Culture in 3 L Bioreactors</i>	41
2.2.8.3	<i>7 L Bioreactor Preparation</i>	41
2.2.8.4	<i>Control and Operation of NS0 Cell Culture in Bioreactors</i>	42
2.2.9	Metabolite Determination	43
2.2.9.1	<i>Glucose Concentration Determination from Cell Culture Supernatant</i>	43
2.2.9.2	<i>Lactate Concentration Determination from Cell Culture Supernatant</i>	44
2.3	Quantitation of GS-NS0 Cell Line IgG Production	45
2.3.1	Optical Biosensor Assay	45
2.3.2	ELISA Assay	45
2.4	Sample Preparation of GS-NS0 Cells for Proteomic Analysis	46
2.4.1	Optimisation of Whole NS0 Cell Protein Extraction	46
2.4.2	Extraction Buffer Solutions	47
2.4.3	Protein Extraction from GS-NS0 Cells	47
2.4.4	Modified Bradford Assay	48
2.5	1-D Electrophoresis	49
2.5.1	1-D SDS-PAGE Sample Buffer	49
2.5.2	1-D SDS PAGE	49
2.6	2-D Electrophoresis	49
2.6.1	Isoelectric Focussing of Protein Mixtures. First Dimension Separation	49
2.6.2	Electrophoresis Buffering Systems	51
2.6.3	Equilibration of IPG Strips Prior to the Second Dimension Separation	52
2.6.4	Sealing of the IPG Strip to the Second Dimension SDS-PAGE Gel	52
2.6.5	Self Casting Polyacrylamide Gels	53

2.6.6	Molecular Weight Markers	53
2.6.7	Mini Gel Second Dimension Separation for 7 cm IPG Strips	53
2.6.8	Large Format SDS-PAGE	54
2.6.9	Large Format SDS-PAGE using the DALT II System	54
2.7	Staining Techniques for Analytical and Preparative 2-D Gels	55
2.7.1	Shevchenko Silver Staining	55
2.7.2	PlusOne Silver Staining Method	56
2.7.3	Bio-Safe Colloidal Coomassie Stain	57
2.7.4	Quantitation of GS-NS0 2-D Gels	57
2.7.4.1	<i>Statistical Assessment of Protein Extraction from NS0 Cells</i>	58
2.7.4.2	<i>Analysis of Variation in 2-D PAGE</i>	58
2.8	Protein Identification	58
2.8.1	De-Staining of Gels	59
2.8.2	Tryptic Digestion of Proteins Visualised on 2-D Gels	59
2.8.3	Desalting of Tryptic Digest Samples	61
2.8.4	MALDI-ToF and Peptide Mass Fingerprinting	61
2.8.5	Database Searching and Protein Identification	61
2.9	Analysis of Active Protein Synthesis in NS0 Cells through <i>in vivo</i> Labelling of Nascent Polypeptides	62
2.9.1	L-[³⁵ S] Methionine Labelling of Nascent Polypeptides	62
2.9.1.1	<i>TCA Precipitation of the Cell Pellet</i>	63
2.9.1.2	<i>TCA Precipitation of Cell Free Supernatant</i>	63
2.9.2	2-D PAGE and Autoradiography of [³⁵ S] Labelled Proteins	63

Chapter 3 Development of the Proteomic Technology Platform

3.1	Introduction	65
3.2	Results	68
3.2.1	NS0 Cell Growth	68
3.3	Optimisation of Whole Cell Protein Solubilisation and Recovery	69
3.3.1	Methods of Cell Lysis	69
3.3.2	Quantitative Assessment of Protein Solubility	69
3.3.2.1	<i>Assessment of Protein Solubility and Recovery using Mini 2-D Gel Electrophoresis</i> ...	70
3.3.3	Quantitative Analysis of Protein Recovery from NS0 Cells	73
3.3.3.1	<i>Optimised Scheme for Sample Preparation of Whole NS0 Cell Extracts</i>	75
3.3.4	Large Format 2-D SDS-PAGE using the Protean II Gel Tank	76
3.3.4.1	<i>Protean II versus DALT II Gel Tanks</i>	76
3.3.5	Selection of IEF pI Resolving Range	78
3.3.5.1	<i>Selection of SDS-PAGE Gel Composition</i>	80

3.3.6	Protein Visualisation Methods	82
3.3.6.1	<i>Protein Visualisation using Colloidal Coomassie Protein Stain</i>	85
3.3.7	Optimised Scheme for Whole NS0 Cell Protein Extraction by Large Format 2-D PAGE	90
3.4	Discussion	91
3.4.1	Sample Preparation	91
3.4.2	Cell Lysis Methodology	91
3.4.3	Qualitative Assessment of Protein Solubility and Recovery	93
3.4.4	Quantitative Assessment of Protein Solubilisation Methodology	94
3.4.5	Large Format 2-D PAGE	94
3.4.5.1	<i>DALT II versus Protean II Gel Tanks</i>	95
3.4.6	Selection of IEF and Second Dimension Gel Percentage Range	95
3.4.7	Protein Visualisation	97
3.4.8	2-D Image Reproducibility	99
3.4.9	Optimised Scheme for Sample Preparation and Analysis of the NS0 Cell Proteome by 2-D Electrophoresis	100
3.5	General Discussion	100

Chapter 4 Analysis of Changes in the GS-NS0 Cell Proteome during Batch Culture

4.1	Introduction	101
4.2	Results	103
4.2.1	Cell Culture	103
4.2.2	Bioreactor Culture	103
4.2.2.1	<i>Monitoring IgG Product Titre in Culture Medium during Batch Culture</i>	103
4.2.3	Analysis of the Whole NS0 Cell Proteome throughout Batch Culture	105
4.2.3.1	<i>Analysis of the NS0 Cell Proteome throughout Batch Culture</i>	106
4.2.3.2	<i>Protein Regulation throughout Batch Culture</i>	107
4.2.3.3	<i>Changes in the Level of Protein Expression throughout Batch Culture</i>	109
4.2.4	The Quantitative Analysis of Regulated Proteins throughout Batch Culture	112
4.2.5	Protein Identification	121
4.3	Discussion	123
4.3.1	Cell Growth	123
4.3.2	Changes in the NS0 Cell Proteome throughout Bioreactor Batch Culture	124
4.3.3	Analysis of Proteins Exhibiting a 2-Fold Change in the Level of Expression	126
4.3.4	Quantitative Analysis and Identification of Specific NS0 Cell Proteins	131
4.3.4.1	<i>BiP (Grp78)</i>	132
4.3.4.2	<i>Heat Shock Cognate-71 (Hsc71)</i>	133
4.3.4.3	<i>Mitochondrial Stress-70 Protein (Grp75)</i>	134

4.3.4.4	<i>Calreticulin</i>	135
4.3.4.5	<i>Heat Shock Protein-60 (Hsp60)</i>	136
4.3.4.6	<i>Protein Disulphide Isomerase (PDI)</i>	137
4.3.4.7	<i>Endoplasmic Precursor (Grp94)</i>	138
4.3.4.8	<i>α-Tubulin</i>	138
4.3.4.9	<i>Disulphide Isomerase ER-60 (Erp60)</i>	139
4.3.4.10	<i>Pyruvate Kinase (PK)</i>	139
4.3.4.11	<i>Elongation Factor 1-Alpha-1 (eEF1A-1)</i>	140
4.3.4.12	<i>α-Enolase</i>	141
4.3.4.13	<i>β-Actin</i>	142
4.3.4.14	<i>Glyceraldehyde 3-Phosphate Dehydrogenase (GAPDH)</i>	143
4.3.4.15	<i>Peptidyl-Prolyl cis-trans Isomerase A (PPIase A)</i>	143
4.3.5	Considerations for Utilising Proteome Analysis Technology	145
4.3.6	Conclusions	146

Chapter 5 Analysis of Protein Synthesis in GS-NS0 Cells during Batch Culture

5.1	Introduction	151
5.2	Results	152
5.2.1	Nascent Polypeptide Synthesis during Batch Culture	152
5.2.1.1	<i>Assessment of Nascent Polypeptide Synthesis throughout the Batch Culture of NS0 Cells</i>	153
5.2.1.2	<i>Quantitative Analysis of Nascent Polypeptide Synthesis throughout Batch Culture</i>	156
5.2.2	Large format (18 cm) 2-D PAGE of the NS0 Cell Proteome for Comparison Against 2-D Autoradiographs	161
5.2.2.1	<i>Analysis of the NS0 Cell Proteome in 18 cm 2-D Gel Format</i>	162
5.2.2.2	<i>Quantitative Analysis of Protein Expression throughout Batch Culture on 18 cm 2-D Proteome Maps</i>	163
5.2.2.3	<i>Comparison of 2-D Autoradiographs versus Silver-Stained Protein 2-D Gels</i>	166
5.3	Discussion	174
5.3.1	Nascent Polypeptide Synthesis during Batch Culture of NS0 Cells	174
5.3.2	Global Analysis of Protein Expression Profiles on 2-D Autoradiographs	175
5.3.3	Analysis of Polypeptides Exhibiting a 2-Fold Change in the Level of Synthesis	177
5.3.4	Analysis of Nascent Polypeptides Showing a Change in the Level of Expression throughout Batch Culture	178
5.3.5	Comparison of Protein Expression on 2-D Autoradiographs and Protein Gels throughout Batch Culture	180
5.3.5.1	<i>BiP</i>	182

5.3.5.2	<i>Hsc71</i>	182
5.3.5.3	<i>Grp75</i>	182
5.3.5.4	<i>Calreticulin</i>	183
5.3.5.5	<i>Hsp60</i>	183
5.3.5.6	<i>PDI</i>	184
5.3.5.7	<i>Grp94</i>	184
5.3.5.8	α - <i>Tubulin</i>	185
5.3.5.9	<i>Erp60</i>	185
5.3.5.10	<i>Pyruvate Kinase</i>	186
5.3.5.11	<i>eEF1A-1</i>	186
5.3.5.12	α - <i>Enolase</i>	186
5.3.5.13	β - <i>Actin</i>	187
5.3.5.14	<i>GAPDH</i>	187
5.3.5.15	<i>PPIase A</i>	188
5.3.6	Implications for rIgG Production	190
5.3.7	General Discussion	191

Chapter 6 A Comparative Proteome Based Analysis of GS-NS0 Cell Lines Differing in Specific Productivities

6.1	Introduction	193
6.2	Results	195
6.2.1	Cell Growth	195
6.2.1.1	<i>Cell Growth in DMEM-F12 Medium Supplemented with 10% dFCS</i>	197
6.2.1.2	<i>Cell Growth Characteristics in Protein-Free Medium Supplemented with 1% dFCS</i> .	198
6.2.2	Bioreactor Culture	200
6.2.2.1	<i>Assessment of GS-NS0 Cell Transfectant Growth during Bioreactor Batch Culture</i> ...	200
6.2.3	Proteome Analysis of NS0 Cell Transfectants at Mid-exponential Growth Phase	203
6.2.3.1	<i>Analysis of NS0 Transfectants at Mid-exponential Growth Phase</i>	205
6.2.3.2	<i>Assessment of Protein Regulation between Transfectants at Mid-exponential Growth Phase</i>	205
6.2.3.3	<i>Changes in the Pattern of Protein Expression between Cell Lines Derived from the same Parental NS0 Cell Host</i>	206
6.2.4	The Quantitative Assessment of NS0 Cell Transfectants at Mid-exponential Growth Phase .	208
6.3	Discussion	211
6.3.1	Cell Growth	211
6.3.1.1	<i>GS-NS0 Transfectant Growth in DMEM, 10% dFCS</i>	211
6.3.1.2	<i>GS-NS0 Cell Growth in Protein-Free Medium</i>	212
6.3.1.3	<i>GS-NS0 Transfectant Growth in 4 L Bioreactor Culture</i>	213

6.3.2	Proteome Analysis of NS0 Cell Transfectants at Mid-exponential Phase during Bioreactor Culture	214
6.3.3	Analysis of Proteins Exhibiting at Least a 2-Fold Change in the Level of Expression at Mid-exponential Growth Phase	215
6.3.4	Quantitative Analysis of Specific NS0 Cell Protein Expression	218
6.3.5	General Discussion	223

Chapter 7 General Discussion and Conclusions

7.1	Final Summary	225
7.2	Implications for Future Engineering Strategies	233
	References	235

Appendices

- Appendix I**
- Appendix II**
- Appendix III**
- Appendix IV**
- Appendix V**
- Appendix VI**
- Appendix VII**

List of Figures

1.1	The history of the NS0 cell line	4
1.2	The formation of glutamine from glutamate through the utilisation of ammonium as an amino group donor	9
1.3	The release of cytochrome <i>c</i> (cyt <i>c</i>) and Smac/DIABLO from the inner membrane space of the mitochondria which is regulated by the Bcl-2 family protein members	12
1.4	A schematic view of the cell-cycle and the various complexes involved in regulating the transitions through 'check points', depicted as a circle running clockwise	15
1.5	The key regulatory networks controlling apoptosis and the G1-S transition of the cell-cycle of mammalian cells	17
1.6	A schematic diagram of antibody folding by BiP	20
1.7	An integrated strategy for rational inverse metabolic engineering	22
1.8	The various elements of proteome technology assessed by 2-D PAGE	24
1.9	Strategies for protein identification from proteins separated by 2-D PAGE	31
3.1	Typical batch culture growth of NS0 cells expressing a recombinant IgG ₁ grown in IMDM medium supplemented with 10% dFCS in a 350 mL spinner	68
3.2	The protein yield using two lysis buffers from 1×10^7 NS0 cells extracted in a 400 μ L volume during mid-exponential phase and death phase of growth	70
3.3	Mini 2-D PAGE of whole NS0 cells extracted from 1×10^7 cells using two different solubilising buffers	72
3.4	Quantitative assessment of protein recovery	73
3.5	Comparison of NS0 whole cell extract analysis by 2-D PAGE, pI 3-10 non-linear resolving range	77
3.6	2-D PAGE images of whole NS0 cell extracts separated in the first dimension using pI 3-10 broad resolving range	79
3.7	Comparison of whole NS0 cell proteins separated on different percentage second dimension gels	81
3.8	Comparison of 1-D mini gel images to assess the detection limits of different staining techniques	84
3.9	Large format (20 x 18 x 0.1 cm) 2-D PAGE of whole NS0 cell extracts	87
3.10	Relationship between protein loads and the number of spots visualised by Coomassie staining.	88
4.1	Batch culture growth of NS0 cells expressing a recombinant IgG in serum-free medium in a controlled bioreactor culture	104
4.2	Large format 2-D PAGE (24 cm, pI 3-10 non-linear resolving range) of whole NS0 cells extracted from 1×10^7 cell samples taken throughout batch culture	106
4.3	Difference maps derived from analysis of whole NS0 cell extracts carried out throughout batch culture showing proteins exhibiting two-fold changes in protein expression levels	108

4.4	The total number of protein spots detected on samples extracted throughout the batch culture of NS0 cells in a bioreactor fermentation by 2-D electrophoresis	112
4.5	The whole NS0 cell proteome at mid-exponential growth phase	113
4.6	Proteins 1-8 from Figure 4.5 matched to protein spots from different sample points throughout the growth curve of NS0 cells in bioreactor culture	114
4.7	Proteins 9-17 from Figure 4.5 matched to protein spots from 2-D gels run from extracts taken throughout bioreactor batch culture of NS0 cells	115
4.8	The quantitative analysis of proteins 1 to 9 in Figure 4.5 whose expression level changed throughout a batch culture of NS0 cells in a controlled 1.5 L bioreactor culture	116
4.9	The quantitative analysis of proteins 10 to 17 in Figure 4.5 from whole NS0 cell proteins throughout bioreactor batch culture	117
4.10	The quantitative assessment of proteins 1-9 on 18 cm 2-D gel images derived from key time points during the bioreactor batch culture experiment	119
4.11	The quantitative assessment of proteins 10-17 on 18 cm 2-D gel images derived from key time points during the bioreactor batch culture experiment	120
5.1	Total protein synthesis of NS0 cells expressing IgG throughout a 1.5 L bioreactor batch culture	152
5.2	Two-dimensional autoradiographs of NS0 whole cell proteins during batch culture	154
5.3	Comparison of nascent polypeptide synthesis throughout batch culture of NS0 cells expressing a recombinant IgG ₁ on 2-D autoradiographs	155
5.4	Comparative analysis of nascent polypeptide synthesis throughout a batch culture of NS0 cells	158
5.5	Large format 2-D PAGE (18 cm, pI 3-10 non-linear resolving range) of NS0 whole cell proteins extracted throughout batch culture	162
5.6	Comparative analysis of protein expression throughout the batch culture of NS0 cells	164
5.7	Comparison of protein expression profiles on 18 cm protein gels and 18 cm autoradiographs ..	167
5.8	Putative protein spot identification	169
5.9	Proteins 1-8 from Figure 5.8B matched to protein gels run from different sample points throughout the bioreactor culture of NS0 cells	170
5.10	Proteins 9-17 from Figure 5.8B matched to protein spots from 2-D gels run from extracts taken throughout the growth curve of NS0 cells	171
5.11	The quantitative analysis of proteins 1 to 9 expression identified in chapter 4, Table 4.5 throughout a bioreactor batch culture of NS0 cells	172
5.12	The quantitative analysis of proteins 10 to 17 expression in chapter 4, Figure 4.5 throughout a bioreactor batch culture of NS0 cells	173
6.1	Batch culture growth of NS0 cell transfectants expressing rIgG ₄ in DMEM-F12 supplemented with 10% dFCS (Batch culture 1), and protein-free media supplemented with 1% dFCS (Batch culture 2) in 100 mL shaker flasks	196
6.2	Batch culture growth of NS0 cell transfectants expressing rIgG ₄ in protein-free medium supplemented with 1% dFCS in 4 L working volume fermenters	202

6.3	Large format 2-D PAGE (24 cm, pI 3-10 non-linear resolving range) of whole NS0 cell transfectants extracted at mid-exponential phase	204
6.4	Difference maps derived from the analysis of NS0 cell lines at mid-exponential growth phase during bioreactor culture	206
6.5	The semi-quantitative analysis of proteins 1-9 expression of NS0 cell transfectants identified in chapter 4, Table 4.5 at mid-exponential growth phase in controlled bioreactor culture	209
6.6	The quantitative analysis of proteins 10-17 expression from NS0 cell transfectants at mid-exponential growth phase	210

List of Tables

1.1	Examples of licensed therapeutic proteins produced in mammalian cells currently in the marketplace	2
2.1	NS0 protein solubilisation buffers	47
2.2	Modified Bradford assay	48
2.3	Focussing protocols for first dimension separations of whole cell NS0 protein extracts	50
2.4	Focussing protocols for protein loads of greater than 100 µg on IPG strips	51
2.5	Components of SDS-equilibration buffer	52
2.6	Bio-Rad broad range molecular weight markers	53
2.7	Novex mini-gel pre-set programme for Tris-glycine gels	54
2.8	Running protocol for protean II Xi cell large format gel tank	54
2.9	Electrophoresis running conditions for second dimension separations with the DALT II tank..	55
2.10	Adapted Shevchenko silver stain	56
2.11	The PlusOne silver staining method	56
3.1	Number of protein spots visualised with silver stain on 2-D mini-gels using the two solubilising conditions described in the methods section	71
3.2	Number of protein spots visualised with silver stain detected using ImageMaster™ software ..	77
3.3	Maximum resolving range for proteins separated on single percentage SDS-PAGE gels	80
3.4	Limits of sensitivity for various protein stains	82
3.5	Comparison of overloaded 2-D gels with variable protein concentrations to investigate the relative staining sensitivity of colloidal Coomassie to silver stain	88
4.1	Maximum viable cell density, growth rate (μ), doubling time (Td), and maximum IgG concentration (qMAb) in a 1.5 L volume batch bioreactor culture of NS0 cells in serum-free medium	104
4.2	Total number of protein spots detected on 24 cm 2-D gels from key points in the growth curve of NS0 cells during controlled bioreactor batch culture	106
4.3	Number of proteins newly synthesised, no longer expressed and up- or down-regulated by at least 2-fold throughout the batch culture of NS0 cells	111
4.4	Total average number of protein spots detected on triplicate 18 cm 2-D gels	118
4.5	The identification of proteins of interest excised from proteome maps of whole NS0 cell extracts and identified by MALDI-ToF ms	122
5.1	Total number of nascent polypeptides detected on 2-D autoradiographs during controlled bioreactor batch culture of NS0 cells	155
5.2	The total number of polypeptides up- and down-regulated at least 2-fold, newly synthesised, no longer expressed or unchanged throughout the batch culture of NS0 cells as assessed by 2-D autoradiography	159
5.3	Total number of protein spots detected on 18 cm 2-D gels throughout the growth curve of NS0 cells during controlled bioreactor batch culture	163

5.4	The total number of proteins up- and down-regulated by 2-fold or greater, newly synthesised, no longer expressed and unchanged proteins throughout the batch culture of NS0 cells assessed by 18 cm 2-D PAGE	165
5.5	The total number of polypeptides on autoradiographs matched to the equivalent protein spot on protein gels from the same day of the batch culture experiment	166
6.1	Maximum viable cell density, growth rate (μ), doubling time (Td), and maximum rIgG concentration (qMAb) in 100 mL shaker flasks in DMEM supplemented with 10% dFCS during period of maximum growth	197
6.2	Maximum viable cell density, growth rate (μ), doubling time (Td), and maximum rIgG concentration (qMAb) in 100 mL shaker flasks of various NS0 cell lines in protein-free medium supplemented with 1% dFCS	198
6.3	Growth kinetics for the 4 L fermentation of GS-NS0 cell transfectants in protein-free medium supplemented with 1% dFCS	201
6.4	Growth kinetics for the duplicate 4 L fermentation culture of GS-NS0 cell transfectants in protein-free medium supplemented with 1% dFCS	201
6.5	Total number of protein spots detected on 24 cm 2-D gels of cell lines derived from the same parental NS0 host cell line at mid-exponential growth phase during controlled bioreactor culture	205
6.6	Number of proteins observed that were unchanged, newly synthesised and up- or down-regulated by at least 2-fold when compared against the blank transfectant at mid-exponential phase of growth	208

List of Schemes

3.1	Optimised protocol for the preparation of whole NS0 cell extracts for 2-D electrophoresis	75
3.2	Optimised procedure for the analysis of the whole cell NS0 proteome by 2-D PAGE	90

Abbreviations

Abbreviations which are used throughout this thesis are listed and described below.

ADP	Adenosine diphosphate
APS	Ammonium Persulphate
ATP	Adenosine triphosphate
BiP	Immunoglobulin heavy chain binding protein/glucose regulated protein 78 kDa (Grp78)
BSA	Bovine serum albumin
cdk	Cyclin dependent kinase
CHAPS	(3-[(3-Cholamidopropyl)-dimethylammonio]-1-propanesulfonate
CHO	Chinese hamster ovary
CH ₃ CN	Acetonitrile
μCi	Micro Curie
CO ₂	Carbon dioxide
cpm	Counts per minute
2-D	Two-dimensional
2-DE	Two-dimensional gel electrophoresis
2-D PAGE	2-dimensional polyacrylamide gel electrophoresis
ddH ₂ O	Double distilled water (18 MΩ cm purity)
dFCS	Dialysed foetal calf serum
DHFR	Dihydrofolate reductase
DIGE	Difference gel electrophoresis
DMEM	Dulbecco's Modified media
DMSO	Dimethyl sulphoxide
DNA	Deoxyribonucleic acid
D.O	Dissolved oxygen
DOT	Dissolved oxygen tension
DTE	Dithioerythritol
DTT	Dithiothreitol
EDC	<i>N</i> -ethyl- <i>N</i> '-dimethylaminopropylcarbodiimide
eEF1A-1	Elongation factor 1-alpha-1
ELISA	Enzyme linked immunosorbent assay
EPO	Erythropoietin
ER	Endoplasmic reticulum
ERp60	Disulphide isomerase ER-60
ESI	Electrospray ionisation
ESI-ms	Electrospray ionisation mass spectrometry

ES-ms	Electrospray mass spectrometry
EST	Expressed sequence tag
F _c	Crystallisable fragment of immunoglobulin molecule
GAPDH	Glyceraldehyde 3-phosphate dehydrogenase
Grp75	Glucose regulated protein 75 kDa/mitochondrial stress-70 protein
Grp94	Glucose regulated protein 94/endoplasmic
GS	Glutamine synthetase
GSK	GlaxoSmithKline
h	Hour
HCl	Hydrochloric acid
hCMV	Human cytomegalovirus
HK	Hexokinase/glucose assay kit
Hsc71	Heat shock cognate 71 kDa protein
HBS	HEPES-buffered saline
HEPES	N-(2-Hydroxyethyl)piperazine-N'-(2-ethanesulfonic acid); 4-(2-Hydroxyethyl)piperazine-1-ethanesulfonic acid
HSP	Heat shock protein
Hsp60	60 kDa heat shock protein
IAA	Iodoacetic acid
ICAT	Isotope-coded affinity tags
IEF	Isoelectric focussing
Ig	Immunoglobulin
IgG	Immunoglobulin G
IMEM	Iscove's Modified Dulbecco's medium
IPG	Immobilised pH gradient
IPG Strip	Immobiline™ DryStrip gel
KDa	Kilo Daltons
MAb	Monoclonal antibody
MALDI	Matrix-assisted laser desorption-ionisation
MALDI-ms	Matrix-assisted laser desorption-ionisation-mass spectrometry
MALDI-ToF-ms	Matrix-assisted laser desorption-ionisation -Time of Flight-mass spectrometry
Max	Maximum
µm	Micron
Min	Minimum
mRNA	Messenger ribonucleic acid
M _r	Molecular weight
ms	Mass spectrometry
MSX	Methionine sulphoximine
MTX	Methotrexate
NAD	Nicotinamide adenine dinucleotide

NaOH	Sodium hydroxide
NHS	<i>N</i> -hydroxysuccinimide
NS0	Non-secreting murine myeloma cells
O.D.	Optical density
PAGE	Polyacrylamide gel electrophoresis
PBS	Phosphate buffered saline
PDI	Protein disulphide isomerase
pI	Isoelectric point
PK	Pyruvate kinase
PMF	Peptide mass fingerprinting
PPIase A	Peptidyl-prolyl <i>cis/trans</i> isomerase A
PSD	Post source decay
PST	Peptide sequence tag
qMAb	Maximum specific antibody titre
rMAb	Recombinant antibody
RNA	Ribonucleic acid
r.p.m	Revolutions per minute
RT	Room temperature
SDS	Sodium dodecyl sulphate
SDS-PAGE	Sodium dodecyl sulphate- polyacrylamide gel electrophoresis
SV40	Simian virus 40
TBP	Tributyl phosphine
TCA	Trichloroacetic acid
Td	Doubling time
TEMED	<i>N, N, N, N</i> ,- tetramethylethylenediamine
Temp	Temperature
TFA	Trifluoroacetic acid
TGS	Tris glycine SDS electrophoresis buffer
Tiff	Tagged-image file format
TMB	3, 3', 5, 5' Tetramethylbenzidine
TRIS	Trimethylol aminomethane
UKC	University of Kent at Canterbury
UK	United Kingdom
UPR	Unfolded protein response
USA	United States of America
μ	Specific growth rate
V/hr	Volts per hour applied to IPG strip during IEF

Chapter 1 Introduction

1.1 Cell Engineering

1.1.1 Recombinant Therapeutic Protein Production

The production of recombinant therapeutic protein products from mammalian cell lines (and linked vector systems) has increased exponentially since the first recombinant protein was approved for marketing in 1982 (Chu and Robinson, 2001; Cudna and Dickson, 2003; Reichert, 2000). Between the USA and Europe, approximately 50 different recombinant protein products have been licensed/approved (Kelly, 2001) and the impact of proteins as therapeutic agents in human health and the pharmaceutical industry continues to increase with experts predicting there will be a surge of protein, antibody and peptide drugs reaching the marketplace in the next 10 to 20 years (Chu and Robinson, 2001).

Mammalian cells are the most common host of choice for the production of recombinant proteins and currently dominate the marketplace in the production of monoclonal antibodies (MAbs) (Kelly, 2001). Some examples of therapeutic proteins produced from mammalian cells currently on the market are shown in Table 1.1 below (Cudna and Dickson, 2003; Lubiniecki, 1998). Many of the products expressed by mammalian cells rely on mechanisms involving the secretory processes of host cells (Barnes et al., 2000; Cudna and Dickson, 2003). Mammalian cell hosts are the only expression system currently capable of performing the correct post-translational modifications, specifically glycosylation, which are required for the full function and activity of many therapeutic products (Cudna and Dickson, 2003).

Many challenges lie ahead in the production of therapeutic proteins derived from animal cells. The requirement to use mammalian cells limits the ability to harvest secreted recombinant proteins (Cudna and Dickson, 2003). The high expression and transport of recombinant proteins into and through the secretory pathway (particularly through the endoplasmic reticulum (ER)), and the associated post-translational processing may act as a rate-limiting step or secretory 'bottleneck' in protein production (Cudna and Dickson, 2003; Schroder et al., 2002). These limitations may also be linked to the alterations in cell function caused by the process of recombinant protein production. That is, the movement of proteins through the ER and the response of ER quality control mechanisms may inhibit protein translation, cell growth and may activate apoptosis, thereby decreasing viable cell numbers (Cudna and Dickson, 2003).

1 Introduction

To produce the required amount of protein product to meet the increasing demand will inevitably strain the current technologies available for large-scale production (Kelly, 2001; Voisard et al., 2003). To maximise the cell culture productivity of therapeutic recombinant proteins researchers have investigated methods to increase the viable cell density, extend the culture lifetime (to increase the productive cell lifetime) and to maintain optimum cellular productivity. Apoptosis has been recognised as the main mechanism of cell death under culture conditions, and is a critical factor that limits some, or all, of the above attributes under culture conditions. Attempts to engineer cell lines to halt the cell-cycle (to divert energy from cell proliferation towards synthesis of recombinant proteins) or the overexpression anti-apoptotic genes (to extend the viable cell lifetime) to improve recombinant protein production have had some success in terms of increasing cellular productivity (Fussenegger et al., 1998a; Meents et al., 2002; Watanabe et al., 2002). Others have predicted that the development of inverse metabolic engineering strategies promises to provide the rational means of targeting proteins for improved functional phenotypes (Bailey et al., 1996).

Table 1.1 Examples of licensed therapeutic proteins produced in mammalian cells currently in the marketplace (adapted from Cudna and Dickson, 2003; Chu and Robinson, 2001; Lubiniecki, 1998)

Host Cell Line	Product	Clinical Application
BHK (baby hamster kidney)	Novo Seven (Factor VIIa)	Haemophilia
CHO (Chinese hamster ovary)	TNKase (recombinant glycoprotein)	Reduction in mortality associated with myocardial infarction
CHO	Activase/ Actilyse (Tissue plasminogen factor (tPA))	Thrombolytic agent, after myocardial infarction/ stroke
CHO	Neorecormon/ Epogin/ Eprex (Epo, erythropoietin)	Anaemia
CHO	Pulmozyme (DNase I)	Cystic fibrosis
CHO	Follistim/ Gonal-F (FSH, follicle stimulating factor)	Infertility
CHO	Rebif (Interferon- β 1a)	Multiple sclerosis
Murine Myeloma	Infliximab/ Remicade (MAb)	Crohn's disease
Murine Myeloma	Simulect (MAb)	Acute organ rejection
NS0 myeloma	Zenapax (humanised antibody)	Kidney transplant rejection
NS0	Synagis (humanised antibody)	Respiratory tract virus

1.1.2 Mammalian Cell Systems

The use of animal cells has many advantages over other systems (e.g. bacterial and plant systems) including the synthesis, processing and secretory signals that are generally properly and efficiently recognised (Barnes et al., 2003). The protein products are also

usually folded and processed correctly including the formation of disulphide bonds and have the correct post-translational modifications which are required for proteins to be functionally active. The most commonly used animal cell lines for the production of recombinant proteins are Chinese hamster ovary (CHO) cells and non-secreting (NS0) murine myeloma cells, which are the system of choice in this study.

1.1.2.1 NS0 Cell History

Murine myeloma NS0 cells have had a long and complicated history. The development of NS0 cells began more than 40 years ago when Potter and Boyce injected mineral oil into the intraperitoneal region of a female BALB/c mouse inducing plasma-cell neoplasmas (Barnes et al., 2000; Cudna and Dickson, 2003; Potter and Boyce, 1962) (Figure 1.1). Briefly, BALB/c mice were induced to form tumours, and one tumour MOPC21 (mineral oil induced plasmacytoma number 21) was observed to secrete IgG₁ and was used to form a continuous tissue culture line. These cells were then maintained as ascites in mice before re-culturing. This heterogeneous population of cells, which grew in suspension culture, were then named P3K cells and were also observed to secrete IgG₁ (Barnes et al., 2000). This cell population was cloned giving rise to P3-X27, a clonal cell line once again capable of synthesising IgG₁ (Barnes et al., 2000). The P3-X27 cells were cloned again giving rise to two cell lines, 289-16 and P3-X63, which were developed separately.

The 289-16 cell line did not secrete IgG₁, synthesising the light chain but no heavy chain (Barnes et al., 2000). At this stage the cell line was re-named the NSI/1 and clones which were resistant to 8-azaguanine were isolated. One clone from the NSI/1 cell line only expressed intracellular light chains, and was called P3/NSI/1-Ag4-1. This cell line was cloned again to generate a sub-cell line, which did not synthesise heavy or light chains of immunoglobulin (Ig), and was called a non-secreting NS0/1 cell line (Galfre and Milstein, 1981). The resulting NS0 cell line has been used as a fusion partner in the production of hybridoma cells for the production of antibodies. Furthermore this cell line has also been used on its own for the production of therapeutic recombinant proteins, particularly when coupled with the glutamine synthetase (GS) system (Barnes et al., 2000; Bebbington et al., 1992).

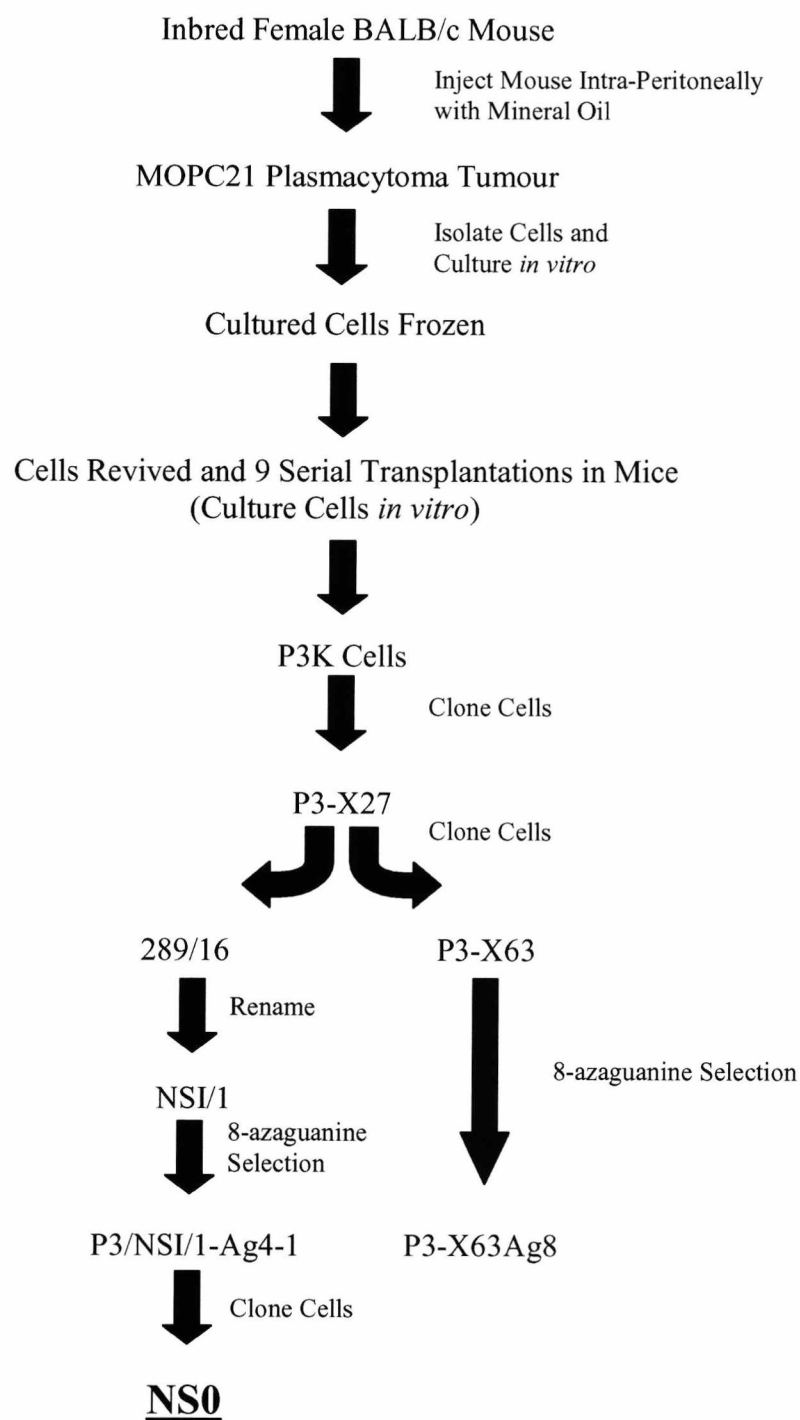


Figure 1.1 The history of the NS0 cell line (reproduced from Barnes *et al.*, 2000).

1.1.3 Strategies for Improved Cell Performance

In order to maximise process productivity a great deal of attention has been focussed towards bioreactor design, culture media development, improved expression systems (and gene amplification systems) and cell line development to optimise cell growth conditions (Laken and Leonard, 2001; Sauerwald *et al.*, 2003).

1.1.3.1 Cell Culture Media

The first development of cell culture medium was the use of precise quantities of amino acids, vitamins, salts and carbohydrates in combination with serum which contains growth factors and signalling molecules required for cell growth and survival. For the routine culture of animal cells today the early formulations of culture media are still in use, with a few modifications including additional carbohydrate in Dulbecco's Modified Medium (DMEM) and Iscove's Modified Dulbecos's Medium (IMDM, DMEM medium modified to include additional selenium, amino acids and vitamins, sodium pyruvate, HEPES buffer and potassium nitrate instead of ferric nitrate). IMDM was found to specifically support murine B lymphocytes, T lymphocytes and a variety of hybrid cells (Iscove et al., 1980; Iscove and Melchers, 1978).

However the use of serum has major disadvantages, in that it is undefined with respect to its chemical composition and may contain substances that induce unwanted cellular behaviour (Hesse and Wagner, 2000). As a result of the cost of downstream processing and bio-safety concerns, serum-free and protein-free media have been developed for the production of biopharmaceuticals (Birch and Froud, 1994a; Hesse and Wagner, 2000). The main objective of these media types is to replace undefined serum with more defined supplements, and in the case of protein-free, medium containing no animal derived products.

Lambert and Merten established that the utilisation of serum-free culture medium resulted in increased MAb production rates in mouse hybridoma cell lines compared to serum-containing medium (Lambert and Merten, 1997). The results indicated that the medium formulation can positively influence MAb production. Furthermore, the addition of serum to the serum-free medium had a pronounced negative effect on MAb productivity (Lambert and Merten, 1997). However, some of the serum-free components such as hydrolysates are not clearly defined (Hesse and Wagner, 2000). These problems have led to the development of protein-free media consisting only of chemically defined components which are not animal derived (Gorfien et al., 2000; Hesse and Wagner, 2000). However, upon serum removal the nutrient balance of the media may need to be optimised and additional nutrients added in place of serum (Dempsey et al., 2003), including cholesterol, peptones and the enrichment of the culture environment through addition of glucose, amino acids, transferrin (or alternatives such as tropolone and ferric ammonium citrate) and phosphate feeding during cell growth which have had a positive impact on MAb

1 Introduction

product titre and can prolong culture lifetime (Dempsey et al., 2003; deZengotita et al., 2000).

NS0 cells transfected with the GS gene have different nutritional requirements to untransfected cells (Zhou et al., 1997). By engineering cells to express the GS gene cells are able to grow in medium without glutamine and this reduces the accumulation of ammonia (Zhou et al., 1997). NS0 cells also use more amino acids (particularly glutamate and asparagine) presumably as a metabolic source of ammonia, which is combined with glutamate to produce glutamine using the GS catalysed reaction (Figure 1.2) (Barnes et al., 2000). The reduction in ammonia and lactate accumulation reduces the inhibition of cell growth, which causes necrotic cell death. With successful nutrient control, monoclonal antibody productivity has been shown to increase substantially in GS-NS0 cells by as much as 10-fold (Barnes et al., 2000). However, NS0 cells are cholesterol auxotrophs (Gorfien et al., 2000); therefore cholesterol is essential for optimal growth although NS0 cells can be grown in cholesterol-free media (Birch et al., 1994b; Gorfien et al., 2000). Media osmolarity has also been shown to have a profound effect upon NS0 cell growth and productivity and under some hyperosmotic conditions can improve productivity (Barnes et al., 2000). However, the optimisation of culture media has only been achieved through time-consuming trial and error approaches.

1.1.3.2 Bioreactor Design

The production of recombinant protein from mammalian cells is limited by nutrient depletion and increase in waste product accumulation. The high volume production of recombinant proteins by animal cells is usually carried out in suspension culture in large-scale stirred tank reactors (Voisard et al., 2003). These bioreactors are basically carried out in three modes, batch culture, which is a closed system in which cells and medium are added to the reactor, fed batch, and perfusion culture (Voisard et al., 2003). The implementation of fed batch or perfusion culture where nutrients are fed to the culture during the growth cycle, or in the case of perfusion culture where nutrients are continually fed into the reactor and spent culture and media are removed, have greatly improved the productive lifetime and integral of viable cells during culture and increased recombinant protein yield particularly of humanised monoclonal antibodies from NS0 cells (Birch and Froud, 1994a; Dempsey et al., 2003; Sauer et al., 2000; Zhou et al., 1997). These approaches involve the development of nutrient feeding strategies to avoid nutrient depletion and to reduce lactate and ammonia formation by controlling glucose and

1 Introduction

glutamine concentrations, and have been found to delay apoptotic cell death in NS0 cells (deZengotita et al., 2000; DiStefano et al., 1996; Sauer et al., 2000; Zhou et al., 1997). In mammalian cell culture systems the parameters of pH, CO₂, osmolarity and dissolved oxygen concentration are usually controlled. In most mammalian cell culture systems these parameters greatly affect cell growth and recombinant protein titre and therefore have to be optimised to obtain the highest viable cell densities and yield of recombinant protein for each cell type (Sauer et al., 2000; Zhou et al., 1997).

Temperature is another key environmental parameter that has been shown to influence cell growth and recombinant protein production (Andersen and Krummen, 2002; Yoon et al., 2003). Reduced temperatures have recently been shown to prolong the cell viability either through growth arrest or through modulation of cold-sensitive gene expression in CHO cells (Andersen and Krummen, 2002; Yoon et al., 2003). Many reports have shown a decrease in temperature reduces the specific growth rate, resulting in the cells maintaining high viability for a longer period of time. However, the effect on productivity has met with conflicting results and appears to be dependent on the cell type and the target protein under investigation (Yoon et al., 2003). The developments in bioreactor design have now been more or less optimised for cell growth *in vitro* but this approach cannot improve cellular properties or machinery. This can only be achieved through engineering of cell lines for desired phenotypes.

1.1.3.3 Gene Amplification Systems

The production of therapeutic proteins in greater quantities has led to major advances in expression systems. The efficiency with which mammalian cells take up and express the DNA of interest varies between different cell types. Therefore a method for stably expressing the DNA of interest would be beneficial. Ranges of selectable markers, some of which allow amplification have been developed. In industry two main markers are utilised, the dihydrofolate reductase system (DHFR) and the glutamine synthetase (GS) system (Barnes et al., 2000). DHFR is a non-dominant marker and is best utilised in cells which lack DHFR, and therefore is routinely used in DHFR⁻ mutants such as the DHFR⁻ CHO cell line (Barnes et al., 2000; Kaufman, 1990).

On the other hand the GS system is capable of acting as a dominant marker and can therefore be utilised in cell lines which contain endogenous GS as well as GS⁻ cell lines (Barnes et al., 2000; Bebbington et al., 1992). The GS system is most commonly used in CHO and NS0 cell lines. The GS system usually only requires one single round of

amplification typically taking approximately 3 months to complete, which significantly reduces the development time and is usually sufficient to provide ‘good’ levels of stable recombinant protein expression (Barnes et al., 2000; Bebbington et al., 1992). This contrasts with the DHFR system which often requires multiple rounds of amplification (Barnes et al., 2000). The GS system also requires fewer copies of the marker and recombinant proteins to obtain high levels of expression (typically 4-10 copies per cell after amplification), compared with the DHFR system which requires several hundred copies per cell after amplification through selection with methotrexate (MTX) (an inhibitor of DHFR) (Bebbington and Hentschel, 1985).

Increased product accumulation has been reported to be higher when the GS system has been implemented when compared with DHFR. NS0 cells contain endogenous DHFR, and therefore much higher levels of MTX are required to obtain significant amplification (Bebbington et al., 1992). As a result, the GS system is regarded as the most efficient system for the high-level production of recombinant proteins in NS0 cells (Barnes et al., 2000). However, in order to identify stably transfected, productive cell lines using either system, industry still relies on lengthy and labour intensive rounds of cloning, screening and selection procedures (Sauer et al., 2000). These procedures are time consuming and can result in selection of cells which are unstable in production and therefore often require the presence of the selection agent to maintain the cells in an amplified state.

The GS system has been used in both CHO and NS0 cells but is the preferred system for use in NS0 cells as they lack endogenous GS (Bebbington et al., 1992). As a result lower levels of toxic agents (methionine sulphoximine (MSX)) are required for selection and amplification (Barnes et al., 2000; Bebbington et al., 1992). NS0 cells also have several other potential advantages including the fact that they are suspension cells, and being derived from immunoglobulin producing tumours are adept at producing high levels of secreted protein. Furthermore, the adaptation of NS0 cells to serum-free and protein-free media and their growth in bioreactors is also relatively straightforward (Bebbington et al., 1992).

1.1.3.4 The Glutamine Synthetase (GS) System

Glutamine is a non-essential amino acid, synthesised by a variety of cells and has a major role within cells (Bebbington et al., 1992). It has a significant role in nitrogen metabolism as it provides a nitrogen source, important to many biosynthetic pathways. The amino acid is important in protein synthesis, purine and pyrimidine biosynthesis and in the formation

1 Introduction

of ammonia, as well as having an important role in the biosynthesis of amino acids and some co-factors (Barnes et al., 2000). Cells can also utilise the carbon chain of glutamine as an energy source. The formation of glutamine from glutamate and ammonia requires energy involving the hydrolysis of ATP, and is catalysed by glutamine synthetase (Bebbington et al., 1992) (Figure 1.2).

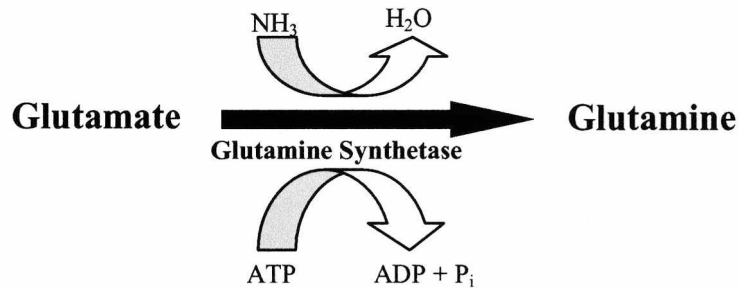


Figure 1.2. The formation of glutamine from glutamate through the utilisation of ammonium as an amino group donor. The reaction is catalysed by glutamine Synthetase (GS) (adapted from Barnes *et al.*, 2000).

The Glutamine Synthetase (GS) system relies on the fact that NS0 cells contain low levels of endogenous GS and therefore when the cells are grown in glutamine-free media, they either require glutamine in an exogenous source or exogenous GS to survive (Barnes et al., 2000; Bebbington et al., 1992). The incorporation of GS in an expression vector enables the selection of stably transfected cells on the basis that cells stably expressing the vector are able to survive in glutamine-free selective medium (Bebbington et al., 1992; Birch et al., 1994b). The construction of the plasmid vector can have a great effect upon productivity (Barnes et al., 2000). The GS coding sequence is usually under the control of a promoter that is weak in lymphoid cells such as simian virus 40 (SV40) (Bebbington et al., 1992). However, the protein coding sequence/s are under the control of a strong promoter such as the human cytomegalovirus (hCMV) promoter (Bebbington et al., 1992; Brown et al., 1992). This methodology ensures that cells successfully transfected survive in a glutamine-free environment, whilst producing high levels of heterologous protein as a result of the strong promoter (hCMV) (Barnes et al., 2000). The GS sequence is usually placed upstream of the recombinant gene to prevent occlusion without compromising transformation efficiency (Bebbington et al., 1992). If the hCMV gene (which is used to direct transcription of the heavy and light chain genes of the antibody) is placed upstream of the SV40 promoter, which directs GS expression, no selection of glutamine-independent cell lines is possible (Barnes et al., 2000; Bebbington et al., 1992).

This system is now widely accepted and utilised routinely in the selection process for NS0 and GS transfected cells (Dempsey et al., 2003). NS0 cells have very low to no endogenous GS activity (Dempsey et al., 2003), and therefore only cells successfully transfected with the GS system will survive in the selection medium. Additionally, the inclusion of MSX, an inhibitor of GS activity, can enable further selection of clones only expressing high levels of the enzyme and the associated heterologous protein coupled to it (Brown et al., 1992). Typically the gene copy number can be increased in this way from 1 to 4-10 copies per cell. Any gene that is co-transfected with the GS-amplifiable marker such as heterologous recombinant protein will be simultaneously amplified. Unlike NS0 cells, CHO cells have endogenous expression of GS, and therefore these cells require permanent toxic MSX selection at relatively high levels to actively select only those cells with the expression vector. This significantly adds to the production costs of using CHO cells with the GS system and prolongs the toxic effects upon cells (Barnes et al., 2000; Bebbington et al., 1992).

1.1.4 Metabolic Engineering Strategies for Improved Cell Specific Productivity

The methods discussed to this point have optimised the culture medium and environment for improved productivity and the considerable progress towards devising effective plasmids for the delivery and expression of genes. However, very little work has been carried out towards optimising the host cell line itself for improved performance. It has therefore become apparent that there is a need to target the 'cell' to enhance metabolic machinery through genetic means. This has led to the field of metabolic cellular engineering (Bailey, 1991). Metabolic engineering strategies have proven useful for the control of apoptosis to extend culture viability, cell-cycle arrest for increased product titre and product quality through glycosylation engineering and these strategies are discussed in more detail below (Fussenegger and Betenbaugh, 2002; Fussenegger et al., 1998b).

1.1.4.1 Control of Apoptosis to Improve Cell Specific Productivity

The production of therapeutic recombinant proteins currently relies on the large-scale culture of eukaryotic cells that secrete the protein of interest into the medium (Laken and Leonard, 2001; Meents et al., 2002). It has recently been recognised that programmed cell death (apoptosis) may pose a significant hurdle to production cell lines, which must be overcome to maximise productivity in these systems (Laken and Leonard, 2001). Cells in culture are constantly exposed to changing conditions in their environment. As a result

non-optimal conditions can result in cell death by one of two mechanisms, (1) necrotic death, as a result of severe insults such as collision with the bioreactor wall (shear effects) or (2) programmed cell death as a result of chronic insults such as nutrient depletion and toxic waste product accumulation (Laken and Leonard, 2001; Sauerwald et al., 2003). Serum components have been identified as major apoptosis-protective agents, although, in modern biopharmaceutical processes serum is not utilised due to fears over BSE and the need to fully characterise culture conditions. This results in cell lines with an increased sensitivity to programmed cell death (Chu and Robinson, 2001; Meents et al., 2002).

It has been proposed by many researchers that solving the problems associated with serum deprivation by understanding the events which cause apoptosis could provide future strategies for the control of apoptosis to enhance volumetric productivity (Dickson, 1998; Laken and Leonard, 2001; Meents et al., 2002). Apoptosis has evolved as a concerted critical pathway in the development and homeostasis of multicellular organisms and occurs in commercial cell types (Laken and Leonard, 2001). The process of programmed cell death is frequently a barrier in maintaining high viable cell densities and possibly as a consequence limits cell specific productivity (Dickson, 1998). Therefore, the prevention of apoptosis could, in theory at least, contribute to maximising the production of recombinant proteins in bioreactor culture (Laken and Leonard, 2001).

The most studied regulatory mechanism in apoptosis involves the Bcl-2 family of proteins (Laken and Leonard, 2001) which consists of pro- and anti-apoptotic members. The most common anti-apoptotic members are Bcl-2 and Bcl-x_L (Laken and Leonard, 2001). These proteins modulate induction of the intrinsic apoptotic pathway involving caspase-9-dependent apoptosis and prevent the release of cytochrome *c* from mitochondria which acts to initiate activation of the caspase cascade and programmed cell death (Laken and Leonard, 2001). Many researchers have initiated a variety of physiological and metabolic engineering strategies for reducing the induction of apoptosis (Meents et al., 2002). In particular, the overexpression of Bcl-2 and Bcl-x_L has been investigated and shown to inhibit apoptosis in several different mammalian cell culture systems (Andersen and Krummen, 2002; Mastrangelo et al., 2000). However, the overexpression of Bcl-2 has been reported to have different effects in various cell types, and despite protecting cells from apoptosis, conflicting results have been obtained as to whether an appreciable increase in recombinant protein production results (Laken and Leonard, 2001). Figure 1.3 below shows an outline of the processes regulated by Bcl-2 and Bcl-x_L leading to initiation or inhibition of apoptosis.

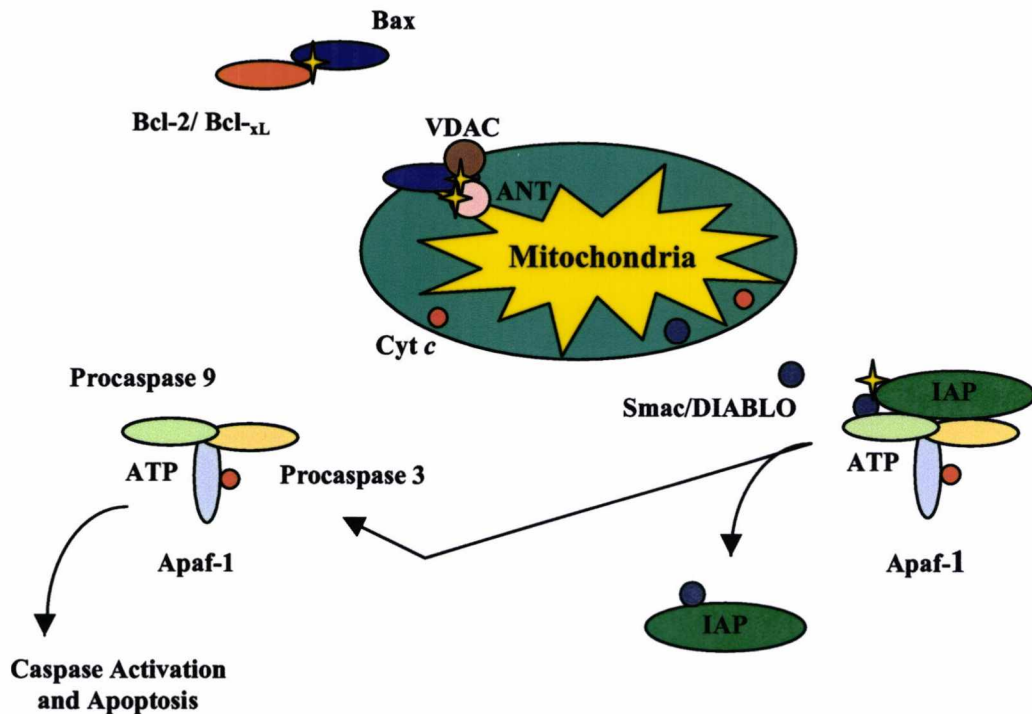


Figure 1.3 The release of cytochrome *c* (cyt *c*) and Smac/DIABLO (a mitochondrial inner membrane associated protein, which has pro-apoptotic activity when released from mitochondria) from the inner membrane space of the mitochondria which is regulated by the Bcl-2 family protein members. For simplicity only two members of the Bcl-2 family are shown here, Bax and Bcl_{xL}. One model for Bcl_{xL} intervention of Bax function is shown; Bcl_{xL} or Bcl-2 is binding Bax in the cytoplasm, which acts to inhibit translocation to the mitochondria. There is an alternative model (not shown), whereby the functional interaction of Bcl_{xL} and Bax occurs in the mitochondrial membrane. Members of the mitochondrial megachannel, voltage-dependent anion channel (VDAC) and adenine nucleotide translocator (ANT) span the inner membrane space of mitochondria and may also contribute to the formation of a Bax-containing channel. Finally caspase activity in the apoptosome can be inhibited by the overexpression of an inhibitor of apoptosis protein (IAP) (reproduced from Huang and Oliff, 2001).

The reasons for the differing results are not clear although it is likely that differences between the cell lines and the specific culture conditions employed have significant effects on the outcome of these cell line engineering strategies (Laken and Leonard, 2001). The differences between cell lines is perhaps not surprising given the complexity of the system and the redundancy of the regulatory pathways involved in apoptosis. Therefore, multifaceted approaches may be required to achieve better results (Andersen and Krummen, 2002).

An alternative strategy has also been investigated which involves the inhibition of activation of the caspase cascade which results in apoptosis (Andersen and Krummen, 2002). The addition of chemicals to mammalian cell culture provides a straightforward method for inhibiting caspases in order to delay the progression of apoptosis, although it is

1 Introduction

a costly method (Sauerwald et al., 2003). An alternative approach is the engineering of cell lines with genes that code for caspase inhibitors (Sauerwald et al., 2003). For example, Sauerwald and co-workers investigated the effect of chemical inhibitors (Z-IETD.fmk and Z-LEHD.fmk) and two genetic caspase inhibitors (XIAP and CrmA) together with mutants of each in CHO and human embryonic kidney (HEK) cell lines (Sauerwald et al., 2003).

There are three classes of genetic caspase inhibitors, p35 from *Autographa californica* nuclear polyhedrosis virus, CrmA (cytokine response modifier A) from cowpox virus and the inhibitor of apoptosis protein (IAP) family. CrmA offers resistance to apoptosis through the extrinsic death receptor pathway by protecting the cell against cell death induced by the TNF (tumour necrosis factor) receptor family. The engineering of this inhibitor into numerous cell lines has resulted in inhibition of cell death and prevents apoptosis caused by a variety of insults (Sauerwald et al., 2003). XIAP is a human member of the IAP family and is a potent inhibitor of caspases. XIAP functions in the intrinsic mitochondrial pathway by preventing the processing of pro-caspase 9, as a result of cytochrome *c* release from the mitochondria to prevent activation of downstream effector caspases (Sauerwald et al., 2003). XIAP has been found to confer protection against many apoptotic inducers (Sauerwald et al., 2003). p35 is more promiscuous and inhibits a wide range of caspases (Cryns et al., 1998).

Investigations utilising these inhibitors suggest that the genetic inhibitors afforded the greatest protection against apoptosis and that the apoptosis pathways induced, and the level of protection afforded by each of the inhibitors, varied with the type of cellular insult (Sauerwald et al., 2003). There was also cross talk of apoptotic pathways inhibited by genetic and chemical treatments. The differences in protection from apoptosis may be due to differences in the mechanisms and pathways used to initiate apoptosis; therefore the progression of cell death may be stalled to different degrees depending on the applicability of the caspase inhibitor used (Sauerwald et al., 2003). If the primary insult which leads to cell death can be elucidated this type of strategy may be useful in combating the particular insult. However, our knowledge of apoptosis is still incomplete, and until our understanding of the mechanisms involved in apoptosis pathways improves, researchers will not be able to create 'designer' cell lines capable of extending viabilities beyond that currently possible (Sauerwald et al., 2003).

Other groups have focussed on the expression of proteins involved with apoptosis, including GADD153 (Lengwehasatit and Dickson, 2002). The GADD153 gene has been

implicated in the cellular response to stresses linked with the initiation of apoptosis and is induced by stress conditions including nutrient deprivation and inhibition of ER function (Lengwehasatit and Dickson, 2002). It has been reported that the addition of glucose, glutamine or amino acid mixtures to batch cultures of NS0 cells suppresses GADD153 expression and delayed apoptotic and non-apoptotic cell death but did not prevent it (Lengwehasatit and Dickson, 2002). Another recent report has shown the transfection of NS0 cells with the *HSP70* gene increased the cells resistance to apoptosis (Lasunskaja et al., 2002). The Hsp70 protein plays an important role in cell protection against a variety of cytotoxic factors, which may include apoptosis (Lasunskaja et al., 2002; Parcellier et al., 2003). The report revealed that NS0 cells were protected against metabolic stress normally observed at the end of stationary phase (Lasunskaja et al., 2002).

1.1.4.2 Cell-Cycle Arrest Strategies to Increase Cell Specific Productivity

In recent years metabolic engineering techniques have been utilised to construct mammalian cell lines in which viability and proliferation can be controlled to optimise culture conditions and productivity (Watanabe et al., 2002). Optimisation of production processes requires active cell growth without the accumulation of toxic metabolites or limiting the conditions that will confer loss of cell viability and productivity (Ibarra et al., 2003). An ideal production process would allow the expansion of cells until they reach their optimal production phase. This phase would then be preserved by the induction of growth or cell-cycle arrest to divert energy towards synthesis of recombinant protein products rather than for cell division (Ibarra et al., 2003). An improved knowledge of the pathways which regulate cell death and growth will, in theory at least, make it possible to modify specific aspects of cellular behaviour by introducing and expressing genes that are known to influence cell survival or proliferation (Watanabe et al., 2002).

The control of the cell-cycle and cell proliferation is based on the activity and level of expression of cyclin-dependent kinases (cdks) and their inhibitors (Watanabe et al., 2002). This family of proteins are regulated by association with cyclin regulatory subunits and phosphorylation mechanisms and can be inhibited by the binding of cdk inhibitors, including p21^{cip1} and p27^{kip1} (Ibarra et al., 2003). The inhibitors p21^{cip1} and p27^{kip1} induce cell-cycle arrest at the G1 checkpoint by inhibiting cyclin E-dependent kinase cdk2 and cdk4 activity respectively (Fussenegger et al., 1997; Ibarra et al., 2003; Watanabe et al., 2002). The manipulation of the cell-cycle in this way should make it possible to keep cells viable in the culture for longer periods of time and as a result the protein production phase

1 Introduction

of culture should continue for a greater period of time (Ibarra et al., 2003). Figure 1.4 shows the cell-cycle and outlines some of the strategies utilised to cause cell-cycle arrest.

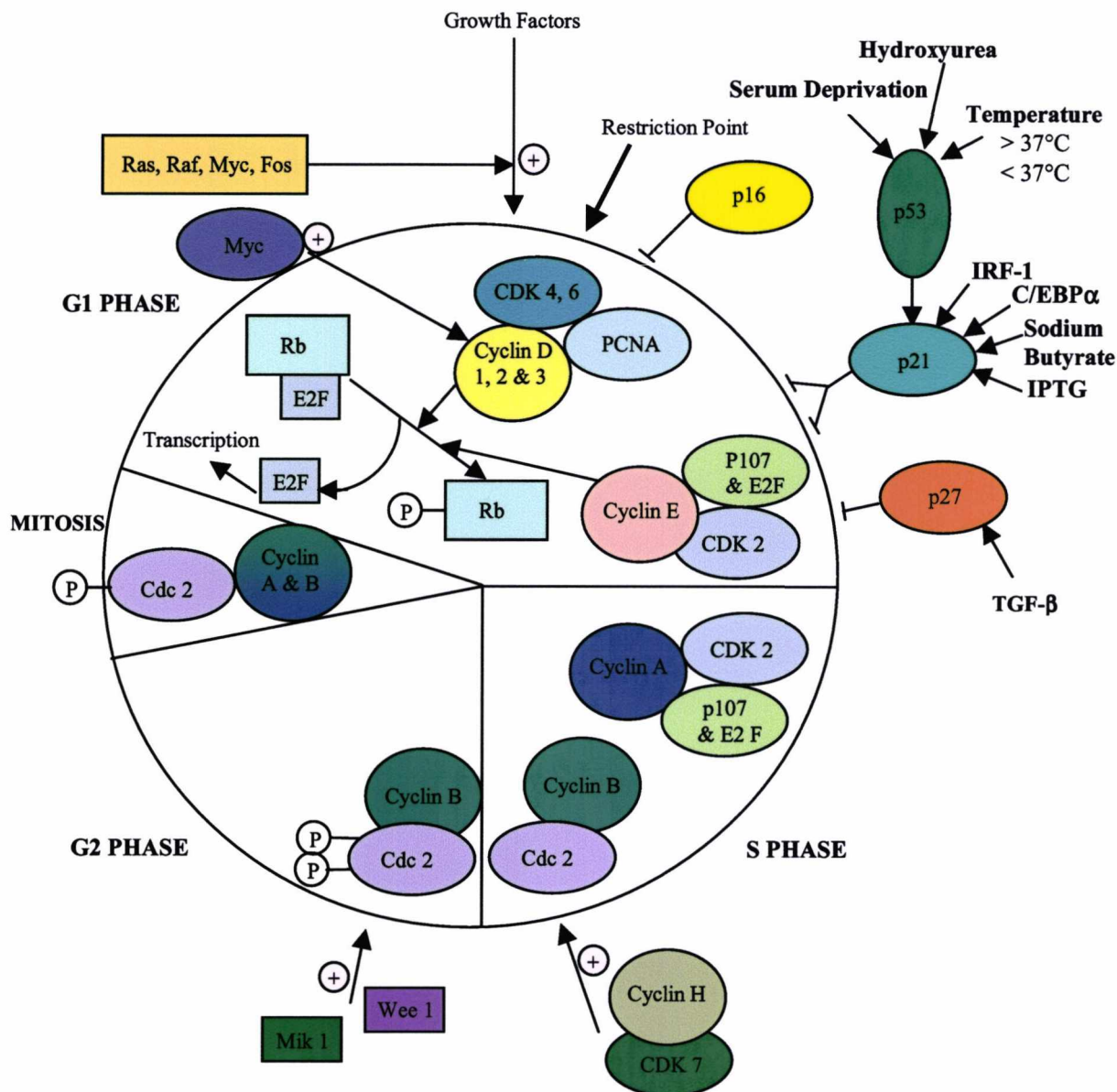


Figure 1.4 A schematic view of the cell-cycle and the various complexes involved in regulating the transitions through 'check points', depicted as a circle running clockwise (adapted from Bailey *et al.*, 1996). Several strategies have been implemented to induce cell-cycle arrest including additives to the culture medium in the form of, hydroxyurea, butyrate and TGF- β . Serum deprivation has also been shown to induce cell growth arrest. Other strategies for arrest at G1-S phase include alterations (an increase or decrease) in culture temperature. Metabolic engineering strategies have had differing levels of success in different cell lines, and include the overexpression of p21, p27 and p53.

Previous efforts to establish inducible cell-cycle arrest by regulated overexpression of p21^{cip1} using a one-gene approach failed (Fussenegger et al., 1998b). However, Fussenegger and co-workers utilised a tetracycline-repressible multigene approach to stabilise and induce p21^{cip1} expression which resulted in the successful inducible

1 Introduction

overexpression of p21^{cip1} and cytotaxis in CHO cells concomitant with a 10-15 times increase in secreted alkaline phosphatase (SEAP) protein production (Fussenegger et al., 1997; Fussenegger et al., 1998b). Cytostasis has also been successfully induced in NS0 cells using the Lacswitch system (Stratagene, U.K.) (Watanabe et al., 2002). Cell numbers were observed to remain stable over a period of 6 days which was concomitant with a 4-fold enhancement in productivity in low-density culture in NS0 cells expressing a chimeric IgG₄ (B72.4) independent of the inducible promoter activity used to promote cytotaxis (Ibarra et al., 2003; Watanabe et al., 2002). In the study p21^{cip1} expression was induced through addition of IPTG to the culture medium in NS0 cells (Watanabe et al., 2002).

Fussenegger *et al.* also investigated the regulatory protein p27^{kip1}, which induces cell-cycle arrest at the G1/S phase border (Fussenegger et al., 1997; Fussenegger et al., 1998a). This study also used tetracycline-repressible multicistronic vectors encoding cdk inhibitors together with genes including secreted alkaline phosphatase SEAP (Fussenegger et al., 1998a; Watanabe et al., 2002). The overexpression of p27^{kip1} in CHO cells using this multigene metabolic engineering approach was found to result in up to a 30-fold increase in cell specific productivity of SEAP (Andersen and Krummen, 2002; Fussenegger et al., 1998a; Watanabe et al., 2002). However, the increased yield of cells with p21^{cip1} and p27^{kip1} expression was established by comparing a control in which SEAP was introduced on a construct lacking a cdk inhibitor. Therefore, any increase in product titre may have occurred as a result of variations in the tetracycline promoter activity at different sites of gene integration (Watanabe et al., 2002). Furthermore, SEAP and cdk inhibitor expression were linked by a shared promoter, and it is therefore possible that the cell lines selected on the basis of cytotstatic arrest are expressing higher levels of both proteins (Watanabe et al., 2002).

Strategies to combine anti-apoptotic proteins such as Bcl-2 and Bcl-x_L with cdk inhibitors have also been implemented with the aim of improving cell viability and increasing cell specific productivity. However, these strategies have met with conflicting results, due to the complexity of mammalian cell systems (Fussenegger et al., 1998a; Ibarra et al., 2003; Tey et al., 2000). Figure 1.5 below outlines the regulatory networks controlling apoptosis and the G1-S transition of the cell-cycle.

1 Introduction

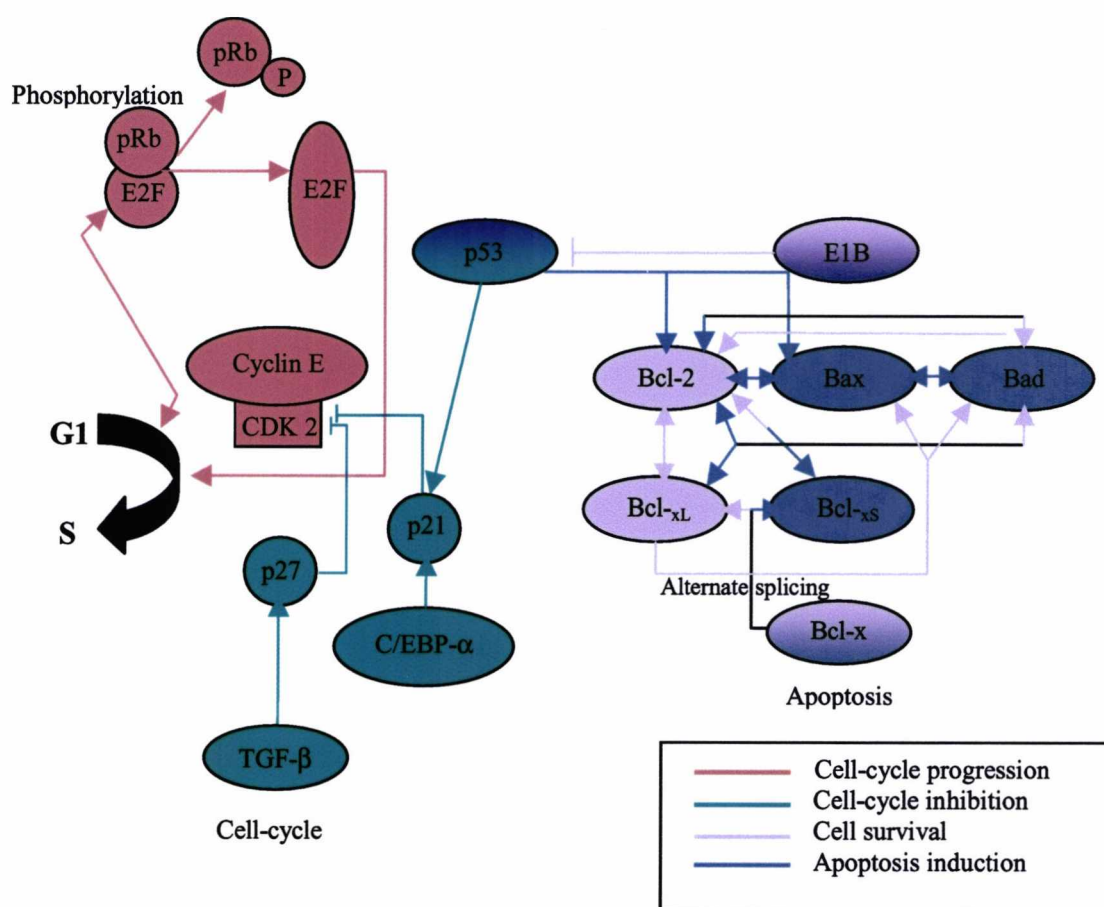


Figure 1.5 The key regulatory networks controlling apoptosis and the G1-S transition of the cell-cycle of mammalian cells. The two major cyclin-dependent kinase inhibitors p21 and p27 negatively control cell proliferation by binding to the cyclin E/cyclin-dependent kinase 2 complex together with other cyclin/cyclin-dependent kinase complexes. Tumour suppressor p53 is a transcriptional activator of several genes including *p21* and induces stable growth arrest at the G1 checkpoint (through *p21*) or programmed cell death through induction of redox genes and Bax. Differentiation factor C/EBP- α up-regulates *p21* expression and stabilises p21 at the protein level. Both positive and negative signals are involved with triggering or suppressing apoptosis. Among them are the anti-apoptotic proteins Bcl-2 and Bcl-x_L, which have been extensively utilised for the inhibition of apoptosis in a variety of human and animal cells with differing levels of success (adapted from Papoutsakis, 1998).

In another recent study rapamycin was fed to hybridoma cultures producing a monoclonal antibody in an effort to reduce cell death via cell-cycle modulation. A beneficial effect was observed on both cell growth and productivity (Andersen and Krummen, 2002; Balcarcel and Stephanopoulos, 2001). Rapamycin is an mTOR (mammalian target of rapamycin) protein kinase signalling molecule inhibitor, immunosuppressant and G1-phase arresting agent (Balcarcel and Stephanopoulos, 2001; Dufner and Thomas, 1999; Rhoads, 1999; Sehgal, 1998). Treatment with rapamycin slightly increased the population of hybridoma cells in the G1-phase of the cell-cycle and significantly enhanced monoclonal antibody production during batch culture (Balcarcel and Stephanopoulos, 2001). Rapamycin also delayed cell death for 48 hours enabling

1 Introduction

viable proliferation to reach higher maximum viable cell densities. The specific monoclonal antibody titre achieved in the hybridoma cell culture was increased by up to 100% during high viability growth (Balcarcel and Stephanopoulos, 2001). The effects of rapamycin are likely to be mediated by its role in inhibiting mTOR, which can influence a wide range of cellular effects (Balcarcel and Stephanopoulos, 2001). Rapamycin has specific and global effects on mRNA translation and protein synthesis and may aid in elucidating the regulation processes involved in cell death, as well as changes during cell-cycle progression, metabolism and specific protein production that occur during the course of fed-batch culture (Balcarcel and Stephanopoulos, 2001).

1.1.4.3 Glycosylation Engineering

The addition of oligosaccharides to proteins and the modification of these structures is a significant metabolic event that separates eukaryotic systems from prokaryotic systems (Fussenegger and Betenbaugh, 2002). These post-translational modifications are of great importance to biotechnological processes as a product's glycosylation pattern affects its biological activity and its effectiveness as a therapeutic agent *in vivo* (Fussenegger and Betenbaugh, 2002; Minch et al., 1997; Robinson et al., 1994). Fussenegger *et al.* recognised that the particular glycosylation pattern for a particular protein depends on the polypeptide sequence, the host cells glycolytic machinery (glycosyltransferases and glycosidases for the addition and removal of sugars), and the environment of the host cells (Fussenegger et al., 1999; Fussenegger and Betenbaugh, 2002). In particular, serum-free cell culture has been shown to influence the glycosylation of murine IgG (Robinson et al., 1994).

Metabolic engineering techniques have been utilised to alter host cell glycosyltransferases involved in processing bottlenecks through augmentation of biosynthetic pathways to generate glycoforms previously unknown in a cell line and the manipulation of the factors that control competition between particular glycoform distributions (Bailey et al., 1998). Efforts have included engineering of the glycosylation pattern on monoclonal antibodies to improve antibody-dependent cellular cytotoxicity (ADCC) reactions, reducing the dosage of antibody required for a therapeutic effect in the patient and reducing health care costs (Fussenegger and Betenbaugh, 2002). Furthermore, Hills *et al.* have reported that changes in the pattern of *N*-glycosylation on MAbs can be achieved by differing feeding/media constituents (specifically of cellular nucleotide sugars or their precursors) in NS0 cells (Hills et al., 2001). This report suggested that genetic

strategies to improve glycosylation of the crystallisable fragment of the immunoglobulin molecule (Fc) region of IgG could improve MAb efficacy (Hills et al., 2001).

1.1.4.4 Current Limitations of Metabolic Engineering

Most of the successes outlined above utilising metabolic engineering have been achieved through the addition of one gene into the host genome. However, this strategy does not access the full potential of engineering cells for a desired phenotype (Fussenegger et al., 1998b; Papoutsakis, 1998). Improved expression systems (plasmid amplification and promoter enhancement) for further increasing the product yield have been shown to result in a high-level of gene transcription, although the levels of secreted proteins are not always correlated to the increased level of mRNA produced (Lambert and Merten, 1997). Furthermore, in the production of MAb by hybridoma cell lines it has been established that the steady-state levels of mRNA coding for the heavy and light chains of Ig do not correlate with the production rate (Lambert and Merten, 1997).

It is believed that one of the major rate-limiting steps in the production of recombinant proteins occurs in the endoplasmic reticulum (ER) and involves the retention of unfolded protein and the transport of nascent polypeptides from the ER to the Golgi complex (Cudna and Dickson, 2003; Downham et al., 1996). However, in batch culture the mRNA levels for the light and heavy chains have been reported to follow the specific growth rate, suggesting the bottleneck in the production of MAb by hybridomas is post-translational (Lambert and Merten, 1997). As a result many investigations into the relationship between the overexpression of various ER resident proteins (involved with protein folding, assembly and post-translational modifications) and MAb production have been initiated in a bid to increase recombinant protein production through alleviating this potential cellular bottleneck. For example Figure 1.6 below shows a schematic model for the role of BiP (glucose regulated protein 78) during the oxidative folding of antibodies. Such an approach has shown some success: for example, Lambert and Merten established a link between cellular levels of protein disulphide isomerase (PDI) and glucose regulated protein 94 (Grp94) and the specific MAb production rate in hybridoma cells cultured in serum-free medium (Lambert and Merten, 1997). However, no correlation between BiP and MAb production was observed (Lambert and Merten, 1997), even though BiP is known to have an intrinsic role in the folding and assembly of antibodies *in vitro* (see Figure 1.6) (Lee et al., 1999; Mayer et al., 2000). In a similar study Downham *et al.* investigated BiP, Grp94 and ERp72 during batch culture of NS0 cells expressing a mouse-

1 Introduction

chimeric MAb (B72.3) (Downham et al., 1996). The expression of the ER resident proteins was observed to increase during batch culture in correlation with MAb production and changes in the culture environment (Downham et al., 1996).

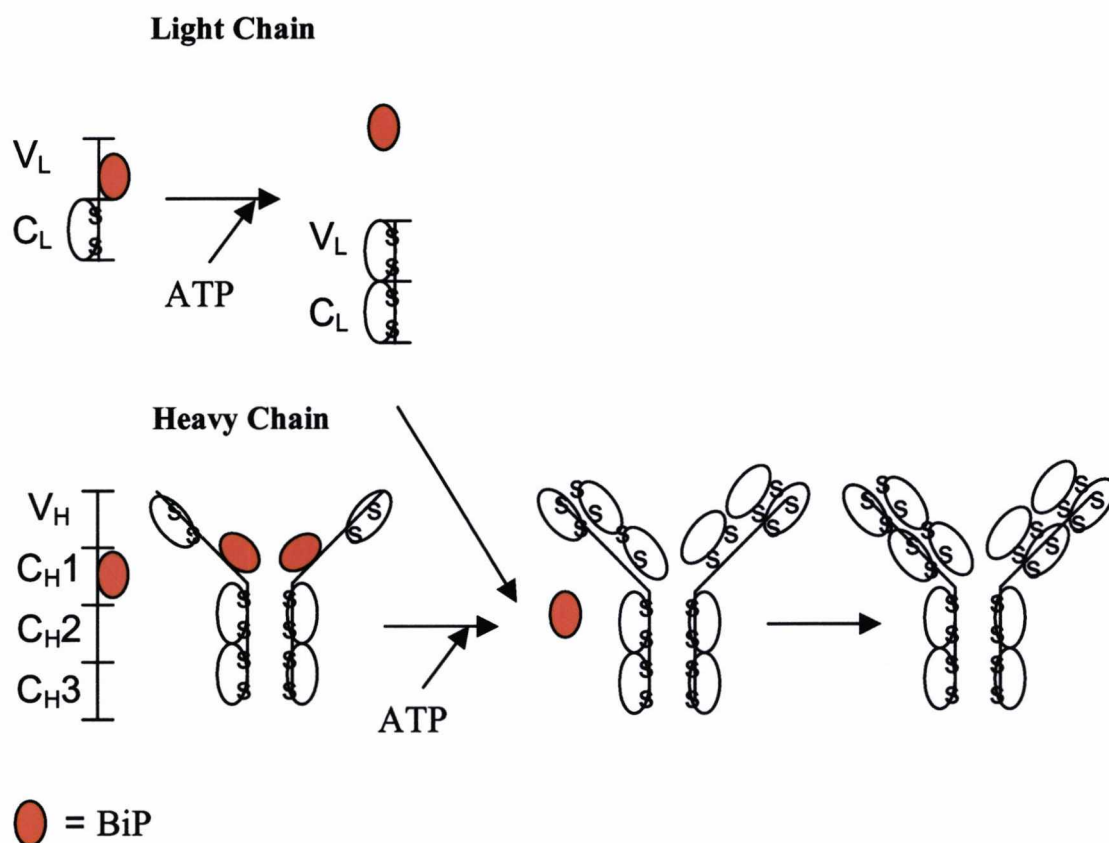


Figure 1.6 A schematic diagram of antibody folding by BiP. Although BiP can associate transiently with other immunoglobulin heavy chain domains, the C_{H1} domain is the main site of BiP binding that is responsible for the retention of heavy chains within the ER. Unlike other heavy chain domains, the C_{H1} domain remains unfolded and unoxidised in the absence of light chains. The synthesis and binding of a folding competent light chain to the heavy chain promotes the release of BiP via an undefined mechanism and allows the C_{H1} domain to fold. The completely folded and assembled immunoglobulin molecule is then transport competent (adapted from Lee *et al*, 1999).

1.1.5 Inverse Metabolic Engineering

The classic method of metabolic engineering described has traditionally been used to identify the rate limiting steps in a pathway to alleviate potential cellular bottlenecks via the over-expression of proteins of interest (Bailey, 1991; Bailey et al., 1996). The metabolic engineering process has been described as the 'improvement of cellular activities by direct manipulation of enzymatic, transport, and regulatory functions of the cell with the use of recombinant DNA technology' (Bailey, 1991). The application of this technology has an important part to play in the field of biotechnology, in the development of new products and new processes as well as improving existing technologies (Bailey et

al., 1996). Metabolic engineering is therefore based on the knowledge of a metabolic system of interest, in which a genetic manipulation can be designed to give an improvement in cellular performance based on the expected outcome (Bailey et al., 1996). This has resulted in much research in this area, but to date has met with limited success and in many cases the metabolic consequence of the genetic change based on this strategy differs substantially from that desired (Bailey, 1991).

This limited success is likely to be due to the extent of our current knowledge of metabolic pathways. In many cases the interplay of individual proteins in different pathways are not known. As a result this often negates this direct approach (Bailey et al., 1996). Firstly, any 'network' that is to be manipulated inevitably involves a subnetwork of a much larger and more complex global metabolic networks, at least at the level of the cell, extending to an interacting multi-cellular population (Bailey et al., 1996). This subnetwork is likely to interact with many different pathways, cofactors and metabolites and furthermore, the specific function of some proteins which mediate critical functions of the cell are often regulated by a complex control system, including phosphorylation/dephosphorylation for activation/inactivation.

The limited success to date of metabolic engineering has prompted the development of a different but complementary strategy, termed inverse metabolic engineering (Figure 1.7) (Bailey et al., 1996). The starting point in an inverse metabolic engineering strategy for an improved industrial organism is the identification of a desired phenotype in the heterologous organism or in a related model system (Bailey et al., 1996). This is then followed by an inverse strategy, whereby the genetic basis for the desired phenotype is determined to design new systems with this phenotype. This genetic basis can then be engineered into the chosen industrial organism or by an environmental manipulation to achieve the desired outcome (Bailey et al., 1996). Several successful attempts at using inverse metabolic engineering strategies have been reported including the engineering of CHO cells to successfully grow in culture without growth factors (basic fibroblast growth factor and insulin) (Bailey et al., 1996; Fussenegger and Betenbaugh, 2002; Renner et al., 1995).

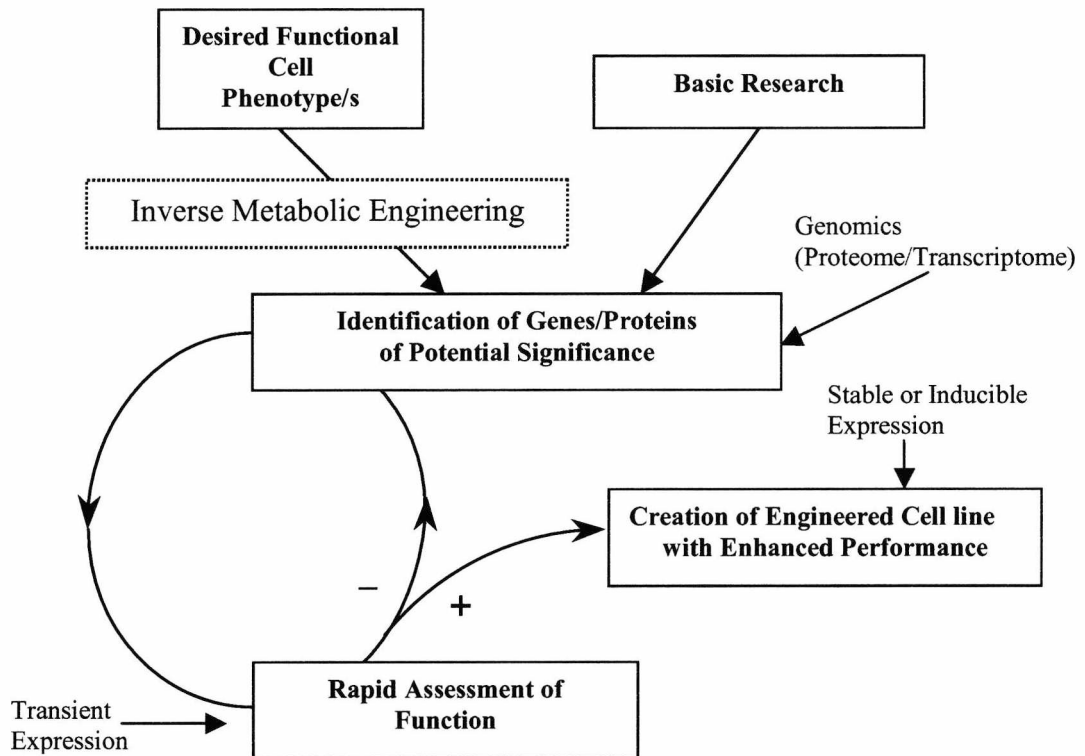


Figure 1.7 An integrated strategy for rational inverse metabolic engineering. The critical step in inverse metabolic engineering is the identification of the genetic basis for a desired phenotypic characteristic. Genetic engineering is utilised in an attempt to transfer that phenotype to the target organism.

Renner and co-workers also utilised inverse metabolic engineering to identify regulators of the cell-cycle to enable cells to grow in protein-free medium (Renner et al., 1995). As part of the experiment, wild type CHOK1 cells were stimulated to proliferate with basic fibroblast growth factor (bFGF) and insulin or both stimulators. They revealed that the wild type CHOK1 cells stimulated with bFGF exhibited the desired phenotype of a long G1 phase and a short S phase, and expressed elevated levels of cyclin E. This prompted the researchers to transfect CHOK1 cells with a vector containing cyclin E, resulting in cells that grew rapidly in protein-free medium without the presence of mitogens (Lee et al., 1996; Renner et al., 1995). The cells were observed to have similar cyclin E levels, distributions of nuclear cell-cycle times and cell morphologies as the bFGF stimulated CHOK1 culture (Renner et al., 1995).

The above experiments were accomplished using proteomics technology, specifically 2-D PAGE, to identify potential targets to implement inverse metabolic engineering strategies. In the following study a proteomic approach was also utilised to understand the changes in the NS0 cell proteome during batch culture. The technology underlying proteomics is discussed in detail below.

1.2 Introduction to Proteomics and the Post-Genome Revolution

1.2.1 Proteome Analysis - Current Technologies

The advent of the genomic era, where DNA sequencing was applied to predict information on gene products (Blackstock and Wier, 1999) has resulted in the generation of extremely large and powerful data sets. However, the majority of predicted proteins have no known function (Blackstock and Wier, 1999), and the behaviour of gene products is proving difficult to predict from the genome alone (Dove, 1999). For example, DNA analysis alone cannot identify when gene products are to be translated by a cell, the concentration of gene products obtained, post-translational modifications such as phosphorylation and glycosylation, and/or their over-expression (Pennington et al., 1997; Zong et al., 1999). Furthermore, the number of mRNA copies per cell often does not necessarily reflect the number of functional protein molecules (Celis, 1998a). Therefore, an emerging area of research incorporating the protein products of an organism's genome, 'proteomics', has emerged which investigates systems at the protein level and is an alternative to mRNA microarray analysis (Unlu, 1999).

The term proteome (the 'PROTEins expressed by an organisms genOME') was originally coined at the Sienna 2-D-electrophoresis meeting in 1994 and was subsequently adopted in the literature in July 1995 to describe the total protein complement of an organism's genome (Wasinger et al., 1995). The term is now utilised to describe the study of protein properties, the expression level, post-translational modifications and interactions to obtain a global integrated view of cellular processes, networks and disease processes, at the protein level in a given genome, cell or tissue type (Blackstock and Wier, 1999). The most commonly utilised technology for proteome analysis involves two-dimensional sodium dodecyl sulphate polyacrylamide gel electrophoresis (2-D SDS-PAGE) and has remained largely unchanged since its first implementation in 1975 by O'Farrell (Figure 1.8). The technology involves the separation of proteins by two different physical parameters, isoelectric point (through isoelectric focussing) and apparent molecular mass (by SDS-PAGE). There has recently been a marked increase in interest in proteomics as a result of improvements in the core technologies involved particularly those post-2-D such as mass spectrometry which allow the identification of proteins from very small amounts (≤ 1 ng). Other advances include the introduction of immobilised pH gradient (IPG) strips for the first dimension separation and the second dimension SDS-PAGE gel tanks which

can run up to 12 gels simultaneously which have greatly improved 2-D PAGE reproducibility.

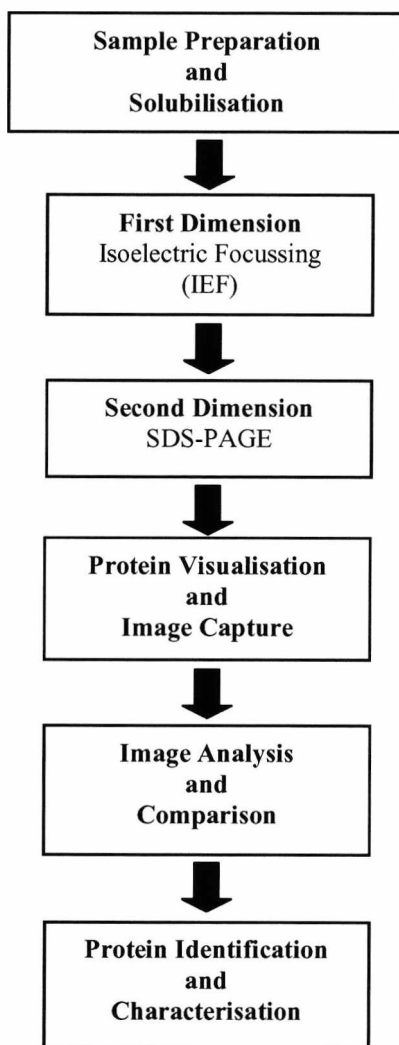


Figure 1.8 The various elements of 2-D PAGE proteome technology.

Advances in image analysis software and improved sensitivity of mass spectrometers together with more complete sequence databases for the identification of proteins have been the main contributors to the increased interest in proteomic studies (Patton, 1999). These technical improvements have enabled proteomic technology to become more reproducible and accurate and have enabled greater loading capacities for improved visualisation of low abundance proteins (Humphery-Smith and Blackstock, 1997a; Wilkins et al., 1996). Two-dimensional electrophoresis is currently the only system capable of simultaneously separating thousands of proteins within a sample resulting in a two-dimensional array, with each protein spot (at least in theory) representing one protein (although it is possible for more than one protein to co-localise in one spot) (Gorg, 2000a).

Proteome technology complements genome sequencing by determining whether predicted gene products are translated (Patton, 1999) and actively required by the sample under investigation at any given moment in time. That is to say, proteomics investigates genes which are actively required to carry out life processes within cells or tissues under varying physiological conditions (Fields et al., 1999; Urquhart et al., 1998). Although it is unlikely that an entire protein complement of an animal cells genome will be expressed at the same time, proteomics enables a real time 'snap shot' to be taken of a cell and its global protein expression pattern and distribution at that moment in time. This allows the analysis of responses to environmental stresses and disease to be investigated (Patton, 1999).

Unlike the genome of an organism, the proteome is not a static feature (Williams, 1999). The proteome changes with development and the variations in environmental conditions in which the organism finds itself (Humphery-Smith and Blackstock, 1997a). Proteomic technology endeavours to complement existing molecular biology techniques including DNA microarrays, expressed sequence tags (ESTs) and serial analysis of gene expression (SAGE) in addressing complex biological problems (Forster et al., 2002; Patton, 1999). New techniques including isotope-coded affinity tagging (ICAT), difference gel electrophoresis (DIGE), multiplexed proteomics (MP) and protein micro- and macro-arrays (Lopez and Pluskal, 2003) are also currently being pursued, which should greatly enhance the applicability of 2-D PAGE with respect to addressing fundamental questions related to global changes in protein expression and post-translational modifications (Patton, 2002).

A major problem facing 2-D PAGE has been the difficulty in obtaining reproducible results in the form of 2-D gel patterns (Dunn, 1997), although this has been improved with the implementation of IPG strips for the first dimension and pre-cast gels for the second dimension separation (Corbett et al., 1994). However, differences in electrophoretic conditions also cause variability, highlighting the importance of equipment that allows up to twelve gels to be run simultaneously in both the first and second dimension separations. Other limitations associated with current 2-D technology include the visualisation of low abundance proteins together with those that are highly basic (beyond pH 10) (Celis et al., 1998b). Two-dimensional electrophoresis technology is also not capable of resolving high molecular weight proteins (above 150 kDa) and hydrophobic membrane proteins (Celis et al., 1998b). However, other technologies currently available

1 Introduction

are incapable of simultaneously separating complex protein mixtures, therefore 2-D PAGE remains the method of choice for proteome analysis.

1.2.1.1 Sample Preparation and Extraction

In proteomic investigations the sample preparation solution used to extract protein samples is critical. No methods are currently available to amplify the proteins present within a sample, unlike those which exist for DNA analysis in the form of the polymerase chain reaction (PCR) (Blackstock and Wier, 1999; James, 1997a; Lopez and Pluskal, 2003). As a result, sample handling and sensitivity are critical issues which have not been totally overcome. The lysis buffer should result in a fully reduced and solubilised solution all of the proteins within a given sample without altering the charge of the proteins as well as being compatible with the techniques used in protein analysis in order to obtain an accurate representation of the protein population (Haynes et al., 1998; Quadroni and James, 1999). This involves the utilisation of reagents without charge, and traditional solubilising solutions include the reducing agent dithiothreitol (DTT) and the neutral chaotrope urea in varying quantities. The addition of zwitterionic detergents such as CHAPS have also been utilised to ensure complete solubilisation of the samples, preventing protein aggregation through hydrophobic interactions (Patton, 1999). Carrier ampholytes or IPG buffers are an important addition to the solubilising buffer, acting to enhance protein solubility through minimising protein aggregation due to charge-charge interactions. It is important to realise the main goal of the analysis, whether to have complete representation of the sample or whether to have a clear and reproducible 'map'. Additional sample preparation steps can improve the final 2-D result, although, for each additional step, selective protein losses may occur and therefore there is a clear trade-off between improved sample quality and complete protein representation (Quadroni and James, 1999).

By optimising the first stage of proteome analysis to solubilise all proteins within a sample, whilst keeping the solution simple, potentially as much of the proteome as possible under investigation can be accurately and reproducibly visualised within the constraints of the technology currently available. However, the range over which the proteome is visualised can also be optimised to allow the whole proteome to be visualised over wide range pIs or zoomed in on using narrow pI range IPG strips (Zuo et al., 2001). With the utilisation of narrow pI range IPG strips the first dimension can be spread out and a series of gels can be used to create a set of overlapping gels (Hoving et al., 2000) which can be used to form a composite gel image. This procedure reduces the overcrowding of proteins

1 Introduction

on one gel, and can potentially enable the resolution of more proteins including those of lower abundance which are often masked on wide range gels, and reduce the co-migration of proteins (Lilley et al., 2001; Zuo et al., 2001).

1.2.1.2 Two-Dimensional Gel Electrophoresis

The technique of 2-D PAGE was developed independently in two laboratories by O'Farrell and Klose (Klose, 1975; O'Farrell, 1975). The two laboratories showed that proteins could be separated on two separate physical parameters: their isoelectric point (pI) using isoelectric focussing and also by their molecular weight (M_r) by SDS-PAGE (Celis, 1998a; James, 1997b). The basic technology has remained unchanged since this time with the first dimensional separation (isoelectric focussing) based on differences in the charge of individual proteins and the second dimension is based on the molecular mass of the polypeptide molecules (Lefkovits, 2003). The technology of 2-D PAGE remains unequalled in its ability to simultaneously separate complex mixtures of proteins and to follow the multigenic phenomena at the level of the whole cell or tissue (Humphrey-Smith et al., 1997b). The resolution of protein spots visualised on 2-D gels is increased by the size of gel implemented for the first and second dimension separations (for example it has been reported that up to 10000 protein spots may be visualised on a 20 x 20 cm gel (Klose and Kobalz, 1995)). The technique can also be used to identify proteins that have been post-translationally modified (Blackstock and Wier, 1999; Humphrey-Smith and Blackstock, 1997a; James, 1997b; Kovarova et al., 2003).

1.2.1.3 First Dimension: Isoelectric Focussing

Isoelectric focussing (IEF) is an electrophoretic method that separates proteins on the basis of charge (Lefkovits, 2003). Proteins are amphoteric molecules carrying positive, negative or zero charge depending on the pH of their surroundings, and the pI is the specific pH where the net charge of a protein is zero (Humphrey-Smith et al., 1997b; Lefkovits, 2003). For IEF the presence of a pH gradient is critical as in an electric field proteins will migrate to a position where their net charge is zero. If a protein diverts from its pI in an electric field the proteins will immediately gain charge and migrate back to the 'correct position' (this is termed the 'focussing effect'), which enables proteins to be separated effectively based on the smallest of charge differences (Humphrey-Smith et al., 1997b).

The use of immobilised pH gradients (IPG strips) has replaced the use of carrier ampholytes and has greatly improved the reproducibility of 2-D gels. The ampholytes are

applied in concentrations of less than 1% to computer standardised pre-dried IPG strips and therefore enhanced focussing of proteins occurs as a result of the buffering effect of the ampholytes (Humphrey-Smith et al., 1997b). In this form of electrophoresis the carrier ampholytes are added to the sample mixture covalently bound to the polyacrylamide matrix. This aids protein entry into the gel matrix through increasing conductivity within the immobiline system, improving the reproducibility of the system and enables between laboratory comparisons of results (Humphrey-Smith et al., 1997b; Lefkovits, 2003; Wilkins et al., 1996). Non-linear, wide range IPG strips can also be used to produce a sigmoidal pH gradient which spreads out the acidic region of the gel, increasing spot definition in areas where protein spots are more focussed across the central zone (Bjellqvist et al., 1993).

1.2.1.4 Second Dimension: SDS-PAGE

Reducing SDS-PAGE is the most common method used to separate proteins from complex mixtures (Davidsson et al., 1999; Klose, 1999). The method is based upon the well-characterised Laemmli system (Laemmli, 1970). The most common procedures utilise acrylamide gradient gels consisting of 10–20%, or alternatively slab gels of between 10–15% acrylamide (Lefkovits, 2003). The resulting gels provide a graphical representation of the proteome, where a spot or a series of spots represents each protein. These can then be described in terms of pI, molecular weight and an intensity related value (Binz et al., 1999).

1.2.1.5 Protein Visualisation

The staining methodology (visualisation of proteins) utilised in 2-D gels is improving as proteome technology develops and the sensitivity is constantly being improved to enable greater visualisation and quantification of protein spots. Current methods of staining have to balance the limits of detection with those of the mass spectrometric methods used to identify proteins (Lauber et al., 2001). The most common protein stains currently used in laboratories which are compatible with mass spectrometry include Coomassie Blue, colloidal Coomassie and various silver staining methodologies. Fluorescent stains including the SYPRO stains (Orange, Red and Ruby) are also sensitive and compatible with mass spectrometry (Lauber et al., 2001; Malone et al., 2001), but specialised equipment is required to detect these stains and the method is relatively expensive (Patton, 2002).

1 Introduction

Coomassie Blue stain can visualise greater than 500 protein spots on a gel at the sub-picomole range and is an endpoint stain (Champion et al., 1999; Patton, 2002). Colloidal Coomassie stain is an alternative to Coomassie Blue and has the advantage of not requiring excessive destaining (Lefkovits, 2003). The stain provides a linear response over a 10-30-fold range (which is the same as for Coomassie Blue), although the stain does not penetrate the gel matrix resulting in preferential staining of proteins (Patton, 2002). However, many proteins on a 2-D gel may be present at attomole levels, far below the limits of detection of Coomassie Blue (Heukeshoven and Dernick, 1988). Silver staining methods, adapted to be compatible with mass spectrometry by the omission of glutaraldehyde (Lauber et al., 2001), are approximately 100 times more sensitive than Coomassie staining (Shevchenko et al., 1996) and can extend the detection limit below the sub-picomole range to femtomole levels (Champion et al., 1999). This method of protein visualisation has the potential of visualising more than 10000 protein spots on an individual gel (Klose and Kobalz, 1995). There are problems associated with silver staining including the negative staining of highly abundant proteins. The stain can also be negatively selective for protein post-translational modifications, particularly glycosylated proteins (Lauber et al., 2001; Malone et al., 2001). This is problematic as many proteins are post-translationally modified, particularly by glycosylation and phosphorylation (Kovarova et al., 2003). Finally, silver stain has a very limited linear dynamic range which reduces its use for comparable expression analysis.

Staining methods have now been developed which have further increased the limit of detection to sub-attomole sensitivity (Berggren et al., 2000; Patton, 2002). The fluorescent staining methods rival silver and Coomassie stains (Coomassie Blue and colloidal Coomassie) and compared with traditional fluorescent stains are compatible with mass spectrometry (Patton, 2002). The SYPRO stains (Orange, Red and Ruby) may be utilised to accurately and rapidly detect nanomolar quantities of sample (Berggren et al., 2000; Lauber et al., 2001), can identify protein subcellular redistribution events (Patton, 1999) and have a relatively large linear dynamic range. The SYPRO stains bind non-covalently and bind to the SDS surrounding the proteins; therefore staining is not selective for particular polypeptides (Steinberg et al., 1996). The stains have a similar sensitivity to silver (1-2 ng). Staining with fluorescent dyes is also much less labour intensive and is completed in a one step procedure, which takes approximately 30 to 60 minutes to complete with no de-staining procedure required (Patton, 1999; Steinberg et al., 1996). In

1 Introduction

some instances the analysis of gels containing mammalian cells using these stains has proven easier than those stained with silver (Steinberg et al., 1996).

Alternative methods for the detection of low abundance proteins or low-level expressed proteins include the pre-fractionation of cells into subcellular organelles (Lopez, 2000). Microsomal (Galeva and Altermann, 2002), mitochondrial (Hanson et al., 2001; Taylor et al., 2003) and membrane proteins (Molloy, 2000) have been successfully fractionated and assessed by 2-D PAGE. Other alternative methods for the detection of proteins on 2-D gels include the use of autoradiography through incorporating ^3H , ^{14}C , ^{35}S , ^{32}P , ^{33}P or ^{125}I into proteins (Patton, 2002), although the most common labelling procedures involve the incorporation of [^{35}S] methionine into nascently synthesised polypeptides (Lefkovits, 2003). These technologies have a wider dynamic range and provide better detection sensitivity (Patton, 2002). Radiolabelling experiments have been widely utilised for *in vivo* metabolic experiments and coupled with the use of organic dye or silver staining methods can be used to simultaneously assess total protein expression levels and total protein synthesis rates (Patton, 2002; Westbrook et al., 2001).

1.2.1.6 Protein Identification and Characterisation

Once an alteration in the pattern of protein expression has been identified the protein itself must be identified in order to interrogate the significance of the change. Figure 1.9 below shows the strategies that may be utilised for the identification of proteins after 2-D PAGE. Sensitive, accurate and rapid methods are required to analyse the proteins expressed by a genome (Hochstrasser, 1998). Many techniques may be utilised to aid in the identification of protein spots, which may be directly excised from a gel, or taken from a nitrocellulose or polyvinylidene fluoride (PVDF) membrane blot to enable a more durable copy of the gel to be obtained (Dunn, 1997; Kemper et al., 2001; Lui et al., 1996; Michalski and Shiell, 1999). However, the current method of choice, which has developed greatly in both speed and sensitivity through the advent of 'soft' ionisation techniques, is mass spectrometry (ms). The two predominant forms of ionisation currently in use for proteomic analyses include matrix desorption ionisation (MALDI) ms and electrospray ionisation (ESI) ms (Lauber et al., 2001). The technique most often utilised for protein identification from proteins separated by 2-D PAGE is MALDI-ms and peptide mass fingerprinting (PMF) (Binz et al., 1999; Gevaert and Vandekerckhove, 2000). Using a PMF approach proteins and peptides are digested either chemically or enzymatically to produce unique degradation 'fingerprints' which can then be analysed by mass spectrometry (Binz et al.,

1 Introduction

1999). However, if the proteins prove difficult to identify electrospray may be implemented. The level of sensitivity for peptide detection by MALDI-ToF is in the femtomolar range, whilst ES-ms based on triple quadrupole, ion trap and Fourier transform approaches have extended the sensitivity to the attomole range (Godovac-Zimmermann et al., 1999; James, 1997a).

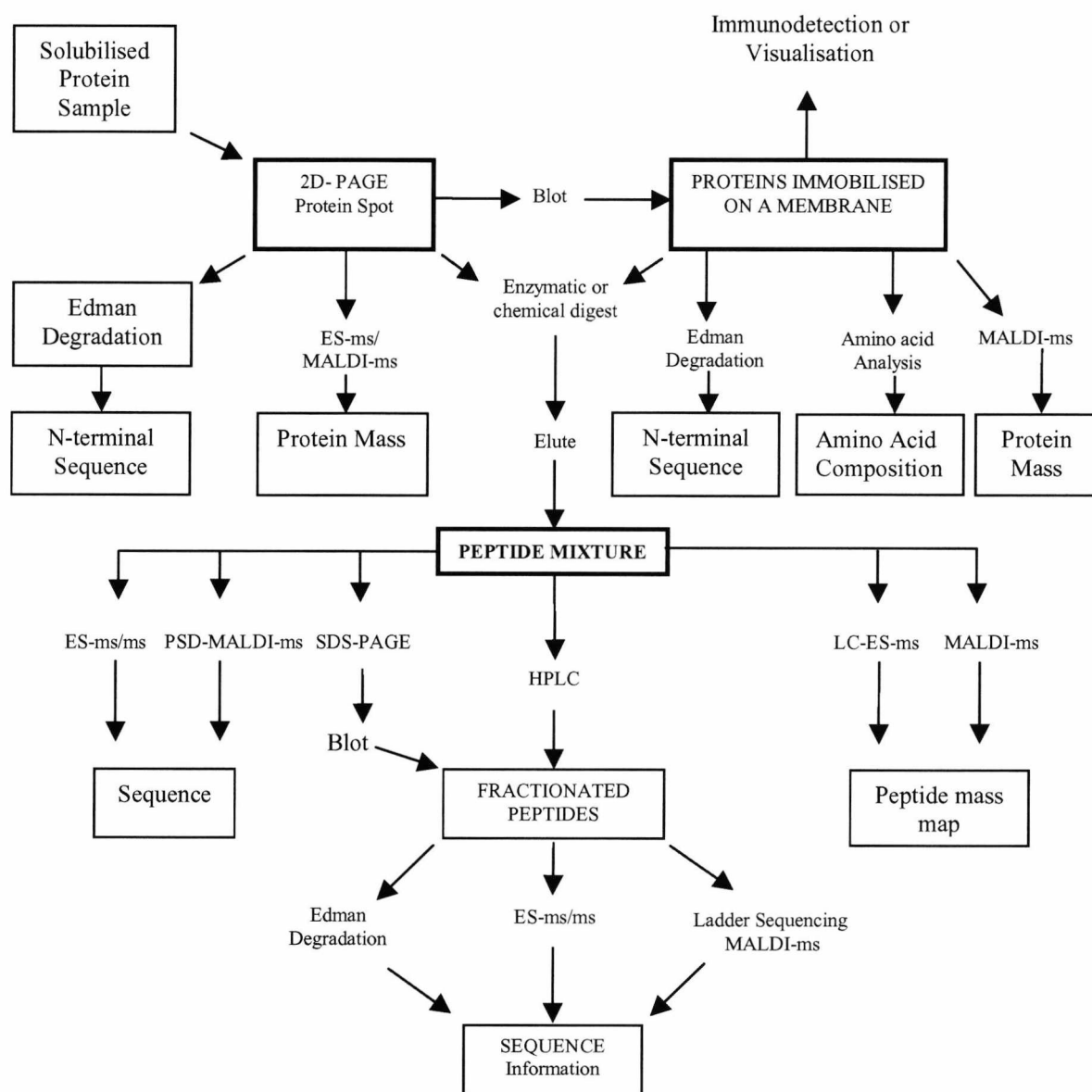


Figure 1.9 Strategies for protein identification from proteins separated by 2-D PAGE (reproduced from Michalski and Shiehl, 1999).

While PMF has become the method of choice for high throughput protein identification, where necessary peptide sequence tags may be generated to aid in protein identification by fragmentation of selected peptides in an ES-ms-ion trap. Peptide sequence tags are short stretches of amino acid sequence data (consisting of 3-10 amino

acids) which can be generated by tandem mass spectrometry techniques. Sequence tags can be used in tandem with the information derived from PMF for identification. For characterising post-translational modifications tandem mass spectrometry is the method of choice (Blackstock and Wier, 1999; Mann and Jensen, 2003). Sequence tags also result in less ambiguous protein identifications than PMF and is fast becoming the 'new' method of choice for protein identification.

Sophisticated bioinformatics plays a key role in the characterisation of data generated by PMF and peptide sequence tags (Soskic et al., 1999) and a variety of databases are available for routine protein identification. Searches can be based on sequence tags or intact protein mass, and interrogation of protein and EST web-based bioinformatic databases including ExPASy (which includes the SWISS-PROT 2-D PAGE database) and Mascot can be used with high specificity (Hoogland et al., 1999; Perkins et al., 1999; Quadroni and James, 1999).

1.3 Complementary Technologies to 2-D PAGE

Other technologies have been developed to complement 2-D PAGE for the comparison of different protein profiles (Patton, 2002). The main aim of proteomics is to increase the information content through multiplexed analysis. Difference gel electrophoresis (DIGE), isotope-coded affinity tags (ICAT), multiplexed proteomics (MP) and protein micro-arrays provide ideal methods for the accurate quantification of low copy number proteins which play key regulatory roles in cells or tissues (Lopez and Pluskal, 2003; Patton, 2002). DIGE was developed to overcome the inherent reproducibility problems associated with 2-D PAGE as the technology relies on the comparison of images of at least two samples (Tonge et al., 2001; Unlu, 1999). The process involves the utilisation of succinimidyl esters of cyanine dyes, Cy2, Cy3 and Cy5 to fluorescently label as many as three different complex proteins populations prior to mixing them together and running on one 2-D gel simultaneously (Patton, 2002; Unlu, 1999). Images of the 2-D gels are then acquired using up to three different excitation/emission filters. The ratio of the differently coloured fluorescent signals is then used to find the differences in protein expression between samples (Patton, 2002). The most important aspect of DIGE is that the technique enables two or three individual samples to be separated under identical electrophoretic conditions, which greatly simplifies the down stream image analysis, particularly the matching of gel images (Unlu, 1999). However, one drawback of the technology is that the labelling

1 Introduction

process is only capable of detecting about half as many proteins visualised by conventional silver staining (Tonge et al., 2001), missing low abundance proteins.

The multiplexed proteomics (MP) platform was designed to enable the determination of protein expression levels as well as certain functional attributes of proteins, such as the post-translational modifications and drug binding or metabolising capabilities (Patton, 2002). MP technology involves the utilisation of the same fluorophore to measure proteins across all gels in a database, and employs other fluorophores with different excitation/emission characteristics to allow the specific functional attributes of individual proteins to be investigated. MP has many advantages over DIGE in that the bandwidth is much broader enabling more information to be obtained and many more gels can be assessed than possible with DIGE (Patton, 2002).

Isotope-coded affinity tag (ICAT) peptide labelling is utilised to quantitatively assess two populations of proteins using isotope ratios (Goshe and Smith, 2003; Tao and Aebersold, 2003). The isotope tags used in ICAT are reagents consisting of a protein reactive group, an ethylene glycol linker region and a biotin tag (Patton, 2002). Current ICAT reagents are specific for cysteine residues in proteins and peptides. Two types of isotope tags are produced using linkers that contain either eight hydrogen atoms (d0, light reagent) or eight deuterium atoms (d8, heavy reagent) (Goshe and Smith, 2003; Han et al., 2001). Two samples are derivatised with either the light or heavy reagents, and are then mixed together and proteolytically digested with trypsin or Lys-C to generate fragments (Patton, 2002; Tao and Aebersold, 2003). The sample is then fractionated by avidin affinity chromatography so that only cysteine-containing peptides are retrieved (Han et al., 2001). The peptides may be further separated by microcapillary reverse-phase chromatography, followed by tandem mass spectrometry (Goshe and Smith, 2003; Tao and Aebersold, 2003). The ratios of the isotopic molecular mass peaks differ by 8 Da and can provide a measure of the relative amounts of each protein from the original samples. Nanoscale liquid chromatography-electrospray ionisation mass spectrometry (LC-ES-ms) is utilised to perform quantitative assessments of peptides based on the relative abundance of the heavy and light peptides, whilst qualitative information based on peptide molecular mass and amino acid sequence information is derived from nanoscale liquid chromatography combined with electrospray ionisation tandem mass spectrometry (LC-ES-ms-ms) (Mo and Karger, 2002; Patton, 2002). It is also possible to combine ICAT technology with 2-D PAGE to enable a single differential display to be achieved, similar to

the DIGE methodology, although the combined technology has some significant improvements upon the DIGE technology (Patton, 2002).

Early applications of microarray technology centred on DNA, although microarrays have now found an application in proteomics as a protein based screening tool (Lopez and Pluskal, 2003). Antibody arrays and phage display technologies have formed the starting point for proteomic microarray technology for the creation of protein chips (Lopez and Pluskal, 2003; Scrivener et al., 2003; Wingren et al., 2003). Variations of protein chips have now been developed and include affinity ms capture (surface-enhanced laser-desorption/ionisation (SELDI)), which consists of a MALDI target plate surface that has been modified with affinity ligands to capture proteins of interest. The target plate can be used to directly identify the proteins (Gygi and Aebersold, 2000). Other methods include the use of chips that utilise surface plasmon resonance to quantify the target captured (Lopez and Pluskal, 2003).

Protein/peptide arrays have been created through the application of proteins directly onto chips to enable protein-protein interactions to be investigated (Lopez, 2000; Lopez and Pluskal, 2003). The use of protein chips enables high throughput screening studies to be carried out on a large scale (Lopez, 2000). For example, researchers at the Max Planck Institute created a library of 15000 non-redundant His-tagged proteins from a human brain cDNA library. Fusion proteins were arrayed on a glass surface and probed with antibodies. Researchers have also used the technology to identify post-translational modifications (glycosylation) of proteins in microarrays (Lopez and Pluskal, 2003; Scrivener et al., 2003). Protein/protein interactions have also been investigated using a system termed the yeast two-hybrid, which involves the use of yeast 'bait' proteins fused to transcription activation DNA domains which can be probed with 'prey' (other yeast) proteins fused to DNA binding domains (Lopez and Pluskal, 2003).

1.4 Aims of this Study

This study utilises a proteomic based approach to investigate murine myeloma NS0 cells and the specific cellular constraints on NS0 cells during batch culture which limit the production of recombinant proteins. The cell lines utilised in this study have been engineered to produce recombinant antibodies and are of a type routinely utilised in industry. These include a GS-NS0 cell engineered to produce an IgG₁ raised against CD38⁺, which was used to investigate changes in the NS0 cell proteome throughout batch culture to answer the following questions; (1) for cell lines selected for high-level

1 Introduction

recombinant protein production are specific cellular processes up- or down-regulated during the course of batch culture?, (2) when do NS0 cells in culture perceive stress? and (3) how do the observed changes during batch culture relate to the specific productivity and viability of the cell line *in vitro*?

Following the above investigation, a series of GS-NS0 cell transfectants derived from the same NS0 parental host cell line engineered to produce an antibody (IgG₄, expressing B72.3) were utilised to assess the differences in GS-NS0 cell line protein expression at mid-exponential phase during controlled batch culture. The specific similarities and differences in global protein expression between a 'mock' GS-NS0 cell transfectant and a series of GS-NS0 cell lines differing in their range of productivities were assessed to answer the following question: Are there specific alterations in functional gene expression which enable mammalian cells to maintain high-level recombinant protein production? The overall aim of this study was to further our understanding of cell functioning during culture to ultimately derive a rational 'knowledge based' strategy for the identification of protein targets for cell engineering for desired functional phenotypes.

Chapter 2 Materials and Methods

2.1 Chemicals

All chemicals and reagents used were Sigma analytical or cell culture grade (Sigma Aldrich Ltd., Poole, Dorset, U.K.), except where indicated.

2.2 Cell Culture

2.2.1 NS0 Cell Line

The glutamine synthetase, (GS) selection system (Bebbington et al., 1992; Brown et al., 1992) is an important expression system utilised in industrial processes for the high-level expression of recombinant therapeutic proteins. Murine myeloma NS0 cells are a non-secreting cell line that was derived from tumour cells of the spleen of BALB/c mice in the 1960s (Barnes et al., 2000). This expression system has been widely utilised in industry, particularly in the production of recombinant therapeutic antibodies from NS0 cells (Zhou et al., 1997) including two human therapeutic antibody products Zenapax[®] and Synagis that have recently reached the marketplace (Barnes et al., 2001; Cudna and Dickson, 2003). Glutamine synthetase catalyses the formation of glutamine from glutamate and ammonia; NS0 cells are GS deficient (Barnes et al., 2001; Brown et al., 1992); therefore when the glutamine synthetase selection/amplification system is utilised together with the gene/s of interest for recombinant therapeutic protein production, only the product of interest will be synthesised and secreted (Brown et al., 1992). Therefore, when used in combination with NS0 cells, the GS system allows the simple identification of successfully transfected cell lines by the exclusion of glutamine from the growth medium. Under such conditions NS0 cells lacking the GS system have no energy source and die. The advantages of this system are the much faster development times and also the fact that fewer copies of the recombinant gene per cell are required than in other systems (Brown et al., 1992).

2.2.2 NS0 Cell Culture

Both the NS0 cell lines utilised in this project have been engineered with the glutamine synthetase (GS) gene, which permits them to grow in glutamine free culture medium.

2.2.2.1 Growth Conditions for GS-NS0 Cells Secreting anti-CD38 Antibody

NS0 cells secreting a humanised recombinant therapeutic IgG₁ (anti-CD38⁺) were donated by GlaxoSmithKline (GSK., Beckenham, Kent, U.K.). Cells were routinely maintained in glutamine and serum-free Iscove's Modified Eagle's Medium (IMDM) (Sigma., Poole, U.K.), containing the following supplements; L-glutamic acid (60 µg mL⁻¹), L-asparagine (60 µg mL⁻¹), adenosine, guanosine, cytidine and uridine (7 µg mL⁻¹), and thymidine (2.4 µg mL⁻¹); 0.01% (w/v) cyclodextrin (Sigma), 0.001% chemically defined lipid concentrate (Gibco BRL., Paisley, U.K.), 0.01% Insulin-transferrin-selenium-X supplement (Gibco), and bovine serum albumin (BSA) fraction V (5 mg mL⁻¹) (Bayer Corp., Kankakee, IL, U.S.A.). Alternatively, NS0 cells were cultured in IMDM supplemented with 10% serum (PAA Laboratories Ltd., Kingston Upon Thames, U.K.), amino acids and nucleosides as outlined above. For proteomic analysis cells were grown in 100 mL shake flasks, 1 L spinner vessels and 3 L bioreactors to a working volume of 1.5 L.

2.2.2.2 Growth Conditions for GS-NS0 Cells Secreting B72.3

NS0 cells were transfected with the glutamine synthetase (GS) system carrying the heavy and light chain genes for human-mouse chimeric B72.3 IgG₄ antibody by LONZA Biologics plc (Slough; U.K.) specifically for this project (see chapters 5 and 6). Details of this procedure are outlined in section 2.2.3. Cells were then maintained in high glucose Dulbecco's Modified Eagle's Medium (DMEM)-F12 Nutrient mix (Gibco), supplemented with 10% (v/v) dialysed foetal calf serum (PAA Laboratories Ltd., Kingston Upon Thames, U.K.), non-essential amino acids (Gibco) (10 mL L⁻¹), L-glutamic acid and L-asparagine amino acids (60 µg mL⁻¹), adenosine, guanosine, cytidine and uridine (7 µg mL⁻¹) and thymidine (2.4 µg mL⁻¹) (Sigma).

2.2.3 Transfection Procedure

Specifically for this study LONZA Biologics plc (Slough, U.K.) generated GS-NS0 cell transfectants producing varying amounts of IgG₄ after undergoing the following transfection procedure. Parental NS0 cells were transfected with a glutamine synthetase (GS) expression vector containing the B72.3 heavy and light chain genes by electroporation using a Gene Pulser II (Bio-Rad., Herts, U.K.) in protein-free medium. Primary transfectants were identified by transferring the cells into medium containing 10% (v/v) dFCS and 2mM glutamine before limiting dilution in 96-well microtiter plates. After 24 h the B72.3 and GS genes were co-amplified by inclusion of 10 mM methionine

sulphoximine (MSX) supplement and the exclusion of glutamine from the culture medium. The plates were then left before screening for colonies. From this point, cultures were no longer cultivated in medium containing glutamine or MSX. Once the cells had recovered from the transfection and screening process, colonies were transferred to 24 well plates and routinely cultured in DMEM-F12 medium containing 10% (v/v) dFCS (PAA) without supplements of glutamine or MSX in Erlenmeyer flasks (Corning).

2.2.4 Determination of Viable NS0 Cells

Viable cell density of NS0 cells during culture was determined by the trypan blue dye exclusion method. Cell culture broth (50 μ L) was added to 50 μ L of trypan blue dye (Sigma), and following mixing the cells were counted using an improved Neubauer haemocytometer with an inverted microscope. Viable cells (pink in colour) were counted within five marked squares of the counting chamber and the average cell number calculated. Cell viability was determined by dye exclusion, the dead cells staining blue through taking up the dye. The number of live and dead cells in 1 mL of culture medium was then calculated from the average count for one of the marked squares (which represents 10^{-4} mL) multiplied by the dilution factor $\times 10^4$.

2.2.5 Creation of Master and Working Cell Banks

Master cell banks were produced from a single vial of GS-NS0 cells engineered to produce the recombinant IgG₄, B72.3 as described in section 2.2.3. The vial was rapidly thawed into a medium flat flask containing 20 mL of 10% (v/v) serum containing DMEM-F12 medium. Cells were routinely passaged at a cell concentration of at least 1×10^6 cells mL⁻¹ and split to a concentration of 2.5×10^5 cells mL⁻¹ until they were successfully cultured to a 100 mL volume in Erlenmeyer flasks (Corning Incorporated., Corning, New York, U.S.A.), and had reached at least 90% viability. For cryopreservation cells were frozen at a density of 2×10^7 cells mL⁻¹ by pelleting 2×10^8 cells mL⁻¹ at $50 \times g$ for 5 minutes and then re-suspending the cell pellet in 10 mL of freezing mixture containing growth medium supplemented with 10% (v/v) dimethyl sulphoxide (DMSO) (Sigma). Aliquots of 1 mL were added to 1.5 mL cryovials (NUNC™ Brand Products., Nalge Nunc International, Denmark) and stored at -20°C for 4 hours before being transferred to -80°C for 12 hours and finally into a liquid nitrogen phase cryostat (-196°C) for long term storage as the master cell bank. The same protocol was followed to form a working cell bank. Cells

were grown and frozen at the same density as stated above. To form stocks of cells for the weaning process (see section 2.2.7), one vial of cells from the working cell bank was utilised, and after reaching a culture volume of 100 mL, the cells in DMEM medium were sequentially weaned into GSK generic medium containing 1% serum. After two passages in each new serum concentration, 10 vials of cells were frozen at a density of 2×10^7 cell mL⁻¹ in order to form new master cell banks of 5% (v/v) and 1% (v/v) serum containing stocks.

2.2.6 Resuscitation of Frozen Cell Lines

Cryovials were thawed quickly to prevent formation of ice crystals in the freezing medium by gentle agitation in a water bath heated to 37°C. The cells were then slowly transferred into a 50 mL tube and the cells re-suspended in 25 mL of pre-warmed medium to dilute and minimise the toxic effects of DMSO. The tube was then spun down to re-pellet the cells at 50 x g for 5 minutes. The supernatant was then poured off and the cell pellet re-suspended in 1 mL of fresh medium and transferred to a 25 cm² flat culture flask containing 10 mL of pre-warmed medium (if 1×10^6 cells were frozen) or into a 75 cm² flat flask containing 20 mL of pre-warmed medium (if 2×10^7 cells were frozen). The flasks were then placed into a 5% CO₂ incubator at 37°C and left until 100% viable. Once the cells were actively growing and dividing they were transferred into a 125 mL Erlenmeyer flask in a 10 mL volume or into a 250 mL Erlenmeyer flask (Corning) in a 50 mL volume and gassed (with 5% CO₂ in air), then left until they reached mid-exponential phase of growth after which time cells were treated as stated in section 2.2.2 and 2.2.5.

2.2.7 Adaptation of NS0 Cells Expressing B72.3 Antibody to 1% Serum in Characterised Protein-Free Medium

In industry, mammalian cells are required to be routinely cultured in media containing no animal derived products due to the risks of viral and prion contamination such as BSE. Media containing no animal products not only simplify downstream purification of the recombinant protein, but also reduces batch-to-batch variations of nutrients which is inevitable with serum. The utilisation of serum free medium also has the advantage of being prepared to standard formulations and protein-free media can be totally chemically defined. GS-NS0 cell clones provided by LONZA Biologics plc were sequentially weaned from DMEM-F12 medium (Gibco) containing 10% (v/v) dFCS into GSK, R87 protein-free

medium supplemented with 1 mL L⁻¹ L-26 lipid solution (Gibco) and 1% (v/v) serum (additionally supplemented with a stepwise reduction of dFCS). The criteria adopted prior to each dFCS reduction was viability greater than 90% whilst in exponential phase of growth. Cells were routinely passaged at a concentration of 1 x 10⁶ cells mL⁻¹ and split at a seeding concentration of 3 x 10⁵ cells mL⁻¹ into fresh medium. Cells were then weaned off 10% (v/v) serum by reducing the serum content to 5% (v/v) and finally to 1% (v/v) dFCS (PAA) containing medium after at least 2 passages at each serum concentration. Master and working cell banks were created as previously described above (section 2.2.5).

2.2.8 Bioreactor Culture

In order to maintain a controlled cell culture environment (which is not possible with shaker or spinner flasks) batch cultures of NS0 cells in 3 L and 5 L working volume bioreactors (Applikon., Tewkesbury, U.K.) were performed as outlined below.

2.2.8.1 3 L Bioreactor Preparation

A 3 L Applikon bioreactor was utilised to examine changes in the GS-NS0 cell proteome throughout batch culture under controlled conditions of cells engineered to produce anti-CD38⁺. Oxygen and pH were measured by electrodes manufactured by Broadley James (supplied by Applikon). The reactor vessel was assembled according to the manufacturer's instructions followed by the attachment of silicon tubing between the reactor head plate ports and medium transfer, NaOH feed and drain outlets. All gas entry and exit ports were sealed using Midisart 2000, 0.2 µm air filters (Sartorius., Epsom, Surrey, U.K.). The reactor vessel was then filled with ddH₂O to just above the level of the pH and dissolved oxygen (D.O) probes to prevent drying out and gate clamps were used to seal off all lines that reached below the probes. Prior to sterilisation and insertion into the reactor head plate, the pH probe was calibrated according to the manufacturers instructions using pH 4 and pH 7 standard solutions. A Rodwell autoclave (Hornchurch, U.K.) was used for sterilisation of the bioreactor and associated glassware for 45 minutes at 121°C. Calibration of the D.O probe was performed following vessel sterilisation as detailed below. A constant stream of nitrogen was sparged into the reactor following inoculation of the vessel with fresh medium. Once anoxic conditions had been reached the Bio-controller was set to 0% dissolved oxygen. The Bio-controller was then set to continuously sparge

with air for approximately 30 minutes, and once a maximum reading was reached this value represented 100% air saturation.

2.2.8.2 Control and Operation of NS0 Cell Culture in 3 L Bioreactors

GS-NS0 (producing anti-CD38⁺) cell inoculum was prepared in 100 mL shaker flask cultures (as previously described in section 2.2.2, 2.2.4 and 2.2.5) to a combined volume of approximately 300 mL prior to seeding the bioreactor at a concentration of 2×10^5 cell mL⁻¹ in a 1.5 L culture volume. Cells that had reached mid-exponential phase of growth were utilised to minimise lag-phase duration.

The medium used for cell culture of the anti-CD38⁺ producing GS-NS0 cells was serum-free IMDM (described in section 2.2.2.1) additionally supplemented with 1 part per million antifoam C to prevent shear stresses (Sigma). Fermentation conditions were automatically maintained during culture using an Applikon BioController 1030 and BioConsole 1035. Dissolved oxygen concentration was kept constant at 40% air saturation by sparging 0.2 µm filtered air or N₂ gas through a microporous sparger. A slow trickle of air was also perfused into the headspace of the fermenter to maintain gaseous flow and to prevent accumulation of CO₂. Temperature was maintained at $37^\circ\text{C} \pm 0.5^\circ\text{C}$ by a water jacket, and the pH of the culture was maintained at 7.2 ± 0.2 by the sparging of CO₂ using a bicarbonate buffering system and the addition of 0.5 M NaOH as required. Cells were agitated at a constant power to volume ratio of 5×10^{-3} W/L using a small marine impeller at a speed of 150 rpm.

Supernatant samples were withdrawn from the culture on a daily basis for off-line analyses for cell growth, productivity, glucose depletion and lactate accumulation. Larger volumes were taken throughout the culture (at lag-phase, day1; exponential phase, days 3 and 5; and death phase, day 7) for preparation of extracts for proteome analysis and protein synthesis (see section 2.4.3 for details). The fermentation run was terminated when cell viability reduced to less than 40%.

2.2.8.3 7 L Bioreactor Preparation

Four 4 L working volume Applikon Bioreactors were used for the comparison of B72.3 producing GS-NS0 cell transfectants under controlled conditions. All 4 L fermentation work was carried out at GSK (Beckenham, Kent, U.K.). Fermentation conditions were controlled by Applikon BioController 1030 and BioConsole 1035 as above for the 3 L

bioreactor in section 2.2.8.1 and 2.2.8.2. The reactors were all matched and each bioreactor was equipped with a marine type impellor. Oxygen was measured using Applisens D.O probes (Applikon), and pH was determined by Mettler Toledo combination pH probes (Mettler-Toledo Ltd., Beaumont Leys, Leicester, U.K.). The reactors were assembled according to the manufacturers instructions, except a 'Y' junction was used on the waste port to enable large sample volumes of up to 2 L to be removed from the bioreactor. Silicon tubing, air filters and gate clamps were attached to all sample ports as described above. The pH probes were then calibrated (as above in section 2.2.8.1) and the dissolved oxygen tension (DOT) was set to 0% on the D.O probes by removing them from the bioreactor and passing nitrogen gas over them to purge oxygen. The reactor vessels were then filled with 1.5 L PBS to cover all probes and then autoclaved. After autoclaving the pH probes were recalibrated if necessary and the D.O saturation level was set to 100% after saturating the bioreactor with oxygen. Once calibration was complete the PBS was removed from the bioreactor and 2 L of fresh medium, R87 (GSK), 1% (v/v) serum (HyClone, Perbio Science U.K., Ltd., Cheshire, U.K.), placed into the reactors.

2.2.8.4 Control and Operation of NS0 Cell Culture in Bioreactors

GS-NS0 cell inoculum was prepared to 200 mL volumes in shaker flask cultures (as previously described in section 2.2.2 and 2.2.5) to a combined volume of 500 mL prior to seeding the bioreactors at a viable cell density of 2.5×10^5 cells mL⁻¹ in a 2.5 L culture volume for a three-day passage. Cells in mid-exponential phase of growth were employed to minimise lag-phase duration. Once the cells had reached mid-exponential phase of growth, the culture volume was adjusted and made up to 4 L at a final viable cell density of 2×10^5 cells mL⁻¹ for the beginning of the fermenter run. For the 4 L batch culture, fermentations were carried out in duplicate; cultures one and two were inoculated using the same working cell stock, but with a further 4 cell generations for culture 2, except for the parental cell line and transfectant 4R which were cultured in duplicate simultaneously.

The medium used for the 4 L batch cultures was protein-free R87 medium provided by GSK (Beckenham, Kent, U.K.) supplemented with 1% (v/v) FBS (HyClone) and 1 mL L⁻¹ L-26 lipid solution (Gibco). Fermenter conditions were controlled by Applikon BioController 1030 and BioConsole 1035 units. Dissolved oxygen (D.O) was kept constant at 15% saturation, controlled by sparging 0.2 µm filtered oxygen through a microporous sparger. Temperature was maintained at 36°C ± 0.5°C by a heating jacket

with mixing by a marine impellor at a constant speed of 150 rpm. The pH was kept at 7.2 ± 0.2 through the addition of CO_2 using a bicarbonate buffering system and 1.0 M NaHCO_3 .

Supernatant samples were withdrawn from the culture at 24 h intervals for analysis of cell growth, glucose depletion and lactate accumulation together with glutamate reduction and glutamine. Larger volumes were also taken at set points throughout the culture (at lag-phase, day 1; exponential phase, day 3 or 4; and death phase, day 7 or 8) for preparation of extracts for proteome analysis (see section 2.4.3). The fermentation runs were terminated when cell viability reduced to less than 40%.

2.2.9 Metabolite Determination

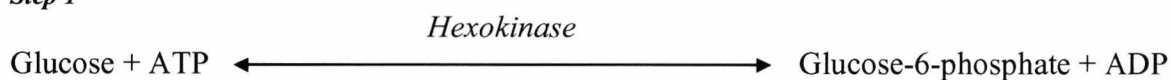
Glucose and lactate concentrations in cell free supernatant samples were quantified by glucose (hexokinase) and lactate dehydrogenase kits (Sigma), adapted to 96 well format. For both assays, the absorbance was read at 340 nm using a MRX™ plate reader (Dynatech., Billinghamurst, U.K.).

2.2.9.1 Glucose Concentration Determination from Cell Culture Supernatant

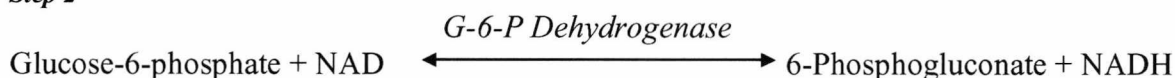
A glucose kit (Sigma) was utilised for routine determination of glucose concentration in cell free supernatants. The assay is based upon the phosphorylation of glucose by adenosine triphosphate (ATP) to yield glucose-6-phosphate, which is then oxidised to 6-phosphogluconate in presence of nicotinamide adenine dinucleotide (NAD). During the oxidation process an equimolar amount of NAD is reduced to NADH which in turn corresponds to an increase in absorbance at 340 nm.

Assay Principle:

Step 1



Step 2



A sample (2 μL) of cell free supernatant was added to 200 μL of glucose (HK) assay reagent (Sigma) in a flat bottom, 96 well ELISA microtitre plate. A blank containing glucose (HK) reagent only together with a range of glucose standards (0-30 μg) was also

2.3 Quantitation of GS-NS0 Cell Line IgG Production

2.3.1 Optical Biosensor Assay

Recombinant monoclonal antibody (rMAb) secretion by GS-NS0 cells expressing anti-CD38⁺ (IgG₁) was quantified in cell free supernatant samples using direct measurement of the rate of binding of rMAb to immobilised recombinant protein L (Actigen., Cambridge, U.K.). Recombinant protein L binds the light chain of IgG₁ specifically and the amount bound was determined using an optical biosensor (Model 2000, Biacore., Uppsala, Sweden.), four channel serial flow biosensor instrument and the following conditions; running buffer, HBS (HEPES-buffered saline, 10 mM HEPES, 0.15 M NaCl, 3.4 mM EDTA and 0.05% P-20 surfactant, pH 7.4), CM5 sensor chip and other immobilisation reagents were all supplied by BiaCore AB (Stevenage, U.K.).

For Biacore determination of rMAb secretion, protein L was immobilised on a CM5 sensor chip surface (Biacore) via amide linkages using standard *N*-ethyl-*N'*-dimethylaminopropylcarbodiimide (EDC) and *N*-hydroxysuccinimide (NHS) chemistry according to the manufacturers instructions. Unbound groups on the CM5 sensor chip were then blocked with 40 μ L ethanolamine (1.0 M ethanolamine hydrochloride, pH 8.5). Samples were injected over the CM5 chip sensor surface at a flow rate of 10 μ L min⁻¹ using the in-built autosampler, and calibrated against a standard curve generated from injections of known concentrations of MAb in IMDM (0-100 μ g mL⁻¹). The standard curve was generated by calculating the relative change in initial rate of binding (RU min⁻¹) for each standard concentration. The sensor surface was regenerated by the application of 20 μ L of 0.1 M HCl, pH 3.0 over the sensor surface at 10 μ L min⁻¹.

2.3.2 ELISA Assay

The concentration of human-mouse chimeric antibody B72.3 (an IgG₄) was quantified using a sandwich enzyme-linked immunosorbent assay (ELISA). The assay was carried out in 96 well microtitre plates (Dynatech Immulon B plates, Thermo Lifesciences., Basingstoke, U.K.). Each well was coated with 100 μ L of primary antibody, AffiniPure F(ab')₂ Fragment Goat anti-human, Fc (gamma) fragment specific IgG heavy and light chain (Jackson ImmunoResearch., Stratech Scientific Ltd, Luton, Bedfordshire, U.K.) diluted to a concentration of 16.6 μ g mL⁻¹ in coating buffer (10 mM sodium carbonate, 30 mM sodium hydrogen carbonate, pH 9.7) and incubated for at least 16 h at 4°C. Unbound

2 Materials and Methods

human IgG was removed by washing the plate twice with wash buffer (5.84 g NaCl, 1.15 g Na₂HPO₄, 0.29 g NaH₂PO₄·H₂O, 3.72 g EDTA, 200 µL Tween-20, 10 mL L-butanol per litre, pH 7.2). The plates were then blocked with 200 µL of blocking buffer (5 g casein L⁻¹ in 10 mM sodium carbonate, 30 mM sodium hydrogen carbonate buffer, pH 9.7), incubated for 1 h at room temperature and then washed twice as previously described. Samples of cell free supernatant were prepared at a dilution of 1:500 and human IgG standards (Sigma) of known concentration prepared in sample buffer (12.1 g Tris, 5.84 g NaCl, 0.2 mL Tween-20 in a total volume of 1 litre, pH 7.0). After washing, test and standard IgG samples were applied to the plate at appropriate dilutions in a volume of 100 µL per well and incubated at room temperature for 1 h. The plate was then washed again and incubated with 100 µL of secondary antibody (affinity isolated purified anti-human Kappa light chains (bound and free)-peroxidase conjugate from goat (Sigma)), prepared to a final dilution of 1:10000 with sample buffer, and loaded into the appropriate plate wells for 1 h followed by two further washes. Subsequently, 100 µL of substrate mixture consisting of 3, 3', 5, 5' tetramethylbenzidine (TMB) (Sigma) in 10 mL of substrate solution (TMB 0.1 mg mL⁻¹ in 0.1 M sodium acetate citrate buffer, pH 5) containing 100 µL of DMSO and H₂O₂ was applied to each well. The plate was then left to develop and the reaction was stopped by the addition of 50 µL of 2.5 M H₂SO₄ once a colour change was observable in the lowest standard. The optical density of each well was measured at 450 nm using an MRX™ Dynatech plate reader (Dynatech) and the concentration of each sample was calculated from the standard calibration curve by interpolation.

2.4 Sample Preparation of GS-NS0 Cells for Proteomic Analysis

2.4.1 Optimisation of Whole NS0 Cell Protein Extraction

Prior to lysis of GS-NS0 cells by extraction in the appropriate lysis buffer, salts and other substances, which can interfere with the isoelectric focussing (IEF) step of 2-D electrophoresis, must be removed. This was achieved by two gentle washes of the cell pellet with phosphate buffered saline (PBS), followed by a further wash with 0.35 M sucrose to remove any remaining contaminants present in the growth medium without placing osmotic tension or undue stress on the cells. Between each wash step the cells were re-pelleted by centrifugation. Several methods of cell lysis were investigated before a gentle lysis method using chemical detergents was optimised as animal cells are easily

disrupted. After the initial washes to remove contaminants, cells were exposed to strongly denaturing extraction solutions to rapidly inactivate proteases and other enzymes. These enzymes are usually compartmentalised in membrane bound vesicles, but are liberated upon exposure to extraction buffer. Proteases are capable of modifying other proteins within the sample and can adversely affect 2-D reproducibility and the proteome; therefore it is essential these proteins are inactivated.

2.4.2 Extraction Buffer Solutions

Two variations of a commonly used lysis solution (Berkelman and Stenstedt, 1998) published by Amersham Biosciences (Buckinghamshire, U.K.) containing a cocktail of reducing agents and solubilising agents were assessed (Table 2.1). Both lysis solutions contained high concentrations of urea to inhibit proteolytic activity, although lysis buffer 1 contained thiourea in addition to urea in an attempt to improve the solubilising conditions according to a method published by Rabilloud (Rabilloud et al., 1997). Different concentrations of dithiothreitol (DTT) (Melford Laboratories Ltd., Ipswich, Suffolk, U.K.) and CHAPS ((3-[(3-Cholamidopropyl)dimethylammonio]-1-propane-sulphonate)TGS) (Sigma) were also added to the lysis solutions. DTT was added as a reducing agent to maintain the proteins in their fully reduced state and CHAPS was utilised as a zwitterionic detergent to ensure complete sample solubilisation and to prevent aggregation of sample proteins through hydrophobic interactions. Carrier ampholytes or IPG buffer were also included in the sample solution to enhance protein solubility and to aid the focussing of proteins within the pI range of the ampholyte during IEF.

Table 2.1 NS0 protein solubilisation buffers

Component	Lysis Buffer 1 Final Concentration	Lysis Buffer 2 Final Concentration
Urea	8 M	9.5 M
Thiourea	2 M	-
CHAPS	4%	2%
DTT	1%	1%
Pharmalytes (pI 3-10)	-	1%
IPG Buffer (pI 3-10)	0.80%	-

2.4.3 Protein Extraction from GS-NS0 Cells

GS-NS0 cells (approximately 1×10^7) were harvested by centrifugation at 50 x g for 5 minutes at room temperature in an MSE ChilSpin 2 bench top centrifuge (Fisons). For each sample time point during culture ten replicate extractions were undertaken (i.e. $1 \times$

2 Materials and Methods

10^8 cells were harvested and split into 1×10^7 cell aliquots). The supernatant was discarded and the pellet was then washed twice with two 10 mL volumes of PBS (Oxoid., Basingstoke, Hampshire, U.K.) followed by a single wash with 0.35 M sucrose (5 mL). Protein extraction was then achieved by the addition of 400 μ L of lysis buffer for 1 h at room temperature, after which time the resulting solution was re-pelleted by centrifugation at 4000 rpm for 30 minutes. All extracts were then stored at -80°C until analysed by 2-D electrophoresis. The resultant cell extracts were rapidly assessed for protein solubilisation and recovery by the modified Bradford assay for protein content (section 2.4.4) and mini gel format 2-D PAGE for rapid method development (section 2.6) to select the optimal solubilising conditions. Based on the results from these studies (see chapter 3, section 3.3) lysis buffer 2 was selected for all future analyses, as unlike lysis buffer 1 it did not liberate DNA to yield a viscous solution and also provided the highest resolution of proteins when analysed on a 2-D gel.

2.4.4 Modified Bradford Assay

The protein content (concentration of protein in the 400 μ L extraction buffer) from extracted NS0 cells was quantified using a modified Bradford assay (Bradford, 1976) based on the method published by Ramagli (Ramagli, 1999). A calibration curve was generated with known concentrations of bovine serum albumin (BSA) prepared in doubling dilutions from a stock solution of 5 mg mL^{-1} (Table 2.2). For each extraction sample the assay was performed in triplicate and the average value reported.

Table 2.2 Modified Bradford assay

[BSA] ($\mu\text{g mL}^{-1}$) equivalent	BSA (μL)	Lysis Buffer (μL)	0.1 M HCl (μL)	ddH ₂ O (μL)
0	0	10	10	80
500	1	9	10	80
1000	2	8	10	80
2000	4	6	10	80
4000	8	2	10	80
5000	10	0	10	80

The above was added to 3.5 mL of Bio-Rad protein assay reagent diluted 1 in 4 and then the absorbance (O.D) determined at 600 nm, and unknown protein concentrations determined using regression analysis.

2.5 1-D Electrophoresis

2.5.1 1-D SDS-PAGE Sample Buffer

For all 1-D sample preparations and separations, Laemmli Sample Buffer was utilised (Bio-Rad).

2.5.2 1-D SDS-PAGE

Pre-cast (Tris-glycine 4-20% (Invitrogen)) or self-cast mini-gels 12.5% (section 2.6.7) were used for 1-D protein separations using Tris/Glycine/SDS (TGS) running buffer (section 2.6.2). Samples were diluted 1:1 with Sample Buffer (section 2.5.1) and heated to 100°C for 5 minutes to fully denature the proteins prior to loading into the gel wells. Molecular weight markers were also added to one of the wells in order to provide an estimate of the molecular mass of the bands visualised in the gels (section 2.6.6). A Novex Vertical Xcell II™ Mini-Cell electrophoresis system was used to run all gels according to the pre-set programme (Table 2.7). After completing the run (once the loading dye front had reached the base of the resolving gel), the gels were visualised with either silver or colloidal Coomassie stain (section 2.7).

2.6 2-D Electrophoresis

2-D electrophoresis is the most widely utilised technique to separate proteins in complex mixtures according to two separate physical parameters: isoelectric point (pI) and relative molecular mass (M_r). The first dimension isoelectric focussing (IEF) separation involves the separation of proteins based on their pI. Proteins are applied to an electric current under which the proteins migrate until they reach the point where their net charge is zero. The second dimension involves the separation of proteins based on their molecular weight by reducing SDS-PAGE.

2.6.1 Isoelectric Focussing of Protein Mixtures. First Dimension Separation

Isoelectric focussing separates proteins according to their isoelectric point (pI). Immobilised pH gradient dry gel (IPG) strips are available in a variety of lengths (7, 11, 13, 18 and 24 cm) and pI ranges from Amersham Biosciences and Bio-Rad. IPG strips are also available in either a linear or non-linear form and also available in either broad or narrow pI, depending upon the desired separation range. For this study three IPG strip

lengths (7, 18 and 24 cm in pH 3-10 linear and non-linear form) (Amersham Biosciences) were utilised. Each IPG strip length requires different focussing times, together with different focussing conditions in order to obtain maximum resolution (for details see Table 2.3 below). During the focussing procedure, proteins are subjected to two types of voltage increase, either 'step-n-hold', which refers to a single applied voltage increase to the next step mode without graduation, or 'gradient mode', which subjects the proteins to a gradual increase in voltage over the specified time. Together with IPG strips, a buffer containing carrier ampholytes (IPG buffer or pharmalytes) is also applied to protein samples prior to IEF. This buffer is complementary to the pI range of the IPG strip, and enhances the focussing of proteins when the Ettan IPGphor™ apparatus applies a charge to the IPG strip.

Table 2.3 Focussing protocols for first dimension separations of whole cell NS0 protein extracts

Step Mode	7 cm IPG DryStrip, pI 3-10 L/NL, 10 µg Protein Load		18 cm IPG DryStrip, pI 3-10 L/NL, 80 µg Protein Load		24 cm IPG DryStrip, pI 3-10 NL 100 µg Protein Load	
	Voltage (V)	Time (h:min)	Voltage (V)	Time (h:min)	Voltage (V)	Time (h:min)
Step-n-hold	30	14:00	30	12:00	30	12:00
Step-n-hold	200	00:30	200	01:00	500	01:00
Step-n-hold	500	00:30	500	01:00	1000	01:00
Step-n-hold	1000	00:30	-	-	-	-
Gradient	1000-8000	00:30	500-8000	01:00	-	-
Step-n-hold	8000	01:30	8000	04:00	8000	09:30
Total Vhr	8000		27000		65000	

Amersham Biosciences supplies two pieces of equipment which can be utilised for IEF, the Multiphor™ II system or the IPGphor™ Isoelectric Focussing System. In this study the IPGphor™ was routinely utilised as it simplifies the first dimension separation by using IPG strip holders as both the rehydration and IEF chamber. The IPGphor™ is also an integrated system with both temperature control and power supply built in. Prior to IEF, whole cell NS0 protein samples were assessed for protein content by the modified Bradford assay (as described in section 2.4.4), as the manufacturers recommendations state optimum separations of proteins occurs within a given concentration range (total protein load) for each IPG strip type. For 7 cm IPG strip separations the optimum protein load is reported as 10 µg in 125 µL loading volume. Therefore, protein samples were diluted in lysis buffer to the required concentration and volume, a few grains of Bromophenol blue added and then the solution placed into a ceramic strip holder. After the plastic backing

was removed from the IPG strip it was then applied gel side down onto the solution and overlaid with 1 mL DryStrip cover fluid (Amersham Biosciences) in order to minimise urea crystallisation during focussing. The plastic lid was then placed on top of the strip holder (which had previously been placed on the IPGphor™ platform between the positive and negative plates) and the IEF procedure commenced using the pre-programmed method described in Table 2.3. The focussing procedure was stopped when 8000 Vhr were accumulated in the case of 7 cm IPG strips. The focussing procedure and volt hours were extended when longer length IPG strips of 18 and 24 cm were employed (Table 2.3).

For preparative gels (more than 100 µg of protein loaded onto 18 and 24 cm IPG strips) it was necessary to extend the focussing time to enable entry of all the proteins into the gel strip, and subsequent migration to the point of neutral charge (Table 2.4). After IEF, IPG strips were washed with ddH₂O to remove excess cover fluid and then placed in either 15 mL Falcon tubes for 7 cm IPG strips, or 10 mL graduated sterile pipettes for 18 and 24 cm IPG strips, and stored at -80°C until required for the second dimension separation.

Table 2.4 Focussing protocols for protein loads of greater than 100 µg on IPG strips

Step Mode	18 cm IPG DryStrip, pI 3-10 NL, 500 µg Protein Load		24 cm IPG DryStrip, pI 3-10 NL 350 µg Protein Load	
	Voltage (V)	Time (h:min)	Voltage (V)	Time (h:min)
Step-n-hold	30	14:00	30	12:00
Step-n-hold	200	00:30	500	01:00
Step-n-hold	500	00:30	1000	01:00
Step-n-hold	1000	00:30	-	-
Gradient	1000-8000	00:30	-	-
Step-n-hold	8000	04:00	8000	09:30
Total Vhr	40000		110000	

2.6.2 Electrophoresis Buffering Systems

A pre-mixed 10 X concentrate of Tris/Glycine/SDS (TGS) running buffer (Bio-Rad) was utilised as the main electrophoresis buffer for 2-D electrophoresis experiments unless otherwise stated. The TGS concentrate was diluted to a 1 x solution prior to use to give a final concentration of 25 mM Tris-HCl, 192 mM glycine, 0.1% (w/v) SDS. For separations utilising the DALT II tank (section 2.6.9) and Ettan DALT pre-cast gels the manufacturers buffer system was utilised according to manufacturers instructions (Amersham Biosciences). The buffer kit consists of two separate buffers (cathode and anode buffer) for the upper and lower chambers of the gel tank to generate a discontinuous

buffering system which in theory gives rapid results with sharper and more reproducible proteomic maps.

2.6.3 Equilibration of IPG Strips Prior to the Second Dimension Separation

Prior to the second dimension separation, the first dimension IPG strips were equilibrated in a Tris-HCl buffer (pH 8.8) to maintain the IPG strip in a pH range suitable for electrophoresis. In addition urea and glycerol were included in the equilibration buffer in order to reduce effects of electroendosmosis, which can interfere with protein transfer to the second dimension gel. The constituents of the equilibration buffer are outlined below (Table 2.5). The solution was aliquotted and stored at -70°C until required.

Table 2.5 Components of SDS-equilibration buffer

Component	Final Concentration
1.5 M Tris-Cl, pH 8.8	50 mM
Ultra Pure Urea	6 mM
Glycerol	30% (v/v)
SDS	2% (w/v)

Equilibration of IPG strips was carried out immediately prior to the second dimension separation by SDS-PAGE. The process modifies the side chain of the amino acid cysteine on proteins. Prior to the second dimension separation each strip was incubated with a 10 mL volume of equilibration buffer (Table 2.5) containing 100 mg of DTT (Melford Laboratories Ltd., Ipswich, Suffolk, U.K.) with gentle agitation for 15 min to ensure all proteins remained in their fully reduced state. After 15 min the solution was removed and the strip washed with ddH₂O to remove any remaining DTT. The strips were then incubated in equilibration buffer containing 250 mg of iodoacetamide (10 mL) for a further 15 min with agitation to alkylate thiol groups which reduces the appearance of streaking in the second dimension. After the equilibration step the IPG strips were washed and then placed onto the second dimension gel and sealed in place.

2.6.4 Sealing of the IPG Strip to the Second Dimension SDS-PAGE Gel

An agarose sealing solution was used to allow the flow of the focussed proteins into the second dimension and to prevent the IPG strip from moving or floating in electrophoresis buffer prior to and during the second dimension separation by SDS-PAGE. Agarose type VIII (Sigma) was solubilised in 1 x TGS running buffer to a final concentration of 0.5%

(w/v). The solution was heated in a microwave, aliquotted and stored at room temperature until required. When required, the agarose sealing solution was melted by heating it to 100°C in a heating block. Once in solution, approximately 1 mL of sealing solution was applied to provide a seal between the IPG strip and the second dimension gel.

2.6.5 Self Casting Polyacrylamide gels

All self-cast SDS-PAGE gels were prepared from a 30% acrylamide/bis 37.5:1 monomer stock solution (Bio-Rad) which was adjusted to a final concentration of 12.5%. Self-cast mini-gels for 1-D separations were cast with an additional 4% acrylamide stacking gel. Once the gels had been cast they could be stored at 4°C in zip-lock bags containing 1 x TGS running buffer for up to two weeks without loss of performance/resolution.

2.6.6 Molecular Weight Markers

Broad range calibrated molecular weight markers were purchased from Bio-Rad in order to estimate the molecular mass of protein bands or spots in gels.

Table 2.6 Bio-Rad broad range molecular weight markers

Protein	Calibrated MW (Da)
myosin	211000
β-galactosidase	122000
bovine serum albumin	80000
ovalbumin	51000
carbonic anhydrase	35900
soybean trypsin inhibitor	28600
lysozyme	20800
aprotinin	6700

2.6.7 Mini Gel Second Dimension Separation for 7 cm IPG Strips

For rapid method development, 7 cm IPG strips were separated in the second dimension on 12.5% self-cast or 4-20% pre-cast Tris-glycine mini 2-D gels (Invitrogen). A Novex Vertical Xcell II™ Mini-Cell electrophoresis system (Invitrogen) was utilised that could run two mini gels in each tank simultaneously using 1 x TGS buffer as the running buffer (section 2.6.3). The equilibrated IPG strips (section 2.6.3) were sealed on top of the second dimension SDS-PAGE gels and markers were applied into a separate lane on the side of the gel to estimate the molecular mass of proteins within the gel (section 2.6.4 and 2.6.6). All such gels were run using a pre-selected programme (see Table 2.7 below).

After the run was completed the gels were removed from their cassettes and placed separately in gel boxes containing fixative for silver staining, and then agitated for approximately 30 minutes for staining the same day or left in fixative overnight for staining the following day (section 2.7.1).

Table 2.7 Novex mini-gel pre-set programme for Tris-glycine gels

Constant Voltage (V)	Current Start (mA)	Current End (mA)	Duration (h:min)
125	30-40	8-12	01:20-01:40

2.6.8 Large Format SDS-PAGE

Large format 18 cm IPG strips were separated on 18 x 20 x 0.1 cm, 12.5% self-cast SDS-PAGE gels (section 2.6.5). Four large format 2-D gels could be run simultaneously using two Protean II Xi Cell vertical gel tanks powered by the same power pack (Bio-Rad). The system was maintained at 12°C using a refrigerator bath to circulate cooled water around the central core of each tank during electrophoresis (Techne TempHC TE-8A). The running protocol is described in Table 2.8 below.

Table 2.8 Running protocol for protean II Xi cell large format gel tank

Constant Voltage (V)	Current (mA)	Constant Power (W)	Duration (h:min)
275	40	300	06:30:00 (approx)

2.6.9 Large Format SDS-PAGE using the DALT II System

To obtain reproducible 2-D gel images an ETTAN DALT II gel tank (Amersham Biosciences) was utilised for large format second dimension separations. The DALT II system enables twelve 2-D gels to be run simultaneously and the second dimension separation is performed more rapidly than with the Protean II Xi system. Unlike the Protean II Xi tank, the power is equally distributed between all gels in the DALT II system so they run under identical conditions during separation. The gels are also larger, with the system utilising 24 cm IPG strips for the first dimension and 26 x 20 x 0.1 cm SDS-PAGE gels for the second dimension separation. Therefore greater separation of the cellular proteins is obtained. The SDS-PAGE gels utilised for separations using the DALT II system were either commercially available pre-cast with a plastic backing (Amersham Biosciences) or self-cast (12.5% acrylamide/bis) (section 2.6.5). The pre-cast DALT gels were homogeneous 12.5% polyacrylamide gels cross-linked with bisacrylamide

(Amersham Biosciences). Electrophoresis was performed under constant power in two steps with controlled temperature (20°C) using the Ettan running buffer kit (section 2.6.3). During the initial migration and stacking period where the proteins are transferred from the IPG strip to the second dimension, the current applied was approximately half of the value required for separation. After transfer (approximately 30 minutes) the current was increased for the remainder of the run. The details are described in Table 2.9 below.

Table 2.9 Electrophoresis running conditions for second dimension separations with the DALT II tank

Step	Constant Power (W/gel)	Duration (h:min)
1	5 W/gel	00:35
2	11 W total	07:00:00 (approx)

2.7 Staining Techniques for Analytical and Preparative 2-D Gels

Two staining techniques were utilised for protein visualisation on 2-D gels. These were selected because of their compatibility with mass spectrometry for protein identification, their sensitivity of staining and ease of use. Silver staining was carried out using either an adaptation of the Shevchenko method (Shevchenko et al., 1996) or an adaptation of the PlusOne silver stain (Amersham Biosciences) for analytical protein loads of 100 µg or less for the maximum sensitivity (section 2.7.1 and 2.7.2). Bio-Safe colloidal Coomassie (Bio-Rad) was utilised for preparative protein loads of up to 1000 ng protein for visualisation of more abundant protein spots (section 2.7.3).

2.7.1 Shevchenko Silver Staining

The Shevchenko silver stain method (Shevchenko et al., 1996) was developed to be compatible with mass spectrometry techniques (Table 2.10). Silver stain results in the visualisation of many more protein spots within gels with less than 5 ng of protein per spot than traditional Coomassie staining techniques. For convenience the fixation step was extended to an overnight step without affecting the final gel image.

Table 2.10 Adapted Shevchenko silver stain

Step	Reagents	Time (mins)
Fixing	50% methanol 5% glacial acetic acid	30 minimum, usually overnight
Wash	50% methanol	10
Sensitise	0.03% Sodium thiosulphate	1
Wash	2 x ddH ₂ O	1
Silver	0.1% Silver nitrate	20
Wash	2 x ddH ₂ O	1
Develop	0.04% formaldehyde 2% sodium carbonate	~ 5
Stop	5% glacial acetic acid	30
Storage	1% glacial acetic acid at 4°C	4 weeks

2.7.2 PlusOne Silver Staining Method

The PlusOne silver stain method was undertaken in accordance with the manufacturer's instructions except glutaraldehyde was omitted from the sensitising step for compatibility with mass spectrometry. When using the PlusOne staining methodology, spot inversion was less frequent than when using the Shevchenko method (section 2.7.1) and therefore protein abundance could be more accurately quantified (section 2.7.4). Plastic backed pre-cast gels were also stained using the PlusOne method, however, it was necessary to increase the staining times and staining volumes due to reagent access being limited to one side of the gel (Table 2.11).

Table 2.11 The PlusOne silver staining method

Step	Reagents	Time (mins)	Time (mins) Backed Gels
Fixation	40% Ethanol 10% Acetic acid	2 x 60 minimum usually overnight	overnight
Sensitise	30% Ethanol 5% (w/v) Sodium thiosulphate Sodium acetate 68 g L ⁻¹	30	60
Wash	ddH ₂ O	3 x 5	5 x 10
Silver	2.5% Silver nitrate Formaldehyde 37% (w/v) 400 µL L ⁻¹	20	60
Wash	ddH ₂ O	2 x 1	4 x 1
Develop	Sodium carbonate 25 g L ⁻¹ Formaldehyde 37% (w/v) 200 µL L ⁻¹	~5	~5
Stop	EDTA-Na ₂ .2H ₂ O 14.6 g L ⁻¹	10	60
Wash	ddH ₂ O	3 x 5	5 x 10
Store	glycerol 87% (w/v) 100 mL L ⁻¹	4 weeks	4 weeks

2.7.3 Bio-Safe Colloidal Coomassie Stain

Protein loads of up to 1000 ng could be visualised on 2-D gels using Bio-Safe colloidal Coomassie stain (Bio-Rad). After completion of the second dimension gels were washed three times for 15 min with ddH₂O and then incubated with colloidal Coomassie stain overnight with gentle agitation. Gels were then de-stained in ddH₂O until the protein spots were clearly visible and the background clear. On completion of the staining gels were stored in zip-lock bags for several months. Colloidal Coomassie staining has a much wider linear dynamic range than silver stain so more accurate quantitation of protein expression levels is possible. However, due to the much lower sensitivity of Coomassie staining it could not be used on its own but rather as a complementary stain to silver.

2.7.4 Quantitation of GS-NS0 2-D Gels

Resultant 2-D gel images were captured using a calibrated ImageScanner™ flatbed optical scanner utilising LabScan software (Amersham Biosciences) at 200 dpi and 256 greyscales in transmissive mode. The process of scanning each gel to acquire a digital image was carried out immediately after completion of staining. The scanner was always calibrated prior to use with a calibrated grey-scale photographic step wedge (Genomic Solutions Ltd., Huntingdon, Cambridgeshire, U.K.). The scanned digital images were then imported into ImageMaster 2-D Elite software™ v4.1 (Amersham Biosciences) for rigorous quantitative analysis (Lopez, 2000). The software was used to detect and filter individual protein spots using a set of parameters which were utilised throughout the analysis procedure (Volume >1200, Circularity >0.3, Sensitivity 9369, Noise factor 5, Operator size 17 and Background 15). In some cases due to differences in staining, the sensitivity was increased to make the spot detection more accurate and comparable between gels in a series. However, all other parameters were kept consistent. Spots that were erroneously detected were manually edited from each gel, and protein spots that had not been automatically identified or split were also manually edited when required. The background was removed from each gel using the Mode of Non-Spot tool, which was set to 45 pixels surrounding each protein spot. Protein spot matching was then achieved through the manual addition of User Seeds followed by automatic spot matching. The software was also used to create averaged gels; therefore where possible from two (ideally three) gel images a composite gel was created for use as a standard reference gel for all other comparisons. The analysed gels were then normalised to total spot volume, which applied a multiplication factor of 100 to produce

values in the form of a percent total. In doing this the volume of a protein spot within many gels could be easily and accurately compared. Although the software provides the data in the form of a percentage, it was further normalised to provide the data in a more usable format by taking the highest normalised spot volume to equal 1. Each protein spot could then be accurately compared between a set of gels relative to the protein spot with the highest volume.

2.7.4.1 Statistical Assessment of Protein Extraction from NS0 Cells

In order to accurately assess the error involved with optimisation of NS0 cell sample preparation, batch cultures of NS0 cells were sampled at various time points in the growth curve and extracted in two different lysis buffers. Once the lysis condition was optimised for NS0 cell solubilisation and recovery, various cell numbers were extracted at mid-exponential growth phase to optimise the cell number to lysis buffer volume ratio. At least three extracts were prepared for each sample. Following extraction, each sample was subjected to a modified Bradford assay to quantify the protein content as outlined in section 2.4.4. Each sample was assessed in triplicate and the resultant concentrations were subjected to error analysis in the form of standard deviation, indicated by error bars.

2.7.4.2 Analysis of Variation in 2-D PAGE

Throughout the project, statistical analysis was utilised to a limited extent to assess the quantitative results obtained from the image analysis software. Ideally replicate 2-D gel images should result in the same number of protein spots being detected and ensure that the same spots migrate to the same position in a 2-D gel each time the gel is run. Unfortunately, 2-D gels are subject to process variation, which arises as a result of sample preparation, gel running (in both the first and second dimension separations) and staining (which is particularly applicable when a non end-point stain such as silver is utilised) and can affect any results obtained. Therefore, limited statistical analysis in the form of standard deviation was utilised to assess the errors associated within individual protein spot volumes between replicate 2-D gels and is also indicated by error bars.

2.8 Protein Identification

Proteome analysis currently involves the separation of proteins by 2-D electrophoresis, followed by identification by peptide mass fingerprinting (determined by matrix-assisted laser desorption/ionisation time of flight mass spectrometry (MALDI-ToF-ms) or by

partial sequencing (using electrospray ionisation tandem mass spectrometry (ESI-ms/ms)) (Lauber et al., 2001; Westbrook et al., 2001). Both methods enable the accurate measurement of the molecular masses of biomolecules. The method of choice in protein identification by ms is peptide mass fingerprinting (PMF) (Yanagida, 2002). In this method proteins are separated by electrophoresis and digested with a sequence-specific endopeptidase such as trypsin, followed by analysis by ms. The resultant molecular masses are then compared with theoretical values of protein masses registered in peptide mass databases to yield identified proteins listed according to the statistical accuracy of correspondence between experimental and theoretical masses of the peptides. The PMF method is the most rapid way of identifying proteins of organisms with completely sequenced genomes. A MALDI-ToF mass spectrometer is also most suitable for PMF since it is capable of high throughput performance.

2.8.1 De-staining of Gels

Silver or colloidal Coomassie stain was removed from gels using the method outlined by Gharahdaghi (Gharahdaghi et al., 1999), which is compatible with ms. Silver stained gel spots of interest were excised from the gel and incubated with a solution containing 100 mM sodium thiosulphate and 30 mM potassium ferrocyanide (150-200 μ L) combined 1:1 for 10-40 min with gentle shaking. The de-staining solution was then removed and the gels washed with ddH₂O until the yellow coloration disappeared. For colloidal Coomassie stained gels, the protein spots of interest were excised and de-stained in a solution containing ammonium bicarbonate (0.1M)/acetonitrile (150–200 μ L) mixed 1:1 for 15 minutes. This was then repeated for gel pieces that were still blue after the initial wash.

2.8.2 Tryptic Digestion of Proteins Visualised on 2-D Gels

ImageMaster 2-D software™ (Amersham Biosciences) was used to detect protein spots of interest that exhibited different patterns of expression between 2-D gels. The final step in the proteome analysis was to identify these proteins by mass spectrometry (ms). Individual protein spots were prepared for ms analysis by undertaking in-gel digestion with trypsin. Protein spots were excised from colloidal Coomassie and silver stained 2-D gels using clean scalpel blades and then placed in 1 mL siliconised eppendorf tubes (Bio-Rad) pre-washed with 50% CH₃CN/1% trifluoroacetic acid (TFA) (100 μ L) to minimise the loss of peptide fragments through adhesion to the tube walls. The gel pieces from silver stained

2 Materials and Methods

gels were then vortexed in 200 μL of HPLC grade H_2O for 20 minutes to remove excess acetic acid. The water wash was then discarded and the gel pieces incubated at room temperature in 200 mM ammonium bicarbonate (200 μL) for 60 minutes. After the incubation excess liquid was removed and the gel pieces were rinsed with dd H_2O before the silver and colloidal stained gel pieces were subjected to different de-staining processes (section 2.8.1). The gel pieces from silver stained gels were incubated in a solution consisting of 30 mM potassium ferrocyanide and 100 mM sodium thiosulphate mixed (1:1) for 40 minutes at 37°C. The de-staining solution was then removed and the gel pieces washed twice with HPLC grade H_2O . Colloidal Coomassie stained gels were also placed in pre-washed siliconised eppendorf tubes and vortexed in 200 μL of HPLC grade H_2O . To de-stain the gel pieces, they were washed twice in a solution containing ammonium bicarbonate (0.1M)/acetonitrile (150-200 μL) combined 1:1 (15 minutes for each wash). Once the de-staining process was complete the solution was removed and the gel pieces washed twice with HPLC grade H_2O . The protein spots were then subjected to in-gel digestion as detailed below.

Following de-staining the protein spots from colloidal Coomassie and silver stained gels were subjected to a common in-gel digestion procedure. Gel pieces were incubated in 200 mM ammonium bicarbonate/50% CH_3CN (v/v) (100 μL) for 45 minutes at 37°C. This solution was then removed and the process repeated. The gels pieces were then dried in a Speed Vac (ThermoSavant SC210A, Thermosavant., Holbrook, U.S.A.) on medium setting for 45 minutes. The gel pieces were then subjected to enzymatic digestion with 0.02 $\mu\text{g mL}^{-1}$ sequencing grade modified porcine trypsin (Promega., Madison, WI, U.S.A.) prepared in 40 mM ammonium bicarbonate/10% CH_3CN (v/v) (20 μL) at 37°C for 45 minutes in order to re-hydrate the gel pieces. After 45 minutes a further 50 μL of 40 mM ammonium bicarbonate in 10% CH_3CN (v/v) was added to each gel piece which were then left to incubate for a further 18 h at 37°C. On completion of the incubation period, tryptic peptides were extracted by pipetting the supernatant into fresh siliconised eppendorfs. Fifty microlitres of 50% CH_3CN (v/v)/0.1% TFA (v/v) was then added to each gel piece, vortexed and incubated for a further 25 minutes at 37°C to extract further peptides from the gel piece. The supernatant was then removed and added to the supernatant prepared previously. The peptides were then concentrated under vacuum using a Speed Vac (ThermoSavant) on a low setting to a reduced sample volume of 5-10 μL . The samples

were then stored at -20°C until desalting (section 2.8.3) and mass spectrometric analyses were undertaken (section 2.8.4).

2.8.3 Desalting of Tryptic Digest Samples

MALDI samples that had been subjected to in-gel digestion and stored at -20°C were allowed to thaw at room temperature. To achieve the concentration and desalting of samples prior to MALDI-ms, C18 ZipTips were utilised (Millipore., Watford, U.K.) according to manufacturers instructions. The ZipTips were washed twice with 50% CH_3CN (v/v) (10 μL) and equilibrated by washing twice with 0.1% TFA (v/v) (10 μL). Samples (10 μL) were then titrated through the ZipTips (repeated five times), followed by two further washes with 0.1% TFA (v/v) (10 μL). The peptides from each sample were then eluted into siliconised 500 μL eppendorf tubes using 80% CH_3CN (v/v)/0.1% TFA (v/v). Following this procedure the peptide samples were ready for MALDI analysis (section 2.8.4), or alternatively could be stored at -20°C until required.

2.8.4 MALDI-ToF and Peptide Mass Fingerprinting

Due to the high throughput capabilities and accuracy of the mass data acquired, mass spectra were recorded using a time-of-flight (ToF) delayed extraction MALDI mass spectrometer. Samples were mixed with an equal volume of matrix (0.5 μL) (α -cyano-4-hydroxy cinnamic acid solubilised in 60% CH_3CN (v/v), 0.02% TFA (v/v)) and spotted onto MALDI target plates and left to air dry. Samples were then analysed using a Bruker Ultraflex MALDI-ToF mass spectrometer (Bruker Daltonics Incorporated, U.S.A.), at the University of Kent or at GSK, Beckenham, Kent. Internal calibration was achieved using porcine tryptic autolysis digestion products.

2.8.5 Database Searching and Protein Identification

Since the genome of the mouse has been sequenced, peptide mass fingerprinting was conducted for samples using the search engine Mascot (matrixscience.com), which compared sample-specific masses with theoretical peptides calculated for all known proteins (Perkins et al., 1999). The search engine enables searching to be carried out using peptide mass fingerprinting, a sequence query or an ms/ms ion search using un-interpreted ms/ms data. The experimental mass values are compared with calculated peptide mass or fragment ion mass values, obtained by applying cleavage rules to the entries in a sequence

database. The resultant protein identifications are then given a matrix (probability) score out of 100% to aid in identifying the closest match for the protein of interest (Perkins et al., 1999). By being probability based a result can easily be judged to be significant or not, which is useful particularly in guarding against false positives. Proteins were identified through searching the database for mouse by considering a mass accuracy of 100 ppm, and a maximum of 1 missed cleavage.

2.9 Analysis of Active Protein Synthesis in NS0 Cells through *in vivo* Labelling of Nascent Polypeptides

2.9.1 L-[³⁵S] Methionine Labelling of Nascent Polypeptides

In order to analyse the total rate of protein synthesis, NS0 cells were labelled with L-[³⁵S] methionine. NS0 cells from a batch fermentation were removed from the fermenter at various time points (lag phase, day 1; exponential phase, day 3 and 5; and death phase, day 7). The cells (2×10^6 cells) were then re-suspended in 150 μ L of IMDM methionine free medium (Sigma). The re-suspended cells were then aliquoted into 1×10^6 cell lots and added to two wells of a 24 well plate (Beckton-Dickinson., Oxford, U.K.). [³⁵S] methionine label (10 μ Ci) (Amersham Biosciences) was then added to each well. After 1 hour, the plate was agitated, the cells removed from each well and placed into a 15 mL centrifuge tube. The samples were then pelleted by centrifugation at 50 x g for 5 minutes at room temperature in a bench top centrifuge. The supernatant was then carefully removed and kept at -70°C for liquid scintillation analysis (see below for TCA precipitation of cell free supernatant) (section 2.9.1.2). The remaining pellets were washed twice by centrifugation at 50 x g for 5 minutes at room temperature with 1 mL PBS buffer.

One of the cell pellets was lysed by adding 100 μ L 2% (w/v) SDS. The other pellet (that was to be carried forward for 2-D electrophoresis and autoradiography) was given a further wash with 0.35 M sucrose (5 mL) and then extracted in 400 μ L of lysis buffer 2 (Table 2.1). Cellular debris was then removed by passing both cell lysates through a 0.2 μ m ultracentrifuge filter (Millipore., Watford, Hertfordshire, U.K.), and samples were kept for liquid scintillation analysis (see below for TCA precipitation of the cell pellet) (section 2.9.1.2).

2.9.1.1 TCA Precipitation of the Cell Pellet

Trichloroacetic acid (TCA) (10% (w/v), 1 mL) was added to 50 μ L of lysed cells (either in SDS or lysis buffer) and cooled on ice for 1 hour. The precipitated protein was then collected on glass-fibre (GF/C) filters (Whatman., Maidstone, Kent, U.K.) using a vacuum manifold (Millipore., Watford, Hertfordshire, U.K.). The filters were washed twice with 1 mL of PBS, followed by 1 mL of 95% (v/v) ethanol and dried. The filters were then covered with 2 mL of scintillation fluid [OptiPhase HiSafe 3 (Eg & G Wallac., Milton Keynes, U.K.)] and subjected to liquid scintillation counting.

2.9.1.2 TCA Precipitation of Cell Free Supernatant

The amount of [³⁵S] methionine labelled protein within the cell culture supernatant was determined by adding 1 mL of trichloroacetic acid (10% (w/v)) to 50 μ L of supernatant which was then cooled on ice for 1 hour. The precipitated protein was collected as previously described on glass-fibre GF/C) filters (Whatman) using a vacuum manifold (Millipore). The filters were washed twice with 1 mL of PBS, followed by 1 mL 95% (v/v) ethanol and dried, before being covered with 2 mL of scintillation fluid [OptiPhase HiSafe 3 (Eg & G Wallac., Milton Keynes, U.K.)] and subjected to liquid scintillation counting. The amount of [³⁵S] methionine label remaining within the cell-free supernatant was determined by subjecting 10 μ L of cell supernatant to liquid scintillation counting.

2.9.2 2-D PAGE and Autoradiography of [³⁵S] Labelled Proteins

After TCA precipitation and scintillation counting of the samples extracted in lysis buffer 2, 1 x 10⁶ cpm for each sample (day 1, 3, 5 and 7 of batch culture) was loaded in a 350 μ L volume onto 18 cm, pH 3-10 NL IPG strips. The IPG strips were then run as detailed in Table 2.3. After completion of the run, the IPG strips were washed with ddH₂O, and then equilibrated for the second dimension separation (section 2.6.3). The IPG strips were then sealed to the second dimension gel and run using a Protean II Xi gel tank (Bio-Rad) using the programme detailed in Table 2.8. After the run was completed the gels were stored separately in gel boxes containing 1% acetic acid to fix the proteins in the gels and stored at 4°C overnight. The following day, the fixative was removed and gels were exposed to Amplify™ fluorographic reagent (Amersham Biosciences) to increase the [³⁵S] signal sensitivity, the gels were dried with filter paper and then exposed to Hyperfilm™ MP, ECL (Amersham Biosciences), in autoradiography cassettes and stored for 4 weeks at -70°C

2 Materials and Methods

before developing automatically using a Hyperprocessor (Amersham Biosciences). The resultant autoradiograph images were then captured using a scanner at 200 dpi and 256 greyscales in transmissive mode followed by analysis using ImageMaster™ software as detailed in section 2.7.4, except protein spots were detected using the following parameters (Sensitivity 9500, Noise factor 5, Operator size 99 and Background 33). Some manual editing was required especially for larger protein spots using an edge grow tool and manual splitting tools, which reduced individual user input errors. Protein spot matching was achieved by planting User Seeds followed by automatic matching, and individual protein spot volumes were normalised according to the total spot volume resulting in values that were comparable between data sets.

Chapter 3 Development of the Proteomic Technology Platform

3.1 Introduction

Proteome analysis attempts to 'quantitatively analyse the protein complement of a genome' (Verhaert et al., 2001), for example, to compare differences between a control and a diseased tissue type to analyse the mechanisms of gene expression and control that result in the disease state. It has now been documented in several reports that there is often a poor correlation between DNA or mRNA levels and the level of active functional protein expressed within a given system (Gabor Miklos and Maleszka, 2001; Smolke and Keasling, 2002). Furthermore, it has also been estimated that 40% of putative genes from sequenced genomes have no function assignable by homology searches (Westbrook et al., 2001). Therefore, by studying the proteome of a cell or tissue type, global changes in the level of protein expression and their post-translational modifications can be directly investigated by 2-D electrophoresis, which, to date, cannot be studied in detail using any other technique alone (Lopez, 2000; Yanagida, 2002). The core technique of proteomics has remained virtually unchanged since its initial impact in 1975 when O'Farrell first published the method of 2-dimensional sodium dodecyl sulphate polyacrylamide gel electrophoresis (2-D PAGE) (O'Farrell, 1975), although the technology (hardware) has improved dramatically in recent years. Two-dimensional SDS-PAGE involves the separation of proteins from within complex mixtures on two different physical parameters; on the basis of charge in the first dimension separation by isoelectric focussing (IEF), and the second dimension involving the separation of proteins by size utilising SDS-PAGE (Herbert et al., 1997). However, due to the inherent difficulties in obtaining a reproducible 2-D gel pattern and also in achieving total proteome coverage (that is, a 2-D gel image that represents all proteins within a given sample at the time of initial sampling and extraction) the technology is not ideally suited for such investigations. Other current technologies that exist, however, are incapable of separating all proteins within a sample simultaneously and, therefore, 2-D PAGE currently remains the fundamental technology for proteome analysis (Zhou et al., 2001).

Unlike the genome, the proteome for any given organism is not 'fixed'. The proteome is a dynamic system (Fey and Larsen, 2001), which constantly changes due to alterations in the environment, and during different stages of the cell-cycle (Wasinger and Corthals, 2002). The amount of 'active' protein is also controlled by production and

degradation rates (Oh-Ishi and Maeda, 2002), and at any one time a gene may be expressed at different levels and translated into different functional products, for example, by alternative splicing or post-translational modifications (Kettman et al., 2002). Proteins may have a different mode of action depending upon their cellular location, and may also have different functional lifetimes and half-lives (Gabor Miklos and Maleszka, 2001). Therefore, due to the inherent differences in the pattern of gene expression it is very difficult to obtain a truly representative picture of the proteome with current technologies, but with 2-D electrophoresis a real-time 'snap-shot' of the pattern of cellular proteins can be obtained (Yanagida, 2002). New technologies (including zoom gels which separate proteins over narrow pI ranges) mean it is now possible to separate up to 10000 proteins in any one experiment, when a composite image is analysed (Gorg et al., 2000b). Despite the difficulties of 2-D PAGE, it is unsurpassed in terms of resolving power, and is currently the only technology capable of separating thousands of proteins within complex mixtures from a single extract (Zhou et al., 2001).

In order to achieve good reproducibility of 2-D gels, it is important to note that compromises need to be made. Sample preparation is arguably the most important step in proteome analysis and this initial stage of preparation must be optimised for each cell type and kept as simple as possible to limit proteome bias. However, during protein solubilisation, there is likely to be a play off between proteins that are easy to solubilise and those that are not (Harry et al., 2000; Molloy, 2000). Proteins which play a pivotal role in cell functioning are also most likely to be proteins of the lowest abundance (Kettman et al., 2002; Oguri et al., 2002), and therefore it is unlikely these proteins will be visualised using current technologies due to limitations in staining techniques. Furthermore, proteins that are more basic together with those which are hydrophobic (such as membrane proteins) may also be difficult to focus or 'lost' during the first dimension separation (Harry et al., 2000; Lopez, 2000). These difficulties must be taken into consideration when choosing a solubilisation method, and the investigator must be clear whether the aim is to produce the most accurate representation of the proteome or whether the end result should be the most reproducible 2-D gel pattern.

In mammalian systems it is also possible to carry out cell fractionation techniques which enable cellular compartments to be separated; for example, mitochondrial or microsomal fractions (Galeva and Altermann, 2002; Hanson et al., 2001; Lopez, 2000). However, it must be recognised that the proteome may become compromised with selective protein losses with each subsequent manipulation in sample preparation, resulting

in a false representation of the sample proteome; therefore quantitative analysis may not be possible.

Recent improvements in 2-D PAGE technology in the form of IPG DryStrips with immobilised pH gradients and zoom gels have resulted in a significant increase in gel reproducibility and proteome coverage. Furthermore, 2-D gel image detection software for accurate quantitative analysis of protein expression has also been more highly developed in recent years (Butt et al., 2001; Miller Jr et al., 2001). The accurate analysis of complex 2-D gel images is highly dependent on computer analysis and data processing. This results in the production of protein expression databases, which enable the identification of proteins that are up- or down-regulated between samples or multiple gels of the same sample and most importantly allow quantitative analyses to be undertaken (Harry et al., 2000). There have also been many technological improvements in the identification of proteins from within 2-D gels in the form of the Q-TOF MALDI-ms and databases available on the Internet (Butt et al., 2001; Verhaert et al., 2001).

The following chapter describes the development and optimisation of a proteomic platform which has been implemented to accurately investigate (1) changes in the NS0 cell proteome throughout batch culture and (2) differential expression in NS0 cell transfectants exhibiting different levels of productivity in order to identify proteins involved with recombinant protein production in NS0 cells.

3.2 Results

3.2.1 NS0 Cell Growth

NS0 cells were routinely cultured in 10% or serum-free IMDM medium as previously described (chapter 2, section 2.2.2). For experiments cells were either cultured to 100 mL volume in Erlenmeyer flasks or in spinner vessels to 350 mL or 1 L volume. An example of the growth of NS0 cells under standard batch conditions in a 350 mL spinner vessel is shown in Figure 3.1 below. NS0 cell cultures were inoculated at 2.25×10^5 cells mL^{-1} and samples were taken daily to assess the characteristics of cell growth and cell viability, together with cell-free supernatant samples for glucose and lactate determination (chapter 2, section 2.9.9.1 and 2.9.9.2 respectively). During culture the cells grew exponentially for approximately 5 days after inoculation attaining a final viable cell density of 14.8×10^5 cells mL^{-1} . During the batch culture very little glucose was utilised (Figure 3.1), although glucose was utilised by the cells during exponential growth phase and the onset of a decline in viable cell density was observed to coincide with the reduced glucose level. The concentration of lactate was not observed to increase significantly during batch culture (Figure 3.1).

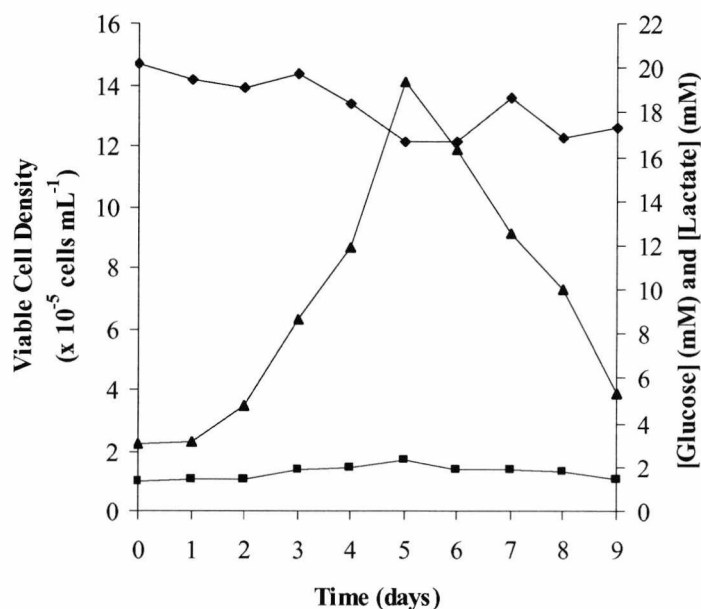


Figure 3.1 Typical batch culture growth of NS0 cells expressing a recombinant IgG₁ grown in IMDM medium supplemented with 10% dFCS in a 350 mL spinner. Samples were taken at the times indicated to determine the viable cell density (\blacktriangle), glucose (\blacklozenge) and lactate (\blacksquare) concentration during the course of the culture. Results are derived from one single batch culture experiment.

3.3 Optimisation of Whole Cell Protein Solubilisation and Recovery

3.3.1 Methods of Cell Lysis

In order to carry out proteome analysis by 2-D PAGE, NS0 cells must be disrupted to liberate cellular contents (Molloy, 2000). Chemical detergents were utilised routinely for the extraction of NS0 cell proteins as mammalian cells are easily extracted under gentle lysis conditions (Gorg, 1998). However, the extraction procedure can liberate enzymes such as proteases. Therefore cells were exposed to an extraction buffer containing high concentrations of detergents and reducing agents to inhibit proteolysis of extracted proteins. Two chemical based detergents (chapter 2, section 2.4.2) were investigated to determine which gave the maximum protein solubilisation efficiency and recovery conditions.

3.3.2 Quantitative Assessment of Protein Solubility

All samples were sourced from a batch culture of NS0 cells in IMDM medium supplemented with 10% dFCS in a 350 mL spinner vessel (Figure 3.1). Cells were cultured until they reached mid-exponential phase of growth and were then extracted according to the method outlined in chapter 2, section 2.4.3. Samples were then analysed for protein content by the modified Bradford assay (chapter 2, section 2.4.4) followed by mini-gel 2-D PAGE analysis to rapidly assess protein solubilisation, recovery and 2-D gel resolution (chapter 2, section 2.6.1, 2.6.7 and 2.7.4.2). Figure 3.2 represents the protein yield from two solubilising buffers used to extract NS0 cell samples (1×10^7 cells) derived from the same batch culture of NS0 cells extracted at mid-exponential and death phase of growth. Cells were also extracted in a sample buffer containing DNase/RNase. However, the protein content of samples extracted in buffers containing DNase/RNase could not be measured by the modified Bradford assay as they contained β -mercaptoethanol, which interferes with the assay. This extraction buffer was therefore not utilised further in this study.

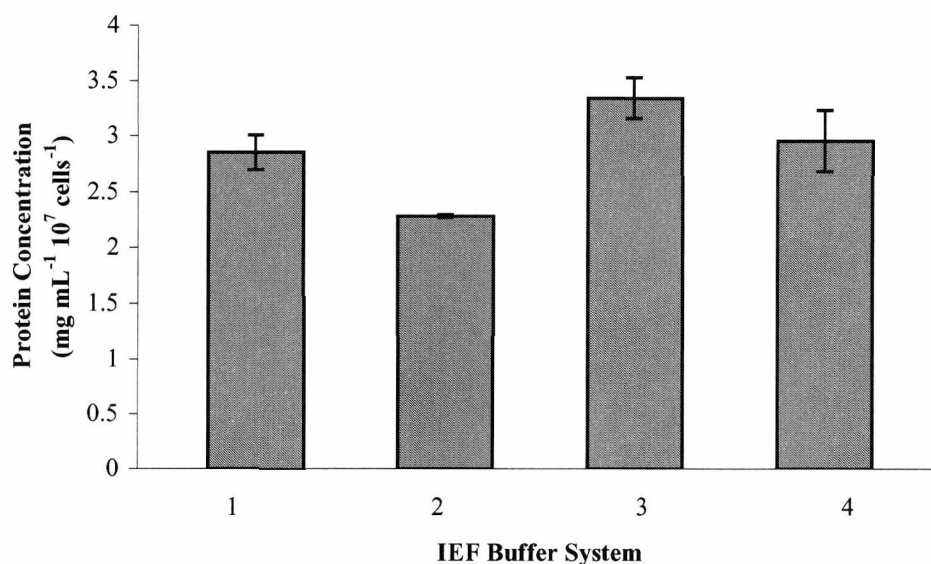


Figure 3.2 The protein yield using two lysis buffers from 1×10^7 NS0 cells extracted in a 400 μL volume in triplicate during mid-exponential phase and death phase of growth. 1. Lysis Buffer 1, mid-exponential phase extract. 2. Lysis Buffer 1, death phase extract. 3. Mid-exponential phase NS0 cells extracted in Lysis Buffer 2, and 4. NS0 cells extracted in Lysis Buffer 2 at death growth phase. Error bars represent the standard deviations derived from three replicate samples each assayed in triplicate.

The results from the modified Bradford assay show that the protein yield with both solubilising buffers (lysis buffer 1 and 2) (chapter 2, section 2.4.2) was similar, although the protein yield from NS0 cells during death phase was less for each solubilising buffer than that obtained from cells extracted during mid-exponential phase of growth. The reduction in protein recovery was due to the increased number of dead cells present at death phase of growth and the reduced number of viable cells. In order to obtain the same number of 1×10^7 viable cells for extraction at death phase of growth, a larger volume of cells was required which resulted in a larger pellet requiring solubilisation. Therefore, the number of cells fully solubilised in the set volume of 400 μL was reduced. In order to qualitatively and quantitatively assess which lysis method resulted in the most highly resolved 2-D gel pattern, mini 2-D gels were carried out on extracts of NS0 cells in both detergents at mid-exponential phase of growth.

3.3.2.1 Assessment of Protein Solubility and Recovery using Mini 2-D Gel Electrophoresis

In order to optimise 2-D gel resolution and NS0 cell proteome coverage the two solubilising buffers (chapter 2, section 2.4.2) were assessed. For each solubilising condition, the extraction procedure was carried out on at least 10 samples of NS0 cells and a modified Bradford assay was carried out to assess protein content on each sample

3 Development of the Proteomic Technology Platform

(chapter 2, section 2.4.3 and 2.4.4). One extract (with the median protein content) from each solubilising condition was then subjected to mini 2-D gel electrophoresis for rapid method development using 7 cm, pI 3-10 IPG strips for the first dimension separation (chapter 2, section 2.6.1 and Table 2.3), and Invitrogen (7 x 7cm, 1 mm thickness) 4-20% Tris-glycine, pre-cast mini gels for the second dimension (chapter 2, section 2.6.7). The resultant mini 2-D gels were visualised using the Shevchenko silver staining method (chapter 2, section 2.7.1) followed by scanning and importing the resulting digital image into ImageMaster™ 2-D Elite software to detect the total number of protein spots on each 2-D gel (chapter 2, section 2.7.4) (Table 3.1 and Figure 3.3).

Table 3.1 Number of protein spots visualised with silver stain on 2-D mini-gels using the two solubilising conditions described in the methods section. Gel images were analysed by ImageMaster™ 2-D Elite software to detect the average total number of protein spots present on each mini 2-D gel

Lysis Buffer	Total Visualised Protein Spots with pI 3-10 NL Resolving Range
Lysis Buffer 1	464
Lysis Buffer 2	480

The image analysis software detected the total number of protein spots for two repeat mini 2-D-gels run for each solubilising condition. Two sample mini 2-D gel images together with the image analysis of whole NS0 cells extracts in lysis buffer 1 and 2 are shown below in Figure 3.3.

3 Development of the Proteomic Technology Platform

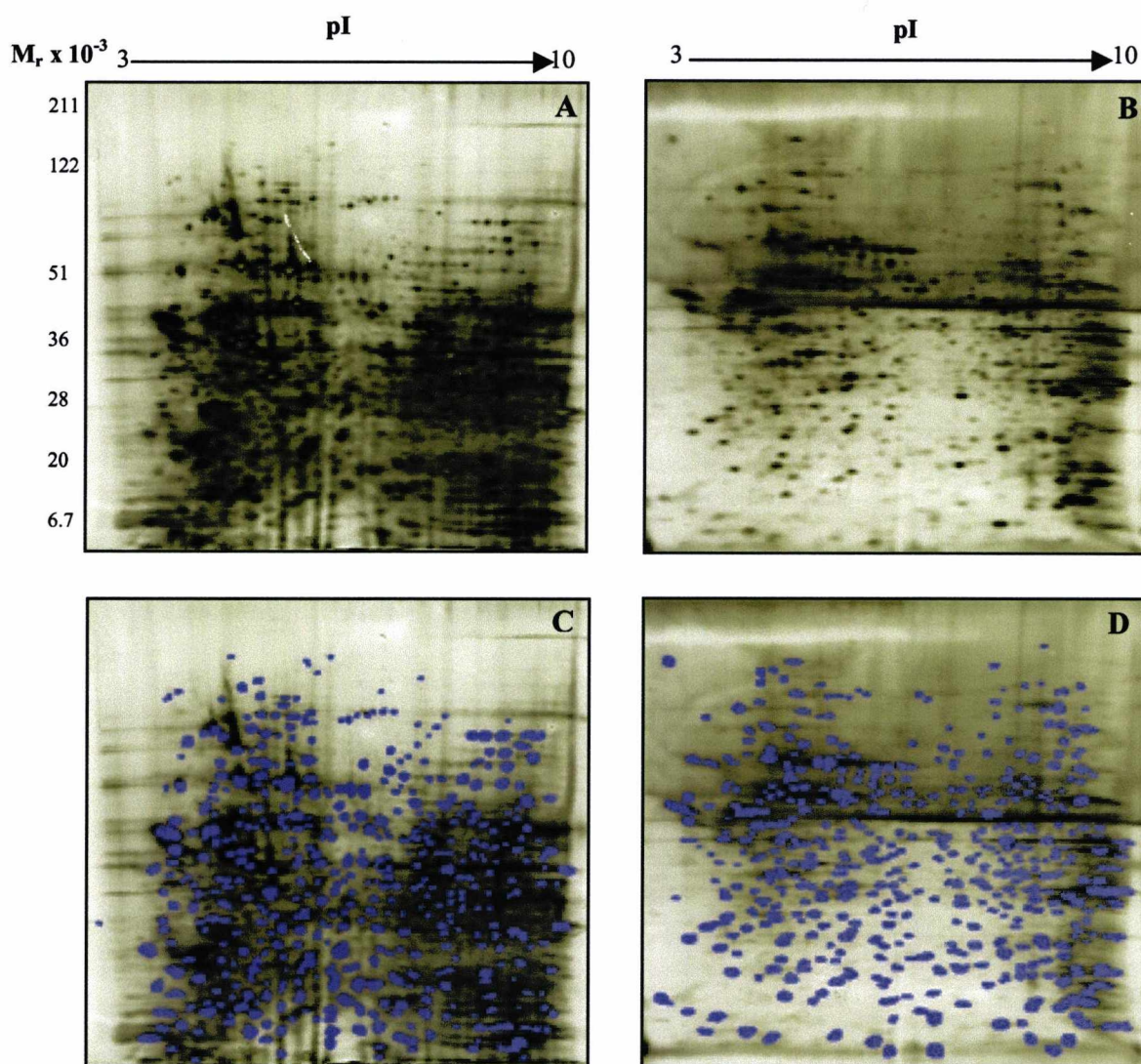


Figure 3.3 Mini 2-D PAGE of whole NS0 cells extracted from 1×10^7 cells using two different solubilising buffers. A, Mini 2-D PAGE of whole NS0 cells extracted using Lysis Buffer 1, visualised with silver stain. B, As for A except whole NS0 cells extracted using Lysis Buffer 2. Figure C, digital image displaying 464 discrete protein spots from Figure A using ImageMaster™ 2-D Elite software and D, 480 protein spots detected in Figure B analysed by ImageMaster™ software.

The above Figure clearly shows that good reproducibility of protein spot patterns was obtained with both lysis solutions. Both lysis buffers yielded a good depiction of the NS0 cell proteome with low abundance proteins well represented. However, when NS0 cells were extracted in lysis buffer 2, followed by subjection to 2-D electrophoresis, a gel of higher resolution was obtained with sharper protein spots and lower background staining, producing a superior image that was more suitable for analysis by 2-D software. The extract solubilised in lysis buffer 1 also liberated DNA resulting in a viscous protein solution; therefore sample handling was made more difficult particularly with respect to pipetting and protein loading. As a result lysis buffer 2 was chosen as the lysis solution for

all further standard procedures. Although the image analysis of these images was not detailed it enabled a quantitative assessment of each 2-D gel to be undertaken and therefore analysis was not only based on a qualitative assessment of protein solubilisation and 2-D gel resolution.

3.3.3 Quantitative Analysis of Protein Recovery from NS0 Cells

In order to reduce proteome bias towards proteins that are easy to solubilise and those that are not, the cell number to extraction buffer volume ratio was optimised to ensure total cell disruption. NS0 cells were seeded at 2×10^5 cells mL^{-1} and cultured in serum-free IMDM medium, in a 1 L volume spinner vessel (chapter 2, section 2.2.2.1). Once the cells had reached mid-exponential phase of growth, five extracts for each different NS0 cell number were prepared using 1×10^5 , 1×10^6 , 5×10^6 , 1×10^7 , 5×10^7 and 1×10^8 cells according to the method outlined in chapter 2, section 2.4.3. Each extracted sample was then assessed for protein yield by the modified Bradford assay outlined in chapter 2, section 2.4.4 and 2.7.4.1 (Figure 3.4).

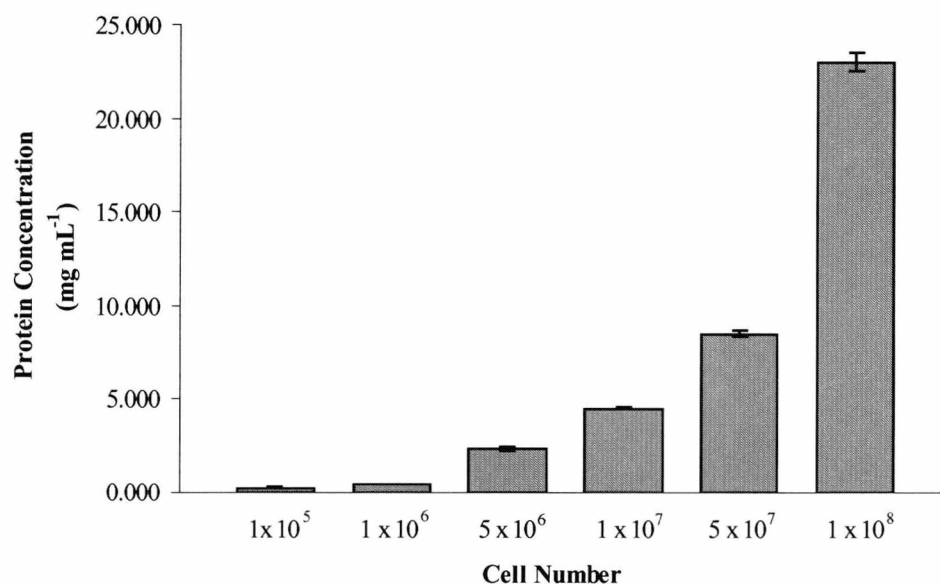


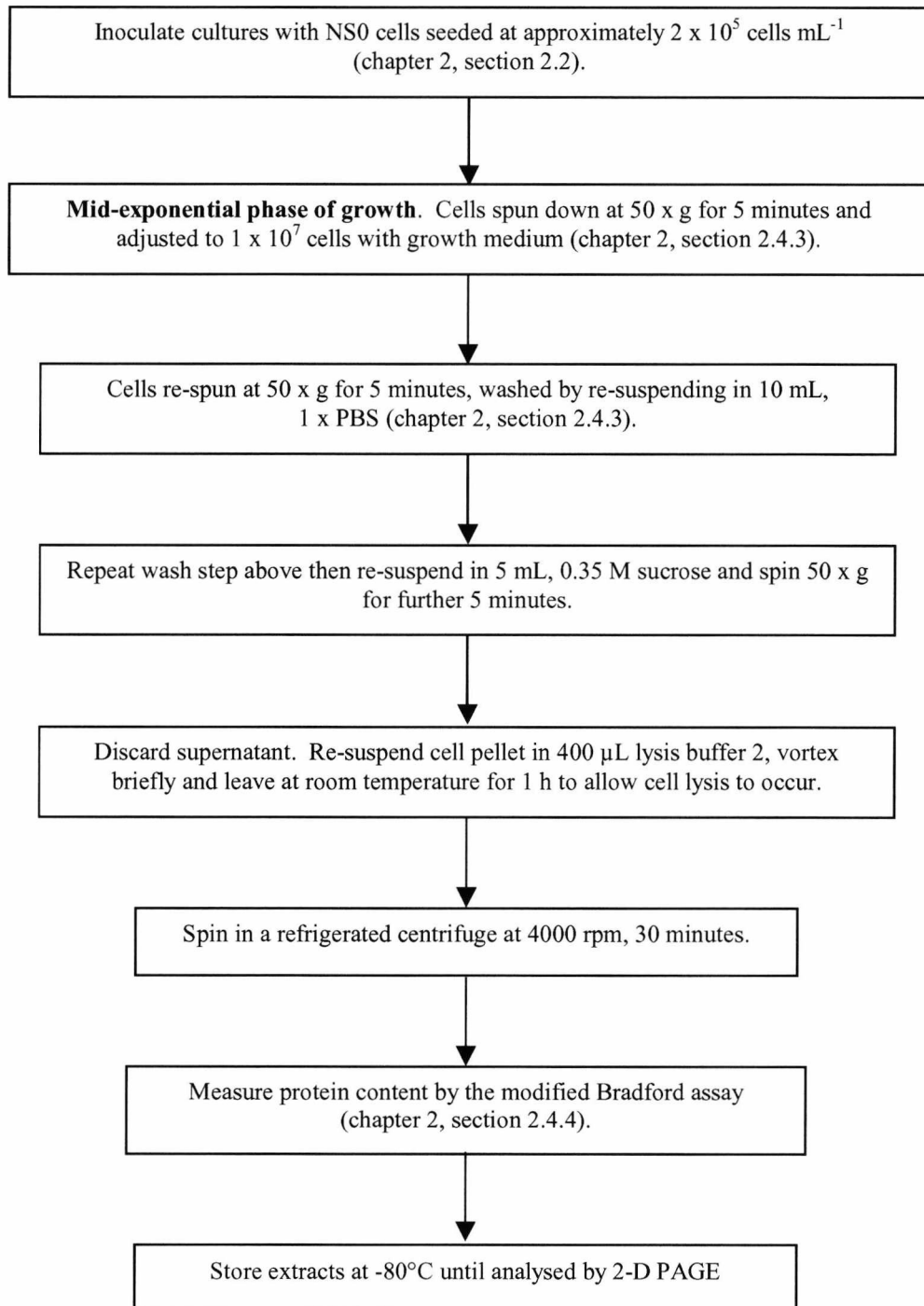
Figure 3.4 Quantitative assessment of protein recovery. Total solubilised protein content was determined from various cell numbers extracted at mid-exponential phase of growth. The data above is derived from NS0 cells extracted from samples of the same batch culture in $400 \mu\text{L}$ of Lysis Buffer 2. The protein concentration is based on the mean of at least three separate repeat sample preparations assessed by the modified Bradford assay in triplicate. The error bars represent the standard deviations based on at least three replicate samplings assayed in triplicate.

3 Development of the Proteomic Technology Platform

The Figure above shows the protein recovery obtained for different numbers of NS0 cells from the same batch culture extracted in a 400 μL volume of lysis buffer 2. The whole cell protein values are seen to increase with cell number, until 1×10^8 cells were extracted. The ratios of protein values between 1×10^6 and 1×10^7 are approximately 10:1, which correlates with the difference in cell number. The same can be seen for cell numbers 5×10^6 and 5×10^7 . However, at lower cell numbers of 1×10^5 and 1×10^6 the solubilised protein ratio is lower, and this is most likely due to loss of the cell pellet during the washing steps before extraction. Between 1×10^7 and 1×10^8 cells there is also a lower ratio of 5:1 observed for solubilised protein, which is probably as a result of the extraction buffer volume (400 μL). When this large number of cells was extracted, not all the cells would be solubilised due to the small volume of lysis buffer, leading to a bias in the proteome towards proteins that are more soluble. The proportional increase in protein recovery between 1×10^6 and 1×10^7 cells suggests that at cell numbers greater than 5×10^7 , the maximum solubilising power has been reached for that cell number and volume of solubilising buffer. As a result solubilisation of 1×10^7 cells in an extraction buffer volume of 400 μL was adopted for all further work, as if greater cell numbers were extracted in this volume a bias in protein solubilisation would occur, leading to an inaccurate representation of the protein complement when subjected to 2-D PAGE.

3.3.3.1 Optimised Scheme for Sample Preparation of Whole NS0 Cell Extracts

As a result of the development and optimisation of analytical technologies, a standardised protocol for the preparation of NS0 cells for whole cell extraction for analysis by 2-D PAGE was devised and is presented below (scheme 3.1).



Scheme 3.1 Optimised protocol for the preparation of whole NS0 cell extracts for 2-D electrophoresis.

3.3.4 Large Format 2-D SDS-PAGE using the Protean II Gel Tank

In order to investigate the whole NS0 cell proteome more accurately, large format 2-D electrophoresis was adopted. By increasing the size of the first and second dimension gels, separation of whole NS0 cell proteins could occur over a greater analytical area, increasing the total number of protein spots visualised. The transition to large format 2-D gel electrophoresis occurred in two parts. Firstly, NS0 cell proteins were solubilised using the optimised protocol (described in chapter 2, section 2.4.3 and scheme 3.1) and the transition to large format 2-D PAGE was achieved through implementing 18 cm IPG strips in replacement of 7 cm IPG strips. By increasing the size of the first dimension IPG strip to 18 cm, the maximum protein load could be increased from 10 µg to 80 µg when 2-D gels were to be visualised using silver staining methodology (chapter 2, section 2.6.1 and 2.7.1). The second dimension gel was also increased in size to 20 x 18 x 0.1 cm for separation using a Protean II gel electrophoresis tank (chapter 2, section 2.6.8). Figure 3.5A below shows an example of a large format 2-D gel run using the Protean II gel tank.

3.3.4.1 Protean II versus DALT II Gel Tanks

Although large format 2-D gels run on the Protean II gel tank were quantifiable, only 4 gels could be run simultaneously in two tanks powered by the same power pack; therefore gel reproducibility was a problem. In order to overcome this, a DALT II tank (chapter 2, section 2.6.9) was utilised in replacement of the Protean II gel tank. The DALT II gel tank is capable of running 12 large format pre-cast or self-cast 2-D gels (26 x 20 x 0.1 cm) simultaneously. Due to the larger size of the second dimension SDS-PAGE gels, the protein load for the first dimension separation of 24 cm pI 3-10 non-linear IPG strips could also be increased further to 100 µg. These changes resulted in a further increase in the number of protein spots visualised on each 2-D gel together with improved reproducibility between 2-D gels when compared against the 2-D gels run using the Protean II gel tank. Figure 3.5 compares two gels run using the same sample of whole NS0 cell proteins separated using the Protean II and the DALT II SDS-PAGE systems and visualised with silver stain.

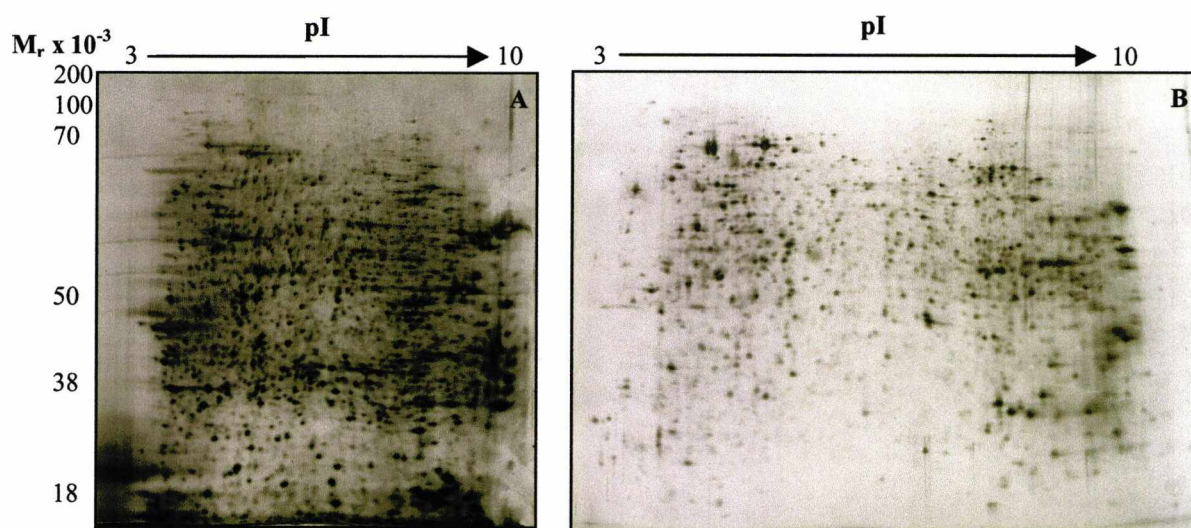


Figure 3.5 Comparison of NS0 whole cell extract analysis by 2-D PAGE, pI 3-10 non-linear resolving range. A, 12.5% self-cast large format 2-D gel (20 x 18 x 0.1 cm) of whole NS0 cell extract (80 μ g protein load) using the Protean II xi vertical electrophoresis gel tank, visualised with silver stain and B, 12.5% pre-cast 2-D gel (26 x 20 x 0.1 cm) of NS0 cell extract (100 μ g protein load) run on the DALT II electrophoresis system.

The first dimension separation was completed using an IPGphor system and 18 cm or 24 cm, pI 3-10 non-linear IPG DryStrips according to the method described in chapter 2, section 2.6.1. The Figure above allows the comparison of whole NS0 cell proteins separated using the Protean II xi Cell vertical electrophoresis system (A) and the Ettan DALT II electrophoresis tank (B). The gel shown in Figure 3.5B was run in the second dimension using a pre-cast, 12.5% backed gel. In this format the gels do not stretch or shrink as part of the staining process, which further increases the reproducibility of the 2-D gel images. This is very important for analysis of multiple gel images by ImageMaster™ software. However, since the gels are backed the capability of the proteins to enter the gel is reduced leading to a reduction in the number of protein spots visualised on each gel when compared against those run using self-cast SDS-PAGE gels. Table 3.2 shows a comparison of the number of discrete protein spots detected using ImageMaster™ software for 2-D gels run using the Novex mini gel system, Protean II and DALT II gel systems for the second dimension separation of NS0 cell proteins.

Table 3.2 Number of protein spots visualised with silver stain detected using ImageMaster™ software

Electrophoresis System	pI Range	Gel Size (cm)	Total Number of Protein Spots Detected
Novex Mini Gel	3-10 NL	7 x 7	450
Protean II xi Cell	3-10 NL	20 x 18	1500
DALT II	3-10 NL	26 x 20	1700

From Table 3.2 above it can be clearly seen that the Protean II and DALT II gel tanks significantly increase the total number of protein spots separated and detected on 2-D gels when compared to the Novex mini gel tank system. Although the total number of protein spots detected using the Protean II tank is similar to those obtained using the DALT II system, the DALT II tank simplified 2-D electrophoresis. The DALT II tank is capable of running 12 gels simultaneously, and 12 IPG strips could also be run simultaneously for the first dimension separation using the IPGphor, this minimised run-to-run variability and greatly simplified the downstream image analysis of the 2-D gel images. Only 4, 18 cm IPG strip holders were available for the separation of proteins in the first dimension, which were run in the second dimension using the Protean II tank. This further increased sources of variation in the 2-D process when comparing more than 4 gels and as a result large differences occurred in 2-D gel spot patterns run from the same sample, which led to complications in image analysis of the 2-D gels. Therefore, by utilising the IPGphor to separate 12 samples simultaneously, together with utilisation of the DALT II gel tank, reproducibility was greatly improved. The use of self-cast gels for separation using the DALT II tank therefore superseded the Protean II xi gel tank for large format protein separations.

3.3.5 Selection of IEF pI Resolving Range

The utilisation of the large 2-D gel format increased the range over which proteins could be separated and resulted in an increase in the number of proteins visualised, including those of lower abundance, when 18 and 24 cm IPG strips were implemented for the first dimension separation. However, due to the broad range separation necessary to visualise the whole NS0 cell proteome, the first dimension resolving range had to be optimised. Therefore, large format 2-D gels were run using pI 3-10 linear and non-linear IPG strips to investigate which produced 2-D gels with the best resolving range (Figure 3.6).

3 Development of the Proteomic Technology Platform

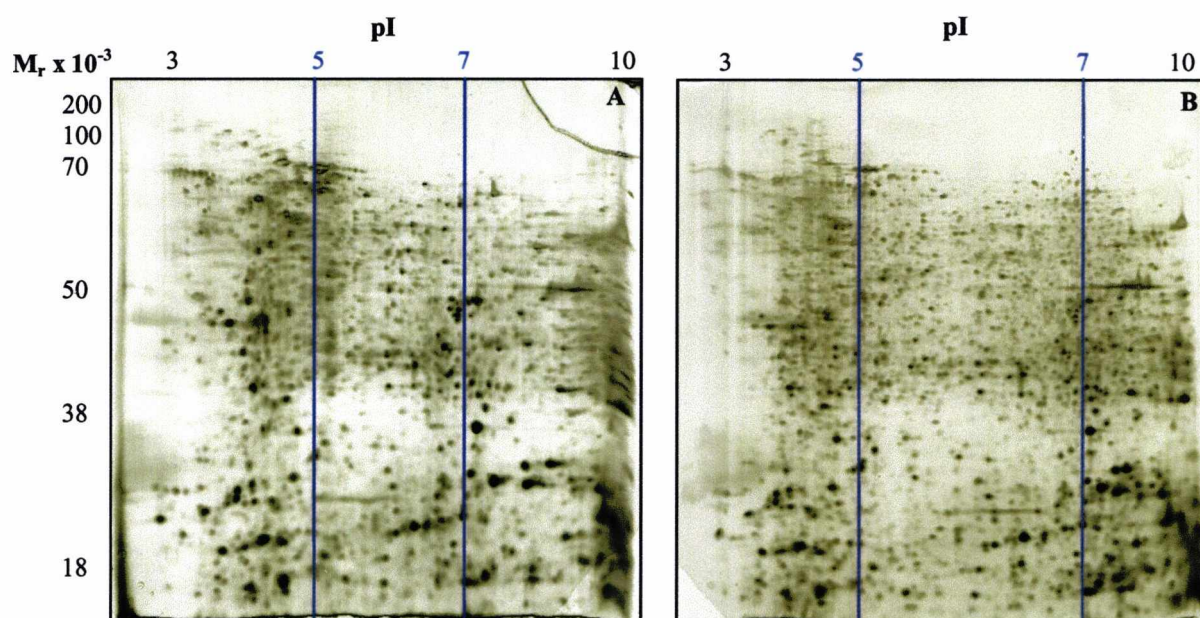


Figure 3.6 2-D PAGE images of whole NS0 cell extracts separated in the first dimension using pI 3-10 broad resolving range. Figure A, large format (20 x 18 x 0.1 cm) 2-D gel separated in the first dimension by pI 3-10 linear resolving range with approximately 1200 protein spots detected by ImageMaster™ software. The gel has been sub-divided to show the pH region between pH 5-7. Figure B, large format 2-D gel separated using a pI 3-10 non-linear resolving range, divided to show the region of increased resolution between pH 5-7 with approximately 1500 protein spots detected with ImageMaster™ software.

The Figure above shows the resolving range of 18 cm, pI 3-10 linear and non-linear IPG strips run using a Protean II gel tank for the second dimension separation. The linear range pI 3-10 IPG strip enabled an overview of protein distribution to be obtained. An estimate of the proteins' isoelectric point could also be obtained relatively easily. However, the basic region of gels run with a linear gradient were not well resolved. When a non-linear pI 3-10 gradient was employed the proteins were more evenly distributed across the second dimension SDS-PAGE gel with increased resolution between pI 5-7. When the images were assessed by ImageMaster™ 2-D Elite software in the extended pI 5-7 region on the non-linear pI 3-10 gradient 677 proteins were detected, which accounted for nearly 50% of the total protein spots detected on the gel. The non-linear gradient resulted in more protein spots visualised on the gel when compared against the linear gradient, which detected 468 protein spots within the same pI 5-7 region, accounting for approximately 40% of the total protein spots detected on the gel. The total number of discrete protein spots visualised on the non-linear gradient gels was also increased with approximately 1500 protein spots detected, whereas on the linear gradient gels approximately 1200 protein spots were detected. The more basic region of the gel between

pH 7-10 was also more greatly resolved when a non-linear gradient was utilised, albeit over a smaller gel area. The stretched out region between pH 5-7 with the pI 3-10 non-linear IPG strips was advantageous as many proteins involved with protein folding and energy metabolism occur within this pI range of 5-7. Therefore pI 3-10 non-linear range IPG strips were utilised for all subsequent standard protocols.

3.3.5.1 Selection of SDS-PAGE Gel Composition

Together with the optimisation of the first dimension IPG DryStrip resolving range, it was necessary to optimise the second dimension gel acrylamide composition to enable the greatest coverage of proteins present within the sample. A range of gels was tested for proteome coverage including 11%, 11.5%, 12% and 12.5% acrylamide. Table 3.3 below shows the approximate resolving ranges for various acrylamide concentrations.

Table 3.3 Maximum resolving range for proteins separated on single percentage SDS-PAGE gels

Acrylamide in Resolving Gel (%)	Approximate Separation Range ($M_r \times 10^{-3}$)
10	14-200
11	14-175
11.5	14-150
12	14-125
12.5	14-100
15	14-60

A major problem associated with 2-D PAGE is the failure of large molecular weight proteins of greater than 150 kDa to migrate into the second dimension gel (Harry et al., 2000; Yanagida, 2002). In Table 3.3 above it can be seen that if a greater concentration of acrylamide is utilised, selective protein losses will occur in the upper range of the gel with larger proteins not transferring into the gel. The opposite can be seen if a lower percentage gel is utilised. Figure 3.7 below shows large format 2-D gels of whole NS0 cell proteins run using pI 3-10 non-linear IPG strips for the first dimension, separated in the second dimension using different percentage gels. It can clearly be seen that at lower percentages of acrylamide (11 and 11.5%), losses of proteins in the lower molecular weight region occur, with no apparent increase in the visualisation of proteins in the high molecular weight region of the gels. The optimum protein separation was observed when either a 12 or 12.5% acrylamide gel was utilised. As a result, gels of 12.5% acrylamide were routinely utilised for the second dimension as they enabled visualisation of the large

3 Development of the Proteomic Technology Platform

molecular weight proteins without undue loss of proteins in the low molecular weight region of the gel when compared against gels of lower concentrations of acrylamide.

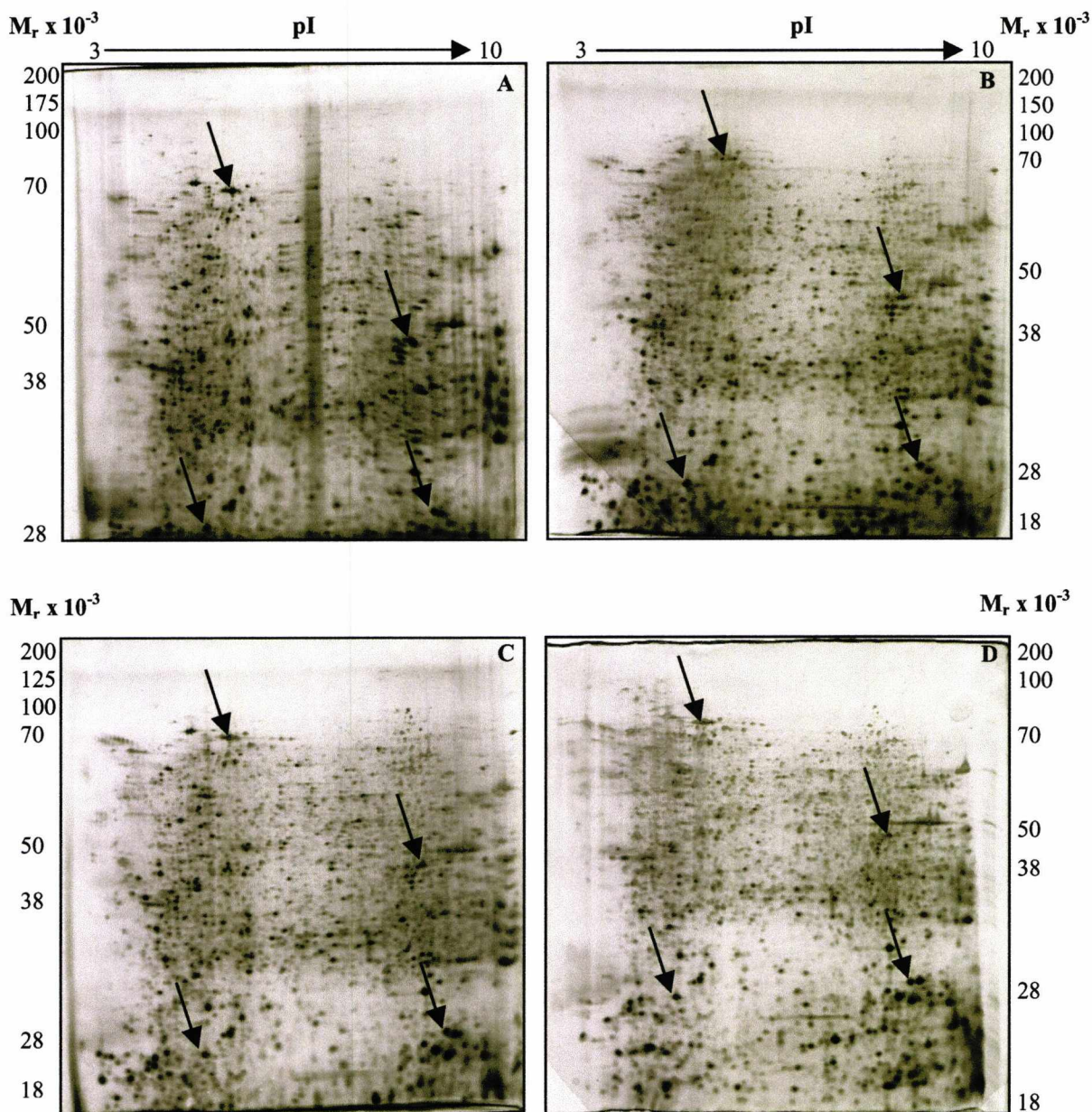


Figure 3.7 Comparison of whole NS0 cell proteins separated on different percentage second dimension gels. Figure A, large format 2-D PAGE separated in the first dimension by broad range pI 3-10 non-linear IPG strip, separated in the second dimension an 11% acrylamide SDS-PAGE gel, visualised by silver stain. Figure B, as for A except separation in the second dimension was on an 11.5% acrylamide gel. Selective loss of low molecular weight proteins is clearly visible with very few proteins below 18 kDa visible. Figure C, as for A except second dimension separation was on a 12% SDS-PAGE gel and, Figure D, a 12.5% acrylamide gel. The arrows indicate landmark proteins present in all gels showing the enhanced resolution of low molecular weight proteins on gels due to higher concentration of acrylamide, without loss of proteins of high molecular weight.

Figures 3.5, 3.6 and 3.7 clearly show that by implementing a strategy whereby whole NS0 cell proteins were focussed on 24 cm, 3-10 non-linear IPG strips followed by

separation in the second dimension by 12.5% acrylamide SDS-PAGE gels run using the DALT II electrophoresis gel tank and finally visualised with silver stain, an increased area over which whole NS0 cell proteins could be visualised was obtained together with increased separation, resolution and detection of protein spots. The gels were also more reproducible, and therefore the image analysis of the 2-D gels was simplified, resulting in less time being required to accurately analyse and quantify changes in protein expression between samples.

3.3.6 Protein Visualisation Methods

A variety of protein stains were assessed for protein visualisation on 2-D gels. Each protein stain was investigated on the basis of sensitivity of staining, ease of use, reproducibility and compatibility with ms (Lopez, 2000). Staining methods investigated included the PlusOne and Shevchenko silver stains (Shevchenko et al., 1996) (chapter 2, section 2.7.1 and 2.7.2) and colloidal Coomassie (Patton, 2002) (chapter 2, section 2.7.3). Other staining methods including SYPRO[®] Orange and Ruby were also assessed (Lauber et al., 2001). However, due to costs and equipment needs the use of these stains was prohibitive (Patton, 2002). The approximate limits of sensitivity and the linear range for each of these stains are given in Table 3.4 below.

Table 3.4 Limits of sensitivity for various protein stains

Protein Stain	Limit of Sensitivity	Linear Dynamic Range
Coomassie Blue	50-100 ng	10-30 fold
Colloidal Coomassie	20 ng	10-30 fold
SYPRO [®] Orange/Red	10 ng	1000 fold
SYPRO [®] Ruby	3-5 ng	1000 fold
Silver Stain Plus	5-10 ng	10 fold
Shevchenko Silver Stain	3 ng	10 fold
PlusOne Silver Stain	3 ng	10 fold

Figure 3.8 below shows 1-D mini-gels of standard protein concentrations stained with two different silver and colloidal Coomassie stains. Each sample was loaded on self-cast 12.5% Tris-glycine 1-D mini-gels and run using a Novex mini-gel system (chapter 2, section 2.5.2 and Table 2.7). For mini gel A and B, a standard mixture of proteins of known molecular weight (HSA, 60 kDa; and lysozyme, 14 kDa) were used to generate a dilution series ranging from 2000 ng to 1.9 ng of total protein to assess the limit of sensitivity for each staining method. The two standard proteins making up the dilution

series were mixed together and loaded into separate lanes as described in Figure 3.8. For mini gel C a standard protein mixture containing HSA and lysozyme was prepared as above except an additional protein, ovalbumin (30 kDa), was included in the sample mixture. The standard proteins were diluted to generate a dilution series ranging from 1000 ng to 1.9 ng and the highest standard was loaded into lane one as above. The proteins were then visualised using the different staining methods and assessed for the limits of sensitivity (chapter 2, section 2.7).

Figure 3.8 and Table 3.4 above show that the silver staining methods gave a higher sensitivity than Coomassie, providing the best visualisation of protein spots. The limit of detection for silver stained gels was approximately 1.9 ng protein. However, the linear range of each stain must also be taken into consideration. Silver staining methods have both the highest sensitivity and the lowest linear range of staining, and therefore the quantitative range of the stain is also very narrow (Gorg et al., 2000b; Patton, 2002). However, this range does encompass the range in which most proteins visualised on 2-D gels fall. Colloidal Coomassie has a mid-range sensitivity of staining and is also linear over a much wider range (Lauber et al., 2001). However, due to the relatively low sensitivity of this technique (20 ng), many proteins present on 2-D gels are not visualised, and therefore, this method of staining could not be used for analytical protein loads. An experimental strategy was therefore devised whereby the first dimension IPG strips could be overloaded followed by 2-D PAGE and visualisation by staining with colloidal Coomassie to enable a more quantitative assessment of protein expression (Oguri et al., 2002) (chapter 2, section 2.6.1 and 3.6.6.1).

3 Development of the Proteomic Technology Platform

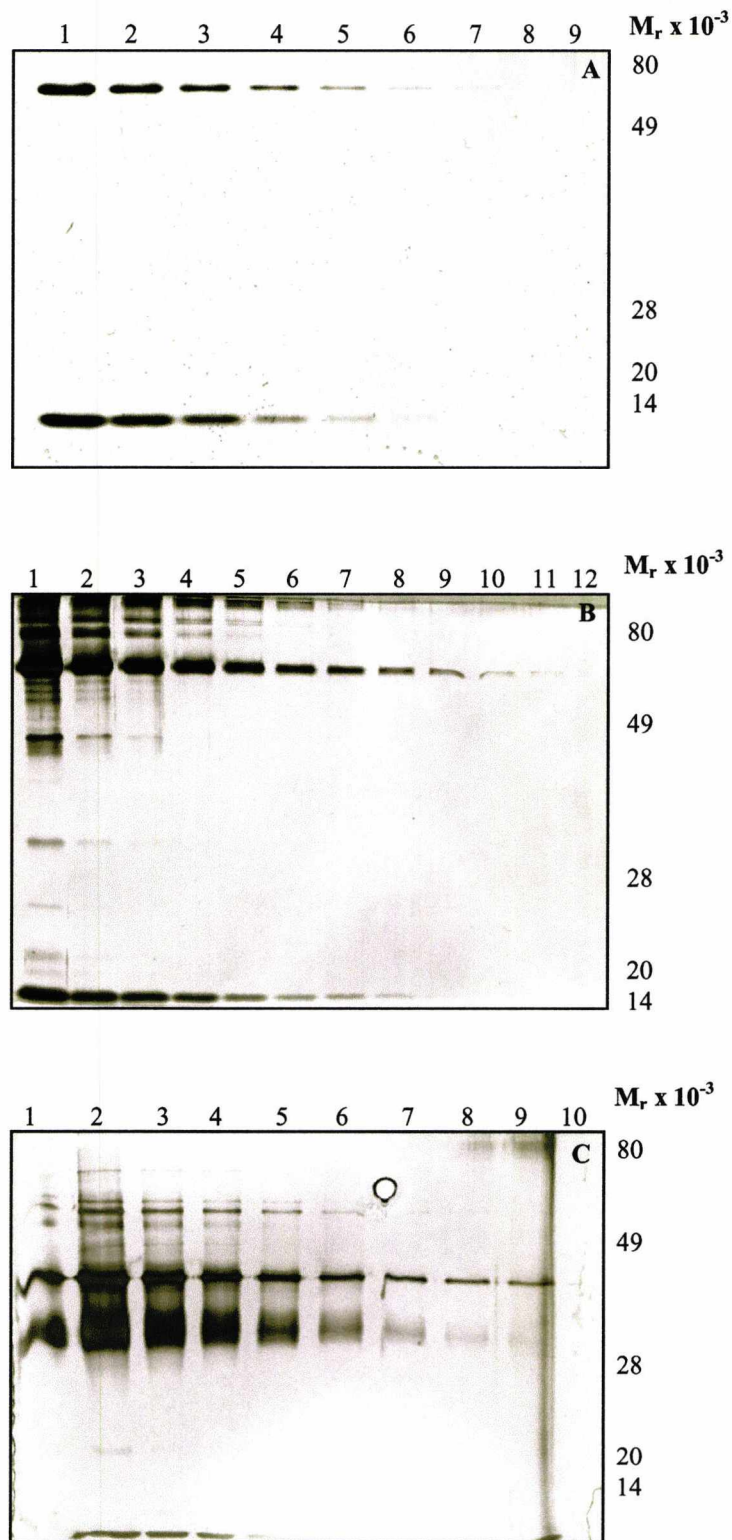


Figure 3.8 Comparison of 1-D mini gel images to assess the detection limits of different staining techniques. Figure A, Colloidal Coomassie stained 1-D gel separation of a standard protein mixture containing HSA and lysozyme diluted to give a series ranging from 2000 to 1.9 ng concentration. The two standard proteins making up the dilution series were mixed together and loaded into separate lanes, 2000 ng lane 1, 1000 ng lane 2, 500 ng lane 3, 250 ng lane 4, 125 ng lane 5, 62.5 lane 6, 31.25 ng lane 7, 15.6 ng lane 8, 7.81 ng lane 9, 3.9 ng lane 10, 1.9 ng lane 11. Figure B, as for A, except stained by the Shevchenko silver stain method. Figure C as for A except, the dilution series ranged from 1000 ng to 1.9 ng and included ovalbumin (30 kDa) in the standard protein mixture, followed by visualisation by the PlusOne silver stain method.

Shevchenko silver staining (Shevchenko et al., 1996) (chapter 2, section 2.7.1) was utilised for all initial staining procedures on 2-D gels although, problems were encountered when quantitative analysis of gels by ImageMaster™ software was implemented. Many of the most abundant protein spots over stained and in some cases, inversion of silver stained protein spots occurred causing negative values for individual spot intensities and volumes to be obtained when analysed by 2-D software (Gorg et al., 2000b). This staining method combined with the downstream analysis, did not provide a true representation of the NS0 cell proteome. The PlusOne silver stain method was therefore adopted (chapter 2, section 2.7.2). The PlusOne silver stain method did not lead to the inversion of staining with abundant protein spots, and thus a more quantitative assessment of protein expression could be achieved. The PlusOne silver stain is compatible with ms if the glutaraldehyde is omitted from the sensitisation step (chapter 2, section 2.7.2), and this method was therefore adopted as the standard staining method for all further work.

The quantitation of 2-D gels visualised by silver stain is based on the sum of pixel intensities for individual protein spots acquired from a scanned 256 grey-scale image analysed using ImageMaster™ 2-D Elite software (chapter 2, section 2.7.4). If a protein load of higher than 100 µg 350 µL⁻¹ (Gorg, 1998) was loaded on the first dimension 18 cm IPG strip, an abundant protein spot would have a lower measured total spot intensity than a protein spot of lower abundance, due to inversion of staining and the narrow linear/quantifiable range of silver stain. As a result of this observation protein loads of greater than 100 µg were not utilised for silver stained gels, as this would reduce the amount of quantifiable data that could be extrapolated from a 2-D image. Therefore, by loading less than 100 µg of total protein a compromise between visualising as many protein spots as possible and the requirement to extract accurate quantifiable data from each individual protein spot was reached.

3.3.6.1 Protein Visualisation using Colloidal Coomassie Protein Stain

The protein stain Bio-Safe colloidal Coomassie (Bio-Rad., U.K.) is an end-point stain which binds quantitatively to proteins of mid to high abundance (Malone et al., 2001). It is not as sensitive as silver stain and will generally not visualise protein spots containing less than 20 ng of protein (Table 3.4). When 2-D gels run from the same sample were stained with either silver or colloidal Coomassie, it was apparent that the colloidal Coomassie stained 2-D gels contained fewer protein spots (Figure 3.9A). In order to increase the

number of protein spots visualised on colloidal Coomassie stained gels the protein loading was increased in the first dimension separation, as has previously been described (Oguri et al., 2002). However, when increasing the protein load it is necessary to increase the focussing time to enable all proteins to enter the IPG strip and for complete focussing to occur. When an increased load of up to 1000 ng of total protein was applied to an 18 cm, pI 3-10 NL IPG strip, it was necessary to increase the focussing time to approximately 40 hours to obtain the best spot resolution.

In order to investigate the use of colloidal Coomassie stain as a quantitative alternative to silver stain, a range of protein loads of a whole NS0 cell extract were separated by 2-D PAGE and compared against an 80 μg protein load. Overloaded gels of 250 μg 350 μL^{-1} , 500 μg 350 μL^{-1} , 850 μg 350 μL^{-1} and 1000 μg 350 μL^{-1} were all separated on large format 2-D gels and assessed for total protein spot number, using ImageMaster™ 2-D Elite software.

3 Development of the Proteomic Technology Platform

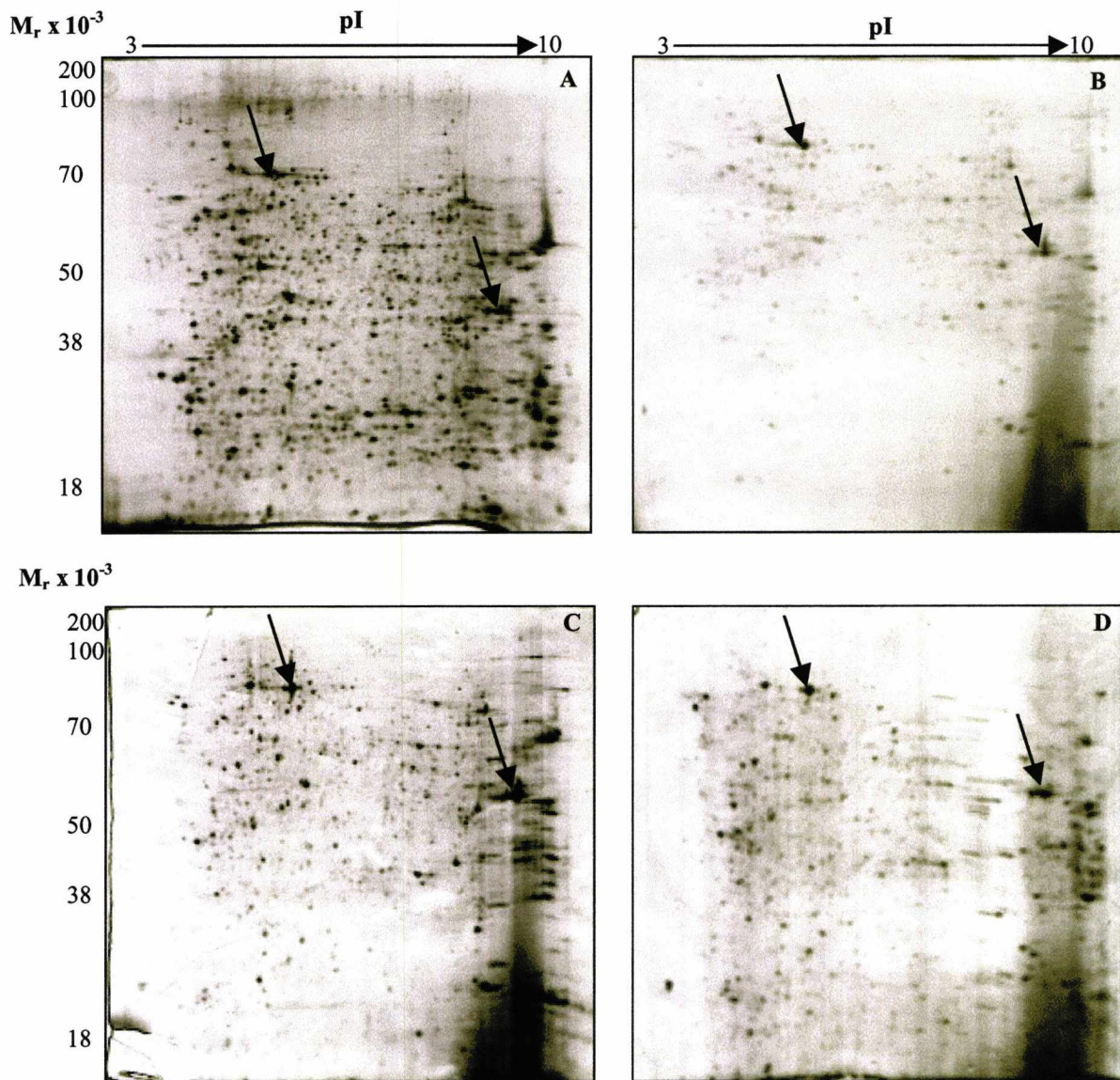


Figure 3.9 Large format (20 x 18 x 0.1 cm) 2-D PAGE of whole NS0 cell extracts. (A), Silver stained 2-D gel with a standard protein load of $80 \mu\text{g } 350 \mu\text{L}^{-1}$. (B), $250 \mu\text{g } 350 \mu\text{L}^{-1}$ protein load visualised with colloidal Coomassie, (C), $500 \mu\text{g}$ protein load visualised with colloidal Coomassie and (D), a large format 2-D gel with a protein load of $1000 \mu\text{g}$ visualised with colloidal Coomassie. Each overloaded 2-D gel was analysed by ImageMaster™ software to enable detection of the total number of discrete protein spots on each gel. The arrows indicate the position of landmark proteins present in all gels.

Figure 3.9 shows colloidal Coomassie stained overloaded 2-D gels (of $250 \mu\text{g}$, $500 \mu\text{g}$, and $1000 \mu\text{g}$ protein loads respectively) from the same sample of extracted whole NS0 cell proteins. The first dimension separation was extended for each of the protein loads to enable entry of the proteins into the IPG strips and complete focussing to occur. Table 3.5 below shows the total number of protein spots detected from the analysed gel images produced by ImageMaster™ software. Protein loads of $80 \mu\text{g}$ and $850 \mu\text{g}$ protein were also analysed in the same way as the images shown above (results not shown).

Table 3.5 Comparison of overloaded 2-D gels with variable protein concentrations to investigate the relative staining sensitivity of colloidal Coomassie to silver stain. Protein spots were detected on 2-D gels and compared to an 80 µg silver stained 2-D gel by ImageMaster™ software

Protein Load (µg)	Staining Method	Number of Protein Spots Visualised
80	Silver	1500
80	Colloidal Coomassie	133
250	Colloidal Coomassie	536
500	Colloidal Coomassie	741
850	Colloidal Coomassie	721
1000	Colloidal Coomassie	763

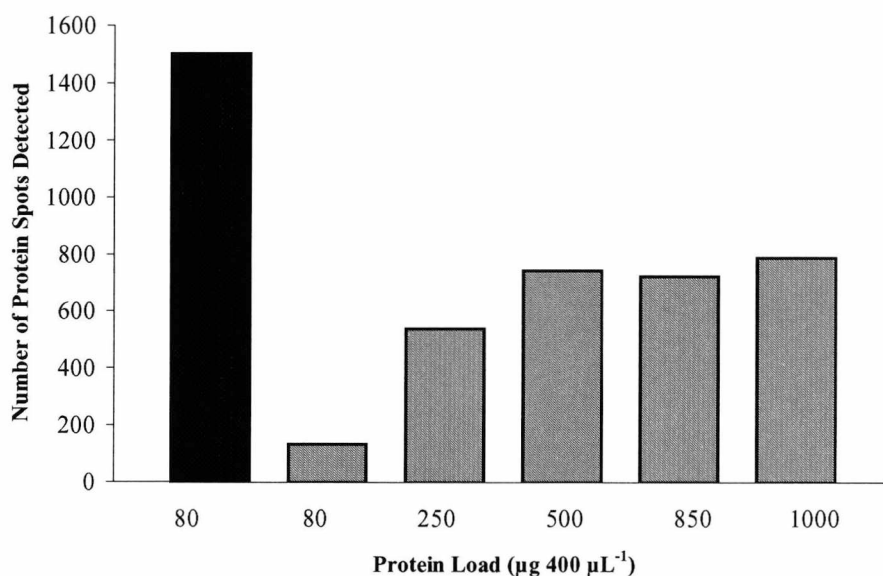


Figure 3.10 Relationship between protein loads and the number of spots visualised by Coomassie staining. Samples of NS0 cells were extracted from a batch culture at mid-exponential phase of growth, followed by subjection to large format (20 x 18 x 0.1 cm) 2-D PAGE and visualisation by silver stain (■) or colloidal Coomassie stain (▨). The total number of protein spots on each gel were detected using ImageMaster™ software as described in the methods section.

The total number of protein spots detected was based on a software generated averaged image and therefore does not include error bars (Figure 3.10). The total number of protein spots visualised on a silver stained 18 cm 2-D gel, loaded with 80 µg whole NS0 cell protein was approximately 1500 as described previously. When the same amount of protein was loaded on a 2-D gel followed by colloidal Coomassie staining only 133 protein spots were visualised, which is less than 10% of the total number of protein spots visualised by silver stain for the same loading. As the protein load was increased the number of protein spots detected on each gel also increased, according to the protein loaded on each 2-D gel. However, even with a total protein load of 1000 µg the number of protein spots detected was only 763 (approximately 50% of that number detected by silver stain with a 80 µg load). The number of protein spots on the overloaded 2-D gels was also

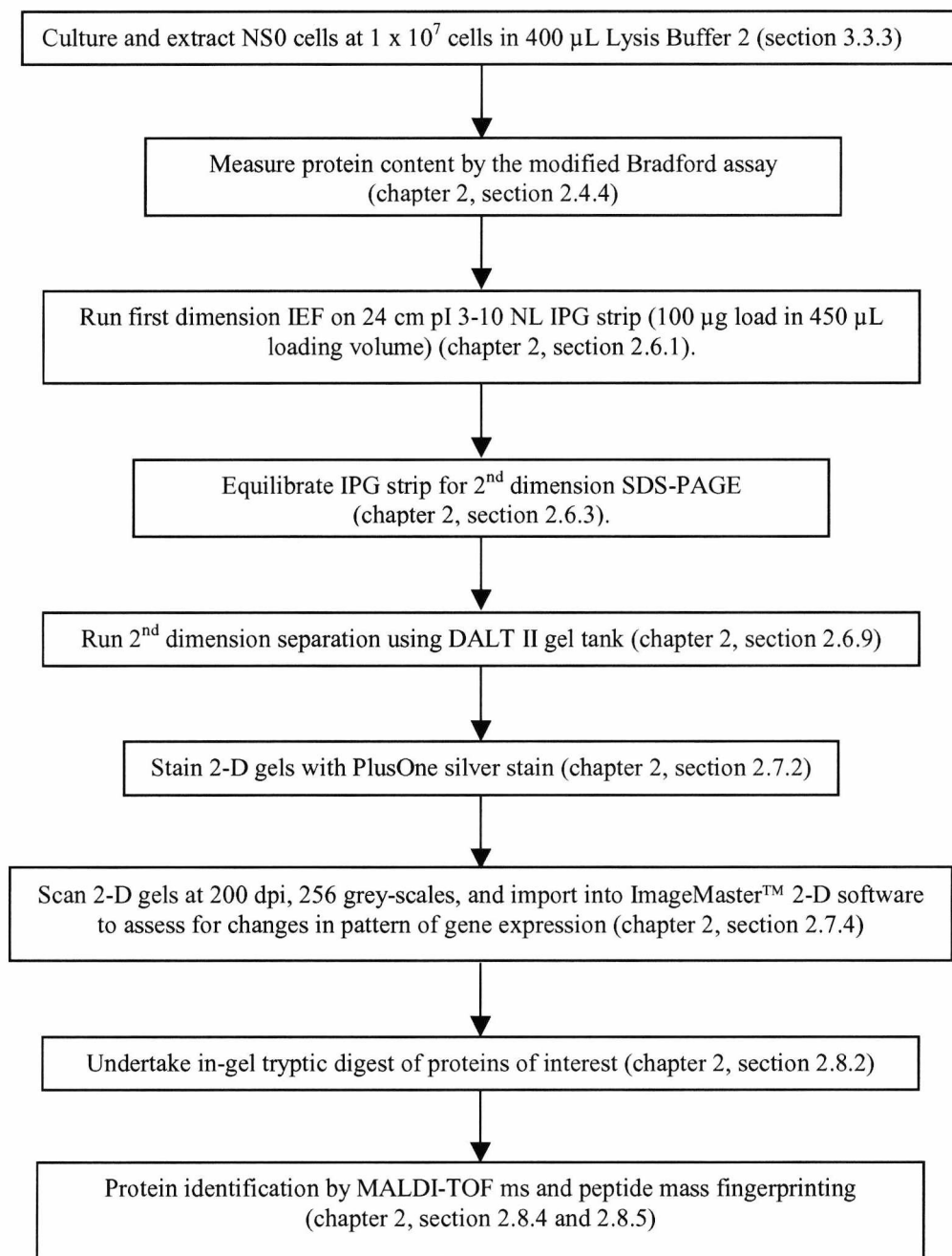
3 Development of the Proteomic Technology Platform

not observed to increase significantly between a 500 μg and 1000 μg protein load, although the intensity of staining for specific protein spots visualised even at low protein loads did appear to increase.

Sequential colloidal Coomassie/silver staining was also investigated for visualisation of both high and low abundance proteins (results not shown) (McDonough et al., 2002). When the gels were stained with colloidal Coomassie followed by silver staining, lower abundance proteins could be visualised but high abundance proteins became highly over developed. As a result this method could not be utilised for the quantitative analysis of the relative expression levels of proteins on the gels.

3.3.7 Optimised Scheme for Whole NS0 Cell Protein Extraction by Large Format 2-D PAGE

The optimised and standardised protocol developed from the work described in this chapter for the treatment of whole NS0 cells for assessment by 2-D PAGE is described below.



Scheme 3.2 Optimised procedure for the analysis of the whole cell NS0 proteome by 2-D PAGE.

3.4 Discussion

3.4.1 Sample Preparation

Through the implementation of a proteomic platform utilising 2-D PAGE, changes in gene expression between samples of interest can be investigated. To accurately obtain the proteome of any sample, the method of protein solubilisation and recovery must be both reproducible and optimised to ensure an accurate representation of the proteins expressed (Molloy, 2000). The method of solubilisation must ensure that the extraction procedure does not 'select' for proteins with certain characteristics, such as their solubilisation or relative abundance, as this will certainly bias the end result of any proteomic analyses. The overall aim of a proteomic study is to be confident that the sample preparation corresponds to the physiological state of the sample at the time the sample was taken, enabling an accurate representation of the proteome to be obtained.

Various methodologies were investigated throughout the optimisation of NS0 cell protein solubilisation and recovery to enable an accurate and reproducible 2-D gel to be produced from any NS0 cell sample. In order to prepare a sample of NS0 cells for 2-D PAGE, the cells must be disrupted to release the cellular proteins without the activation of proteolytic enzymes, which are capable of altering proteins of interest and therefore also capable of altering the proteome (Gorg, 1998). Unlike bacterial cells, mammalian cells do not contain a cell wall, and therefore gentle methods of cell lysis can be implemented in the form of chemical lysis protocols (Gorg, 1998). There are a wide variety of standard solubilising kits and methods available, although, in order to prepare samples for 2-D PAGE, the sample buffer must not contain buffers which contain a charge (such as SDS), as these interfere with the first dimension separation (IEF). Therefore, buffers containing a net charge of zero and low salt concentration are required (Oh-Ishi and Maeda, 2002). To optimise the protein solubility and recovery from NS0 cells, two chemical methods of protein solubilisation were investigated to determine the most efficient method of cell lysis.

3.4.2 Cell Lysis Methodology

In order to carry out successful 2-D PAGE, the solubilising buffer must not only be free of ionic components and achieve complete protein solubilisation without biasing or altering the resultant extract, the sample preparation must ensure complete protein disaggregation, into single polypeptide chains. To fully denature the proteins within a sample, the bonds

which hold proteins in their three dimensional structure must be disrupted; these bonds include disulphide bonds, hydrogen bonds and hydrophobic interactions (Molloy, 2000). These interactions must be permanently disrupted to prevent aggregation of proteins during the 2-D process. Disulphide bridges can be broken through the addition of dithiothreitol (DTT), dithioerythreitol (DTE) or addition of tributyl phosphine (TBP) (Oh-Ishi and Maeda, 2002). All of these additives had been extensively utilised in the preparation process of 2-D PAGE. SDS and β -mercaptoethanol can also be utilised for the reduction of disulphide bonds, although both contain a charge which would interfere with the first dimension separation IEF, resulting in poor focussing and separation of proteins (Rabilloud, 1999). In order to reduce the ionisable effects of these two reducing agents, dialysis would be required before IEF (Oh-Ishi and Maeda, 2002), resulting in an additional preparation step to sample preparation which could result in selective protein losses. These reducing agents therefore were not utilised in this study. Tributyl phosphine (TBP) is a hazardous chemical and requires great care when being used, and it was therefore not investigated for use as a denaturant. DTT was therefore included as the reducing agent of choice in the lysis buffers for NS0 cell sample preparation, due to its effectiveness in reducing the sample.

In addition to reducing the disulphide bonds present within a protein sample, non-covalent interactions must also be disrupted. This was achieved through the addition of the zwitterionic chaotrope, urea, to the solubilising solution. Urea is particularly efficient at destroying hydrogen bonds although it is less effective at breaking hydrophobic interactions and can result in protein aggregation. As a result other chaotropes could be utilised in conjunction with urea including thiourea, which has been reported to enhance the focussing of membrane proteins (Molloy, 2000; Oh-Ishi and Maeda, 2002). Other zwitterionic or non-ionic detergents may also be included in the solubilising buffer such as CHAPS, Triton and sulphobetaines (Oh-Ishi and Maeda, 2002). These zwitterionic compounds can greatly improve focussing and stability of the gradient during IEF. CHAPS was chosen as the zwitterionic compound of choice for the solubilisation of NS0 cell proteins in this study.

Eukaryotic cells are known to contain proteases including serine and metalloproteases, which are compartmentalised in organelles, although, upon cell lysis these are liberated and therefore need to be inactivated as they are capable of modifying other proteins in the sample, thereby altering the proteome. The lysis buffers used to

solubilise NS0 cells did not contain protease inhibitor cocktails as cells were directly lysed in a solution containing a high concentration of urea, which inhibits proteolytic activity (Gorg, 1998).

Two lysis buffers (chapter 2, section 2.4.2) differing in DTT, CHAPS and urea concentration were investigated, as was the effect of the addition of thiourea to the lysis buffer. Figure 3.2 showed that lysis buffer 2 containing (9.5 M urea, 2% CHAPS, 1% DTT and 1% pharmalytes) provided the greatest protein recovery from NS0 cells. This lysis buffer also yielded a protein solution which was easy to handle without liberation of DNA or other contaminating substances, which can form a viscous solution and cause streaking on 2-D gels (Gorg, 1998). Lysis buffer 2 also solubilised similar amounts of protein from whole NS0 cells extracted throughout the growth curve at mid-exponential and death phase of growth and therefore protein yield was shown to be independent of the point in the growth curve that a sample was taken. This was an important observation, as the increase in cell number towards death phase may have adversely affected the reproducibility of the extracted protein sample, resulting in experimental selection towards proteins that are more susceptible to solubilisation. This in turn would have compromised the ability of the sample preparation protocol to represent all proteins within the sample. However, since the protein yields at mid-exponential and death phase of growth were similar we can assume that the samples were less likely to be biased by this extraction method, even at death phase.

3.4.3 Qualitative Assessment of Protein Solubility and Recovery

Protein solubilisation and recovery was assessed by the modified Bradford assay (chapter 2, section 2.4.4). This assay provides a method for evaluating total solubilised protein, but does not allow a qualitative assessment of a buffer's resolving ability. The resolving ability is especially important for buffering systems, as although the lysis buffer may solubilise the greatest amount of cellular proteins, it may not provide a 2-D gel with highly resolved and separated proteins. The buffering system may also cause smearing of proteins across the 2-D gel causing a high level of background staining if it is not completely compatible with 2-D PAGE. If there is a high level of background staining, the downstream image analysis of individual 2-D gels is more difficult. In order to assess the resolving ability of the two selected solubilising buffers, mini 2-D gels were run on whole NS0 cell extracts.

Following 2-D electrophoresis, the ability of each solubilising condition to separate complex protein mixtures was assessed by comparing the total number of protein spots resolved by each solubilising buffer. After spot detection, the results showed lysis buffer 2 produced more highly resolved 2-D gel images and a higher number of discrete protein spots. This lysis buffer was less complex than lysis buffer 1 which contained a higher concentration of CHAPS and thiourea to aid membrane solubilisation (Oh-Ishi and Maeda, 2002). As a result it was clear that lysis buffer 2 solubilised a higher concentration of cellular protein and also resolved a greater number of discrete proteins with less streaking than lysis buffer 1; therefore this lysis buffer was utilised for all further experimental procedures.

3.4.4 Quantitative Assessment of Protein Solubilisation Methodology

In order to provide the optimum solubilising conditions it was necessary that the number of NS0 cells solubilised in a set volume of extraction buffer was quantified. A batch culture of NS0 cells were extracted at mid-exponential phase of growth using different cell numbers (ranging from 1×10^5 to 1×10^8 cells) in a set 400 μL volume of lysis buffer 2 (section 3.3.3). The amount of protein solubilised in each extract was then determined by the modified Bradford assay (chapter 2, section 2.4.4). The number of cells providing the best solubilisation conditions without creating a bias in the proteins' representation was 1×10^7 cells in 400 μL of lysis buffer volume. The protein recovery determined from 1×10^6 to 1×10^7 cells increased in a linear fashion, and therefore the volume of lysis solution to sample pellet did not result in a bias of protein solubilisation. However, if the cell numbers were increased further to 1×10^8 cells, the protein yield did not increase in a linear fashion as the lysis buffer had reached its limit of solubility. In this case a bias towards solubilisation of proteins which were more soluble may have resulted. It was necessary to keep the volume of lysis buffer low due to the limits of volume loading for IEF. If larger volumes of lysis buffer were utilised the resulting protein concentration would have been too dilute.

3.4.5 Large Format 2-D PAGE

For all optimisation experiments and protocol development experiments, mini gel 2-D electrophoresis was utilised as this allowed rapid method development and analysis. However, in order to increase the resolution and number of protein spots visualised, large format 2-D PAGE was adopted. When a Protean II gel tank was utilised the length of IPG

strip for the first dimension separation could be increased to 18 cm meaning more protein (80 µg versus 10 µg) could be loaded onto each strip. The use of large format SDS-PAGE gels resulted in an increase in the total number of protein spots detected (from 450 to 1500, section 3.3.4, Table 3.2). The adoption of the larger gels for 2-D PAGE also increased the analytical area over which a greater number of proteins were separated and resolved.

3.4.5.1 DALT II versus Protean II Gel Tanks

Due to problems with reproducibility when the Protean II large format gel tank was utilised whereby only 4 gels could be run simultaneously with 2 tanks, a DALT II system was implemented. The DALT II gel tank is capable of running 12 large format SDS PAGE gels simultaneously. The first dimension IPG strips were also increased in size in the DALT II system (to 24 cm) and 12 gels could also all be run simultaneously. Therefore a whole set of 12 gels could be run together resulting in simpler downstream analysis of the gels, increasing reproducibility since the running conditions were identical. As a result the DALT II gel tank was adopted as the standard system for running large format 2-D gels in combination with the IPGphor IEF system for consistent 2-D gel patterns.

3.4.6 Selection of IEF and Second Dimension Gel Percentage Range

It has previously been reported that the focussing of basic proteins, membrane proteins and hydrophobic proteins is limited (Molloy, 2000; Santoni et al., 2000). The main limitations are due to instabilities within the buffering systems for basic proteins and in the solubilising conditions for membrane and hydrophobic proteins. Resolution of the basic region of 2-D gels has recently been greatly improved with narrow range IPG strips now available, which are capable of resolving proteins of basic pI up to pH 11 (Gorg et al., 2000b). However, it is still difficult to maintain a stable gradient at basic pH and therefore it remains extremely difficult to obtain consistent results in the basic region of 2-D gels (Hoving et al., 2000; Ohlmeier et al., 2000).

In order to investigate the whole NS0 cell proteome, it was necessary to implement broad range IPG strips of pI 3-10 for the first dimension separation of the proteomic platform. Using the optimised cell lysis conditions and sample preparation (scheme 3.1), the proteome of NS0 cells could be investigated throughout the growth curve. Investigations were carried out using both linear and non-linear pI 3-10 IPG strips to assess which gave the best representation of the NS0 proteome. Linear range IPG strips separate proteins over the range in equal distance and resolved approximately 1200 protein spots.

However, the non-linear IPG strips stretch out the region on the gel between pI 5-7, resolving approximately 677 proteins within this region of the second dimension SDS-PAGE gel compared to 468 protein spots detected on the linear gradient gels in the same pI region. On the non-linear pI gradient gels approximately 50% of the total proteins on the gel were detected in the pI 5-7 region, whereas on the linear gradient gels approximately 40% of the total proteins detected on the 2-D gels were detected within the same region. As a result the total number of proteins resolved using the non-linear gradient was increased to approximately 1500 proteins. The basic region on non-linear gradient gels between pI 7-10 is also better resolved albeit over a narrower area with the same number of proteins resolved when compared to the linear gradient gels. Proteins involved with protein folding and energy transduction are generally found in the acidic region and therefore the pI 3-10 non-linear range was adopted as the standard method for analysis of the NS0 cell proteome throughout all further investigations.

In order to stretch out the resolving range of IPG strips further, 'zoom gels' could have been implemented (Hoving et al., 2000). These IPG strips resolve proteins over very narrow pI ranges and enable a composite image of the proteome to be acquired. These strips also enable visualisation of proteins of very basic pH, for example, when pH 6-11 or pH 6-9 IPG strips are utilised in combination with the paper bridge loading or cup-loading method (Gorg et al., 2000b). However, in this study investigations were restricted to wide range pI 3-10 non-linear IPG strips for maximum coverage of the NS0 cell proteome.

The second dimension SDS-PAGE gel was also optimised to yield the best separation and representation of the NS0 cell proteome. In order to optimise coverage of the whole NS0 cell proteome, SDS-PAGE gels with different concentrations of acrylamide were investigated (section 3.3.5.1). Gels of 11 and 11.5% resulted in loss of low molecular weight proteins and large molecular weight proteins of greater than 150 kDa as these large proteins fail to enter the second dimension gel (Harry et al., 2000). As a result gels of 12.5% acrylamide were routinely utilised. Although the 12.5% acrylamide gel narrowed the separation range of the gel, complicating the downstream image analysis, this separation range was utilised for all further investigations as it produced a more accurate representation of the NS0 cell proteome with a good representation of low and high molecular weight proteins.

3.4.7 Protein Visualisation

The staining method for protein visualisation on 2-D gels must be reproducible and quantitative for image analysis. There are many protein gel stains available such as Coomassie, silver and fluorescent stains including the SYPRO[®] stains (Lauber et al., 2001). The most sensitive stain available for visualisation of proteins of low abundance (reported to be less than 1 ng per protein spot) is silver stain. Many protocols have been published based on the silver nitrate staining technique of Merril, including those that are compatible with mass spectrometry (Merril et al., 1981; Shevchenko et al., 1996). The silver stain method of protein visualisation is much more sensitive than the Coomassie stains, and therefore is often the stain of choice when maximum protein visualisation is the aim. However, if quantitative analysis of protein spots to investigate changes in the level of expression is required, silver staining is, in theory, not the best choice as it is only quantitative over a narrow dynamic range of approximately 10-fold (section 3.3.6, Table 3.4) (Lauber et al., 2001; Spibey et al., 2001). Fluorescent stains such as SYPRO[®] orange and Ruby are quantitative over a much wider linear range than silver and also have been reported to be as sensitive as silver stain in some instances, and are therefore very popular in proteomic research (Kemper et al., 2001; Malone et al., 2001). However, they remain very costly and are dependent on good imaging equipment. Furthermore, the extended quantitative range tends to cover high abundance proteins and it is not at this end of the scale that the extended range is required. Colloidal Coomassie is more sensitive than the standard Coomassie Blue stains, with a detection limit of 20 ng of protein (Lauber et al., 2001). The stain has a greater quantitative range than silver (10-30-fold), is cheaper than fluorescent stains, and does not require any specialised imaging equipment. Protein visualisation using colloidal Coomassie was investigated further with increased protein loads in the first dimension to assess whether visualisation equivalent to silver staining could be achieved (section 3.3.6.1). A series of overloaded IPG strips were carried out over a protein concentration range of 80-1000 µg total protein loads. However, even with protein loads as high as 1000 ng, the same level of visualisation (spot numbers) as that achieved with silver stain could not be obtained on 2-D gels (Figure 3.9 and 3.10 and Table 3.5).

In order to improve protein loading the thickness of the second dimension SDS-PAGE gel could have been increased, but this had the effect of making the gels fragile and difficult to handle. Alternatively the first dimension IPG strip width and thickness could

have been increased (Harry et al., 2000), although, the IPG strips are only supplied in one thickness and width by Amersham Biosciences, and therefore this was not possible. Other methods of increasing the protein loaded on 2-D gels include the use of cup loading and paper bridges, and these methods allow the volume of sample loaded onto IPG strips in the first dimension to be increased (Sabounchi-Schutt et al., 2000). However, for simplicity and to keep the method comparable to analytical loads of 80 μg protein, the concentration of protein loaded onto IPG strips was increased up to 1000 μg 350 μL^{-1} and the separation time was increased from approximately 24 hours to 40 hours to allow focussing of the samples. When the colloidal Coomassie stained gels were analysed by ImageMaster™ software the total number of protein spots increased from 133 when an 80 μg protein load was utilised to 763 protein spots when a 1000 μg load was implemented. However, when 2-D gels of 500 μg , 850 μg and 1000 μg protein loads were investigated, the total number of protein spots visualised was not observed to increase (Figure 3.9 and Table 3.5). Therefore, even at a protein load of more than 10 times the amount required for an analytical 80 μg protein load followed by silver staining, the visualisation of proteins with colloidal Coomassie was still not sufficient to replace silver staining and so was not utilised to replace silver staining but could be used in some cases to complement it.

These results clearly demonstrate that for quantitative analysis a compromise must be made between the staining methodology, the sensitivity or number of protein spots detected and the linear dynamic range over which quantitative data can be collected. Coomassie based techniques allow 'good' quantitative data to be obtained for very abundant proteins only at the expense of not detecting less abundant proteins. However, silver staining techniques allow the detection and measurement of many more (less abundant) proteins although do not provide reliable quantitative information on highly abundant proteins. Therefore, silver staining techniques provide much more information overall and were chosen as the staining technique of choice. However, if reliable quantitative measurements of very highly abundant proteins are to be made the colloidal Coomassie staining method should be employed.

SYPRO® Orange and Ruby stains were also investigated and found to have a staining sensitivity that was similar to the silver stains investigated. However, when proteins of higher abundance were present on gels, a fogging effect occurred, which masked other proteins within the same area on the gel (data not shown). This was likely to be due to the equipment used for capturing the image. As a result of this problem and the

specialised equipment necessary to capture fluorescent stained gels, these staining methods were not pursued further.

One way of identifying proteins from within 2-D gels is to digest the proteins with trypsin and then to analyse the resulting peptides (Washburn and Yates, 2000). The staining technique used for protein visualisation must therefore be compatible with mass spectrometry and identification by peptide mass fingerprinting. To achieve this two silver stains were commonly used, an adaptation of the Shevchenko method (Shevchenko et al., 1996) and the PlusOne silver staining method, which was adapted for ms by omitting glutaraldehyde. The Shevchenko method caused inversion of staining of proteins of high abundance and, therefore for most investigations the PlusOne method was utilised as the standard stain for visualisation of proteins on 2-D gels. The selection of silver staining as the standard method for protein visualisation on 2-D gels was therefore a compromise between the highest sensitivity of staining and the lowest quantitative range. However, as previously described, most proteins on 2-D gels occurred within the linear range of the silver stains utilised.

3.4.8 2-D Image Reproducibility

In order to carry out successful gel image analysis of protein expression profiles, each data set must be obtained from the same concentration of protein, run under the same conditions and finally each gel must be 'equally' stained. Silver stain, unlike SYPRO[®] and colloidal Coomassie stains is not an end-point stain and therefore care had to be taken particularly in the development stage of the staining process. However, as it often takes up to 5 minutes to fully develop each silver stained gel, a standardised method for the staining of 2-D gels by silver could be established, whereby proteins of low abundance which tended to stain last could act as the end-point marker for staining. This allowed some control over the development and stain uptake between gels that were stained at the same time. The narrow linear range of silver stain does not severely limit the amount of quantifiable data that can be obtained from individual proteins, as most proteins tend to lie within this range (Smales *et al.*, 2003). Therefore the utilisation of silver stain is a compromise between sensitivity of staining and quantifiable range.

The utilisation of the DALT II system also enhanced the reproducibility of the 2-D gel images as 12 gels could be run simultaneously. When this was coupled with the first dimension separation, which also enabled 12, 24 cm IPG strips to be run together and the

final staining of the gels, which could be controlled as described above, the whole process became much more reproducible allowing a greater amount of quantitative data to be acquired for different samples.

3.4.9 Optimised Scheme for Sample Preparation and Analysis of the NS0 Cell Proteome by 2-D Electrophoresis

As a result of the optimisation experiments outlined in this chapter, the implementation of a standardised platform for sample preparation, separation and visualisation of whole NS0 cell proteins by 2-D PAGE has been developed. The protocol enables rapid reproducible and quantitative analyses to be undertaken in a systematic way to accurately assess changes in protein expression. The optimised scheme for the preparation of samples for 2-D PAGE is presented in scheme 3.2.

3.5 General Discussion

Through the development and optimisation of the proteomic analysis platform, a standardised scheme for the analysis of GS-NS0 cells has been developed (scheme 3.2). The extraction procedure for GS-NS0 cells was optimised by solubilising 1×10^7 cells in a 400 μ L volume of lysis buffer 2 (section 3.3). Whilst accepting current limitations of proteome technology, compromises have been made in order to obtain a reproducible and accurate representation of the GS-NS0 cell proteome. Broad range 24 cm, pI 3-10 non-linear IPG strips have been adopted for the first dimension to enable maximum coverage of the NS0 cell proteome (section 3.3.5), and the Ettan DALT II gel tank has been implemented for the second dimension so 12 gels can be run simultaneously to increase run reproducibility (section 3.3.4.1). A compromise in protein visualisation to achieve optimal sensitivity of staining and quantifiable range by utilising silver staining techniques has also been implemented (section 3.3.6). Using this optimised system for the proteomic analysis of GS-NS0 cells, in subsequent chapters the investigation of the NS0 cell proteome throughout batch culture under controlled conditions is investigated together with the investigation of NS0 transfectants exhibiting different levels of specific productivities to identify proteins involved with recombinant protein production.

Chapter 4 Analysis of Changes in the GS-NS0 Cell Proteome during Batch Culture

4.1 Introduction

Mammalian cells, in particular murine myeloma NS0 cells, are extensively utilised in the biopharmaceutical industry to produce high levels of recombinant therapeutic antibodies (Barnes et al., 2001; Watanabe et al., 2002). The specific cellular processes which control whether or not a cell line is productive has not been extensively investigated. Most research to date has utilised a reductionist approach whereby the engineering of cell lines with one or two specific proteins has been investigated with limited success. For example, Fussenegger *et al.* engineered CHO cell lines with the anti-apoptotic gene *bcl-2*, which was shown to be successful in delaying the onset of apoptosis; the same was observed in hybridoma cells, although contradicting results have been reported in NS0 cell lines (Fussenegger et al., 2000; Jung et al., 2002; Murray et al., 1996).

The basic functioning of animal cells in culture is a 'black box' with many questions concerning cellular processes and productivity remaining unanswered. It has previously been reported that DNA or message levels (mRNA) often do not correspond to the levels of active protein within cells (Gabor Miklos and Maleszka, 2001; Smolke and Keasling, 2002). Therefore, in order to investigate changes in the protein expression profiles of NS0 cells throughout batch culture any study must be capable of identifying global changes in protein expression. With the utilisation of a proteomic platform an holistic approach has been implemented which, in theory at least, allows the multiple changes in specific proteins implicated with the functional competence of NS0 cells in culture to be characterised and identified.

Using the optimised proteomic platform described in chapter 3, the changes in the functional phenotype of NS0 cells during bioreactor batch culture was investigated and is reported in the following chapters. Bioreactor culture was utilised to allow the investigation of NS0 cell growth and proteome in a defined and controlled environment. Large format 2-D gels were carried out using the optimised protocol outlined in chapter 3, scheme 3.2, followed by rigorous analysis by ImageMaster™ 2-D software and peptide mass fingerprinting to identify proteins that exhibited an increase or decrease in relative expression throughout batch culture and as a result the following questions were addressed;



4 Analysis of Changes in the GS-NS0 Cell Proteome during Batch Culture

(1) for cells cultured under controlled conditions, when do they perceive stress? and, (2) do the changes observed relate to the specific productivity of the cell line *in vitro*?

4.2 Results

4.2.1 Cell Culture

NS0 cells expressing an anti-CD38⁺ IgG₁ were cultured and maintained in serum-free medium as outlined in chapter 2, section 2.2.2.1. Seeding stocks and inocula for the experiment were prepared in shaker flasks up to 100 mL volume, agitated at 100 rpm on a shaker platform maintained at 37°C. Typically cells were introduced at 2.5×10^5 cells mL⁻¹ into fresh medium, followed by gassing with 5% CO₂ for 30 seconds. Cells were then left to grow until they reached mid-exponential growth phase (approximately 1×10^6 cells mL⁻¹) prior to passage or seeding the fermenter vessel (chapter 2, section 2.2.8.1).

4.2.2 Bioreactor Culture

In order to maintain a more controlled culture environment than possible with shaker or spinner flasks, a stirred tank bioreactor with on-line controls for pH and D.O was utilised. Batch culture of GS-NS0 cells was carried out in a 3 L fermenter (chapter 2 section 2.2.2.1, section 2.2.8.1 and 2.2.8.2 for maintenance and culture of NS0 cell line). The culture was inoculated at 2×10^5 cells mL⁻¹ in a 1.5 L working volume. The characteristics of cell growth were monitored from samples taken daily (Figure 4.1A) and the fluxes of glucose and lactate metabolite concentration from cell-free supernatant samples were monitored according to the method described in chapter 2, section 2.2.9 (Figure 4.1B).

4.2.2.1 Monitoring IgG Product Titre in Culture Medium during Batch Culture

The NS0 cell line engineered to produce Immunoglobulin G (IgG) and described above was selected as the model system for this investigation. Throughout the bioreactor batch culture of NS0 cells, cell-free supernatant samples were taken on a daily basis, and assayed for recombinant antibody production by Biacore Optical Biosensor (chapter 2, section 2.3.1) (Figure 4.1A).

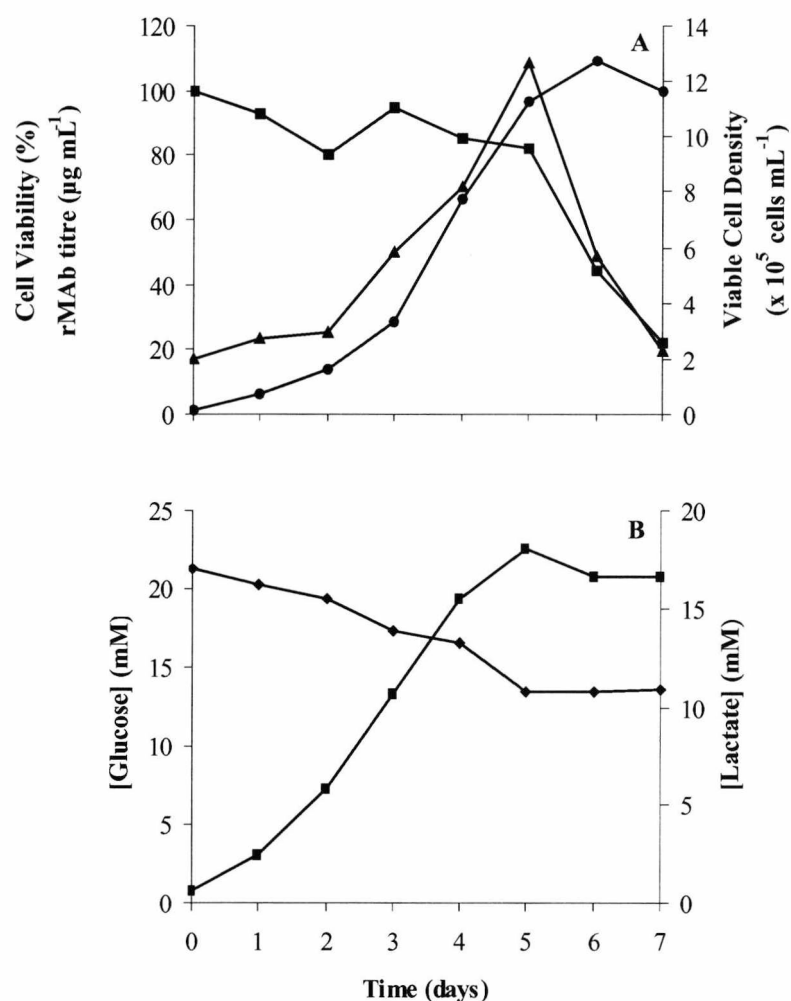


Figure 4.1 Batch culture growth of NS0 cells expressing a recombinant IgG in serum-free medium in a controlled bioreactor culture. A typical culture of NS0 cells expressing IgG is shown above. Figure A, Cell viability (■), rMAb titre (●) and Viable Cell Density (▲). Figure B, Glucose (◆) and Lactate (■) concentration respectively from samples taken during the course of batch culture.

Table 4.1 Maximum viable cell density, growth rate (μ), doubling time (Td), and maximum IgG concentration (qMAb) in a 1.5 L volume batch bioreactor culture of NS0 cells in serum-free medium

μ (h ⁻¹)	Td (h)	Generation number	Max V.C.D. (x10 ⁵ Cells mL ⁻¹)	Max IgG Titre (µg mL ⁻¹)	qMAb (pg Cell ⁻¹ h ⁻¹)
0.02	34	2.11	12.7	109	1.46

Figure 4.1A above shows a typical growth curve for NS0 cells cultured in serum-free medium. GS-NS0 cells had a maximum specific growth rate during exponential growth phase (period of maximum growth rate) of 0.02 h⁻¹ between 48 and 120 h of culture. The minimum doubling time was calculated as 34 hrs, which is similar to previous reports (Downham et al., 1996), and during this time the generation number was 2.11

(Table 4.1). Cell viability was observed to decline rapidly after 120 hrs, although the IgG titre increased further after the cell viability and viable cell density decreased, peaking at $109 \mu\text{g mL}^{-1}$ after 144 hrs of culture. Cell specific productivity (qMAb) was calculated as $1.46 \text{ pg cell}^{-1} \text{ h}^{-1}$ (between 48 and 120 h of culture).

Glucose levels decreased rapidly throughout culture with maximum glucose depletion (qGlu) occurring during exponential growth phase. However, glucose was not completely utilised during batch culture with a final concentration of 13 mM reached by the end of culture (Figure 4.1B). Lactate levels accumulated concurrent with glucose depletion to approximately 18 mM during exponential growth phase. Levels of ammonia were not measured or recorded as cell lines transfected with the GS system utilise ammonia and glutamate for synthesis of glutamine. This attribute allows the cells to refrain from the need for glutamine in the cell culture medium and reduces toxic ammonia accumulation (Sauer et al., 2000; Zhou et al., 1997).

4.2.3 Analysis of the Whole NS0 Cell Proteome throughout Batch Culture

In order to assess the changes in the NS0 cell proteome throughout culture a 1.5 L bioreactor batch culture was run and samples of 1×10^7 cells were extracted in triplicate at key time-points throughout the growth curve (lag phase, day 1; mid-exponential phase, day 3 and 5; and death phase, day 7) as outlined in chapter 3, scheme 3.1. Large format 2-D electrophoresis of whole NS0 cell proteins were separated in the first dimension on 24 cm, pI 3-10 non-linear IPG strips followed by separation in the second dimension on 12.5% pre-cast (26 x 20 x 0.1 cm) acrylamide gels using the optimised protocols detailed in chapter 3, scheme 3.2. Proteins were then visualised by silver staining (chapter 2, Table 2.11) and the resultant images were captured using an ImageScanner (chapter 2, section 2.7.4). The resulting digital images were analysed using the ImageMaster™ 2-D software (v4.01) to accurately assess changes in the NS0 cell proteome throughout batch culture. Figure 4.2 shows the resultant 2-D gel images.

4 Analysis of Changes in the GS-NS0 Cell Proteome during Batch Culture

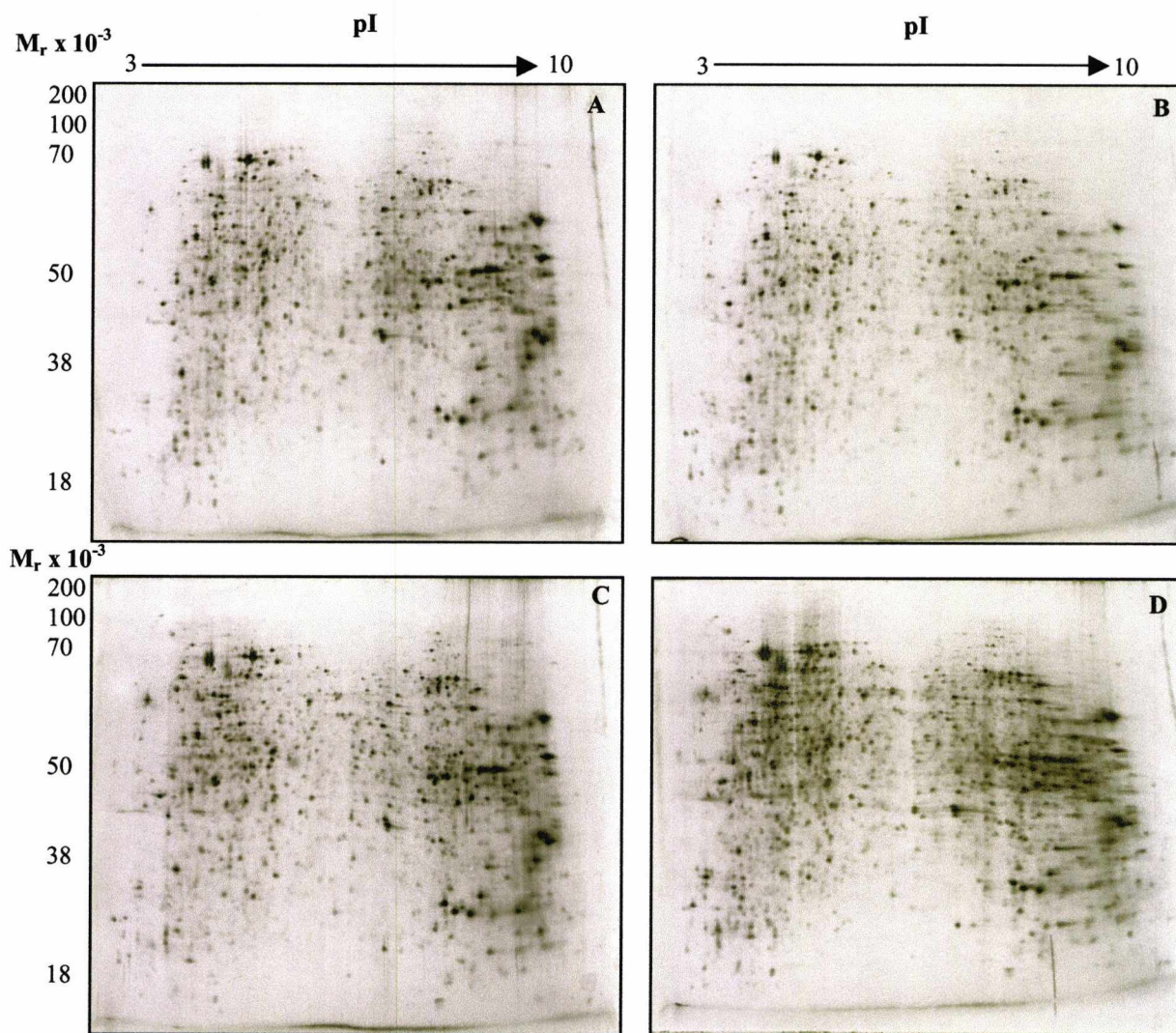


Figure 4.2 Large format 2-D PAGE (24 cm, pI 3-10 non-linear resolving range) of whole NS0 cells extracted from 1×10^7 cell samples taken throughout batch culture. Figure A, lag phase, day 1 2-D gel; Figures B and C extracts from exponential growth phase (day 3 and 5 of the batch culture); and Figure D, death phase (day 7 of the batch culture). All gels were visualised using silver staining methodology.

4.2.3.1 Analysis of the NS0 Cell Proteome throughout Batch Culture

The total number of protein spots determined for each time point are shown in Table 4.2 below.

Table 4.2 Total number of protein spots detected on 24 cm 2-D gels from key points in the growth curve of NS0 cells during controlled bioreactor batch culture

Day of Culture	Number of Protein Spots Detected
1	1398
3	1352
5	1680
7	1859

Table 4.2 above clearly shows the total number of proteins expressed by NS0 cells throughout the bioreactor batch culture increases as the culture progresses. After inoculation at lag growth phase there was an initial decrease in the total number of protein spots detected (1398) when compared with day 3 of the batch culture (1352), a reduction of 46 proteins. The total number of protein spots detected during mid-exponential growth phase was then observed to increase as the culture progressed (from 1352 to 1680 protein spots), an increase of 328 protein spots. At the end of the culture the maximum number of protein spots (1859), was observed, which was a further increase of 179 protein spots.

The global changes in total spot numbers alone using the image analysis software does not allow the quantitative assessment of the expression levels of proteins throughout the batch culture to be determined. In order to determine which proteins were up- or down-regulated, the 2-D gels were compared against a reference gel (day 1 of culture sample).

4.2.3.2 Protein Regulation throughout Batch Culture

Using the gel images reported earlier for the batch culture experiment (Figure 4.2), ImageMaster™ 2-D software was utilised to examine the proteins expressed throughout batch culture and to identify those proteins that showed a two-fold quantifiable increase or decrease in expression levels (chapter 2, section 2.7.4). The digital images created from the batch culture experiment were all compared to a reference gel generated from the 2-D gel from day 1 of the batch culture. This allowed the identification of changes in protein expression throughout the batch culture. The proteomic map showing all proteins up- and down-regulated by a two-fold or greater quantifiable change throughout the batch culture is reported below (Figure 4.3). To identify the proteins exhibiting a change in regulation throughout the batch culture each sample was compared against the 2-D gel from the preceding sample point.

Figure 4.3 clearly shows that the NS0 cell proteome changes throughout batch culture. The greatest increase in proteins that exhibited a change in expression occurred during exponential growth phase. At death growth phase, many proteins were also up-regulated, presumably as a result of the stress response. Of the proteins conserved between all the phases of growth, very few showed a two-fold (or greater) up- or down-regulation of gene expression (Table 4.3).

4 Analysis of Changes in the GS-NS0 Cell Proteome during Batch Culture

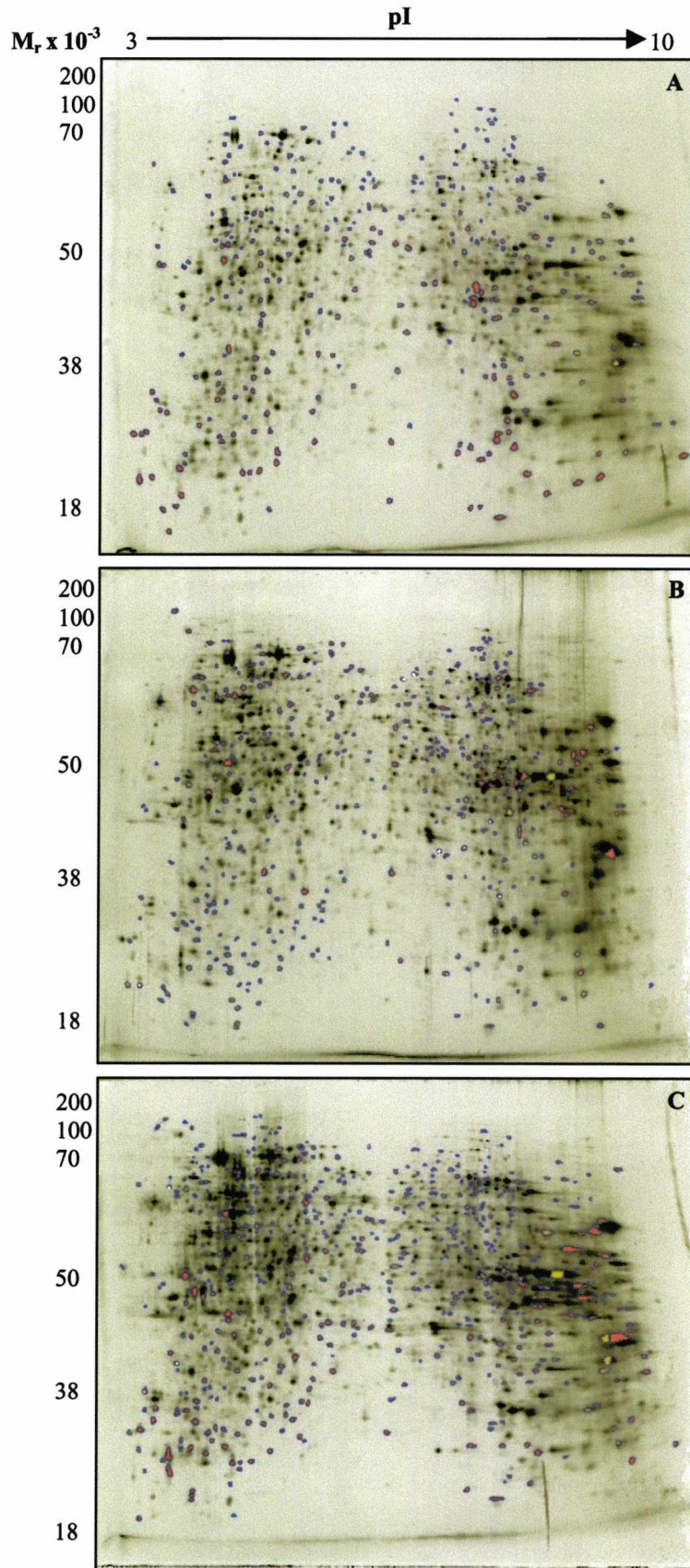


Figure 4.3 Difference maps derived from analysis of whole NS0 cell extracts carried out throughout batch culture showing proteins exhibiting two-fold changes in protein expression levels. Only the proteins matched between samples are shown. Figure A, day 3 versus day 1 of culture, Figure B, day 5 versus day 3 of culture and Figure C, day 7 versus day 5 of the batch culture experiment. (●) Matched proteins exhibiting at least a two-fold increase and (●) matched proteins showing at least a two-fold decrease in protein expression throughout the batch culture.

4.2.3.3 Changes in the Level of Protein Expression throughout Batch Culture

Throughout batch culture many changes in the level of protein expression would be expected. For example, at the start of the batch culture, proteins involved with cell division/replication and energy transduction requirements for cell growth would be expected to be up-regulated. The total number of proteins expressed at exponential phase of growth would therefore be expected to be greater, when compared to the pattern of protein expression at earlier and later stages of cell growth. At this stage of the growth curve the cells have reached the maximum viable cell density and IgG production has also reached maximum levels. Therefore, the proteins involved in cell growth/division and IgG production would be expected to be up-regulated further to cope with the cellular demands. Towards the end of culture the number of proteins up-regulated was observed to increase further, presumably due to the induction of proteins involved with the stress response. Table 4.3 below depicts the global changes in the NS0 cell proteome throughout batch culture.

Utilising image analysis software, the alterations in protein expression were assessed. The sum of all the variables (number of proteins unchanged, up/down-regulated and newly expressed proteins) described in Table 4.3 is equal to the total number of protein spots detected at each sample point. Between days 1 and 3 of the culture 749 protein spots exhibited no change in the level of expression, this number decreased between day 3 and 5 with 677 proteins remaining unchanged. Towards the end of the culture the number of proteins unchanged decreased slightly with 668 proteins unchanged between days 5 and 7. At each stage of the growth curve differences in the pattern of newly synthesised proteins and proteins those that were no longer expressed when compared to the previous sample day were investigated using the same parameters that were defined for the detection of protein spots on the 2-D gels. Between the start of the culture and day 3, 283 proteins were newly synthesised. The number of new proteins later in the culture at mid-exponential growth phase was greater. Between days 3 and 5 of the batch culture 621 newly synthesised proteins were observed and this figure was further increased between days 5 and 7 of the batch culture to 648 newly synthesised proteins.

Although the number of newly synthesised proteins can be accurately measured, this does not tell us anything about the level of up-regulation. The number of protein spots that ceased to be expressed between sampling days was also identified using the image analysis software. Throughout the batch culture between days 1 and 3, 328 proteins were no longer expressed at detectable levels but, as the culture progressed, this number

4 Analysis of Changes in the GS-NS0 Cell Proteome during Batch Culture

decreased with 251 proteins no longer expressed between days 3 and 5 of the culture and towards the end of the culture, the number of proteins that were no longer detected (between days 5 and 7) was 409.

The data clearly shows that the greatest increase in the number of protein spots occurs between day 3 and day 5 of the culture, late exponential growth phase as expected. However, this type of analysis alone does not give any information as to the extent of the changes observed throughout the experiment. As a result, image analysis was further utilised using the difference map tool to identify the proteins which exhibited at least a 2-fold change in expression throughout batch culture. Each sample was compared to the gel image from the preceding days' 2-D gel sample. This type of image analysis enabled the total number of proteins up- or down-regulated to be identified. Table 4.3 below shows the global changes in the NS0 cell proteome throughout batch culture and the total number of proteins that concomitantly increase or decrease in expression by at least 2-fold (100%).

Throughout batch culture the general trend of proteins up-regulated relative to the preceding sample increased. Between days 1 and 3 182 proteins were up-regulated by at least 2-fold. This number decreased between days 3 and 5 with 170 proteins exhibiting a 2-fold increase in gene expression. Towards the end of the culture between days 5 and 7 the greatest increase in protein expression occurred with 271 proteins up-regulated. In common with the pattern of proteins up-regulated, as the culture progressed the same trend was observed for proteins that were down-regulated. Between days 1 and 3, 138 proteins were down-regulated, 212 proteins were down-regulated between days 3 and 5 and 263 proteins between days 5 and 7.

In total the number of newly expressed and up-regulated proteins (by at least 2-fold) throughout the batch culture increases. At lag growth phase between day 1 and 3, the expression level of 465 (34%) proteins was up-regulated while at mid-exponential growth phase between day 3 and 5, 791 (47%) of the total proteins were up-regulated or newly expressed. The greatest number of up-regulated or newly expressed proteins was observed between late exponential and death growth phase with 919 (49%) of the total number of protein spots newly expressed or up-regulated. The total number of proteins down-regulated and no longer expressed was also observed to increase as the culture progressed. Between days 1 and 3, 466 (34%) of the total number of proteins detected were down-regulated or no longer expressed when compared to the previous sample point. Later in the culture (between day 3 and 5 of the culture) 463 (28%) proteins were no longer expressed or down-regulated. Finally between day 5 and 7 of the batch culture the number of down-

regulated or no longer expressed proteins was 672 (36%). Throughout the culture the number of proteins constitutively expressed relative to the previous sample day remained almost constant at approximately 700 (40%) of the total number of protein spots.

Figure 4.4 below shows that throughout the batch culture very few proteins expression levels changed by greater than 2-fold. As the stringency of a change in expression was increased the total number of proteins regulated by the set amount was reduced as expected. As a result a 2-fold change in gene expression was utilised as the standard level with which to gauge significant changes in gene expression.

Along with the assessment of the NS0 cell proteome by global statistics, proteins which have previously been reported to have a significant role with the secretion and processing of IgG including BiP, calreticulin and PDI (High et al., 2000; Mayer et al., 2000; Michalak et al., 1999) (Figure 4.6) were assessed to investigate whether these proteins were significantly altered throughout the batch culture. Using the image analysis software, it was shown that the expression levels of BiP, PDI and calreticulin were observed to change by a maximum of 0.5-fold (50% up- or down-regulation) throughout the batch culture experiment. All three proteins showed the same pattern of gene expression throughout the batch culture with an initial decrease in expression by 1-fold between day 1 and 3, followed by a 0.5-fold increase between day 3 and 5 before decreasing again by 1-fold between day 5 and 7 of the culture (Figure 4.8).

Table 4.3 Number of proteins newly synthesised, no longer expressed and up- or down-regulated by at least 2-fold throughout the batch culture of NS0 cells

Day of Culture	Total Number of Protein Spots	Unchanged*	Up-Regulated*	Down-Regulated*	Newly Expressed*	No Longer Expressed*
1	1398	1398	-	-	-	-
3	1352	749	182	138	283	328
5	1680	677	170	212	621	251
7	1859	668	271	263	648	409

*Indicates number of proteins showing alterations in protein expression relative to the previous sample point

4 Analysis of Changes in the GS-NS0 Cell Proteome during Batch Culture

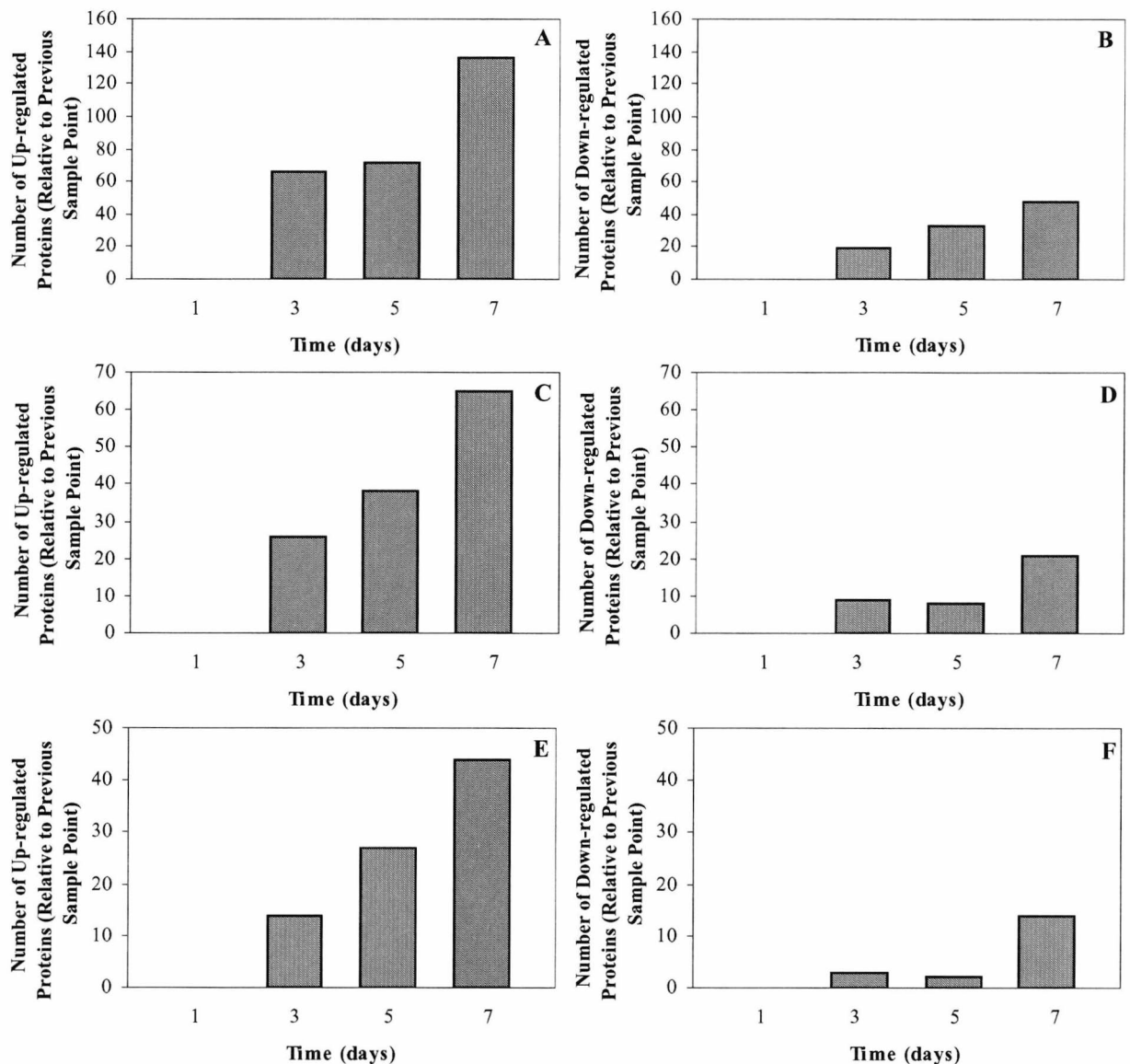


Figure 4.4 The total number of protein spots detected on samples extracted throughout the batch culture of NS0 cells in a bioreactor fermentation by 2-D electrophoresis. The number of protein spots up- and down-regulated by at least 3-fold (Figure A and B respectively), 4-fold (Figure C and D) and 5-fold (Figure E and F) throughout the batch culture experiment. The 2-D gel from each time point was compared to the previous extract to enable the comparison of protein expression throughout the batch culture. Therefore no up- or down-regulation of proteins could be determined for the 2-D gel carried out for the day 1 extract.

4.2.4 The Quantitative Analysis of Regulated Proteins throughout Batch Culture

The image analysis software allowed the identification of those proteins in which the level of expression was observed to increase or decrease by at least 2-fold throughout batch culture (Figure 4.3). Through the comparison of proteome maps available on the Internet and in publications, proteins likely to be of interest in the productivity of the NS0 cell line were investigated. The whole NS0 cell proteome map reported below (Figure 4.5) shows the position of proteins likely to be important in the processing, folding and secretion of

4 Analysis of Changes in the GS-NS0 Cell Proteome during Batch Culture

rIgG *in vitro*. The likely position of these proteins was determined through the comparison of molecular weight and pI together with the position of these proteins as identified on a Chinese hamster ovary (CHO) cell proteome map (Champion et al., 1999). The selected proteins shown below in Figure 4.5 were then subjected to tryptic digestion for confirmation of identification by MALDI-ToF ms (chapter 2, section 2.8). The resultant protein identifications are shown below in Table 4.5.

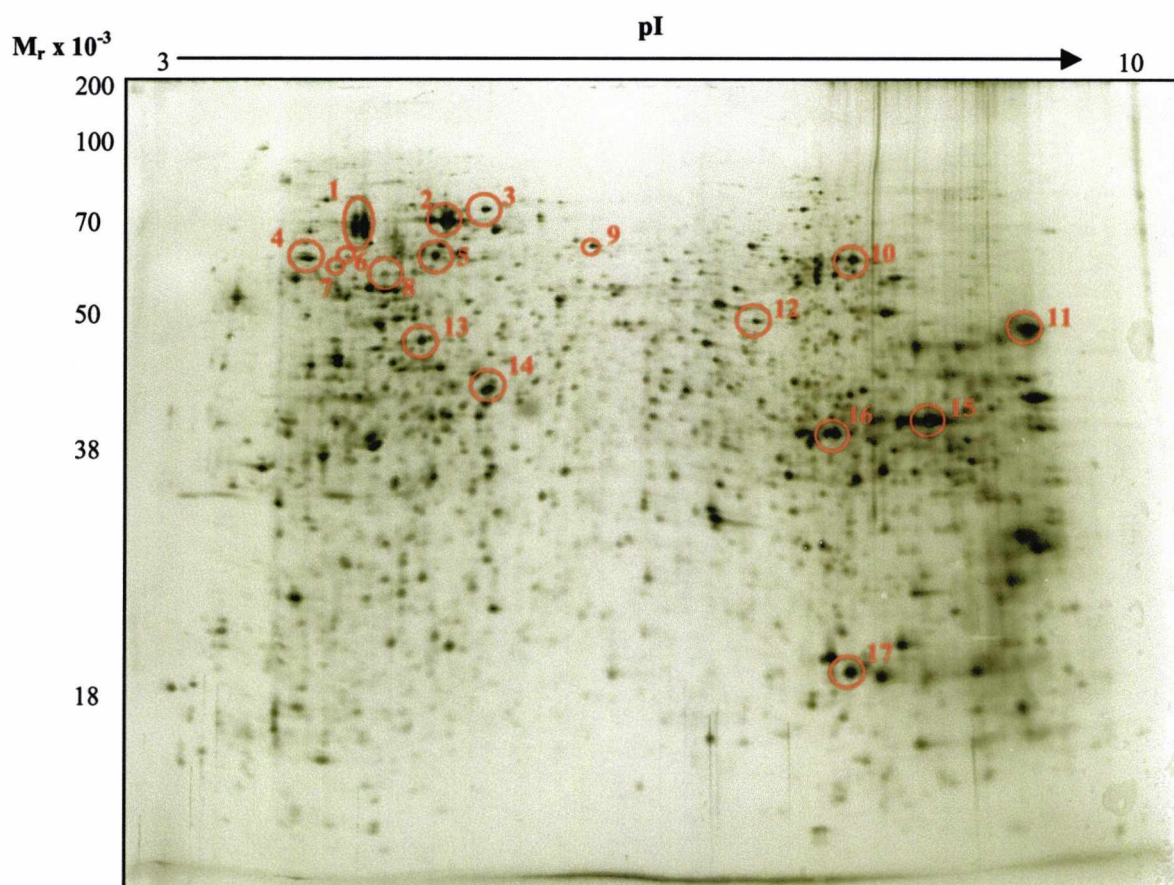


Figure 4.5 The whole NS0 cell proteome at mid-exponential growth phase. The circles highlight proteins of possible importance to the NS0 cell line for growth/division and rIgG production. Each protein was tentatively identified through comparison against other mouse cell types and CHO cell proteome maps on the Internet (www.expasy.com). Each number refers to proteins identified and detailed in Figure 4.6, 4.7 and chapter 4, Table 4.5.

4 Analysis of Changes in the GS-NS0 Cell Proteome during Batch Culture

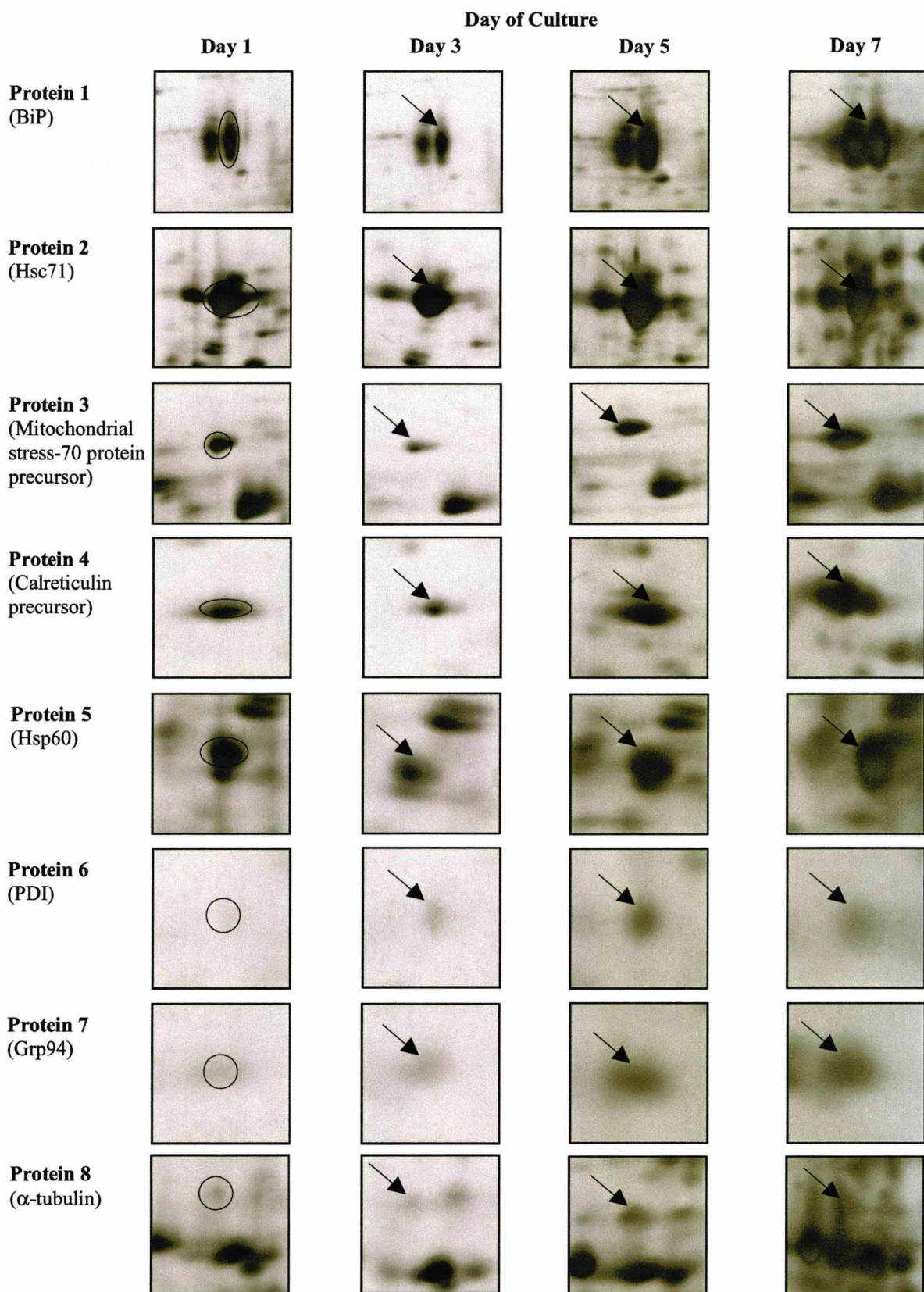


Figure 4.6 Proteins 1-8 from Figure 4.5 matched to protein spots from different sample points throughout the growth curve of NS0 cells in bioreactor culture. The highlighted proteins (circles and arrows) represent expanded areas taken from the different days of sampling, compared against the reference gel (whole NS0 cell day 1 extract).

4 Analysis of Changes in the GS-NS0 Cell Proteome during Batch Culture

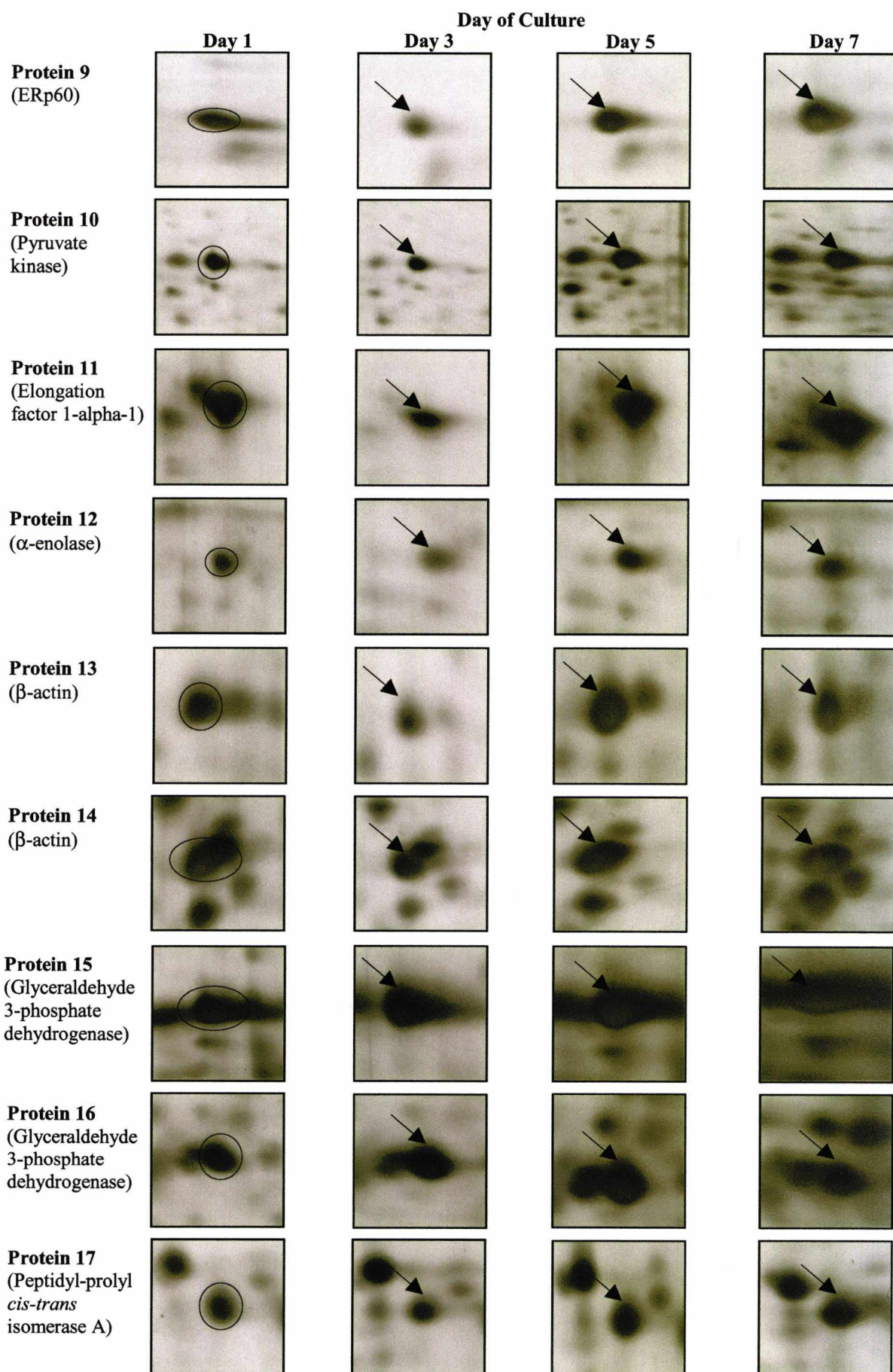


Figure 4.7 Proteins 9-17 from Figure 4.5 matched to protein spots from 2-D gels run from extracts taken throughout bioreactor batch culture of NS0 cells. The proteins highlighted represent expanded areas on each gel from different sample points matched against the reference gel (day 1 whole NS0 cell sample extract).

4 Analysis of Changes in the GS-NS0 Cell Proteome during Batch Culture

The semi-quantitative analysis of the proteins of interest whose level of expression was observed to change throughout batch culture were analysed using the image analysis software as described earlier. The software enables the direct comparison of protein expression between a set of gels through normalising spot volumes (by dividing each individual spot volume by the total spot volume). The Figures below present the semi-quantitative expression profiles of the 17 selected proteins that were highlighted in Figure 4.5. The normalised spot volume data was derived from one set of gels, and therefore was not subject to error bar inclusion.

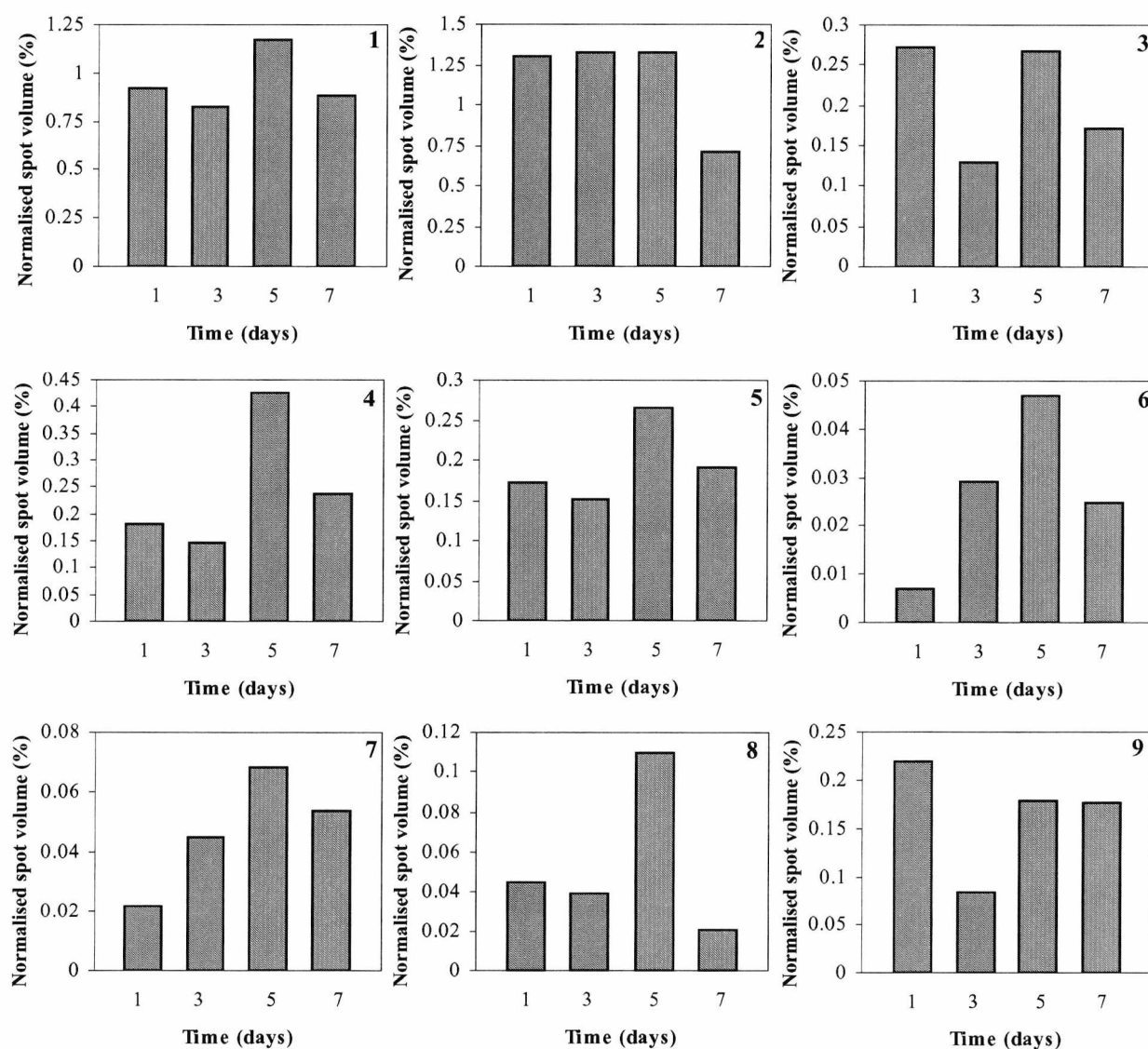


Figure 4.8 The quantitative analysis of proteins 1 to 9 in Figure 4.5 whose expression level changed throughout a batch culture of NS0 cells in a controlled 1.5 L bioreactor culture. The graphs indicate the quantitative assessment of proteins identified from 2-D maps detailed in Table 4.5. Each datum point was derived from a single gel image produced for each time point during the batch culture experiment and therefore was not subject to error analysis.

4 Analysis of Changes in the GS-NS0 Cell Proteome during Batch Culture

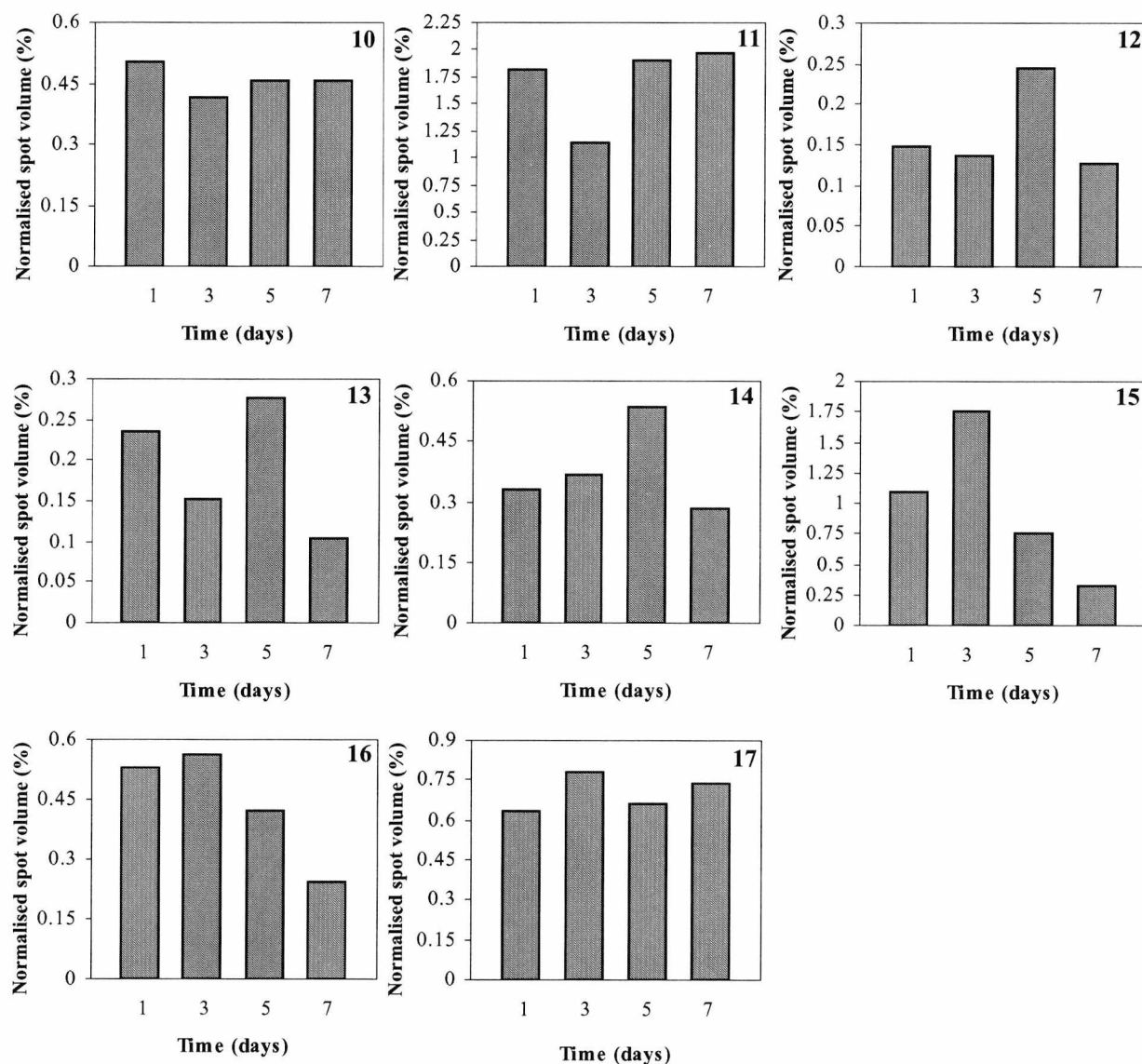


Figure 4.9 The quantitative analysis of proteins 10 to 17 in Figure 4.5 from whole NS0 cell proteins throughout bioreactor batch culture. The graphs represent the quantitative assessment of proteins identified from 2-D maps detailed in Table 4.5. Each datum point originated from individual protein spots on one 2-D gel image prepared for each sample point, and therefore was not subjected to error analysis.

The quantitative analysis described above in Figures 4.8 and 4.9 was not subjected to statistical analysis as only one 2-D gel was carried out for each time point sampled during the batch culture experiment. Therefore for comparative purposes to assess protein spot volume accuracy and reproducibility, replicate 18 cm 2-D gels that were prepared to match against the 18 cm 2-D autoradiographs (discussed in detail in chapter 5) were analysed. Although the samples were separated on a different format similar average spot

numbers were observed on the 18 cm 2-D gels as on the 24 cm gels throughout the culture (Table 4.4) however, at the end of the culture the total number of protein spots detected decreased as expected at this point in the growth curve. The 17 protein spots were assessed for each of the 18 cm 2-D gel images in the same way as for the 24 cm 2-D gels by comparing normalised spot volumes and error analysis in the form of standard deviation (chapter 2, section 2.7.4.2) was performed (Figure 4.10 and 4.11).

Table 4.4 Total average number of protein spots detected on triplicate 18 cm 2-D gels from key time points in the growth curve of NS0 cells during controlled bioreactor culture

Day of Culture	Average Number of Protein Spots Detected
1	1552 ± 89
3	1524 ± 66
5	1570 ± 103
7	1551 ± 105

Figures 4.10 and 4.11 below show the averaged normalised spot volumes achieved for each of the 17 protein spots of interest highlighted previously in Figure 4.5. Although the analysis of the 18 cm gel images was only used for comparative purposes it can clearly be seen that a similar pattern of protein expression was observed for both the 18 cm and 24 cm 2-D gels (Figure 4.9 and 4.10). The error bars indicate that small differences in individual protein spot volumes were apparent between the replicate gel images. The above Figures and quantitative data show that the expression profiles of the selected proteins changed throughout the batch culture experiment, with the expression profiles matching the visual pattern of protein expression (Figure 4.6 and 4.7). The 17 selected proteins of interest were then excised from the 24 cm 2-D gels and subjected to digestion and MALDI-ToF ms for identification by peptide mass fingerprinting (Table 4.5).

4 Analysis of Changes in the GS-NS0 Cell Proteome during Batch Culture

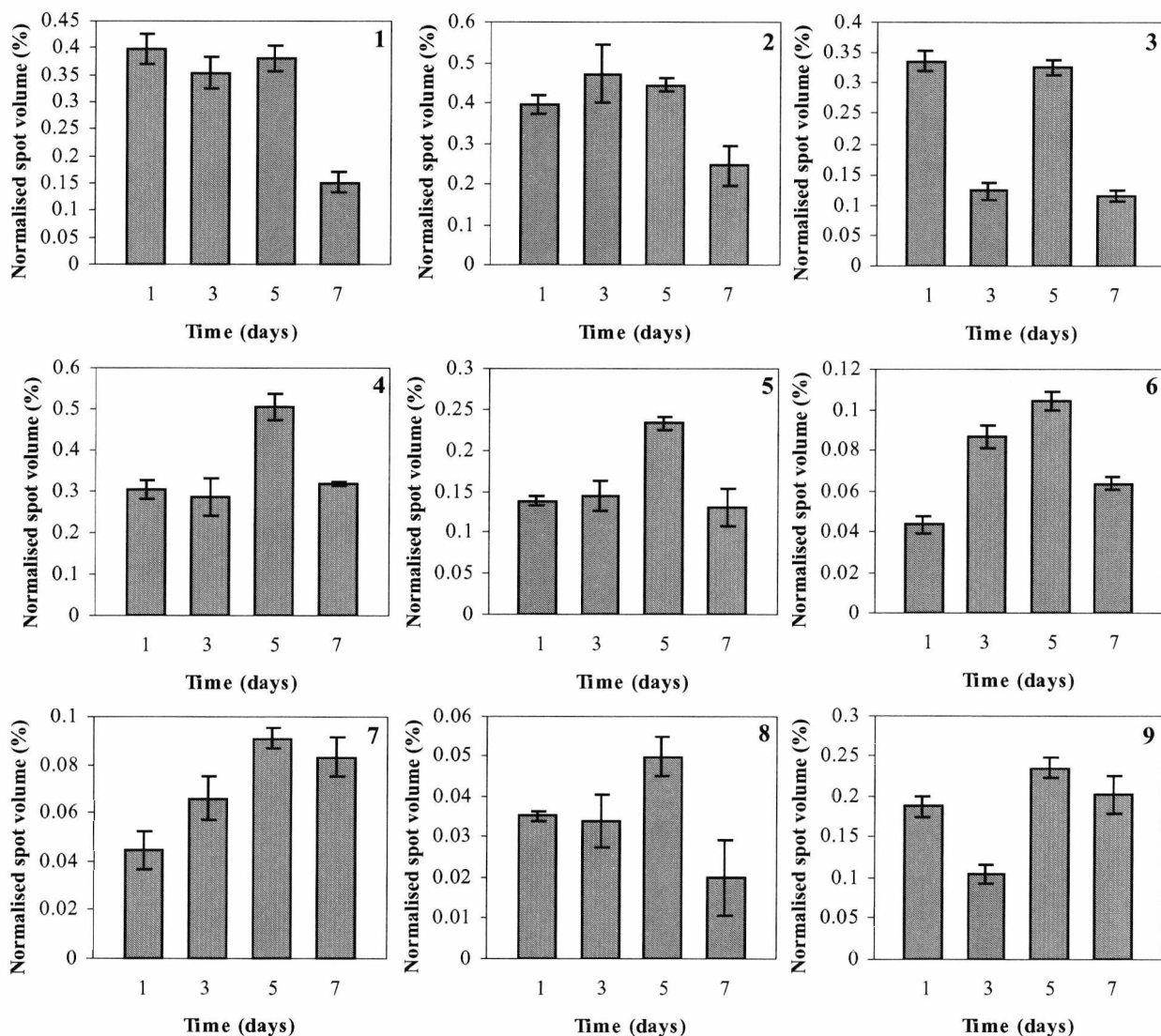


Figure 4.10 The quantitative assessment of proteins 1-9 on 18 cm 2-D gel images derived from key time points during the bioreactor batch culture experiment. Error bars represent the standard deviations of individual normalised spot volumes from triplicate 2-D gel images.

4 Analysis of Changes in the GS-NS0 Cell Proteome during Batch Culture

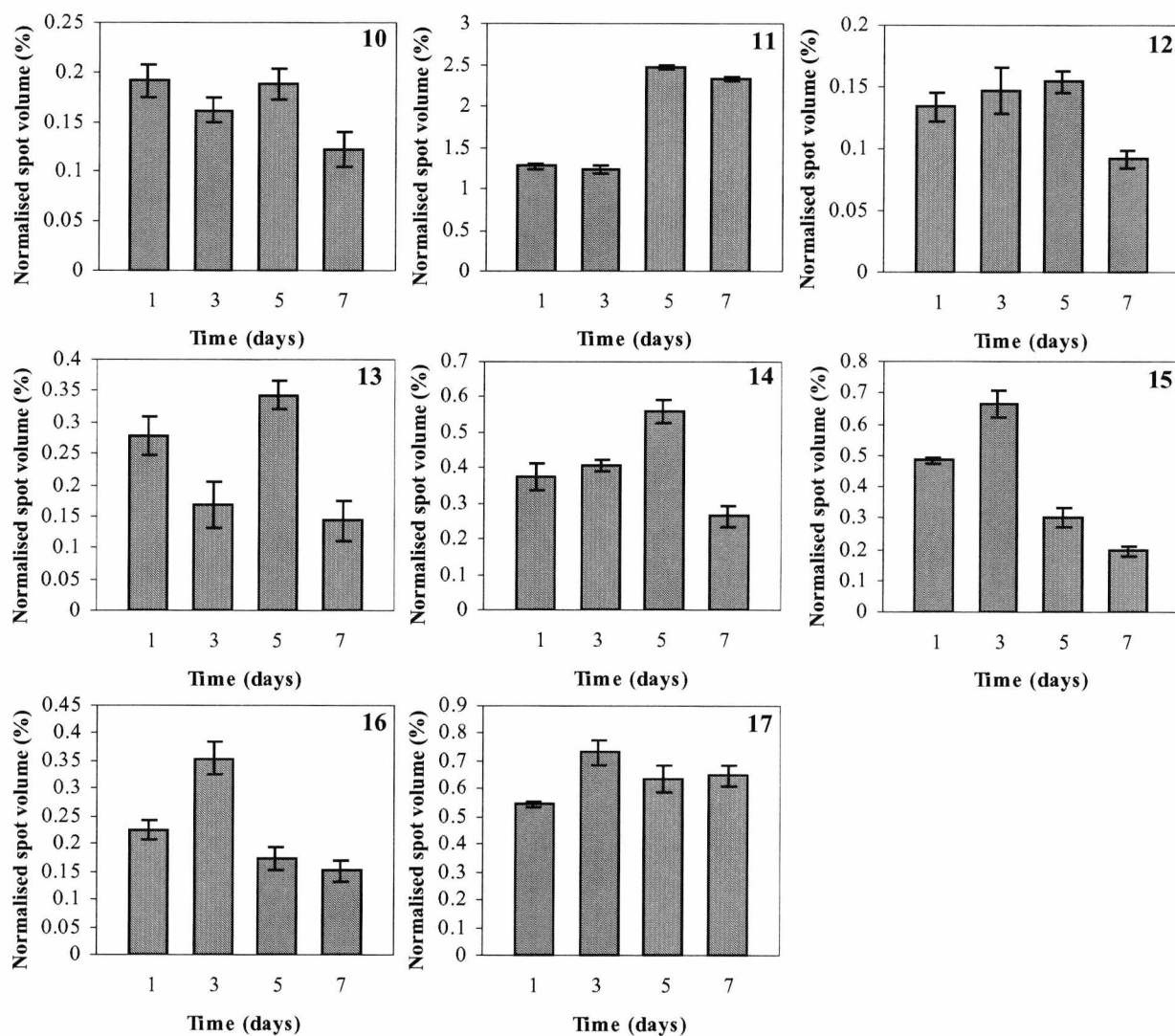


Figure 4.11 The quantitative analysis of protein spot numbers 10-17 on replicate 18 cm 2-D gel images carried out on samples extracted at key time points during the growth curve of NS0 cells in bioreactor batch culture. The error bars represent the standard deviations in individual protein normalised spot volumes on triplicate 2-D gel images.

4.2.5 Protein Identification

Table 4.3 and Figures 4.6 and 4.7 together with the semi-quantitative data represented in Figures 4.8 and 4.9 clearly show that the expression of the 17 selected proteins changed throughout the bioreactor batch culture of NS0 cells. The data represented here is only semi-quantitative as only one 24 cm 2-D gel was utilised for the analysis of each sample. Ideally at least three replicate 24 cm 2-D gels should have been run from the same sample to create a composite gel image so that any changes that observed could be confidently assigned. Although, clearly the 18 cm 2-D gel image analysis derived from the triplicate gel images shown here for the 17 protein spots of interest in Figure 4.10 and 4.11 indicated similar results to those obtained from the individual 24 cm gel images. The pattern of protein expression during bioreactor culture closely correlated with the data produced for the 24 cm protein gels run using the same samples when the normalised percent volume values were compared relative to the day 1 sample. These 17 protein spots were then excised from all four 24 cm 2-D gels and subjected to an in-gel digest with trypsin followed by identification by MALDI-ToF ms and peptide mass fingerprinting (chapter 2, section 2.8). The resultant peptide masses were entered into the Mascot search engine and identified by a probability score. The resultant protein identifications are shown in Table 4.5 below.

The proteins that were successfully identified using MALDI-ToF ms and peptide mass fingerprinting are highlighted in Table 4.5. The peptides were successfully identified from mouse databases available on the Internet (Mascot: matrixscience.com) since NS0 cells are derived from tumourous mouse B cells (Barnes et al., 2000). The protein spots were excised from each of the four 24 cm 2-D gels to confirm the identity of each protein. In order to increase the probability and the confidence of a protein match the experimental pI and molecular weight were also included in the search field (chapter 2, section 2.8.5). Further sequence analyses are detailed in appendix VII.

Table 4.5 The identification of proteins of interest excised from proteome maps of whole NS0 cell extracts and identified by MALDI-ToF ms

Spot Number	ExPASy Accession No.	Protein Identification	Species*	MOWSE Score	PMF**	Sequence Coverage	Theoretical pI	Theoretical kDa	Experimental pI	Experimental kDa	Cellular Localisation
1	P20029	BiP (Grp78)	Mouse	6.57×10^7	19/50	38%	5.07	72.40	5.11	69.50	ER lumen
2	P08109	Hsc71	Mouse	2.19×10^8	13/23	32%	5.37	70.87	5.50	70.90	cytoplasmic
3	P38647	Mitochondrial stress-70 protein precursor	Mouse	1.40×10^5	14/50	22%	5.91	73.53	5.35	75.00	mitochondrial
4	P14211	Calreticulin precursor	Mouse	7.59×10^4	11/42	28%	4.30	47.90	4.44	65.60	ER lumen
5	P19226	Hsp60	Mouse	7.73×10^5	10/50	25%	5.91	60.90	5.25	67.20	mitochondrial
6	P09103	Protein Disulphide Isomerase (PDI)	Mouse	8.28×10^4	9/27	20%	4.79	57.14	4.88	65.60	ER lumen
7	P08113	Endoplasmic precursor (Grp94)	Mouse	5.79×10^6	7/39	29%	4.74	92.48	4.84	60.00	ER lumen
8	P05213	α -tubulin	Mouse	2.86×10^6	11/50	33%	5.06	56.42	5.10	58.00	ER lumen
9	P27773	ERp60	Mouse	1.05×10^8	18/50	41%	5.99	56.62	5.54	59.60	ER lumen
10	P52480	Pyruvate Kinase	Mouse	1.95×10^{13}	26/50	50%	7.42	57.76	6.75	65.45	cytoplasmic
11	P10126	Elongation factor 1-alpha-1	Mouse	2.45×10^4	12/50	31%	9.10	50.16	9.50	52.50	cytoplasmic
12	P17182	α -enolase	Mouse	8.88×10^9	12/19	47%	6.36	47.01	6.25	53.25	cytoplasmic
13	P02570	β -actin	Human	4.39×10^5	9/27	28%	5.22	41.70	5.25	51.15	cytoplasmic
14	P02570	β -actin	Human	1.96×10^6	10/23	41%	5.22	41.70	5.35	50.25	cytoplasmic
15	P16858	Glyceraldehyde 3-phosphate dehydrogenase	Mouse	1.13×10^3	7/50	19%	8.45	35.68	7.66	45.15	cytoplasmic
16	P16858	Glyceraldehyde 3-phosphate dehydrogenase	Mouse	5.68×10^4	7/50	14%	8.45	35.68	6.55	43.20	cytoplasmic
17	P17742	Peptidyl-prolyl <i>cis-trans</i> isomerase A	Mouse	1.78×10^4	9/50	47%	7.88	17.84	6.85	23.50	cytoplasmic

Note: The sign * indicates that proteins were identified in the mouse database

The sign ** indicates the peptide mass fingerprint. The column shows the number of peptides submitted to the search that were matched

For further details of sequence analyses see Appendix VII

4.3 Discussion

4.3.1 Cell Growth

The batch culture of NS0 cells was carried out under controlled conditions in a 1.5 L bioreactor. Throughout the culture cell growth characteristics were assessed in the form of glucose utilisation and lactate accumulation (Figure 4.1B). The maximum viable cell density coincided with the maximum glucose utilisation and lactate accumulation. Following the onset of a decline in viable cell density after day 5 of the batch culture, coincidentally, a halt in further glucose utilisation was observed (Figure 4.1B). As the culture progressed, maximum glucose utilisation was observed at day 5 of the batch culture (Figure 4.1B). Glucose consumption was not depleted, however, with the concentration reducing from 21 mM to just above 13 mM by the end of the culture. Figure 4.1A shows the specific productivity of anti-CD38⁺ (an IgG₁) by NS0 cells during batch growth, which was obviously not glucose limiting. After day 5 of the culture the viable cell density and cell viability reduced however, the IgG titre was observed to reach a maximum after day 5 of the culture. The maximum rIgG concentration was obtained at the end of the culture (109 µg mL⁻¹).

The characteristics of cell growth and antibody production reported here are similar to those reported previously for NS0 cells (Bebbington et al., 1992; Downham et al., 1996). Many studies on growth and antibody production characteristics have revealed that antibody production (in hybridomas) is not associated with cellular growth, as cells exhibit higher specific productivities during the latter stages of batch cultures (Jung et al., 2002). Although, antibody production could be suggested as growth related/associated with low productivity of the cell line occurring during growth and high productivity at stationary phase of the growth curve. The greatest utilisation of glucose occurred during exponential growth (Figure 4.1B). The cessation of further glucose utilisation with the onset of a decline in cell number and viability, despite its availability, has been reported for other mammalian cells in culture (Downham et al., 1996; Kohno et al., 1993). It has been proposed that after exponential growth phase, cells have an inability to utilise glucose rather than its reduced availability. However, the exact mechanism of how and why this occurs remains unclear (Downham et al., 1996). Lactate accumulated in the growth medium as the growth curve progressed increasing to approximately 16 mM (Figure 4.1B). The yield of lactate from glucose has been associated with high specific growth rates

(Hayter et al., 1992). The level of lactate production reached its maximum at day 5 of the batch culture, and dropped off after this time. It has been reported that this shift in lactate production to consumption could be as a result of lactate being converted to pyruvate, which may enter the TCA cycle and/or be partially converted to alanine via the transamination pathway (Zhou et al., 1997). It has also been reported that once lactate consumption begins, cells die rapidly. Similar cellular metabolism has previously been reported in the batch culture of NS0 cells (Zhou et al., 1996). Cell death in NS0 cells has been reported to occur mainly via the mechanism of apoptosis, a phenomenon of programmed cell death (which allows the cell to participate in its own death), controlled by the tight balance between inducer and repressor genes (Jung et al., 2002; Samali and Cotter, 1996).

In common with cells in the *in vivo* environment, cells *in vitro* require constant stimulation by hormonal survival signals and nutrients in order to remain in a viable state (Tey et al., 2000). In many cases the survival signals are provided by factors present in serum (Meents et al., 2002), although the cells utilised in this study were cultured in supplemented serum-free medium. Cell lines cultured in serum-free media have been reported to have an increased sensitivity to apoptosis (Lasunskiaia et al., 2002; Meents et al., 2002), which can be triggered by environmental stresses including oxygen limitation and nutrient deprivation, such as glucose and amino acids (DiStefano et al., 1996; Tey et al., 2000; Zhou et al., 1997). During the batch culture of NS0 cells, glucose was not fully utilised by the cells; therefore it is more likely that the amino acids were limiting. The levels of amino acids were not monitored throughout the batch culture. Mechanisms for the delay of apoptotic cell death in NS0 cells have been implemented, which involve the over-expression of anti-apoptotic determinants including Bcl-2 and Bcl-x_L (Jung et al., 2002; Tey et al., 2000). The methodology has been successfully utilised in hybridoma and CHO cell lines, increasing cell viabilities and in some cases cell specific productivities (Jung et al., 2002; Meents et al., 2002). However Bcl-2 and Bcl-x_L over-expression has had limited success in NS0 cells, whereby, although apoptosis was successfully delayed, a significant increase in cell specific productivity despite an improvement in cell robustness was not observed (Jung et al., 2002; Tey et al., 2000).

4.3.2 Changes in the NS0 Cell Proteome throughout Bioreactor Batch Culture

In this chapter the comparison of whole cell proteome maps throughout the batch culture of NS0 cells was investigated in order to define when cells under controlled culture

conditions perceive stress, and also whether this correlates with the productivity of the cell line. The global results presented here on 24 cm 2-D gels show that as the culture progressed the total number of proteins spots visualised with silver stain at each sample point increased, and therefore the overall protein complement was seen to increase towards stationary and death phase (Table 4.2). Between day 1 and 3 of the batch culture the total number of protein spots visualised decreased from 1398 to 1352. This small decrease may be due to the inherent errors involved in proteomic analysis. The small increased number of proteins visualised at day 1 compared to day 3 may be as a result of the cells being placed in a new environment; therefore the cells may have been subjected to a mild stress. Early in the batch culture cells would be expected to be preparing for growth and proliferation. However, the cells used to inoculate the bioreactor vessel were already growing at an exponential rate; therefore the proteins involved with cell growth/proliferation and production of IgG should already be available to the cell. At the start of the batch culture experiment there was only a short lag phase in cell growth, and by the third day of the culture, the cells were beginning to grow exponentially and to produce rIgG (Figure 4.1A). From the 2-D gel produced from a sample extracted on day 3 of the batch culture, the total number of protein spots detected decreased from day 1. This may be as a result of the NS0 cells no longer being under the mild stress conditions of being introduced into a new culture environment as already stated. However, the 2-D gel from this time point (day 3) is slightly under-loaded/under-stained when compared to the day 1 sample (Figure 4.2), therefore, as a result less proteins were visualised accounting for the decrease in the number of protein spots detected.

At late exponential growth phase (day 5 of the culture), as expected, the total number of proteins detected increased to 1680. This coincided with maximum viable cell density and the maximum rate of production of rIgG (maximum qMAb). The greatest reduction in glucose concentration also occurred at this time point (Figure 4.1B), presumably as a result of the energy requirements for maximum cell growth and rIgG production. At this stage in the growth curve we would expect to observe the maximum change in the NS0 cell proteome. Previous reports suggest at this time we should observe stress protein induction as a result of unfolded rIgG accumulation within the endoplasmic reticulum (ER) and the unfolded protein response (Downham et al., 1996; Kohno et al., 1993). Furthermore, at this point in the growth curve the NS0 cells are likely to be under stress due to nutrient deprivation and the accumulation of toxic waste products within the cell culture medium.

The number of proteins detected on day 7 of the batch culture increased to 1859, an increment of 179 detected proteins. This further increase in spot numbers was not expected. Late in the growth curve (at day 7), most of the cells in the culture were dead or dying, with a reduction in cell viability to 22% (Figure 4.1A). The rIgG titre was also no longer increasing at an exponential rate (Figure 4.1A). Therefore, it was expected that proteins required for cell growth and proliferation would be switched off or down-regulated at this stage in the growth curve as the cells would no longer have a requirement for them. At the same time, we would expect the expression levels of proteins involved with apoptosis and stress responses (such as the pro-apoptotic proteins of the caspase cascade and heat shock proteins including Hsp70) to be up-regulated. The increase in protein spot number observed on the 24 cm format 2-D gel at day 7 of the batch culture was not observed on the 2-D autoradiographs or 18 cm 2-D gels run from the same sample (discussed in chapter 5). Therefore, it is likely that the 2-D gel run for the sample extracted on day 7 was either overloaded or over-stained in comparison to days 1, 3, and 5. Figure 4.2 shows the digital images of the 24 cm 2-D gels run for the batch culture experiment. It is clearly visible that the day 7 gel (Figure 4.2D) is over-stained in comparison to the preceding 2-D gel from day 5 of culture (Figure 4.2C) resulting in more proteins (or artefacts) being visualised. Although the data discussed here is derived from one 24 cm 2-D gel image for each time point sampled, the same general trend was observed for the average spot numbers on the replicate 18 cm 2-D gel images (Table 4.4). As a result, the number of protein spots detected throughout the batch culture experiment on 24 cm format can be confirmed as being accurate, although clearly the number of protein spots detectable at the end of the culture did decrease rather than increase explained by the reasons discussed above.

Observations based on numerical differences alone do not take into account the change in expression levels of the protein complement throughout the batch culture. The number of proteins visualised at each sample point is the end product of increases and decreases in protein expression; therefore it is more informative to investigate the extent of up-and down-regulation of specific proteins throughout the experiment rather than just taking into account global numerical differences.

4.3.3 Analysis of Proteins Exhibiting a 2-fold Change in the Level of Expression

Proteomic analysis has been utilised to identify the changes in protein expression throughout a batch culture of NS0 cells and to determine when NS0 cells cultured under

controlled conditions perceive stress. Initial analysis shows that although all 2-D gels were stained at the same time, some differences in the intensity of staining was apparent. This was accounted for during analysis of individual spots using the normalisation tool in the image analysis software so that all protein spots could be compared between different gels. Approximately 700 (40%) of the proteins across the experimental set of gels did not show any significant alterations in the level of expression throughout batch culture. These proteins are likely to be 'housekeeping' proteins, which are constitutively expressed and essential under normal growth conditions for basic metabolic activities and cell functioning (Table 4.3) (Hartl, 1996). Proteins that are unchanged throughout batch culture are unaffected by stress and changes in the level of nutrient and waste product accumulation.

Proteins that were newly expressed and those whose expression was down-regulated as the culture progressed were investigated throughout the batch culture (Table 4.3), together with proteins whose level of expression changed by at least 2-fold. Proteins that demonstrated less than a 2-fold change in gene expression were not considered as significant changes in expression except in a few cases where the protein spot volume was high and the protein was already highly expressed. For example, BiP, PDI and calreticulin are proteins known to interact with nascent IgG and have important roles in processing and secretion (High et al., 2000; Mayer et al., 2000; Michalak et al., 1999). The expression levels of these proteins were observed to change only by 0.5-fold (50%) throughout the batch culture. However, this result is not surprising (that the expression levels of these proteins only changed by a small amount) since BiP, PDI and calreticulin are involved in many cellular processes and were abundant and highly expressed even on day 1 of culture (Figure 4.6 and 4.8, protein numbers 1, 4 and 6). Therefore, even a small change in the level of expression could be significant (that is, a 50% change in abundance of a highly expressed protein is significant).

The results obtained from the analysis of the NS0 cell proteome maps carried out at key time points throughout the batch culture experiment showed that the expression level of many proteins changed by at least 2-fold (100%) (Table 4.3). Throughout the culture most of the changes in protein expression were observed at exponential growth phase in accordance with the global changes in spot numbers (section 4.3.2, Table 4.2 and 4.3).

Between day 1 and 3 of culture, 34% of the proteins detected were newly expressed and/or exhibited a 2-fold increase in the level of expression, and approximately 34% were no longer present at detectable levels and showed a 2-fold or greater decrease in expression (Table 4.3). Therefore, even early in the culture, the expression levels of two-thirds of all

those proteins expressed were modulated. After the third day of culture, the cells were growing/dividing at an exponential rate and also started to produce rIgG at an exponential rate. Therefore it was not surprising that the expression level of many proteins was modulated by the cell at this point in the growth curve. Between day 3 and 5 (at exponential growth phase), 47% of the proteins detected exhibited an increase in expression levels. Fewer proteins (28%) exhibited a decrease in expression by at least 2-fold. This indicates that many proteins are required to enable exponential cell growth/proliferation and maximum production of rIgG. It is likely that at this stage of the growth curve, the cells would be under a greater amount of stress than during the earlier stages of growth as a result of any unfolded IgG accumulating within the ER, but also due to large energy requirements of the cell to enable protein synthesis, cell growth and division. As a result, proteins involved with glycolysis, proliferation, and the unfolded protein response (UPR) (general stress response proteins) are likely to be induced at this stage of the growth curve. Furthermore, the cells at this stage must respond to increasing levels of toxic metabolites (e.g. lactate), shear stress and other environmental changes.

The greatest change in the level of protein expression occurred towards the end of the culture between day 5 and 7, with 49% and 36% of the proteins detected exhibiting an increase or decrease in gene expression respectively. The maximum change in the pattern of protein expression coincided with the cells reaching maximum viable cell density, and rIgG titre. It has been postulated when large amounts of protein are being produced, the induction of the unfolded protein response results, which in turn induces stress proteins (Patil and Walter, 2001). However, we have shown here that many of the proteins known to be involved with the stress response are already abundant and are constitutively expressed throughout culture (Figure 4.6 to 4.9). This has also been reported elsewhere in B-cell differentiation (van Anken et al., 2003). Therefore, it is likely that these 'global' figures observed may be as a result of an UPR, which has been shown to form part of a more general stress response (Patil and Walter, 2001). It is likely that the cells would be perceiving a great amount of stress late in the culture as a result of the environmental changes and possibly as a result of the accumulation of IgG within the secretory pathway, inducing an UPR. The unfolded protein response describes the effect of unfolded protein accumulation within the ER, and also forms a general stress response (Ellgaard and Helelius, 2001; Harding et al., 2002).

The UPR in mammals can have both cryoprotective and cytotoxic functions, and can result in cell survival through up-regulation of UPR target genes to induce proteins

including the chaperones, or regulated cell death through triggering pro-apoptotic effectors (Patil and Walter, 2001). The decision between the two outcomes is believed to be made during a cell-cycle arrest which is generated in response to ER stress. The delay in the cell-cycle is believed to enable the cell to determine whether adaptation to stressful conditions, mediated by chaperones and other target genes, will be possible and, if not, to continue towards apoptosis (Patil and Walter, 2001). In response to accumulating proteins in the ER, a signal is sent across the ER membrane into the nuclear and cytoplasmic compartments, where effector proteins respond by up-regulating the transcription of target genes and slowing general translation. As a result, the cell is able to survive conditions, which otherwise compromise protein folding within the ER (Patil and Walter, 2001). The ER contains an environment which is optimised for efficient folding, and it is within the ER that proteins translocated into the secretory pathway undergo the modifications and interactions with chaperones that are essential for their maturation into their final conformations.

The main targets for transcriptional up-regulation in response to stress have been identified as the ER-resident chaperones including BiP (a major chaperone of the ER) and proteins involved in every step of the secretory pathway (Patil and Walter, 2001), which act to decrease the concentration of unfolded proteins by increasing the rate of folding, post-translational processing, export and if required, degradation, to efficiently clear the cell of the accumulated proteins to reduce the load on the folding capacity of the cell. If the UPR fails to clear the accumulated proteins from the ER, the caspase cascade is activated, resulting in apoptosis and controlled cell death (Patil and Walter, 2001). During the late exponential growth phase it is possible that the cells would be affected by the UPR as a result of the increased IgG titre at the end of the culture. However, in this case it is likely that the cells would also be under stress as a result of toxic waste product build-up, increased shear pressure, and nutrient deprivation (i.e. environmental stress). Given the relatively low qMAb obtained for these cells and the fact that other reports have shown much higher qMAb in the same cell line (discussed in chapter 6), it is unlikely that the cells had reached their full folding potential. The maximum concentration of glucose was utilised at day 5 of the growth curve, and the concentration remained unchanged until the end of the culture. It has been shown that glucose depletion has a major effect upon inducing stress proteins including endoplasmic reticulum resident proteins including Grp78 and Grp94 (Downham et al., 1996). Therefore it was not unexpected that at this stage in the growth curve many proteins were induced and up-regulated (Figure 4.3C and Table

4.3). In opposition to the anti-apoptotic proteins, we would expect pro-apoptotic proteins involved in activating the caspase cascade to be up-regulated at this late stage of the growth curve. The nutrients within the culture medium at this stage of the growth curve would have been exhausted and the waste products of cell metabolism would also be accumulating to toxic levels, and therefore the stresses upon the cells at this time would be fatal (Patil and Walter, 2001). Furthermore, the greatest decrease in protein expression was observed at this stage in the growth curve with 36% of all the proteins expressed being down-regulated (by at least 2-fold) or no longer detectable. This may be as a result of processes involved with cell growth and division being down-regulated or switched off, as the cells would no longer require them at this late stage in the growth curve.

The results discussed in this section assume that a 2-fold change in protein expression is indicative of a significant change in a proteins expression. Although many proteins on the NS0 cell proteome map are of relatively high abundance and therefore have a high spot volume, the software is only capable of semi-quantifying proteins that are highly abundant and saturated or negatively stained. There is also large error involved in quantifying proteins that are present in low abundance. These lower abundance proteins are often 'masked' by other housekeeping proteins (Mitchell, 2003). Furthermore, it is not possible to determine the 'level of activity' of a given protein on a 2-D gel. Recent reports have shown that a single gene product is capable of yielding up to 10-15 different protein spots, mostly as a result of post-translational modifications (Mann and Jensen, 2003; Mitchell, 2003). For example, β -actin and glyceraldehyde 3-phosphate dehydrogenase have been identified in at least two positions on the NS0 cell proteome map (Figure 4.7). However, the protein spot concentration or spot volume may not always relate to the activity or function of that particular protein. Different proteins have varying half-lives, and may also be degraded at different rates by the cell. Whether a protein is actively being synthesised by the cell at each time point cannot be investigated using the approach described in this chapter and the investigation of post-translational modifications of the proteins present on 2-D gels often requires further molecular tools and biochemical approaches including LC/ms, which can be utilised to detect mass changes due to covalent modifications (Wu and Yates, 2003). We also assume that on each gel, one single protein spot contains one protein, although it is possible for proteins to co-localise in one spot on a 2-D gel (Gorg, 2000a). However, it was beyond the scope of this project to identify

whether this was the case for any of the protein spots detected on the 2-D gels reported here.

The global results reported in this chapter are based on single gels being analysed for each sample point. Ideally at least three gels for each sample point should have been prepared so that the differences in protein expression analysis could easily be confirmed or discounted. However, the global statistics reported in the next chapter, whereby 18 cm 2-D gel images were prepared and analysed from the same samples (chapter 5, Table 5.4), similar patterns of protein expression were observed to the data discussed in this chapter for the 24 cm 2-D gels (Table 4.3). This confirms that the data provided here, although utilising individual gels, accurately describes the changes in the NS0 cell proteome during bioreactor batch culture.

4.3.4 Quantitative Analysis and Identification of Specific NS0 Cell Proteins

The comparative analysis of the NS0 cell proteome throughout batch culture showed that many changes in protein expression were observed. More than 400 proteins were up- or down-regulated throughout the culture (Table 4.3). Proteins that were identified as being of importance to the productivity of the cell line were first tentatively identified through matching the protein spots against a proteome map of CHO cells. The level of expression of 17 proteins were then analysed followed by confirmation of their identity by peptide mass fingerprinting (PMF). The 17 proteins identified by PMF were divided into 3 main groups; molecular chaperones, glycolytic enzymes and structural proteins. The relative position of each protein spot was mapped, and then the expression level of each protein was compared at each time point (Figures 4.5 to 4.9).

The results show that the pattern of gene expression varies according to each protein. The 17 proteins that were chosen for further analysis through identification by MALDI-ToF (Table 4.5) are discussed in greater detail below. Many of the proteins that were identified are chaperones. Approximately a quarter of all chaperones known are stress proteins which undergo up-regulation during conditions of cellular stress, but many are also essential under normal growth conditions (Agashe and Hartl, 2000). Heat shock proteins (HSPs) have typically long half-lives (~48 hr has been reported in human epidermoid cells) (Kiang and Tsokos, 1998). Increased expression of these proteins in many cultured cells has also been reported (Kiang and Tsokos, 1998). Various conditions including nutrient starvation, particularly of glucose, can result in increased expression of many ER proteins. Therefore, it was not unexpected that the increased expression of many

HSPs and chaperones occurred throughout batch culture, particularly when glucose levels were decreased and depleted (Downham et al., 1996). The common factor in many cases whereby increased expression of chaperones and/or HSPs occurs is the accumulation of unfolded proteins within the ER and/or environmental stresses. The protective mechanism is probably mediated by the HSPs capacity to function as molecular chaperones to prevent inappropriate protein aggregation and to mediate the transport of immature proteins to the target organelle for packaging, degradation or repair (Kiang and Tsokos, 1998).

Enolase, glyceraldehyde 3-phosphate dehydrogenase and pyruvate kinase are key glycolytic enzymes. Particularly during exponential growth phase, cell metabolism is expected to increase in order to support the rapid turnover of proteins required during this period of rapid cell growth and proliferation. In accordance with the increase in viable cell density and IgG titre, the level of glucose utilisation was also observed to increase (with the maximum utilisation occurring at day 5 of the culture). As the maximum utilisation of glucose occurred during exponential growth phase it is likely that the induction of these key glycolytic proteins constitute part of the cellular response to increased metabolic requirements following increased cell division and proliferation (Van Dyk et al., 2003).

Structural proteins actin and tubulin were also identified on the NS0 cell proteome map and their level of expression was assumed to remain unchanged as the culture progressed (Lee et al., 1996). However, throughout the culture the expression levels of these proteins did change. Actin and Tubulin have been reported to be involved with remodelling of the cell cytoskeleton and to be involved in the trafficking and secretion of proteins from the cell through microtubules (Thyberg and Moskalewski, 1999). Although the level of expression of these proteins was not expected to change throughout the batch culture, it is possible that the increase in the level of tubulin occurred as a direct result of rIgG accumulating in the ER which required transportation out of the cell. These three groups of proteins (chaperones, glycolytic and structural proteins) are discussed below.

4.3.4.1 BiP (Grp78)

BiP or glucose regulated protein 78 (Grp78), is an Hsp70 molecular chaperone located in the lumen of the endoplasmic reticulum (ER) and was originally identified as the immunoglobulin heavy chain binding protein (Johnson et al., 2001). The analysis reported here showed that the greatest increase in the level of expression of BiP was at exponential growth phase (day 5) when the level of glucose uptake was halted. This has previously been reported to occur towards the end stage of cell growth (Downham et al., 1996). At

this stage of the growth curve both lactate production and rIgG production were at their maximum levels. After this time point the level of expression of BiP decreased, coinciding with a reduction in viable cell density (Figure 4.1A and Figure 4.8, number 1).

BiP has been reported to bind newly synthesised proteins and hydrophobic polypeptides (Johnson et al., 2001) as they are translocated into the ER and maintains them in a state which is suitable for their folding and oligomerisation by preventing intra- or intermolecular aggregation (Gething, 1999). BiP is also an essential component of the translocation machinery and plays a role in retrograde transport across the ER membrane of proteins destined for degradation by the proteasome. BiP interacts synergistically with PDI in the *in vitro* folding of the Fab fragment of IgG and is thought to hold the unfolded antibody chains in a conformation which allows PDI to access the cysteine side chains for the correct folding to occur (Mayer et al., 2000). Like all Hsp70 proteins, BiP has a weak ATPase activity, and the binding of ATP is necessary for the release of peptides bound to BiP. The protein has a binding site selective for hydrophobic residues, and therefore it has been postulated that the binding sequences in BiP for IgG are the light chain and the V_H, C_{H1} and C_{H3} domains of the immunoglobulin (Ig) heavy chain (Mayer et al., 2000). As in previously published data (Champion et al., 1999), BiP is amongst the most dominant ER proteins present in the NS0 cell proteome map.

During batch culture of NS0 cells an increase in BiP expression was observed. This agrees with previous reports (Downham et al., 1996; van Anken et al., 2003). The over-expression of BiP is thought to protect the cell from stress, although there are conflicting views regarding the effect of increased BiP expression on the secretion of recombinant proteins. In several reports the increased expression has been associated with a decrease in the secretion of recombinant protein (Edgington, 1992). However, an alternative viewpoint has been reported suggesting that the over-expression of BiP contributes to an overall increase in the rate of secretion of recombinant protein (Downham et al., 1996). The results reported here suggest that BiP expression was maintained during the stress response, reaching its maximum expression level during late exponential growth phase. The induction of BiP occurred early in culture suggesting NS0 cells perceive stress relatively early during batch culture.

4.3.4.2 Heat Shock Cognate-71 (Hsc71)

Hsc71, heat shock protein cognate-71 (Hsc70, Hsp73) is found in the nucleus and cytoplasm of cells. It belongs to the largest group of chaperones, the Hsp70 family. The

protein is constitutively expressed and is most abundant in growing cells and is not heat-shock inducible (Sorger and Pelham, 1987). In common with other stress proteins, increased levels of these proteins are observed after environmental stresses and under normal physiological processes, although the protein is constitutively expressed in unstressed cells (Kiang and Tsokos, 1998). As expected, Hsc71 was highly expressed throughout batch culture, although expression increased slightly as the culture progressed (Figure 4.8, number 2). At the later stages of culture, (between day 5 and 7) the level of Hsc71 expression decreased to approximately half the level observed earlier in the growth curve.

Hsp70 proteins have a wide range of activities and have been reported to bind up to 20% of nascent and newly synthesised polypeptide chains (Hartl and Hayer-Hartl, 2002). Hsc71 also acts in facilitating the proteolytic degradation of unstable proteins, and in some cases can control the biological activity of folded regulatory proteins including transcription factors. All of these cellular activities require the ATP-regulated association of Hsp70 with short hydrophobic segments in substrate molecules, which prevent the further folding or aggregation by shielding these segments (Bukau and Horwich, 1998).

Under times of stress Hsp70 proteins provide an essential role in preventing aggregation and assist in the refolding of mis-folded proteins (Bukau and Horwich, 1998). The protein may act to prevent apoptosis under times of cellular stress (Kiang and Tsokos, 1998) to promote cell survival by inhibiting caspase-dependent events including changes in cell morphology (Jaattela et al., 1998). These functions fit with the observed changes in the level of expression of Hsc71 throughout the batch culture during days 1 to 5. However, the level of expression of the protein decreased at day 7 of culture. At this stage of the culture, the cells would likely be under a great amount of cellular stress as a result of the decline in nutrients, waste product accumulation and a possible build-up of IgG within the ER. At this late stage in culture, cell viability decreased to 22%; therefore almost all of the cells are dead or dying and expression of large amounts of Hsc71 would serve no purpose to the cell (Figure 4.8, number 2).

4.3.4.3 Mitochondrial Stress-70 Protein (Grp75)

Mitochondrial stress-70 protein (mortalin, Grp75) is a member of the Hsp70 family. The protein has been implicated to be involved in the stress response, mitochondrial biogenesis, intracellular trafficking, control of cell proliferation (cellular aging and survival), and also cell fate determination, by affording apoptosis protection (Kaul et al., 2002). Grp75 may

also act as a molecular chaperone (Kaul et al., 2002). In agreement with the reported properties of Grp75, the semi-quantitative assessment of Grp75 throughout batch culture reported here clearly showed that the protein was up-regulated at the start of culture. This is in agreement with the suggested role of Grp75 in cell proliferation (Figure 4.8, number 3). The expression of Grp75 decreased after this time point, but was then observed to increase again at late exponential growth phase when the cells would be under conditions of maximum stress. At this point in the growth curve we would expect Grp75 to become up-regulated, and the anti-apoptotic characteristics of Grp75 would be expected to take effect in response to the reduction in glucose uptake by the cells (Takano et al., 2001).

4.3.4.4 Calreticulin

Calreticulin is a chaperone found mainly in the lumen of the ER. During the course of the NS0 cell batch culture the level of calreticulin expression was relatively low early in the culture, and was greatly induced at day 5 of the culture. Towards the end of the culture at day 7, the expression level reduced to approximately half the expression level observed at day 5. At this stage in the growth curve, most of the cells were dead, with the culture having a viability of approximately 22%. The increase in the level of expression at day 5 of the batch culture was expected since calreticulin has been reported to become up-regulated during times of stress. Therefore, the results shown here indicate that NS0 cells were likely to be exposed to the maximum 'stress' levels at late exponential phase (day 5) of the batch culture.

The period in the growth curve where maximum IgG was being produced coincided with maximum cell viability and maximum glucose utilisation by the NS0 cells (Figure 4.1A and Figure 4.8, number 4). Calreticulin acts as a glycan recognising chaperone, which either binds peptides through its lectin activity, before or after the chaperone BiP depending on the position of N-linked glycans. The protein is also involved with the regulation of Ca^{2+} signalling and the modulation of gene expression. It has been proposed that calreticulin binds polypeptides through exposed hydrophobic polypeptide sequences. Calreticulin has also been reported to store BiP for quick release during times of stress (Llewellyn et al., 2000). Calreticulin also interacts with its membrane bound homologue calnexin to bind and release newly folded proteins and glycoproteins (Ellgaard and Helelius, 2001). Competition has been reported to occur between this calreticulin/calnexin pathway and the classical BiP/PDI pathway depending on the position of glycosylation in the glycoprotein. Calreticulin is thought to interact with PDI in a calcium dependent

manner affecting and inhibiting PDI chaperone activity. This may result in the release of unfolded proteins from PDI to leave them free to interact with other ER chaperones, which may allow a flux of proteins from one chaperone to another (Michalak et al., 1999). Calreticulin also interacts with ERp60 in a calcium-regulated manner and affects its chaperone activity (Michalak et al., 1999).

Although calreticulin contains an ER retaining sequence (KDEL), when the protein's expression is up-regulated such as during times of cellular stress including apoptosis and necrosis, calreticulin undergoes translocation to the cell surface. Protein glycosylation may also have a role in the cellular distribution of calreticulin. It has been shown in CHO cells that under times of stress the protein becomes glycosylated and this results in the redistribution of the protein within the cell. It has been anticipated that calreticulin is essential to cell survival and proliferation and has a role in regulating apoptosis during times of stress (Johnson et al., 2001). These reported characteristics fit with the changes in the level of expression of calreticulin observed on the NS0 cell proteome map throughout batch culture.

4.3.4.5 Heat Shock Protein-60 (Hsp60)

Hsp60 is a mitochondrial chaperonin. The semi-quantitative analysis of Hsp60 indicated it was expressed at relatively high levels throughout batch culture. However, the maximum level of Hsp60 protein expression was reached at day 5 of the culture. The level of expression reduced by approximately 25% to day 7 of the culture, although the level remained high in comparison with other proteins (including Hsc71 and Grp75, Figure 4.8, number 2 and 3) at the same time point (Figure 4.8, number 5). The observation that the protein expression level remained high to the end of culture correlates with reports which suggest Hsp60 has a role in modulating pro-apoptotic pathways within mammalian cell types (Moller et al., 2002; Samali et al., 1999). The Hsp60 class of proteins are found in all compartments of cells except the ER (Fink, 1999). Hsp60 proteins are constitutively expressed in the absence of heat shock and require a co-chaperonin for full activity (Fink, 1999). Hsp60 proteins bind partially folded intermediates after the Hsp70 proteins, preventing their aggregation and facilitating their folding and correct assembly (Fink, 1999).

Hsp60 proteins have an ATPase activity and ATP binding-directed substrate release is required for the release of correctly folded proteins (Bukau and Horwich, 1998). Hsp60 and Hsp10 have been found to form a complex with pro-caspase-3 the precursor of

caspase-3, accelerating the activation of it by cytochrome *c* and dATP in an ATP-dependent manner (Xanthoudakis et al., 1999). Upon induction of apoptosis, pro-caspase-3 is cleaved to form the active caspase-3 molecule which is dissociated from the HSP complex, this occurs simultaneously with the release of HSPs from mitochondria suggesting these HSPs are positive regulators of caspases during apoptosis (Samali et al., 1999). The release of these HSPs from mitochondria may participate in the amplification of the caspase cascade in the cytosol.

4.3.4.6 Protein Disulphide Isomerase (PDI)

Protein disulphide isomerase (PDI) (Figure 4.8, number 6) is a member of the thioredoxin superfamily and is an oxidoreductase that is present in many cellular locations (Noiva, 1999) and is part of the quality control machinery in the ER. The semi-quantitative analysis of PDI showed that the level of expression increased during exponential growth phase between day 3 and 5. The increased expression of PDI at this stage of the growth curve coincided with the maximum rate of IgG production by NS0 cells (Figure 4.1A). PDI acts synergistically with BiP in the *in vitro* folding of the denatured and reduced Fab fragment of IgG (Mayer et al., 2000). BiP has been reported to bind the unfolded polypeptide chains to keep them in a conformation in which the cysteine residues are accessible for PDI to catalyse the rate-limiting reactions of disulphide bond formation (Ferrari and Soling, 1999). PDI expression has also been associated with events including heat shock and crowding which increase chaperone activity in the cell (Noiva, 1999; Wang, 2002). These reports fit the expression profile of PDI observed throughout batch culture.

During exponential phase, PDI is likely to be required by the cell to process the increasing IgG being produced more efficiently (Noiva, 1999). PDI catalyses the formation, reduction and isomerisation of disulphide bonds depending upon the redox conditions and the nature of the substrate protein (Frand et al., 2000). PDI must be present during the initial stages of folding and reoxidation of antibodies to influence the reaction. During the ATP-dependent cycles of BiP and the Fab region of the IgG, it has been postulated that PDI binds to antibody chains simultaneously with BiP or after BiP is released from the polypeptide chain (Mayer et al., 2000).

4.3.4.7 Endoplasmic Precursor (Grp94)

Endoplasmic precursor (Grp94) is an abundant glycoprotein of the ER lumen. The protein is constitutively expressed in mammalian cells (Argon and Simen, 1999; Downham et al., 1996). Throughout batch culture, the semi-quantitative analysis of Grp94 indicated it was expressed throughout the growth curve, and increased steadily until the end of exponential growth was reached at day 5. The level of expression of Grp94 decreased at day 7, but was still present at higher levels than was observed at earlier stages of culture (Figure 4.8, number 7). Grp94 has been implicated in the folding process and in the transport of secreted proteins. Grp94 may act sequentially with BiP in the assembly of IgG molecules (Melnick et al., 1994) and is part of the complex quality control system for protein folding in the ER (Moller et al., 2002). These reports support the increased level of Grp94 observed during exponential growth phase when rIgG was produced at maximum levels by the cell (Figure 4.1A).

Grp94 activity is thought to be regulated by phosphorylation. The phosphorylated form does not associate with Ig light chains in the cell (Argon and Simen, 1999). Grp94 is thought to interact with Ig differently to other chaperones, the interaction with the light chain being with the late fully disulphide bonded intermediate (Argon and Simen, 1999). Grp94 association persists for the majority of the residence time of the light chain in the ER, in opposition to BiP-Ig interactions which are short-lived, only lasting for the first few minutes after Ig synthesis (Argon and Simen, 1999). It is therefore thought that Grp94 participates in the retention of proteins in the ER but acts downstream of, or in conjunction with, other chaperones (Argon and Simen, 1999).

4.3.4.8 α -Tubulin

α -tubulin is a structural protein which together with β -tubulin is a major constituent of microtubules, which are vital components of cellular architecture, morphology and function. Microtubules are also 'actively' involved in the secretion of proteins (Thyberg and Moskalewski, 1999), and secretory vesicles (Wu et al., 2000). As α -tubulin is involved with cellular architecture and is required for structural integrity, we expected that the expression of α -tubulin would remain more-or-less constant. However, this was not the case and throughout culture the level of α -tubulin expression changed. α -tubulin was present at low levels at the start of culture and up until day 3. After this time, however, the level increased dramatically at day 5 as observed with many other chaperones and stress

proteins as highlighted above. The increase in expression once again coincided with the maximum cell viability and IgG secreted by the cells. It is possible that at this stage in the culture an increase in α -tubulin occurred in order to assist in secretion via the formation of additional microtubules which enable transportation of mature IgG out of the cell. This would also aid in reducing any stress on the cells as a result of IgG accumulation within the ER (Figure 4.8, number 8).

4.3.4.9 Disulphide Isomerase ER-60 (ERp60)

ERp60 is a protein disulphide isomerase precursor and a PDI homologue. The analysis of ERp60 during batch culture indicate it was expressed at high levels at the start of culture, suggesting ERp60 may have a role in cell proliferation. This observation has not been reported before. However, the level of expression decreased by the third day of the culture. It is possible that ERp60 was initially induced early in culture as a result of the cells being placed in a new environment. This can result in the cells being placed under mild stress (Figure 4.8, number 9). The level of expression of ERp60 increased after exponential growth phase, between day 5 and 7 of the culture. However, the levels were lower than those observed at the beginning of the culture. ERp60 did not respond throughout the culture in the same way as BiP and endoplasmic reticulum chaperone, as has been previously reported (Ferrari and Soling, 1999). ERp60, (also called ERp57), has been reported to interact and cooperate with calreticulin and calnexin (by functioning as a co-chaperone) with growing polypeptide chains of monoglycosylated glycoproteins including IgG in the lumen of the ER (High et al., 2000; Michalak et al., 1999) to assist in disulphide bond formation. It is believed that calreticulin binds to the ERp60 molecule and that together these proteins wrap around polypeptide chains to protect the folding chain and to position ERp60 for disulphide bond oxidation (Ellgaard and Helelius, 2001). Association of ERp60 with calnexin stimulates the isomerase activity *in vitro* (Frandsen et al., 2000). ERp60 is induced especially under conditions of stress and responds in a similar way to BiP and Grp94 (Ferrari and Soling, 1999). These reports correspond with the characteristics observed during the culture of NS0 cells.

4.3.4.10 Pyruvate Kinase (PK)

Pyruvate kinase (PK) is a cytoplasmic glycolytic enzyme. The semi-quantitative analysis of PK showed that the expression level remained almost constant throughout the culture.

However, PK was induced at the start of the culture when compared to the rest of the culture. The level of expression reduced at day 3, but increased again at late exponential phase (day 5). PK is a rate-controlling glycolytic enzyme which catalyses the formation of pyruvate and ATP from phosphoenolpyruvate and ADP (Yamada and Noguchi, 1999). Mammalian PKs exhibit allosteric properties and are activated by phosphoenolpyruvate and fructose 1,6-bisphosphate. The activity of PK is regulated by protein synthesis, phosphorylation alterations, and by nutrient and hormone levels (Yamada and Noguchi, 1999). An increase in PK expression has been reported to coincide with S-phase of the cell-cycle. Furthermore, glucose is required for cell proliferation and for induction of other glycolytic enzymes (Yamada and Noguchi, 1999). These reports support the observations that PK was highly expressed at the beginning of the batch culture experiment, a stage in the growth curve where cells were preparing to proliferate. At this early stage of the culture high levels of glucose were also present which would further induce the enzyme. As expected the level of expression of PK remained highly expressed throughout the culture of NS0 cells (Figure 4.9, number 10). It is likely that PK remained highly expressed throughout the culture even at day 7, due to the presence of glucose in the medium, which was not fully utilised by the cells.

4.3.4.11 Elongation Factor 1-Alpha-1 (eEF1A-1)

The elongation phase of mRNA translation is the stage at which the polypeptide is assembled and requires large amounts of metabolic energy. The analysis of elongation factor 1-alpha-1 (eEF1A-1) throughout batch culture indicated that expression was induced at the start of the culture at a time when the cells were preparing for growth and cellular proliferation. Expression of eEF1A-1 then reduced at exponential phase of the culture (day 3). After reaching late exponential growth phase at day 5 of the culture, the level of eEF1A-1 expression increased again to the highest level of expression observed throughout the culture. This was unexpected since most cells would be dead at this stage and protein synthesis, to all intents and purposes, will be switched off (Figure 4.9, number 11). In the cytoplasm of higher eukaryotes, the process of peptide-chain elongation requires two types of ancillary factors, one to recruit the amino acyl-tRNAs to the A-site of the ribosome and one to mediate the translocation step in which the ribosome moves relative to the mRNA by the equivalent of one codon for the decoding of mRNA (Caraglia et al., 2000). Mouse elongation factor 1-alpha-1 (eEF1A-1) is a protein which requires phosphorylation to become active to enable the recruitment of amino acyl-tRNAs to the ribosome (Browne

and Proud, 2002; Proud, 2002). eEF1A-1 binds guanine nucleotides and in its (guanidine triphosphate) GTP-bound form can interact with aminoacyl tRNA to bring it to the A-site of the ribosome. Following hydrolysis of the GTP, eEF1A-1.GDP is released from the ribosome. This form is incapable of binding amino acyl-tRNA and is recycled to the active GTP-bound form which enables further recruitment of amino acyl-tRNAs to the ribosome.

When protein synthesis is activated, translation initiation is stimulated and the loading of ribosomes onto mRNAs increases. It would seem logical that the rate of elongation would also increase to match the rate of attachment of ribosomes to the mRNA to avoid decreasing the translation rate due to elongation. That is, the increased numbers of ribosomes engaged on the mRNA will require increased activity of elongation factors. Therefore, we would expect that elongation factors would be maintained at high levels by the cell. However, it has been shown that elongation activity is inversely related to translational fidelity (Browne and Proud, 2002), and it seems that high-level expression of elongation factors can lead to mis-sense reading errors or premature termination. In order to reduce the rate of protein synthesis, inhibition of elongation ensures the polysomes are retained in the cell even if initiation is also repressed. Therefore translation can be resumed rapidly once protein synthesis is required. The expression level of eEF1A-1 would be expected to be down-regulated towards the end of the culture when protein synthesis would no longer be required, although the level of expression appeared to remain high. However, the software was unable to accurately quantify the changes in the level of expression of eEF1A-1, as it is a very abundant protein spot. This may explain the discrepancy reported here.

4.3.4.12 α -Enolase

α -enolase is a key glycolytic enzyme which catalyses the formation of phosphoenolpyruvate from 2-phosphoglycerate and is important in providing energy to the cell (Sugahara et al., 1998). Throughout batch culture the level of expression of α -enolase was low between day 1 and 3 of the culture, although expression increased greatly at day 5 of the culture (Figure 4.9, number 12). The greatest increase in expression of α -enolase occurred when IgG production was at its maximum and when the cells were at maximum viable cell density. At this stage of the growth curve it is assumed that the cells will have an increased energy requirement to meet that required for cell growth/proliferation and

rIgG production. Therefore, it was not unexpected that α -enolase was up-regulated at this stage of the growth curve.

The level of expression of α -enolase decreased at day 7 of the culture, as expected. Most of the cells would be dead and/or dying at this stage and so would no longer require energy. α -enolase has a wide range of catalytic activities including activity as a stress protein (Aaronson et al., 1995). In hypoxic endothelial cells the protein was observed to become up-regulated and contribute to hypoxia tolerance. In splenic B cells from BALB/c mice exposure to soluble α -enolase was found to induce the secretion of immunoglobulin M (IgM) and IgG that was mediated possibly by augmented transcription, although the exact mechanism is unclear (Babu et al., 2002). Other groups have suggested the enhancement of Ig production by α -enolase occurs between translation and posttranslational events rather than by stimulating secretion (Sugahara et al., 1998). It has also been reported that enolase acts intracellularly as an accessory molecule to stimulate B cells to secrete immunoglobulin (Babu et al., 2002). NS0 cells are derived from splenic B cells of BALB/c mice, and it is possible that α -enolase may exert the same function in NS0 cells.

4.3.4.13 β -Actin

β -actin is a major component of the cellular cytoskeleton (Friso et al., 2001). Throughout the growth curve, the level of β -actin expression was expected to remain constant. However, the expression of the two actin protein spots identified on the NS0 cell proteome map (Figure 4.9, protein number 13 and 14) increased towards exponential growth phase. At this time point the level of IgG production and glucose utilisation were at their maximum, and the transport of IgG out of the cell would be at its maximum requirement. This may have resulted in an increased demand for microtubules and for cytoskeleton reorganisation to enable exocytosis of rIgG from the cell as previously described for α -tubulin. Actin forms filaments, which make up a major component of the cytoskeleton and it is also involved in cell motility. Actin monomers and polymers interact with many actin-binding proteins that participate and regulate microfilament assembly (Schuler, 2001). Actin reorganisation has also been reported to allow for fusion and exocytosis of proteins that have been transported on microtubules such as secretory vesicles (Wu et al., 2000).

4.3.4.14 Glyceraldehyde 3-Phosphate Dehydrogenase (GAPDH)

Glyceraldehyde 3-phosphate dehydrogenase (GAPDH) is an enzyme which is central to the glycolytic pathway with a pivotal role in energy production (Dastoor and Dreyer, 2001). On the proteome maps of NS0 cells, the normalised spot volumes for this enzyme (Figure 4.9, spot number 15 and 16) became saturated as the culture progressed; therefore the values appear very low and the quantitation is unreliable. However, it can clearly be seen that the expression of GAPDH was up-regulated throughout the culture by visual comparison. The results suggest the expression of GAPDH was maintained as stress conditions prevailed towards the end of the batch culture (Figure 4.9, number 15 and 16). Recent studies have proposed a new role for the enzyme or some of its isoforms which are unrelated to its glycolytic activity including apoptosis and oxidative stress (Dastoor and Dreyer, 2001). In particular GAPDH expression has been shown to become three times higher in apoptotic cells and has been shown to make cells more sensitive to agents that induce apoptosis. The apoptotic inhibitor Bcl-2 has also been shown to prevent the nuclear translocation of GAPDH (Dastoor and Dreyer, 2001). It has been proposed that GAPDH acts as a molecular chaperone, acting as a pro-apoptotic enzyme downstream of Bcl-2 in the cell signal transduction cascade of apoptosis (Dastoor and Dreyer, 2001). The enzyme has also been associated with increased immunoglobulin production in human and mouse hybridomas and lymphocytes *in vitro* as a result of increased protein synthesis on the post-transcriptional process rather than as a result of stimulated secretion (Sugahara et al., 1998).

4.3.4.15 Peptidyl-Prolyl *cis-trans* Isomerase A (PPIase A)

Peptidyl-prolyl *cis-trans* isomerase A (PPIase A/immunophilin) is identical to cyclophilin the major intracellular receptor for cyclosporin A, an immunosuppressive drug, and is a folding catalyst rather than a protein disulphide isomerase (Schiene-Fischer and Yu, 2001). Throughout the batch culture of NS0 cells PPIase A was highly expressed, with the greatest increase in expression observed at day 3 and day 7 of the batch culture (Figure 4.9, number 17). The data reported here suggests that the protein is constitutively expressed at high levels and is therefore required at all times by the cell. As in the quantitative analysis of eEF1A-1 and GAPDH, PPIase A was highly expressed throughout the culture, and therefore any changes in the level of expression were difficult to quantify using the software.

There are three conserved families of PPIases and this class of proteins (the cyclophilins) catalyse the specific rate-limiting steps in folding, particularly the *cis-trans* isomerisation of peptide bonds preceding prolyl residues in different folding states of a target protein (Schiene-Fischer and Yu, 2001). The PPIases have also been reported to function as chaperones (Agashe and Hartl, 2000; Hartl and Hayer-Hartl, 2002). The PPIases have also been found to play a critical role in the functional arrangement of components within receptor complexes (Schiene-Fischer and Yu, 2001). If inhibitors to this class of proteins are utilised, the rate of protein secretion from cells is reduced, suggesting that luminal PPIases are important for folding *in vitro* and in model systems evidence suggests that the PPIases can act in synergy with PDI (Freedman et al., 1994). This group of proteins has also been shown to interact directly with Hsp90 proteins, although the function of the interaction has not been established (Jacob and Buchner, 1994).

Although the Shevchenko method of silver staining is not thought to be an accurate method of staining (due to high background levels and negative staining of abundant proteins), image analysis of the 18 cm 2-D gel images prepared for the comparison of 18 cm 2-D autoradiographs resulted in similar patterns of protein expression being observed to those for the 24 cm gels (Figure 4.8–4.11). In many cases small differences in the normalised protein spot volumes between replicate gel images were observed, resulting in small errors being obtained (indicated by error bars) (Figure 4.10 and 4.11). This is in agreement with a recent publication in which it was shown that more abundant protein spots show less gel-to-gel variation with respect to spot volume (Smales et al., 2003). In some cases (for example with protein spot number 8, 12 and 13) slightly larger errors in normalised spot volumes were observed when comparing the standard deviations between the replicate gel images. These protein spots were of lower abundance and therefore were expected to exhibit a higher degree of variation between replicate gel images (Smales et al., 2003). This was likely to be as a result of the protein staining methodology utilised and the imaging equipment. Silver stain is a non end-point stain, and as a consequence differences in staining intensity (and therefore protein spot volume measurements) occurred, which was unavoidable.

The results confirm that with respect to the image analysis data for both the 24 cm and the replicate 18 cm 2-D gel images, an accurate representation of the pattern of protein expression in NS0 cells during batch culture was obtained. Furthermore, other laboratory members have confirmed the results discussed in this chapter utilising methods other than

2-D PAGE to investigate differences in the level of protein expression during bioreactor culture. Immunological approaches were utilised to investigate the expression levels of many of the proteins identified and discussed here including Hsc71, PDI, Grp94 and BiP (results not shown).

4.3.5 Considerations for Utilising Proteome Analysis Technology

The results described in this chapter assume that proteome analysis is 100% accurate, although, there are limitations associated with the technology. It has been estimated up to 10000 proteins can be visualised on one large format (20 x 20 cm) 2-D gel. Clearly this number of protein spots was not visualised on either of the large format 18 cm or 24 cm 2-D gels on which the maximum number of protein spots detected was approximately 1500-1700 respectively (chapter 3, Table 3.2). The estimated number of proteins expressed by an 'average' mammalian cell is 10000 therefore a maximum of 17% of the whole NS0 cell proteome was represented on a large format 2-D gel at each key time point sampled during the batch culture experiment. Although it is unlikely for all proteins to be expressed by a cell at any one moment in time as protein expression is dynamic being dependent on many factors including time and environmental changes/stresses. The amount of active protein expressed is tightly controlled by production and degradation rates (Oh-Ishi and Maeda, 2002) and proteins also have varying half-lives and functional lifetimes (Gabor Miklos and Maleszka, 2001).

Furthermore, high and low molecular weight proteins are also not well represented on 2-D gels, with a 12.5% acrylamide gel (utilised in this project) having a cut off of 100 kDa and 14 kDa (chapter 3, Table 3.3). Membrane proteins also do not easily focus or enter the first dimension IPG strip utilising current focussing methodologies. The visualisation of proteins on 2-D gels can be achieved using a variety of staining methods, including colloidal Coomassie, silver stain and the fluorescent SYPRO[®] stains. The most sensitive methods of staining for proteins are reported to be SYPRO[®] Ruby and silver, although silver staining remains popular due to the high sensitivity achieved and ease of image capture. Protein visualisation utilising silver staining methodology is protein specific (Smales et al., 2003) and the linear dynamic range is reported to be less than that of other protein stains (Lauber et al., 2001). Silver staining although arguably the most sensitive method for protein detection, will only detect proteins down to approximately 1 ng, therefore very low abundance proteins will not be detected.

Low abundance proteins often include those that carry out key regulatory processes, for example, the cyclins which are key regulators of the cell cycle are of low abundance and are only present for a short time during the cell cycle and are not likely to be readily detected on a 2-D gel image. It is assumed that for each individual protein spot visualised one protein will be present. However, it is possible for protein spots to co-localise on a 2-D gel, and this may lead to masking of other proteins (Gorg 2000a). Proteins of a much higher abundance can also mask those of lower abundance. This can lead to misrepresentation and interpretation of the proteome under investigation.

It is important when carrying out any type of proteome analysis to run the greatest number of replicates possible. In many cases three 2-D gels are run, with which to accurately assess the proteome. Ideally more than three replicate gel images should be prepared, although this is not always possible, due to sample availability. The number of time points sampled to assess the NS0 cell proteome throughout batch culture involved lag phase (day1), early exponential and mid-exponential phase of growth (day 3 and 5) and death phase (day 7).

In this chapter it was the complex changes in NS0 cell protein expression during batch culture were assessed. Many proteomic studies to date have been concerned with analysing simple 'on/off' qualitative changes in the proteome through assessing a disease state versus a control rather than assessing quantitative graduated responses in one cell type. As a result of proteins exhibiting different functional lifetimes and half-lives and the inherent differences in the pattern of gene expression due to alternative splicing and/or post-translational modifications (Kettman et al., 2002) it is difficult to assess quantitative changes in the NS0 cell proteome utilising current technologies and image analysis software. Although the general trend of protein expression during bioreactor culture was confirmed through assessing replicate 2-D el images. In order to more accurately define the changes in the NS0 cell proteome, NS0 cells could have been sampled more frequently during the batch culture. However, this was not possible due to sample availability. Larger starting culture volumes would have been necessary to provide the increased number of cells for each harvest, which was not possible at the time the bioreactor culture was carried out.

4.3.6 Conclusions

Regardless of the limitations of proteome analysis discussed above, the results highlighted in this chapter show that many changes in the expression of proteins (particularly of HSPs,

chaperones and glycolytic enzymes) were apparent throughout the batch culture of NS0 cells. The NS0 cell proteome is a dynamic system with many changes in protein expression occurring throughout culture. The expression of approximately 400 proteins were observed to change by at least 2-fold as the culture progressed, in order to adapt to the cells specific requirements at each time point, and the global statistics reflect the global 'position' of the cell at each sample point. However, of the proteins that were identified, many are required for general 'housekeeping' functions in the cell as well as having stress protein properties (Agashe and Hartl, 2000). As a result it is difficult to pinpoint exactly when the cells perceived 'stress' during culture. For example, Hsc71 is a member of a large family of proteins which are constitutively expressed throughout the lifetime of the cell, and are up-regulated as a result of cellular stress. Therefore any changes in the expression profile of Hsc71 cannot be directly attributable to the stress response. Many of these proteins naturally fluctuate throughout the growth curve to provide the necessary machinery for cell growth and proliferation, or to provide energy to the cell, even in non-producing cell lines (see chapter 6 for further details). However, of the 17 proteins that were identified, most were induced or up-regulated at day 5 of the culture, which coincided with the maximum glucose utilisation and lactate production and changes in the culture environment. At this time IgG production was also at its maximum level, suggesting the cells perceived maximum stress during this stage of the growth curve.

NS0 cells have been under constant selective pressure for many years to produce recombinant proteins. As a result the proteins expected to be involved with protein folding, such as molecular chaperones and foldases may have been selected for and therefore constitutively up-regulated. Proteins involved with other housekeeping functions, which were important when the cells were *in vivo*, may have been selectively down regulated as their function is no longer required in the *in vitro* environment. The cell line may therefore appear to be permanently under 'stress' (as the cellular machinery expressed mimics the pattern of proteins involved with the stress response) as a result of the constant engineering process. Reports have shown that the induction of a protein of the stress response, X-box binding protein-1 (XBP-1), a substrate for *IRE1*, which is an essential gene in mice that controls the expression and function of transcription factors, occurs during the conversion of B-cells to plasma cells (Harding et al., 2002). In response to ER stress and the UPR, *IRE1* proteins are up-regulated and activate transcription of target genes including those for BiP. An important feature that differentiates plasma cells from B-cells is the expansion of an extensive ER and secretory apparatus (Harding et al.,

2002). It has been hypothesised that as the B-cell matures, immunoglobulin biosynthesis imposes a load upon the ER, which in turn activates *IRE1* and *XBP-1*. The downstream gene expression program controlled by XBP-1 involves specialised secretory machinery that can cope with the load imposed by the plasma cells (Harding et al., 2002). A similar mechanism may occur in NS0 cells.

Furthermore, many of the results reported in this study correlate with a recently published report in which van Anken *et al.* investigated the differentiation process and sequential changes in cellular machinery reorganisation involved when B cells prepare to become plasma cells using a proteomic approach (van Anken et al., 2003). They used 2-D PAGE to follow the overall changes in protein expression to investigate how Ig secretion and ER development are related to assess whether an increase in secretory proteins (Igs) drive expansion of the ER via signalling cascades programmed to enhance protein folding capacity and limit ER load, via the UPR (Patil and Walter, 2001; van Anken et al., 2003) or whether the development of a protein 'factory' precedes the production and release of antibodies (van Anken et al., 2003).

Many of the proteins identified in NS0 cells in this chapter were investigated. The proteins were grouped similarly to include ER resident proteins of the secretory pathway, (including calreticulin, BiP, Grp94 and ERp57 (also called ERp60)), together with proteins involved with cellular metabolism (including α -enolase and GAPDH). Mitochondrial chaperones (Grp75 and Hsp60) were also investigated, as well as cytoskeletal proteins (α -tubulin and β -actin). Hsc70 was also investigated as a cytosolic chaperone.

During the activation of B cells to become plasma cells, the expression profiles of the ER resident proteins were observed to increase linearly as the activation process progressed during differentiation, to the fourth day of activation. The structural proteins (α -tubulin and β -actin) and the cytosolic chaperone Hsc70 were observed to decrease steadily from the start of activation until the end of the study at day 4. The mitochondrial and cytosolic chaperones were observed to exhibit high expression at the start of activation (day 1), and decreased after this time to day 4 after activation, whereas metabolic enzymes peaked after the third day of activation (van Anken et al., 2003). The cells dramatically increased the production of IgM production after 2 days of activation. The results revealed that the transformation of dormant B cells to secretory plasma cells (like NS0 cells during culture) is a multi-step process with proteins exhibiting sequential waves of expression, which are co-ordinately expressed during the transformation process. After activation, B

cells prepare for their new role as plasma cells before IgM secretion is commenced, by first ensuring that the metabolic capacity and secretory machinery have expanded before IgM is produced (van Anken et al., 2003). IgM in plasma cells is therefore unlikely to be the driving force of the UPR at the initial stages of activation, although during later stages IgM subunits did appear to trigger the classical XBP-1 ER load dependent UPR (van Anken et al., 2003). The results suggest a two-step launch of ER expansion observed in B cells which may be essential to all cells that differentiate to become professional secretors (including NS0 cells). The cells first prepare for the new secretory role, and once the first steps have been taken, results in the increased production of Ig, which may provide an UPR-linked feed-forward circuit which drives further ER protein expansion (van Anken et al., 2003). This clearly suggests that the changes in protein expression (particularly stress proteins) reported here in NS0 cells and by van Anken *et al.* in B cells are closely associated with stress perception and antibody production (van Anken et al., 2003).

A comparison of the proteins expressed at mid-exponential growth phase in a series of transfectants producing different amounts of a rIgG is detailed in chapter 6. The proteomic analysis of these transfectants against the blank, 'mock' transfected NS0 cell line, and the parental NS0 cell line may provide the evidence required to identify those proteins which determine if a given cell line is to be 'productive'.

The results in this chapter have shown that the NS0 cell proteome changes in a dynamic way throughout batch culture, with the up-regulation of many proteins particularly apparent at exponential phase of the batch culture and beyond. The induction of stress proteins during this stage of the growth curve coincided with metabolic changes and maximum productivity of the cell line. However, utilising proteome analysis in the form of 2-D electrophoresis only enables a 'snapshot' of protein expression at one moment in time to be investigated. The data provided by this type of approach enables the protein profile to be interrogated but does not provide information as to which proteins are required by the global cellular population at that time point. Proteins have different half-lives and as a result are degraded at different rates. Although a protein may be present on a proteome map, it may not be 'active'. In order to investigate those proteins being actively synthesised and utilised by NS0 cells throughout the batch culture, nascent polypeptides were labelled with [³⁵S] methionine, at the same time samples were taken for proteome analysis as discussed in this chapter. The labelled proteins were subjected to 2-D electrophoresis followed by autoradiography and the resultant images were assessed for changes in nascent polypeptide synthesis throughout batch culture. The autoradiographs

4 Analysis of Changes in the GS-NS0 Cell Proteome during Batch Culture

were then compared to the silver stained 2-D gels already analysed. The results of this study are discussed in the next chapter.

Chapter 5 Analysis of Protein Synthesis in GS-NS0 Cells during Batch Culture

5.1 Introduction

The classical method of proteome analysis provides a ‘snap shot’ of the proteins expressed in a sample at a specific moment in time. However, the presence of a protein at a particular time point does not mean it is being actively synthesised (i.e. required by the cell) at the specific time point. In order to investigate nascent polypeptide synthesis during batch culture, NS0 cells were labelled with [³⁵S] methionine for the detection of proteins actively being synthesised by the NS0 cell line at a given time point. Radiolabelling with [³⁵S] methionine represents a sensitive method to visualise many of the constitutively expressed and synthesised proteins of the NS0 cell proteome.

Utilising [³⁵S] methionine requires very low total protein loading on a 2-D gel (Westbrook et al., 2001). The images of autoradiographs and protein gels visualised with silver for the comparison of protein spot identification are difficult to match and often do not correspond due to the different principles underlying each method (that is, staining constitutively expressed versus metabolic labelling of newly synthesised proteins) (Westbrook et al., 2001). As a result [³⁵S] methionine labelling has been utilised in this study as a complementary technology to the traditional method of 2-D PAGE. When the changes in protein synthesis were related to secretory productivity and changes in metabolite concentration, a more complete picture of the changes in the NS0 cell proteome throughout bioreactor batch culture has been achieved.

5.2 Results

5.2.1 Nascent Polypeptide Synthesis during Batch Culture

In order to investigate those proteins that were being actively synthesised at specific time points throughout the growth curve, the rate of nascent polypeptide synthesis in NS0 cells was assessed throughout batch culture by monitoring the rate of [³⁵S] methionine incorporation into newly synthesized proteins as outlined in chapter 2, section 2.9. Using this procedure labelled extracellular secreted polypeptides could be distinguished from labelled intracellular polypeptides.

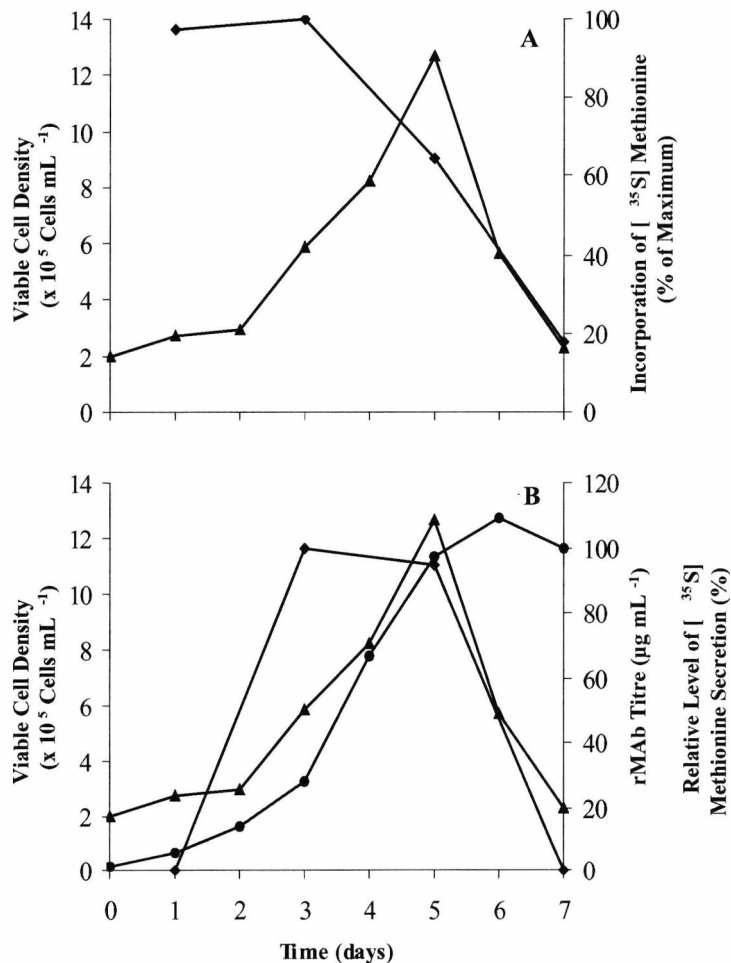


Figure 5.1 Total protein synthesis of NS0 cells expressing IgG throughout a 1.5 L bioreactor batch culture. Samples of 1×10^6 cells were taken throughout the batch culture at lag phase, day 1, exponential growth phase, day 3 and 5, and death phase day 7 of the batch culture (see chapter 4, Figure 4.1 and 5.3 for growth characteristics). Figure A shows the viable cell density (▲) and the total protein synthesis (◆), determined through the incorporation of [³⁵S] methionine as outlined in chapter 2, section 2.9. Figure B represents the secreted protein (◆), measured as [³⁵S] methionine secreted protein over a 1 hour incubation period relative to the labelled protein at 72 hours of culture (maximum rate of incorporation observed) together with the viable cell density (▲) and recombinant IgG (rIgG) titre (●) obtained throughout the batch culture.

Samples of 1×10^6 cells were taken from the batch culture experiment at the same time points as for the protein extracts used for the protein gels detailed in chapter 4 (section 4.2.3). Maximum incorporation of [^{35}S] methionine was observed at early exponential growth phase (day 3 of the culture) (Figure 5.1A). This corresponds to the time in the batch culture of the induction of maximum growth and division. After day 3 of the batch culture the level of [^{35}S] methionine incorporation reduced. The decrease in the incorporation of radioactivity corresponds with a decrease in the viable cell density after day 5 of the batch culture (Figure 5.1A). In correlation with the incorporation of [^{35}S] methionine, the maximum level of secretion also occurred between the third and fifth day of the batch culture when maximum recombinant IgG (rIgG) production and cell growth occurred (Figure 5.1B). After this time the level of secretion rapidly reduced, concomitant with a reduction in the viable cell density.

5.2.1.1 Assessment of Nascent Polypeptide Synthesis throughout the Batch Culture of NS0 Cells

Throughout the 1.5 L batch culture experiment outlined in the previous chapter, samples of NS0 cells were extracted and subjected to large format 2-D PAGE (chapter 4, section 4.2.3). At the same time samples were subjected to *in vitro* labelling with [^{35}S] methionine to investigate nascent polypeptide synthesis for direct comparison against the silver stained 2-D gels. Due to constraints in the size of the autoradiograph gel cassettes and developing machine (which is only capable of developing up to 20 cm films), 18 cm large format 2-D gels were utilised for all the autoradiograph experiments as 24 cm gels could not be processed (Figure 5.2). One individual 2-D autoradiograph was prepared for each sample point.

5 Analysis of Protein Synthesis in GS-NS0 Cells during Batch Culture

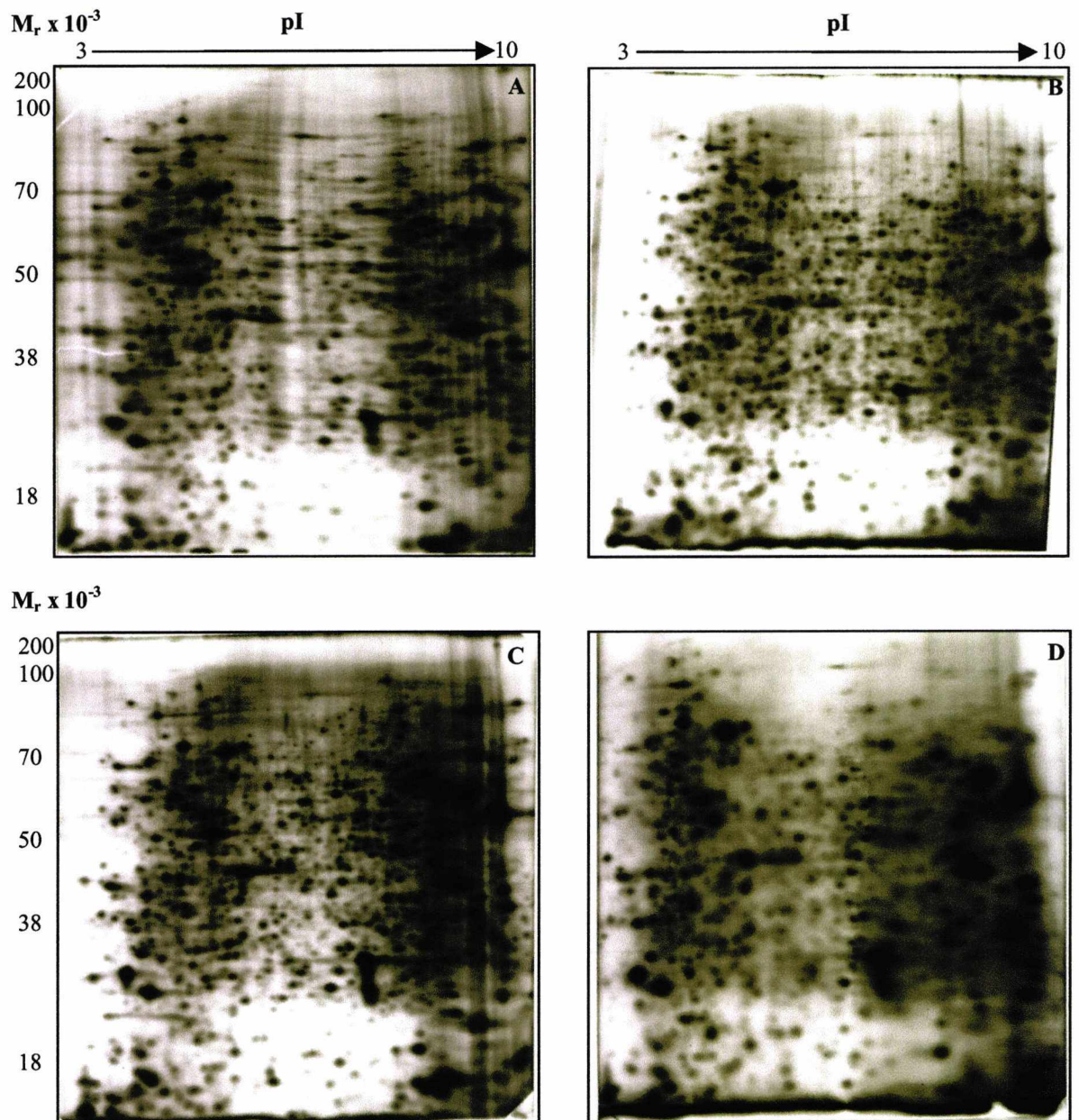


Figure 5.2 Two-dimensional autoradiographs of NS0 whole cell proteins during batch culture. A total of 1×10^6 cpm was loaded from each sample and subjected to large format (20 x 18 x 0.1 cm) 2-D PAGE using pI 3-10 non-linear IPG strips. Following 2-D PAGE, gels were stored separately in fixative overnight at 4°C. The following day, gels were placed in fluoramplify agent (Amersham Biosciences) to enhance the [^{35}S] signal on the autoradiographs. Each gel was dried and then placed in an autoradiography cassette with 'Hyperfilm' and left at -70°C for 4 weeks. The autoradiographs were then developed and scanned at 200 dpi and analysed using ImageMaster™ 2-D software. Figure A, 2-D autoradiograph of 1×10^6 cells labelled with 10 μCi and extracted from day 1 of the batch culture, Figure B, day 3 of the batch culture. Figure C and D respectively were extracted from day 5 and 7 of the bioreactor batch culture.

Table 5.1 Total number of nascent polypeptides detected on 2-D autoradiographs during controlled bioreactor batch culture of NS0 cells

Day of Culture	Number of Protein Spots Detected
1	802
3	866
5	894
7	677

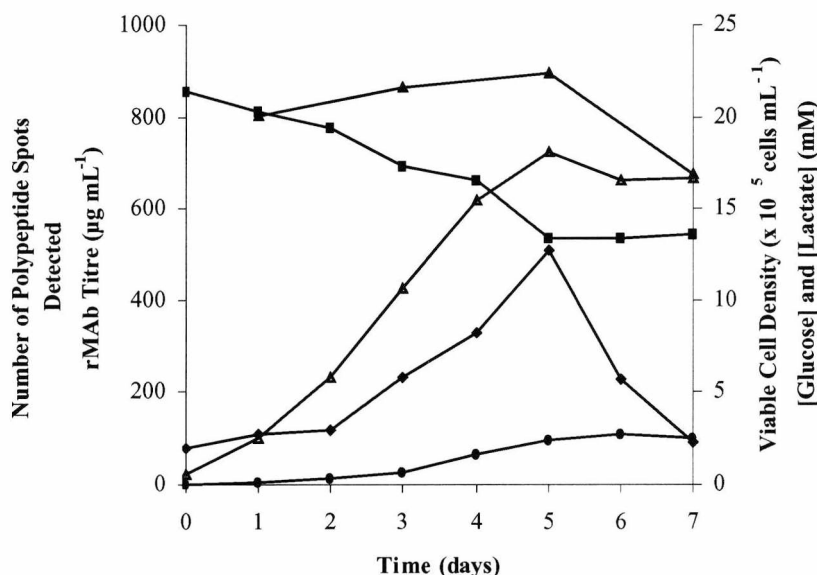
**Figure 5.3** Comparison of nascent polypeptide synthesis throughout batch culture of NS0 cells expressing a recombinant IgG₁ on 2-D autoradiographs. (▲) Number of polypeptide spots detected throughout batch culture. (●) rIgG titre and (◆) viable cell density throughout the growth curve. (■) and (△) glucose and lactate concentration respectively.

Table 5.1 above clearly shows that throughout batch culture the total number of polypeptides being actively synthesised increased and reached a maximum at day 5 of the culture. After inoculation of the bioreactor at day 1 of the batch culture 802 proteins were actively being synthesised. The maximum incorporation and secretion of [³⁵S] methionine also occurred at this time point (Figure 5.1). This data shows that at this time point a large number of proteins are 'required' by the cell, presumably for growth and preparation for division. However, the cells used to inoculate the fermenter were at mid-exponential growth phase, therefore one may expect that the cells will have protein expression profiles consistent with exponential growth.

During early exponential growth phase, the total number of polypeptides being actively synthesised increased to 866, an increment of 64 proteins. At this time point the cells were beginning to actively grow, divide and proliferate. The cells were also

beginning to produce rIgG at relatively high levels ($28 \mu\text{g mL}^{-1}$). By the fifth day of batch culture the number of polypeptide spots detected on the autoradiographs increased to 894 (a small increase of 28 proteins). During late exponential growth phase (day 5), the maximum viable cell density was reached, together with the maximum concentration of glucose utilisation (chapter 4, Figure 4.1B). At this time point the cells were also producing maximum rIgG (qMAb $1.46 \text{ pg cell}^{-1} \text{ h}^{-1}$). At this point in the growth curve the secretion of [^{35}S] methionine was still relatively high (Figure 5.1B), which coincides with the increased number of nascent polypeptides being synthesised.

Towards the end of the batch culture (day 7), the total number of polypeptides being actively synthesised reduced to 677, a large decrease of 217 polypeptide spots. This observation was expected and coincided with reduced cell viability (22%) and reduced viable cell density ($2.3 \times 10^5 \text{ cells mL}^{-1}$). The rate of incorporation and secretion of [^{35}S] methionine was also reduced at this time point (Figure 5.1 and Figure 5.3). Most of the cells at this time in the growth curve were dead, and could not therefore synthesise new proteins. Most of the cellular processes requiring protein synthesis are expected to be switched off or down-regulated at this time point. In order to quantify the differences in polypeptide expression throughout the batch culture, image analysis software was utilised further to identify the polypeptides that exhibited alterations in expression by at least 2-fold throughout the culture.

5.2.1.2 Quantitative Analysis of Nascent Polypeptide Synthesis throughout Batch Culture

Using the digital 2-D autoradiograph images produced from the batch culture experiment (Figure 5.2), ImageMaster™ 2-D analysis software was utilised to explore the changes in polypeptide expression throughout batch culture (chapter 2, section 2.9.2). The digital images created from the batch culture experiment were all compared to the reference gel, which was derived from the 2-D autoradiograph from the day 1 sample extract. The proteome maps for days 3, 5 and 7 of the batch culture showing the polypeptides that were up- or down-regulated by a two-fold or greater quantifiable change throughout the batch culture are shown in Figure 5.4 below. To identify the regulation of the proteins throughout the culture, each autoradiograph image was compared against the preceding sample (Table 5.2).

Figure 5.4 shows that many changes in nascent polypeptide synthesis occurred as the culture progressed. Most of the polypeptides that exhibited at least a 2-fold change in expression were observed at late-exponential growth phase, in accordance with the protein levels as shown in chapter 4 (Table 4.3). The greatest increase in the level of synthesis was during mid-exponential growth phase compared to the start of the culture. During this stage of the growth curve the maximum cell density, glucose utilisation, IgG titre and [³⁵S] methionine secretion occurred. This therefore suggests that the cells were most active at this stage of the growth curve as would be expected. At death phase, other polypeptides were up-regulated, although the total number of proteins synthesised and the secretion of [³⁵S] methionine decreased greatly at this time point in the growth curve.

5 Analysis of Protein Synthesis in GS-NS0 Cells during Batch Culture

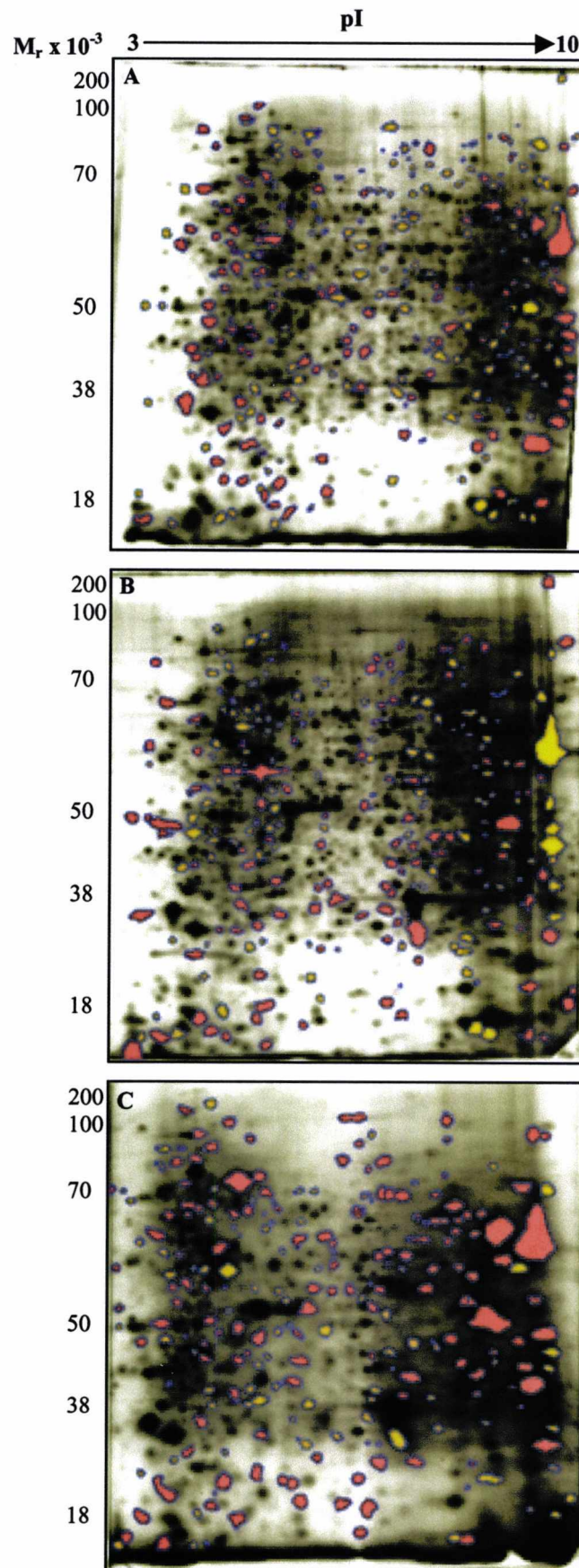


Figure 5.4 Comparative analysis of nascent polypeptide synthesis throughout a batch culture of NS0 cells. The difference maps show the proteins exhibiting at least a two-fold change in the level of nascent polypeptide synthesis. Only proteins that have been matched between samples are shown. Figure A, day 3 versus day 1 of the batch culture, Figure B, day 5 versus day 3 and Figure C, day 7 versus day 5 of the batch culture. Matched proteins exhibiting at least a two-fold increase (●) or decrease (●) in the level of polypeptide synthesis.

Table 5.2 shows the global statistics generated from the 2-D autoradiographs. In common with the pattern of protein expression observed on the 24 cm 2-D gels (chapter 4, Table 4.3), the greatest increase in the total number of newly synthesised polypeptides occurred at day 5 of culture (late in exponential growth phase). However, this type of analysis alone does not yield any information as to the extent of the changes observed throughout the experiment. As a result image analysis was utilised further to assess the total number of polypeptides that exhibited changes in the level of expression throughout the growth curve through comparing the gel images against the preceding day's 2-D gel sample (Table 5.2). This type of image analysis enabled the identification of the total number of nascent polypeptides whose expression level changed by at least 2-fold together with those polypeptides whose expression level was unchanged throughout culture (Table 5.2).

Table 5.2 The total number of polypeptides up- and down-regulated at least 2-fold, newly synthesised, no longer expressed or unchanged throughout the batch culture of NS0 cells as assessed by 2-D autoradiography

Day of Culture	Total Number of Polypeptide Spots	Unchanged*	Up-Regulated*	Down-Regulated*	Newly-Expressed*	No Longer Expressed*
1	802	-	-	-	-	-
3	866	280	122	149	315	250
5	894	254	106	139	393	177
7	677	162	135	91	289	305

* Indicates number of nascently synthesised polypeptides showing alterations in expression relative to the previous sample point

Table 5.2 above shows the global changes in the NS0 cell proteome throughout the batch culture experiment. As observed on the 24 cm protein gels in chapter 4 (Table 4.3), the sum of all variables shown in Table 5.2 (except for the number of proteins no longer expressed) is approximately equal to the total number of polypeptide spots detected on each day of the culture. Throughout the experiment, each gel was matched to the reference gel (created from the day 1 gel). After the matching was complete, the reference gel was rebuilt by adding protein spots from the other gels that were not present at day 1. As a result 405 additional protein spots were added to the reference gel. Therefore, as the culture progressed, 405 new proteins were synthesised. The number of nascent polypeptides that remained unchanged in the level of expression throughout the batch culture was investigated and between day 1 and 3, 280 nascent polypeptides were unchanged. When day 5 was compared versus day 1 this number increased to 303 and finally when the day 1 gel was compared against the day 7 gel, the number of polypeptides

remaining unchanged reduced to 170. During exponential growth phase we would expect that proteins involved with energy transduction, growth and proliferation would be up-regulated. At the end of the culture (day 7), only 170 proteins remained unchanged. This was expected, as late in culture cells are likely to be shutting down protein synthesis, and proteins involved with apoptosis and stress responses would be expected to be up-regulated. General house-keeping proteins and those involved in growth and proliferation would therefore no longer be required by the cell.

Throughout the growth curve the differences in the pattern of newly expressed proteins and proteins that were no longer expressed were compared using the difference map tool and interrogation of the resulting expression tables. The resulting statistics are reported in Table 5.2. Although the number of proteins newly synthesised or no longer detected were accurately defined, these changes do not provide any information as to the extent of the changes. Therefore the level of up- and down-regulation of the polypeptides detected on the 2-D autoradiographs were assessed using the difference map tool (Figure 5.4). Once again the resulting statistics are reported in Table 5.2.

In total the number of newly synthesised polypeptides and those up-regulated (by at least 2-fold) throughout the batch culture increased until late exponential phase. At lag growth phase (between day 1 and 3) 437 (55%) of the polypeptides in total were newly expressed or up-regulated. At mid-exponential growth phase (between day 3 and 5) 499 (58%) of the polypeptides detected were up-regulated and newly expressed. Finally between late exponential and death growth phase (day 5 to 7), 424 (47%) of the polypeptides were newly expressed and up-regulated. The greatest number of up-regulated and newly expressed nascent polypeptides was therefore observed at mid-exponential growth phase, between day 3 and 5 of the batch culture. This result was expected as at this time point the cells require large amounts of energy to sustain growth and division and may also at this time begin 'detecting' stress as a result of nutrient depletion, space reduction, shear stress and the accumulation of rIgG. As a result we might expect that stress proteins would be induced at this time to protect the cells from the cytotoxic effects of accumulated proteins within the ER.

The total number of nascent polypeptides down-regulated or no longer present at detectable levels decreased as the culture progressed. Between day 1 and 3, 399 (50%) of the total number of polypeptides synthesised observed were down-regulated. Between day 3 and 5 of the culture (at mid-exponential growth phase), 316 (36%) of the polypeptides were down-regulated. Finally between day 5 and 7 of the batch culture the number of

down-regulated nascent polypeptides increased to 396 (44%). Throughout the culture the number of proteins constitutively expressed between each sample point remained almost constant at approximately 25% of the total number of polypeptide spots detected at each sample point. However, throughout the batch culture the number of proteins unchanged as the culture progressed (relative to the previous sample) decreased. This was not unexpected, as once the culture had reached exponential growth phase, it is likely that proteins involved with energy partitioning, growth and proliferation would be induced. Finally, towards the end of the culture at day 7, most of the cells were either dead and/or dying, and we would therefore expect that cellular processes requiring protein synthesis would be switched off or down-regulated.

5.2.2 Large Format (18 cm) 2-D PAGE of the NS0 Cell Proteome for Comparison Against 2-D Autoradiographs

The 2-D autoradiographs produced for the analysis of nascent polypeptide synthesis were limited in size to 18 cm x 20 cm as described earlier. Therefore, in order to carry out the comparative analysis of the 2-D autoradiographs against protein gels, 18 cm 2-D protein gels were undertaken on the samples extracted throughout the batch culture and visualised by silver staining. The resultant protein gels were utilised to locate the position of the proteins identified from the 24 cm proteome maps discussed in chapter 4, section 4.2.4 and to enable the direct comparison of the proteome maps for global statistical analysis and to identify the proteins that were regulated throughout the batch culture experiment. Figure 5.5 below shows the resultant individual 18 cm gel images obtained for the batch culture experiment.

5 Analysis of Protein Synthesis in GS-NS0 Cells during Batch Culture

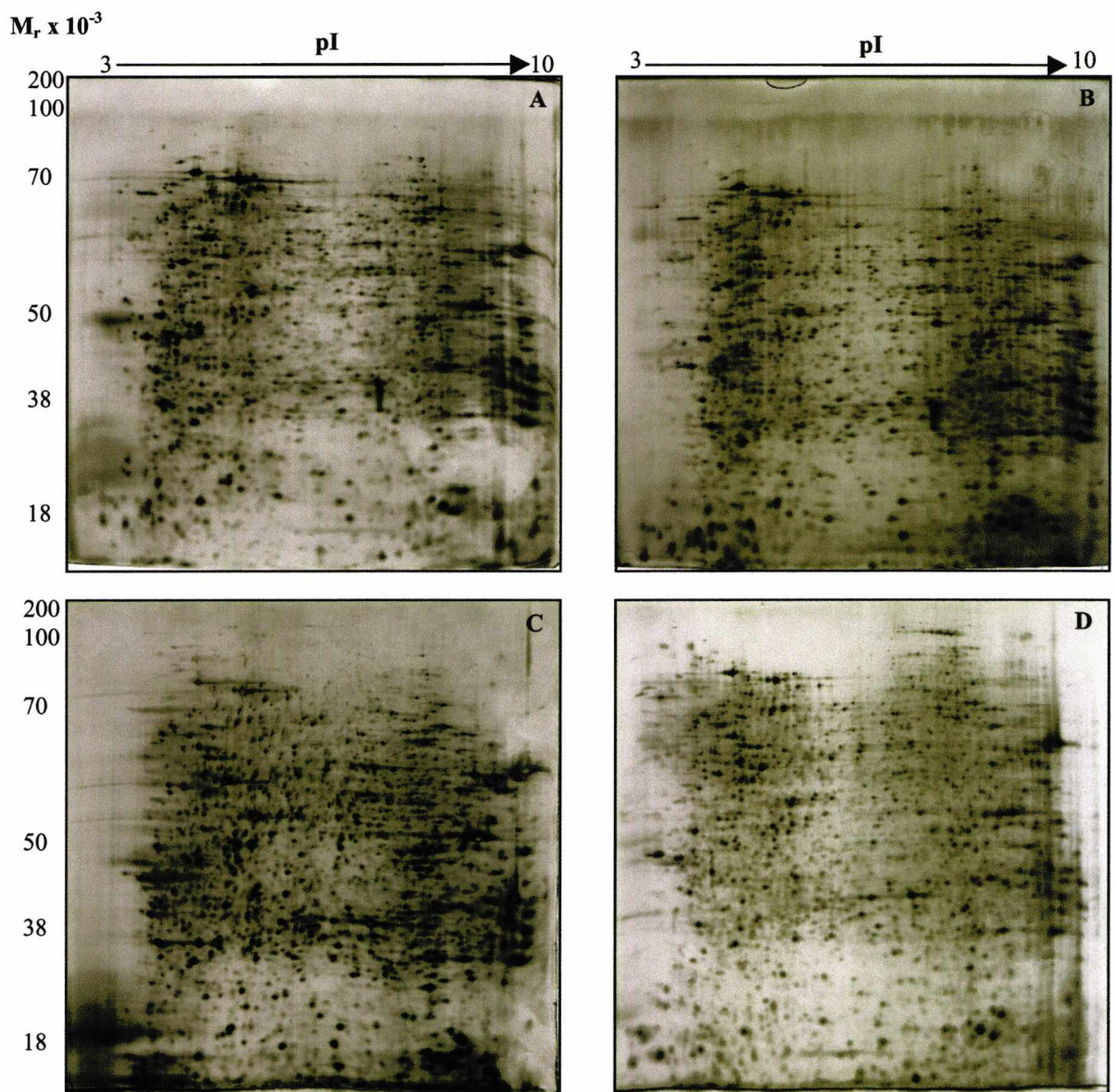


Figure 5.5 Large format 2-D PAGE (18 cm, pI 3-10 non-linear resolving range) of NS0 whole cell proteins extracted throughout batch culture. Figure A, day 1, lag phase 2-D gel; Figures B and C extracts from day 3 and day 5 (exponential growth phase) and Figure D, death growth phase (day 7). All gels were visualised using silver staining methodology.

5.2.2.1 Analysis of the NS0 Cell Proteome in 18 cm 2-D Gel Format

The extracts utilised in chapter 4 for large-scale (24 cm) proteome analysis (chapter 4, section 4.2.3) were used to run 18 cm 2-D gels for the direct comparison of protein gels against the 2-D autoradiographs. The resultant digital images derived from one individual 2-D gel prepared from each time point sampled were treated in the same way as the 24 cm protein gels in chapter 4, and the global statistics are reported in Table 5.3 below.

Table 5.3 Total number of protein spots detected on 18 cm 2-D gels throughout the growth curve of NS0 cells during controlled bioreactor batch culture

Day of Culture	Number of Protein Spots Detected
1	1583
3	1609
5	1704
7	1686

As with the protein gels run for the batch culture experiment in chapter 4, the total number of protein spots detected on each 18 cm gel throughout culture increased until late exponential growth phase (day 5 of the batch culture). However, at the end of culture (day 7) the number of proteins detected decreased as expected. As observed in the autoradiographs, the number of protein spots increased as the culture progressed until the end of the culture was reached (Table 5.1 and 5.3). The largest increase in the number of proteins observed was between early and late exponential growth phase where the number increased by 105. Towards the end of the culture at day 7 (in contrast with the 24 cm 2-D gels) the number of protein spots detected reduced relative to day 5 (a decrease of 18 protein spots). This is consistent with the autoradiograph data, confirming that fewer proteins are present at this phase of the growth curve.

5.2.2.2 Quantitative Analysis of Protein Expression throughout Batch Culture on 18 cm 2-D Proteome Maps

In order to accurately compare the global expression changes on the 2-D autoradiographs, the 18 cm 2-D protein gels were analysed using the same parameters as the 24 cm gels in the previous chapter (chapter 2, section 2.7.4). The resultant digital images (Figure 5.5) were analysed using ImageMaster™ 2-D software to investigate changes in protein expression throughout batch culture. Gel images were all compared to a reference gel which was derived from the 2-D gel extracted on the first day of the culture. The proteome maps for the batch culture, showing the proteins that were matched to the reference gel and shown to be up- and down-regulated by a two-fold or greater quantifiable change, are shown below in Figure 5.6. In order to identify the regulation of the proteins throughout the culture, each gel was compared against the preceding sample.

5 Analysis of Protein Synthesis in GS-NS0 Cells during Batch Culture

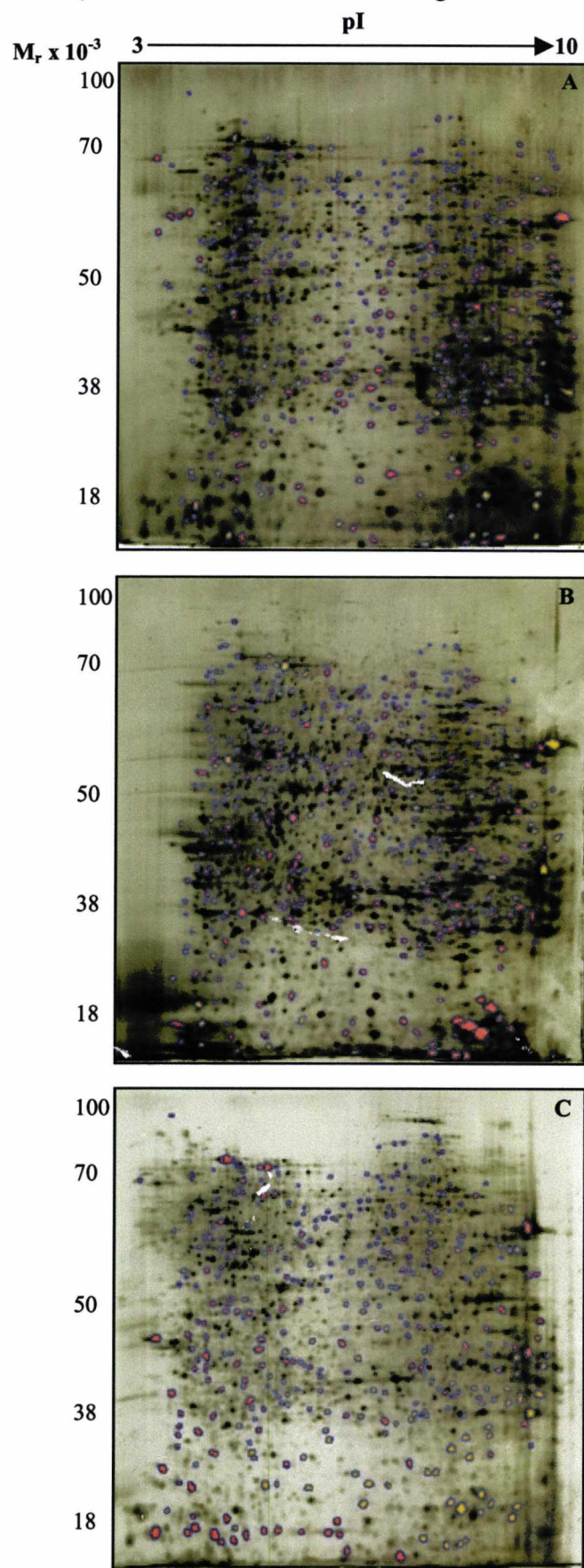


Figure 5.6 Comparative analysis of protein expression throughout the batch culture of NS0 cells. The Figure shows difference maps illustrating the proteins exhibiting at least a two-fold change in the level of protein expression. Only proteins that have been matched between samples are shown. Figure A, day 3 versus day 1 of the batch culture, Figure B, day 5 versus day 3 and Figure C, day 7 versus day 5 of the batch culture. Matched proteins exhibiting at least a two-fold increase (●) or decrease (●) in the level of protein expression.

Table 5.4 The total number of proteins up- and down-regulated by 2-fold or greater, newly synthesised, no longer expressed and unchanged proteins throughout the batch culture of NS0 cells assessed by 18 cm 2-D PAGE

Day of Culture	Total Number of Protein Spots	Unchanged*	Up-Regulated*	Down-Regulated*	Newly Expressed*	No Longer Expressed*
1	1583	1583	-	-	-	-
3	1609	776	183	209	441	415
5	1704	523	197	187	797	545
7	1686	478	178	189	841	554

* Indicates number of protein spots showing alterations in expression relative to the previous sample point

The pattern of protein expression throughout the batch culture experiment was, as expected, very similar to the observations on the 24 cm 2-D gels previously reported (chapter 4, Table 4.3). However, in contrast to the 24 cm protein 2-D gels, the number of protein spots detected at the end of the growth curve decreased (in common with the 2-D autoradiographs). Table 5.4 above shows the global changes in protein expression on the 18 cm 2-D gels for the NS0 cell proteome throughout the batch culture experiment. From the analysis of the 2-D gel images it was determined that after matching the gels to the reference gel (day 1 sample point) and rebuilding by adding protein spots present on gels from sample points other than day 1, 897 new proteins were added to the reference gel. Therefore as the culture progressed 897 proteins were newly expressed at time points other than at the start of the batch culture experiment. Throughout the batch culture, the number of proteins remaining unchanged when compared against the day 1 sample, decreased as previously observed.

As in the 24 cm protein gels (chapter 4, Table 4.3), the total number of proteins newly synthesised and up-regulated by at least 2-fold in total throughout the batch culture was observed to increase until the end of the culture at day 7. At the start of the culture between day 1 and 3, 624 (39%) of the total number of proteins detected were observed to be newly synthesised and/or up-regulated by at least 2-fold. At mid-exponential growth phase between day 3 and 5, 994 (62%) of the total proteins detected were up-regulated and/or newly expressed and finally between late exponential and death growth phase 1019 (60%) of the total number of protein spots detected were newly expressed and/or up-regulated by 2-fold. The greatest number of up-regulated and newly expressed proteins was observed at mid-exponential growth phase between day 3 and 5 of the batch culture. This observation correlates with the data obtained for the 2-D autoradiographs (Table 5.2 and 5.4).

The total number of proteins down-regulated or no longer expressed fluctuated (albeit by a small amount) as the culture progressed until the end of the culture. This was in contrast to the data obtained for the 24 cm gels, where the number increased. Between day 1 and 3, 624 (39%) of the total number of proteins were no longer synthesised and down-regulated. Between day 3 and 5 at mid-exponential growth phase 732 (45%) of the total number of detected proteins were no longer expressed or down-regulated by at least 2-fold and finally between day 5 and 7 the number of down-regulated and proteins no longer expressed increased to 743 (44%). Throughout the culture the number of proteins constitutively expressed between each time point reduced. Approximately 49% of the total number of protein spots between day 1 and 3, 33% between day 3 and 5, and finally between exponential and death growth phase 28% of the matched proteins were unchanged.

5.2.2.3 Comparison of 2-D Autoradiographs versus Silver-Stained Protein 2-D Gels

When the 2-D autoradiographs were compared against the equivalent protein on the 18 cm 2-D gels, the overall spot patterns appeared similar, particularly in the more abundant protein spots. However, when the images were subjected to in-depth analysis significant differences in the pattern of protein expression were observed (Figure 5.7). The total number of proteins detected on the autoradiographs was approximately half the number of proteins observed on the protein gels. The protein gels were also difficult to match against the autoradiographs, and it was possible to only match approximately 50% of the polypeptides to the protein gels (Table 5.5). Figure 5.7 below highlights an example of the visualisation differences between the protein gels and 2-D autoradiographs.

Table 5.5 The total number of polypeptides on autoradiographs matched to the equivalent protein spot on protein gels from the same day of the batch culture experiment

Day of Culture	Number of Polypeptide Spots	Number of Protein Spots	Number of Polypeptides Matched to Protein Gel*
1	802	1583	316
3	866	1609	407
5	894	1704	338
7	677	1686	280

* Indicates nascent polypeptide spots matched to protein spots from the same sample point on 18 cm gel format

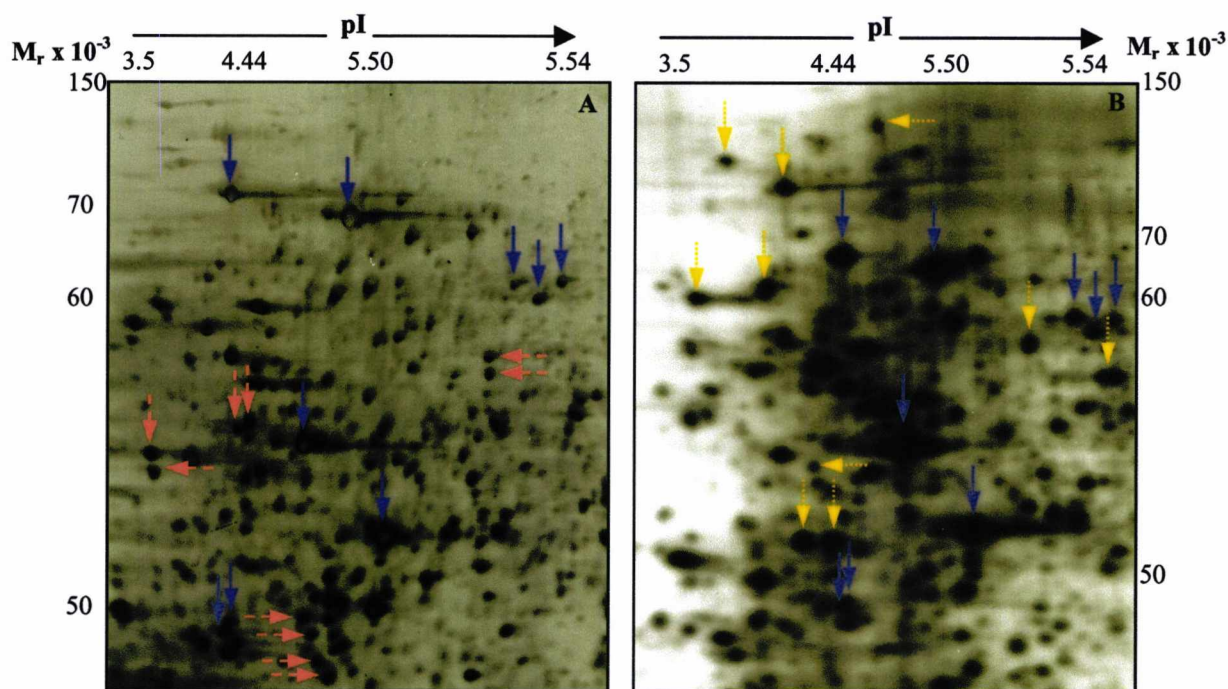


Figure 5.7 Comparison of protein expression profiles on 18 cm protein gels and 18 cm autoradiographs. Figure A, section of the acidic region of a silver stained gel image of a whole NS0 cell extract, and Figure B, autoradiograph image of a whole NS0 cell extract. Both samples were extracted at exponential growth phase. Solid blue arrows represent protein spots that are located on the protein gel and the autoradiograph, the broken red arrows highlight protein spots clearly represented on the protein gels only, and the dotted yellow arrows represent protein spots only clearly visualised on the 2-D autoradiographs.

Figure 5.7 above displays a typical example of the differences between the protein gels and autoradiographs. The variances between the autoradiographs and protein gels may be caused by the detection method utilised, the sensitivity of the method or as a result of differences in protein expression. Due to the differences in the 2-D autoradiographs and the protein gels it was difficult to match and assign protein spots. It is not possible to identify protein spots on autoradiographs using current technologies to confirm protein identity. Therefore, tentative protein identification assignment on autoradiographs was achieved by comparing the relative position of proteins identified from the 24 cm gels in chapter 4, (Figure 4.5 and Table 4.5). The positions of the identified proteins were first located on the 18 cm format protein gels (which were run from the same sample), and these were then utilised to identify the likely positions of the protein spots on the autoradiographs. Figure 5.8 below shows the tentative positions of the proteins identified in the previous chapter. Figure 5.9 and 5.10 below show the visual changes in polypeptide expression throughout the growth curve of NS0 cells on 2-D autoradiographs.

The image analysis software was utilised to investigate the 17 proteins identified in chapter 4 (Figure 4.5 and Table 4.5) on the 2-D autoradiographs in the same way as the

proteins on the 24 cm protein 2-D gels were analysed. Therefore, changes in the level of expression of polypeptides throughout the batch culture could be assessed and accurately compared to the corresponding protein spots on the 24 cm gels. Although the software enables individual spot volumes to be normalised, which allows the direct comparison of protein expression between a set of gels, the data obtained was further normalised (as detailed in the methods section) to obtain data in a more usable format. The relative levels of protein expression between the autoradiographs and 24 cm protein gels were then compared. Figure 5.11 and 5.12 below show the expression profiles of the 17 polypeptides on the autoradiographs that were identified and observed to change in relative expression levels throughout the batch culture experiment on 24 cm protein gels (chapter 4, Table 4.5). The 18 cm protein 2-D gels were not utilised for exploring the relative changes in protein expression as the proteins were visualised using Shevchenko silver staining methodology, which has been shown to result in high background staining and a high degree of saturation and negative staining for abundant protein spots (chapter 3, section 3.3.6) (Gorg et al., 2000b). Although the normalised spot volumes did provide similar results to those observed for the 24 cm gels (chapter 4, Figure 4.8 to 4.11) with small variations between replicate 2-D gel images of the same sample observed (chapter 4, Figure 4.10 and 4.11).

5 Analysis of Protein Synthesis in GS-NS0 Cells during Batch Culture

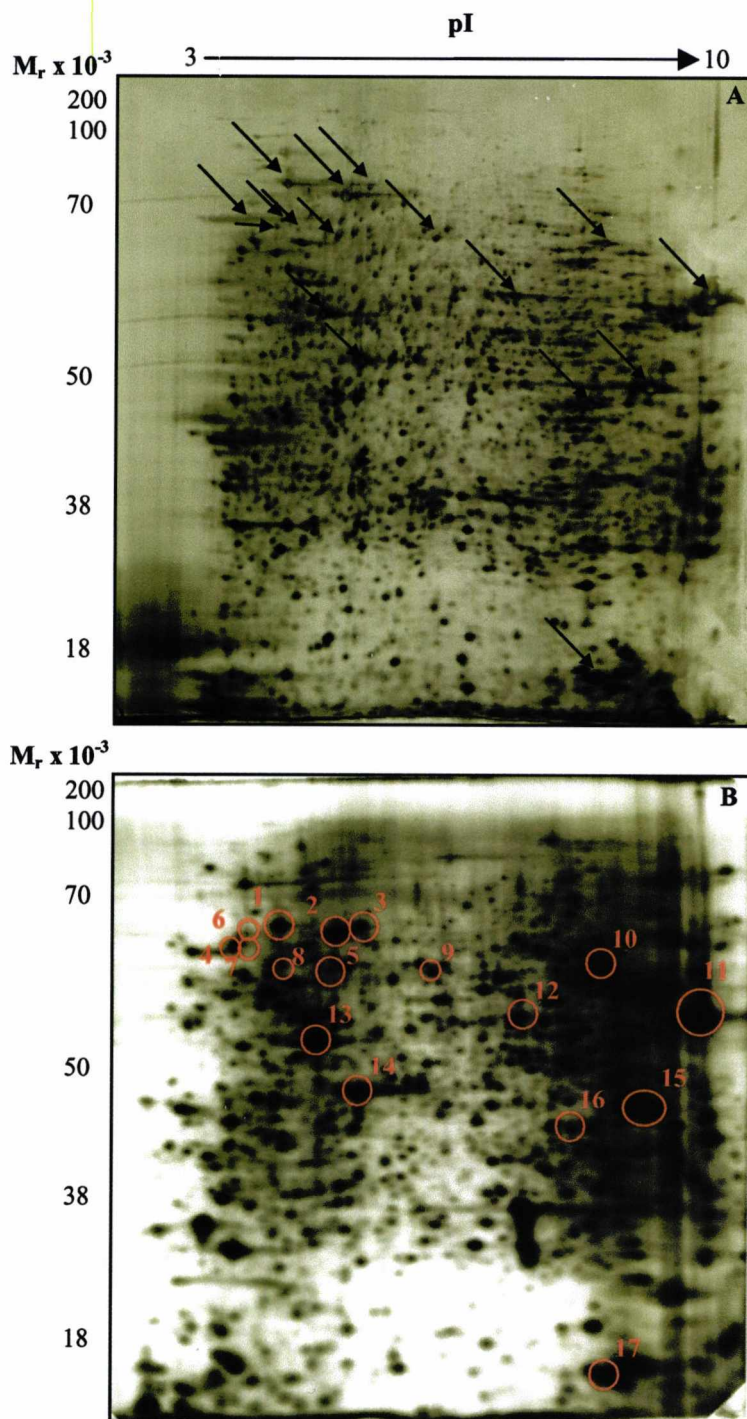


Figure 5.8 Putative protein spot identification. Figure A, silver stained, 18 cm, pI 3-10 non-linear, 12.5% gel image from a sample of whole NS0 cells taken at day 5 (exponential growth phase) of the culture. Figure B, a 2-D autoradiograph image (run on 18 cm, pI 3-10 non-linear IPG strip, 12.5% gel), taken from day 5 of the growth curve. The arrows and circles correspond to the likely position of protein spots on the 18 cm 2-D gel and 2-D autoradiograph identified in chapter 4, Figure 4.5 and highlighted in chapter 4, Table 4.5.

5 Analysis of Protein Synthesis in GS-NS0 Cells during Batch Culture

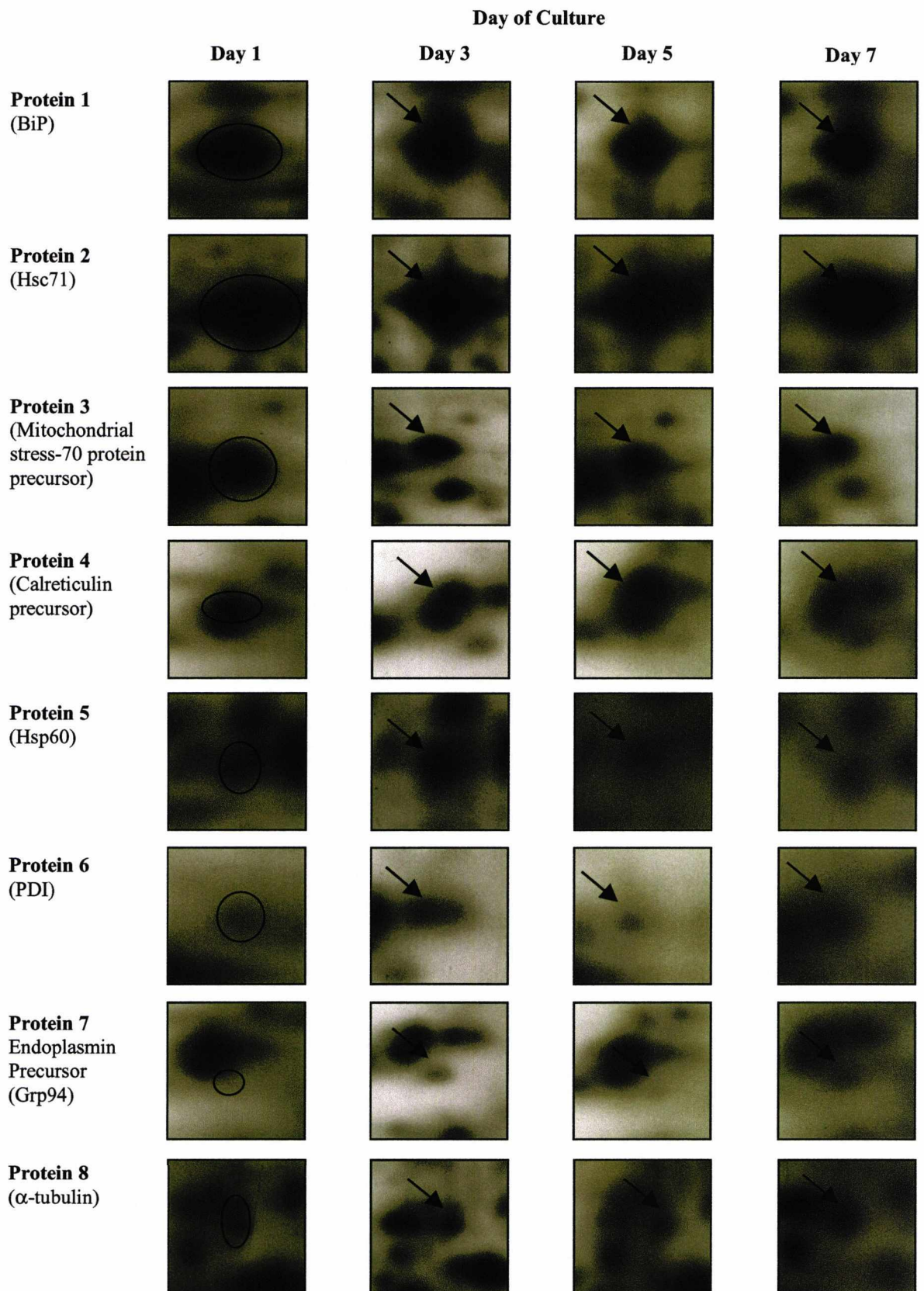


Figure 5.9 Proteins 1-8 from Figure 5.8B matched to protein gels run from different sample points throughout the bioreactor culture of NS0 cells (chapter 4, Table 4.5). The highlighted proteins (circles and arrows) represent expanded areas taken from the different days of sampling, compared against the reference gel (whole NS0 cell day 1 autoradiograph).

5 Analysis of Protein Synthesis in GS-NS0 Cells during Batch Culture

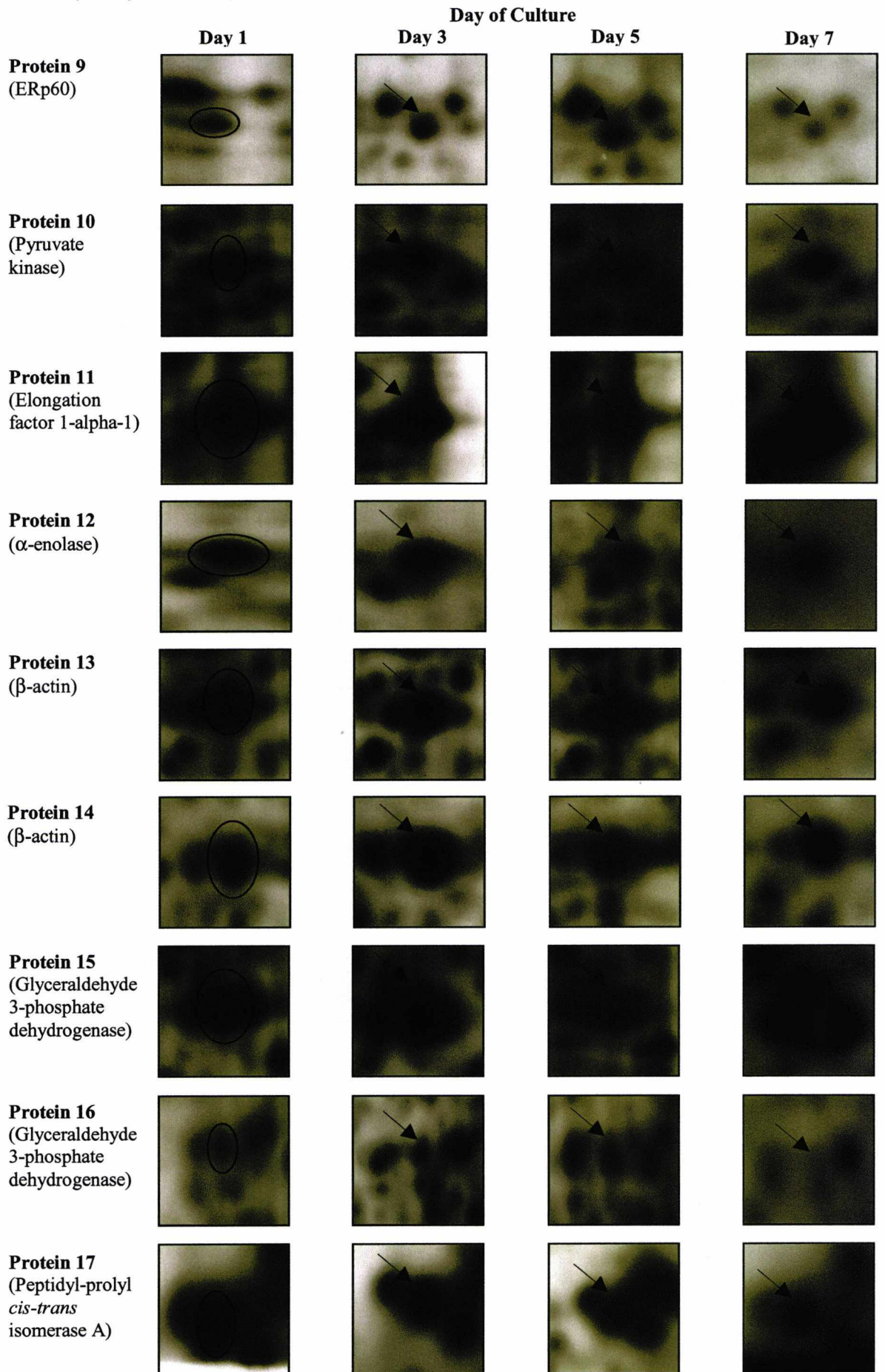


Figure 5.10 Proteins 9-17 from Figure 5.8B matched to protein spots from 2-D gels run from extracts taken throughout the growth curve of NS0 cells. The proteins highlighted represent expanded areas on each gel from different sample points matched against the reference gel (day 1 whole NS0 cell sample extract).

5 Analysis of Protein Synthesis in GS-NS0 Cells during Batch Culture

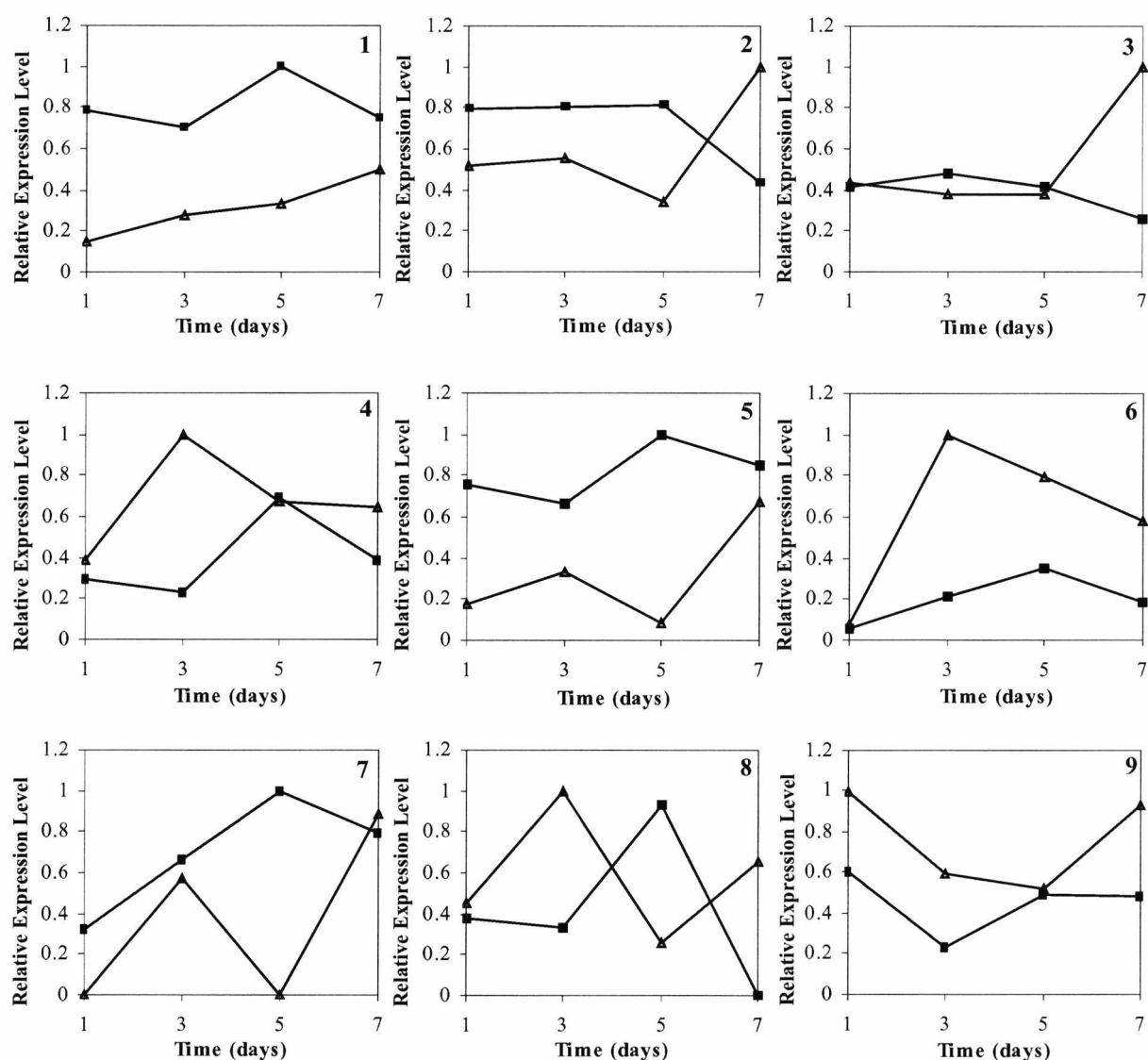


Figure 5.11 The quantitative analysis of proteins 1 to 9 expression identified in chapter 4, Table 4.5 throughout a bioreactor batch culture of NS0 cells. The graphs show the semi-quantitative information of proteins identified from NS0 cell sample extracts detailed in chapter 4, Table 4.5. (■) Relative protein expression profiles from 24 cm 2-D PAGE and (Δ) relative nascent polypeptide expression profiles from 2-D autoradiographs. Each datum point originated from individual protein or polypeptide spots on one 2-D gel image produced for each sample point, and was therefore not subject to error bar inclusion.

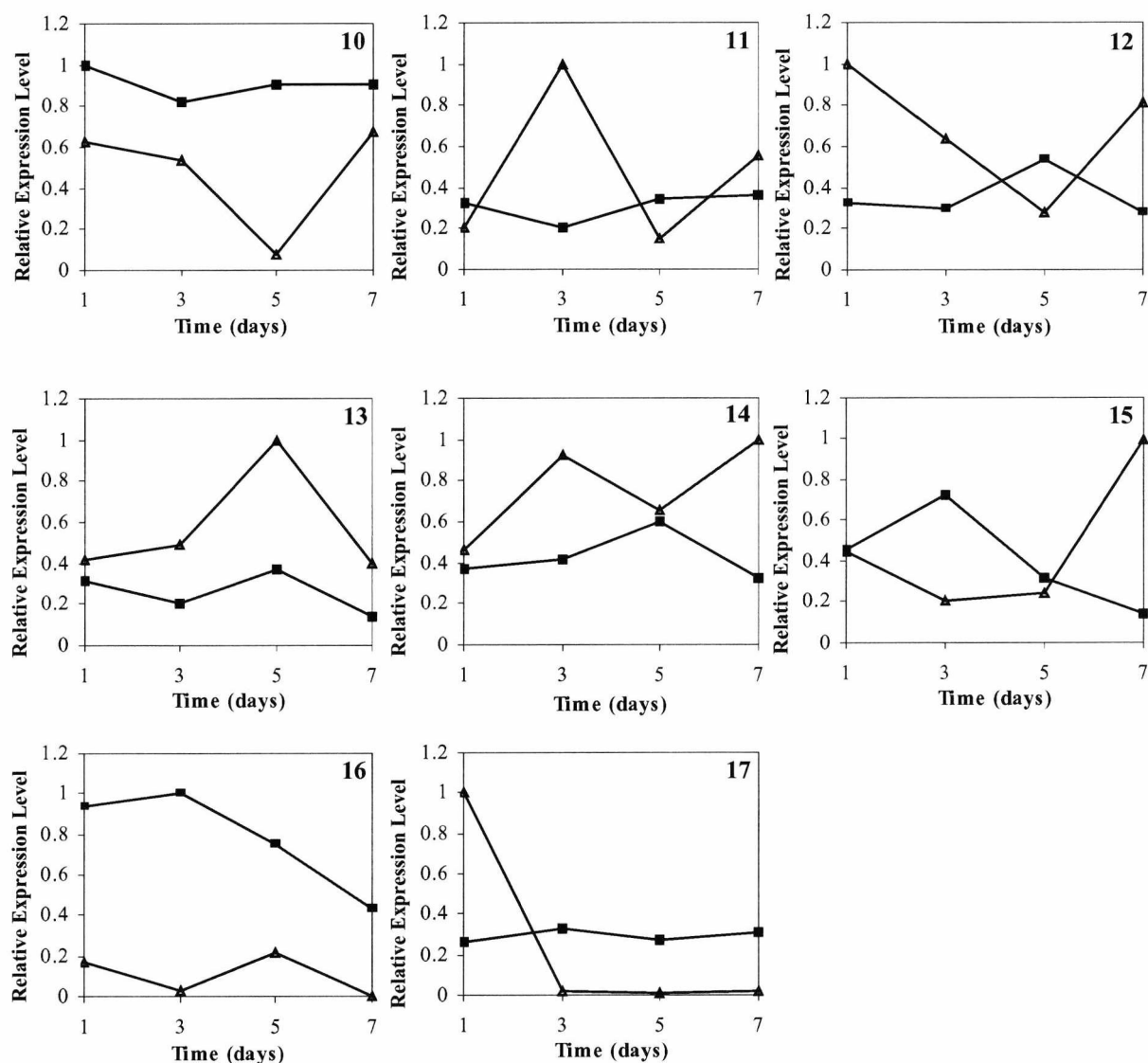


Figure 5.12 The quantitative analysis of proteins 10 to 17 expression in chapter 4, Figure 4.5 throughout a bioreactor batch culture of NS0 cells. The graphs show the semi-quantitative information of proteins identified from NS0 cell sample extracts detailed in chapter 4, Table 4.5. (■) Relative protein expression profiles from 24 cm 2-D PAGE and (△) relative nascent polypeptide expression profiles from 2-D autoradiographs. Each datum point was derived from individual protein or polypeptide spots on one 2-D gel image prepared for each sample point and therefore were not subject to error analysis.

5.3 Discussion

5.3.1 Nascent Polypeptide Synthesis during Batch Culture of NS0 Cells

The growth characteristics of NS0 cells under bioreactor batch culture conditions have been discussed in detail in the previous chapter (chapter 4, Figure 4.1, section 4.2.1, 4.2.2 and 4.3.1). Nascent polypeptide synthesis was assessed throughout the batch culture at key sample points by labelling newly synthesised polypeptides with [³⁵S] methionine (chapter 2, section 2.9 for details). The incorporation and secretion of [³⁵S] methionine labelled newly synthesised polypeptides was assessed to identify when maximum protein synthesis in NS0 cells under controlled conditions during batch culture occurred. The maximum incorporation of [³⁵S] methionine into NS0 cells occurred during early exponential growth phase (day 3) (Figure 5.1A). At this point in the growth curve, cells are preparing for maximum cell division, proliferation and also for producing maximum levels of rIgG. As a result we would expect that the cells would be more actively synthesising proteins at this point in the growth curve, to provide the necessary protein machinery required for energy production, cell division/proliferation and any stress proteins/chaperones required to clear any rIgG accumulating within the ER at this point in time. The cells were utilising the greatest amount of glucose (between day 3 and 5 of the batch culture) in order to provide the energy source required to support the increased cell numbers and cellular processes.

After the third day of the batch culture, the level of [³⁵S] methionine incorporation reduced steadily until the end of the culture was reached at day 7, concomitant with a reduction in viable cell density after day 5 of the batch culture. However, it is unclear why the incorporation of [³⁵S] methionine was not higher at day 5 of the culture. It would have been expected for the incorporation of the radiolabel at day 5 of the culture to be at a higher level than observed at day 3, as a result of the increased requirement for protein synthesis. However this was not observed. Clearly, even at this early stage in culture, the maximum viable cell density has been obtained and therefore the rate of growth and proliferation has slowed considerably. As a result the requirement for protein machinery involved in these processes would be expected to be lower, resulting in less nascent polypeptide synthesis. This is possibly offset to some degree by the synthesis of proteins in response to any stresses the cells may have perceived at this stage in the growth curve. At the end of the culture (day 7), the level of [³⁵S] methionine incorporated into the cells was greatly reduced, as expected. During this late stage of the growth curve, the cell

viability had reduced to 22%. Therefore most of the cells were dead and, as a result, only a very small amount of the radiolabel was taken up by the remaining viable cells.

Throughout batch culture the level of [³⁵S] methionine secreted from NS0 cells into the supernatant was also investigated. The maximum level of secreted protein into the supernatant was observed (as expected) at exponential growth phase between day 3 and 5 of the batch culture (Figure 5.1B). Again, this is in agreement with the observations made from the growth characteristics and protein expression on the 2-D gels (chapter 4, Figure 4.1 and section 4.2.3) whereby the maximum level of labelled secreted protein coincided with the period in the culture where the cells were most actively proliferating.

As previously stated, during this stage of the growth curve maximum rIgG production was observed. During late exponential growth (day 5 of the culture), the maximum rate of glucose consumption was also observed (Figure 5.3). The increase in glucose consumption at day 5 correlates with the increase in protein production required to enable the cells to reach maximum viable cell density. The greatest effect of stress, and therefore stress protein induction, was observed on the protein gels during late exponential growth phase (day 5) (chapter 4, Table 4.3). This observation coincides with the greatest increase in nascent protein synthesis by the cells (Figure 5.1B). Towards the end of the culture at day 7, the level of secreted [³⁵S] methionine labelled proteins decreased below detectable levels. During this period in the growth curve it was expected that protein synthesis would be shut down, or at least reduced, because of the decrease in viable cell numbers. This is confirmed by the observation that no radiolabelled secreted nascent polypeptides were detected at this point in the growth curve.

5.3.2 Global Analysis of Protein Expression Profiles on 2-D Autoradiographs

In the previous chapter samples of 1×10^7 cells were extracted throughout the batch culture and subjected to 2-D PAGE (chapter 4, section 4.2.3). Following image analysis a pattern of protein expression was revealed; however, proteome analysis of the proteins present at any time point does not provide information concerning the proteins that are being actively synthesised, and therefore required, by the cells at a specific time point. In order to obtain a more complete and accurate picture of the proteins being actively synthesised and required by the cells at each time point, samples of 1×10^6 cells were removed from the culture and subjected to *in vitro* labelling with [³⁵S] methionine, which was incorporated into newly synthesised proteins (chapter 2, section 2.9 for details of labelling).

Between day 1 and day 3 of the culture, the total number of newly synthesised proteins expressed increased from 802 to 866, and between days 3 to 5, this number increased again by nearly 100 polypeptides to 894 (Table 5.1). The increase in protein synthesis during the first few days of the culture and on into exponential growth phase may be attributed initially to the new environmental conditions and the cells preparing to begin growth and division. However, it must be noted again that at the early stages of the growth curve (day 1), when the bioreactor vessel was seeded, the cells were already growing at an exponential rate (as the cells were used to seed the fermenter once they had reached a density of 1×10^6 cells mL^{-1}). As a result the proteins required for proliferation and rIgG production would be expected to already be present. The greatest increase in nascent protein synthesis occurred at late exponential growth phase (day 5 of the culture). As already stated, at this time point the cells were at their maximum viable cell density and were also producing the greatest amount of rIgG. It was therefore expected that the level of protein synthesis would increase as a result of increased cell growth and proliferation and possibly due to ER stress as a result of accumulation of rIgG within the ER, which has previously been reported (Downham et al., 1996; Kohno et al., 1993).

During late exponential growth phase the greatest utilisation of glucose occurred, to provide the energy source for rapid cell growth and division of the ever-increasing cell population. At this time maximum recombinant protein production was observed which is also presumably energy expensive. During this stage of the growth curve the expression of proteins that protect the cell from stress as a result of glucose depletion and the UPR would also be expected to be induced. Furthermore, as a result of any protein accumulating within the ER, proteins such as chaperones and heat shock proteins are likely to be induced, and the synthesis of these proteins would be expected to increase (as was observed in the protein profiles of the 2-D gels in chapter 4, Table 4.3). Towards the end of the culture at day 7, the number of newly synthesised polypeptides detected reduced dramatically to 677 polypeptide spots (a decrease of 217 protein spots). This observation was expected, as at this stage of the growth curve most of the cells were dead (with the cells having a viability of just 22%). Therefore it is unlikely that the cells would require new protein synthesis and, as a result, protein synthesis would be shut down. This was confirmed in the pattern of the radiolabel incorporation and secretion throughout the culture, where the maximum incorporation and secretion of [^{35}S] methionine occurred during the earlier stages of growth, and decreased dramatically towards the end of the culture at day 7 below detectable levels (Figure 5.1).

5.3.3 Analysis of Polypeptides Exhibiting a 2-Fold Change in the Level of Synthesis

Image analysis was further utilised to explore the changes in the level of synthesis of nascent polypeptides throughout batch culture to further characterise the changes in the NS0 cell proteome. After normalising the polypeptide spot volumes on each gel (to enable their accurate comparison), approximately 200 (25%) of all the polypeptides synthesised remained unchanged in the level of their expression throughout batch culture. Those proteins present at the same level throughout culture are likely to be 'housekeeping' proteins, which are essential for the growth and survival of NS0 cells (Table 5.2). These proteins are actively synthesised by NS0 cells at a constant rate and remained unchanged throughout culture, without being induced or repressed either as a result of stress being perceived by the cells, or nutrient deprivation.

Throughout the batch culture, the number of proteins exhibiting a reduction in expression fluctuated. This occurred in correlation with the results obtained for the 24 cm 2-D gels discussed in chapter 4 (Table 4.3). Although the results discussed here provide some general information about the global 'position' of the NS0 cells at each time point throughout the growth curve, the level of expression of newly expressed or no longer detectable proteins cannot be quantified. As a result the changes in polypeptide synthesis throughout the batch culture were quantified in the same way as the changes in the protein gels in chapter 4, using the software to investigate polypeptides that exhibited at least a 2-fold change in protein expression.

From the 2-D autoradiographs, many of the nascently synthesised proteins exhibited at least a 2-fold change in the level of expression (Table 5.2). The greatest change in polypeptide synthesis occurred between day 1 and 3 of the culture as previously discussed, with the number of proteins exhibiting a 2-fold increase in expression fluctuating throughout culture. Between day 1 and 3, 122 proteins were up-regulated, 106 between day 3 and 5, and finally at the end of the culture 135 polypeptides showed an increase in expression. This correlates with the results observed for the 24 cm protein gels reported in chapter 4.

Although the greatest number of polypeptides exhibiting a 2-fold change in the level of synthesis was observed at the start of the culture, the greatest number of polypeptides showing a 2-fold increase in expression (together with polypeptides that were newly expressed) occurred at exponential phase of the culture between day 3 and 5 (499, 58% of polypeptides). During this stage of the growth curve we would expect that many proteins would become up-regulated in order to facilitate proliferation and possibly to

assist in (and in response to) the production of rIgG. Proteins involved with the UPR would therefore be expected to become induced or up-regulated at this stage of the growth curve to aid in the clearance of the accumulating unfolded proteins from the ER (Ellgaard and Helelius, 2001). It is also probable that proteins involved with glycolysis would be up-regulated in order to maintain the energy requirements of the cell at this time.

The number of polypeptides exhibiting a decrease in the level of expression by at least 2-fold was also investigated. During exponential growth phase (between day 3 and day 5), the number of proteins down-regulated or no longer detectable numbered 316 (36%). This low decrease in protein expression correlated with the observations on the 24 cm protein gels. During this stage in the growth curve the cells were at their most active and were proliferating and producing rIgG at the maximum level. Therefore it is likely that the cells would be under a great amount of stress as a result of the rIgG accumulating in the ER, and it is also likely that proteins involved with energy production would be up-regulated to enable protein synthesis and cell proliferation to occur.

Finally, between day 5 and 7 (towards the end of the culture) 396 (44%) of all the polypeptides were down-regulated and/or no longer expressed at detectable levels (Table 5.2). The data obtained here correlates with the trends observed on the 24 cm protein gels. At the end of the culture, the number of polypeptides up-regulated was high, and was possibly attributable to the cells being under stress and the cellular response. However, it is also likely that at this stage of the growth curve the cells would sense that the stress they were under was not combatable, and therefore other proteins, such as those which aid in inducing apoptotic cell death, would be up-regulated and the cells would undergo controlled cell death (as discussed in the previous chapter). It can clearly be seen that towards the end of culture the number of proteins down-regulated is less than at exponential growth phase of the culture. However, many more proteins ceased to be expressed at this time when compared to the rest of the culture (Table 5.2).

5.3.4 Analysis of Nascent Polypeptides Showing a Change in the Level of Expression throughout Batch Culture

In order to accurately compare the proteome of NS0 cells versus nascent polypeptide synthesis, the 18 cm proteome maps were subjected to the same type of analysis to identify the global changes in the NS0 proteome. The data obtained for the 18 cm gels visualised with Shevchenko silver stain (Shevchenko et al., 1996) does not yield an accurate representation of changes in the NS0 proteome, particularly with respect to changes in the

level of expression. The staining method causes high background levels and also results in negative staining on highly abundant proteins so that false low values can be obtained for the spot volumes of these proteins (chapter 3, section 3.3.6) (Gorg et al., 2000b). The results obtained could therefore not be utilised to explore in detail the changes in the NS0 cell proteome throughout batch culture. The results are briefly outlined here for comparative reasons only, as the autoradiographs cannot be compared directly to the 24 cm gels because of the differences in resolving range on the gels. Although a similar trend in protein expression was observed on both the 18 cm and 24 cm protein 2-D gels.

Image analysis of the 18 cm protein gels showed that during the early stages of culture 776 protein spots were unchanged (between day 1 and 3), 523 were unchanged at exponential growth phase (day 3 to 5) and 478 at the end of the culture (between day 5 and 7) (Table 5.4). Throughout culture approximately 30 to 40% of all the proteins remained unchanged in the level of expression (Table 5.4). This compares with approximately 40% of all proteins that remained unchanged throughout batch culture on the 24 cm protein gels discussed in chapter 4.

The global analysis of protein synthesis on 18 cm gels throughout the batch culture experiment indicated as the culture progressed the number of newly expressed polypeptides increased until the end of the culture was reached at day 7. This was in contrast with the autoradiographs, which increased until day 5, before the level decreased. The number of newly detected proteins on the 18 cm proteome maps increased greatly as the culture progressed (Table 5.4). This correlated with the changes observed on the 24 cm proteome maps (chapter 4, Table 4.3). The number of proteins that were no longer present at detectable levels was also investigated throughout the culture and was observed to increase. This was again in agreement with the general trend of the autoradiographs and 24 cm protein gels (chapter 4, section 4.2.3.3, Table 4.3 and Table 5.2).

In contrast with the results observed on the autoradiographs and the 24 cm protein gels, the number of proteins down-regulated on the 18 cm gels increased between day 3 and 5 of the culture with 732 (45%) proteins exhibiting a change in the level of expression. This was not expected as at this stage in the culture it was expected that the number of proteins down-regulated would decrease as observed in the 24 cm gels (see chapter 4). However, as observed in the 24 cm protein gels and the autoradiographs an increase in the number of proteins down-regulated was observed towards the end of the culture (between day 5 and 7) with 44% of proteins down-regulated at this time (chapter 4, Table 4.3, Table 5.2 and 5.4). The reasons for this have been discussed previously.

5.3.5 Comparison of Protein Expression on 2-D Autoradiographs and Protein Gels throughout Batch Culture

When the autoradiographs were compared against the protein gels the images appeared very similar, although on closer inspection it was apparent that there were many differences in the pattern of protein and polypeptide expression (Figure 5.7). Firstly the number of actively synthesised polypeptides was much less than the number of protein spots detected on the protein gels. When the autoradiographs were matched against the protein gels, approximately half the total number of polypeptides was matched to the corresponding protein gel (Table 5.5). The differences in protein spot patterns may be explained by slight differences in the running conditions and the different methods utilised for producing autoradiographs and protein 2-D gels, which reflect metabolic and constitutive protein expression respectively (Westbrook et al., 2001).

It has previously been reported that proteins with high turn-over rates are unlikely to accumulate in high enough levels to enable visualisation by silver stain methodology (Westbrook et al., 2001). Conversely, it has also been reported that proteins, which have a slow rate of synthesis and degradation, may only be detectable by silver stained gels and not by 2-D autoradiography (Westbrook et al., 2001). Autoradiographs only visualise proteins that are being actively synthesised and required by the cells at each given time-point, and thus it is unlikely that all the proteins visualised on protein gels would be expressed on the autoradiographs. The 2-D pattern of protein spots on autoradiographs are also more diffuse than those on the protein gels, and as a result it is possible that the more abundant polypeptide spots could mask some of the less abundant protein spots present on the autoradiographs. The autoradiographs also suffered from very high background levels, which is a problem associated with the technique, and as the protein spots also appeared much more diffuse, it proved difficult to match the autoradiographs against the corresponding protein gel.

Despite the problems associated with the two different techniques for analysing nascent polypeptide synthesis and protein expression, many of the protein spots that were identified from the 24 cm protein gels were located on the 18 cm format protein gels and autoradiograph images (Figure 5.8). Once each protein was located, the relative levels of protein and polypeptide expression throughout the batch culture were compared (Figure 5.9 to 5.12). The 17 proteins that were identified in the previous chapter by MALDI-ToF ms, were matched to the 2-D autoradiographs and then compared against the relative expression level on the 24 cm protein gels (Figure 5.11 and 5.12). Although the 18 cm 2-D

gels were utilised to compare the global statistics, the silver staining methodology utilised is unreliable for expression analysis of individual proteins as previously described.

As discussed in the previous chapter (chapter 4, section 4.3.4), the proteins that were identified could be separated into 3 main groups, chaperones, glycolytic proteins and structural proteins. The first two groups of proteins are expected to change in the level of expression throughout the culture, for the reasons previously described, that is to (1) assist in protein folding and transport through the ER and the secretory pathway (Kiang and Tsokos, 1998) and (2) in order to provide the energy required by the cells to support growth, proliferation and the increased metabolic burden of synthesising rIgG (Van Dyk et al., 2003). The third group of proteins were not expected to alter in the level of expression. However, as previously discussed, the level of expression of the structural proteins actin and tubulin were observed to change as the culture progressed. These proteins have been reported to be involved in the trafficking of proteins through the secretory pathway on microtubules (Thyberg and Moskalewski, 1999) and it is possible that the increase in the abundance of these proteins may be a direct result of rIgG production and the requirement to transport ever-increasing amounts of recombinant protein out of the cell.

Comparison of the protein and autoradiograph data for the 17 proteins discussed in chapter 4 shows that, in general, the level of nascent polypeptide synthesis and protein expression follow each other as expected (Figures 5.11 and 5.12). We would expect that an observed increase in nascent polypeptide synthesis would result in an observed increase in protein expression. Conversely, a decrease in nascent polypeptide synthesis should be followed by a decrease in protein expression levels and the general trend of the data confirms this. However, there are discrepancies to this general trend and this is most likely due to the difficulty in obtaining accurate quantitative autoradiograph data and differences in the half-life of individual proteins. The pattern of protein and polypeptide expression for the 17 individual proteins is discussed in greater detail below. Statistical analysis of protein and polypeptide expression was not carried out as only one 24 cm protein gel and one 18 cm autoradiograph was performed for each sample point. Although the variation in the pattern of protein expression for the 17 protein spots on replicate 18 cm protein 2-D gels are shown in chapter 4, Figure 4.10 and 4.11. The function of each protein is discussed in more detail in chapter 4.

5.3.5.1 BiP

BiP (Grp78) (Figure 5.11, protein number 1), as already described (chapter 4, section 4.3.4.1), is a member of the Hsp70 family (Johnson et al., 2001) and is known to interact with IgG heavy chains (Brewer et al., 1997). The relative expression level of BiP polypeptide chains throughout culture increased, reaching the maximum level of synthesis by the end of the culture. This observation occurred in slight contrast with the level of expression observed on the 24 cm protein gels, whereby the level of expression was observed to increase to late exponential growth phase, and then decreased slightly by the end of the culture. This suggests that BiP is increasingly required by NS0 cells throughout culture to assist in protein biogenesis in the ER under 'normal', non-stressed conditions, but is also induced as culture progresses, most likely in response to stress perception as BiP plays an important role in the UPR preventing the build-up of unfolded proteins within the secretory pathway (Brewer et al., 1997).

5.3.5.2 Hsc71

Hsc71 (heat shock protein cognate-71) (Figure 5.11, protein number 2) is a member of the Hsp70 family and is a constitutively expressed protein, which is most abundant in growing cells (Sorger and Pelham, 1987). The relative expression of Hsc71 on the autoradiograph images altered as the culture progressed. Between day 1 and 3 the level remained at approximately the same level, although the expression level decreased at day 5. The level of Hsc71 nascent polypeptide expression was induced at the end of the culture, which was inconsistent with the results observed for Hsc71 protein expression at this time (chapter 4, section 4.3.4.2). While it is possible that the level of Hsc71 was up-regulated late in culture, the protein data (which is more reliable) does not support this observation. The autoradiograph image for the day 7 sample was also blurred, and this would have made the identification of individual spot boundaries by the software programme a difficult task, which may account for the differences in protein spot expression patterns between protein gels and polypeptide gel images.

5.3.5.3 Grp75

Mitochondrial stress-70 protein (mortalin, Grp75) (Figure 5.11, protein 3) has been implicated to have chaperone-like properties, be involved in the stress response, and in determining cell fate by providing apoptosis protection (Kaul et al., 2002). The relative abundance of Grp75 during culture revealed that it was present at relatively high levels at

the start of the culture, in agreement with the 24 cm protein gel data (chapter 4, section 4.3.4.3). Grp75 continued to be synthesised at similar levels throughout until the end of the culture at day 7. Towards the end of the culture the expression level increased greatly. Once again, this was in contrast to the observations on the 24 cm protein gel, which showed a significant decrease in the relative expression level. Visual inspection of the Grp75 expression profile appears to show the greatest increase in expression during exponential growth phase, and that the relative volume does not increase at day 7. It is apparent that the software has yielded higher spot volume values as the protein spot was less diffuse at day 7 compared with the rest of the culture (Figure 5.9, protein spot 3).

5.3.5.4 Calreticulin

Calreticulin (Figure 5.11, protein 4) is an important chaperone of the ER lumen. Throughout batch culture the pattern of polypeptide and protein expression was on the surface very different. The relative expression of calreticulin was observed to increase greatly at the beginning of the culture between day 1 and 3 and reduced to the end of the culture at day 7. This was different to the observations on the protein gels, which exhibited the greatest induction of expression during late exponential growth phase (day 5), reducing to day 7 (chapter 4, section 4.3.4.4). However, closer inspection of the data shows that nascent polypeptide synthesis increased at day 3 and protein synthesis at day 5. It is possible that the level of protein expression was therefore only detected at day 5 (i.e. the cell responded to the need for more calreticulin by initiating synthesis on day 3, but this was only detected at the protein level on day 5). Protein sampling on day 4 may have been expected to show an increase in protein expression levels.

Although the maximum level of expression of calreticulin as determined by image analysis of nascent polypeptide synthesis was shown to occur at day 3 of the batch culture, the visual pattern of expression indicates that the maximum level of expression occurred at day 5 in agreement with the results shown on the 24 cm protein gels (Figure 5.9, spot number 4). These results suggest that, again as a consequence of the diffuse spot patterns and the high background values for the autoradiographs, errors in the spot volumes occurred, resulting in low values being obtained.

5.3.5.5 Hsp60

Hsp60 (Figure 5.11, protein 5) is a chaperonin, which is present in the mitochondria (Moller et al., 2002; Samali et al., 1999). The relative expression level of Hsp60 on the

autoradiograph images was observed to increase at early exponential growth phase, and reduce at day 5 of culture. The level of expression reached its maximum level by day 7 of the culture. This result contrasted with the values obtained for the protein gels (chapter 4, section 4.3.4.5). The level of protein expression was observed to decrease between day 1 and 3, and increased to its maximum level to late exponential growth phase, before decreasing in expression to the end of the culture. Once again, as in the case of calreticulin this may be the direct result of the difference between synthesis and protein accumulation.

5.3.5.6 PDI

Protein disulphide isomerase (PDI) (Figure 5.11, spot number 6) is an important protein involved in the quality control machinery within the ER (Noiva, 1999). The pattern of polypeptide expression differed from the relative abundance of the protein expressed on the 24 cm 2-D gels (chapter 4, section 4.3.4.6). The relative abundance of PDI was induced greatly at the beginning of the batch culture at day 3, early exponential growth phase. The expression of PDI was observed to decrease steadily after this time. A similar pattern of protein expression was observed except the highest level of expression occurred during late exponential growth phase. PDI has been reported to have a role in the *in vitro* folding of IgG, therefore it is likely that the expression of PDI would be increased between day 3 and 5 of the batch culture, a period where most IgG was being actively produced by the cells. PDI has also been associated with heat shock and acts as a chaperone, as well as having a role in catalysing the rate-limiting steps of disulphide bond formation (Noiva, 1999; Wang, 2002). This once again highlights the 'delay' observed between initiation of protein synthesis and increased protein expression.

5.3.5.7 Grp94

Endoplasmic reticulum chaperone (Grp94) (Figure 5.11, spot number 7) is an abundant protein of the ER lumen (Downham et al., 1996). The relative expression level of endoplasmic reticulum chaperone on the autoradiographs was very different to the pattern of protein expression. It is obvious that the point for day 5 (Figure 5.11, number 7) or day 7 is incorrect and this highlights the difficulty in obtaining quantitative data from autoradiographs of 2-D gels.

5.3.5.8 α -Tubulin

α -tubulin (Figure 5.11, number 8) is an important structural protein and is a major constituent of microtubules, which are involved in cell morphology, and also for the transportation and secretion of newly synthesised proteins (Thyberg and Moskalewski, 1999). In common with many of the other polypeptides analysed, the pattern of expression was different to that seen on the protein gels (chapter 4, section 4.3.4.8). The greatest induction of α -tubulin was observed by the third day of the batch culture. After this time the expression of α -tubulin decreased to day 5, before increasing again towards the end of the culture. In contrast to the polypeptide autoradiographs, the expression of α -tubulin on the protein gels was observed to decrease between day 1 and 3 of the culture before increasing to its maximum expression level by the fifth day. After reaching maximum expression levels at day 5, the expression of α -tubulin protein then decreased to below detectable levels by day 7 of the batch culture.

The visual pattern of α -tubulin on the autoradiograph images followed the relative expression graphs. Although it is possible that the expression of α -tubulin increased in expression by day 3, it was not expected that the expression of α -tubulin would increase towards the end of the culture (Figure 5.9, number 8). It would be expected that the expression pattern would have followed that visualised on the protein gels, increasing to the fifth day of the culture, and therefore the level of α -tubulin expression would also be expected to reduce at the end of the culture.

5.3.5.9 ERp60

ERp60 (Figure 5.11, number 9) is a homologue of PDI, and has similar roles in the cell to BiP and Grp94 (Ferrari and Soling, 1999). Throughout the batch culture the pattern of polypeptide synthesis and protein expression were similar. This suggests that initiation of induction of ERp60 synthesis is rapidly followed by increased expression of mature protein. The cell can therefore rapidly respond to the requirement for ERp60. ERp60 has been reported to interact with growing polypeptide chains including IgG in the lumen of the ER (High et al., 2000; Michalak et al., 1999) and is involved with the stress response. As a result we might expect that ERp60 would be up-regulated at day 5 of the batch culture, (where IgG production was at its maximum level and the cells were under stress), in common with BiP and Grp94 expression on the protein gels. As expected, this pattern of expression for ERp60 was observed on the protein gels and autoradiographs.

5.3.5.10 Pyruvate Kinase

Pyruvate kinase (PK) (Figure 5.12, number 10) is a key glycolytic enzyme, which catalyses the rate limiting step of pyruvate and ATP formation from phosphoenolpyruvate and ADP (Yamada and Noguchi, 1999). The pattern of polypeptide expression and protein expression did not appear to agree throughout culture. The pattern of protein expression showed that PK remained constitutively expressed, only fluctuating slightly in the level of expression (chapter 4, section 4.3.4.10), while the polypeptide data fluctuated throughout. However, the visual pattern of polypeptide expression did not correlate with the relative expression levels measured using the ImageMaster™ software (Figure 5.10, number 10). Visually throughout culture the expression of PK increased slightly during the first few days of the culture, reaching maximum expression levels by day 5 of the culture. After day 5 the level of expression appeared to reduce slightly. It appears that the differences in the visual pattern and quantified levels of expression were again due to the diffuse pattern of the polypeptide spots, which the analysis software could not accurately define. The expression levels reflect the requirement for PK on both the autoradiographs and protein gels throughout the culture.

5.3.5.11 eEF1A-1

Elongation factor 1-alpha-1 (eEF1A-1) (Figure 5.12, number 11) is important in the translation of proteins and is involved in the recruitment of amino-acyl-tRNAs to the ribosome (Caraglia et al., 2000). The expression levels of the polypeptide and protein again exhibited contrasting patterns. However, closer inspection once again confirms that there appears to be a delay between increases in polypeptide synthesis and the resulting observed increase in protein expression levels. Furthermore, once again the diffuse nature of the autoradiograph data and the intensity of the polypeptide make accurate measurement of this spot in particular almost impossible with the currently available computer software. However, the visual pattern of polypeptide expression fits with the observations on the protein gels. The increase in eEF1A-1 expression during exponential phase correlates with the proteins' function being involved with translation (Richarme, 1998).

5.3.5.12 α -Enolase

α -enolase (Figure 5.12, number 12) is a glycolytic enzyme, which has a key function in the formation of phosphoenolpyruvate from 2-phosphoglycerate (Sugahara et al., 1998).

Throughout batch culture the polypeptide expression levels on autoradiographs did not correlate with the protein expression levels (chapter 4, section 4.3.4.12). The reasons for the differences in the visual pattern and quantified data were likely again to be due to the diffuse pattern of the polypeptide spot.

However, once again the visual pattern of α -enolase expression did appear to correlate with the relative expression on the protein gels (Figure 5.10, number 12). The explanation for this expression pattern is discussed in chapter 4.

5.3.5.13 β -Actin

β -actin (Figure 5.12, number 13 and 14) is an important structural protein, involved in organisation of the cellular cytoskeleton (Friso et al., 2001). The level of expression of β -actin was not expected to change throughout the culture. On the autoradiographs, however, the level of expression was observed to increase at late exponential growth phase (spot 13) before reducing to the end of the culture. On the β -actin spot (number 14), the polypeptide reached the maximum level of expression by the third day of the culture, before reducing at day 5 and increasing again to the end of the culture. The pattern of expression of spot 13 followed the pattern of expression of β -actin on the protein gels (chapter 4, section 4.3.4), although the changes in expression were more dramatic. The level of expression of β -actin of spot number 14 did not however follow the pattern for the corresponding protein spot.

The visual pattern of β -actin expression followed the same general trend seen for spot number 13 (Figure 5.10, number 13 and 14). Spot numbers 13 and 14, revealed that the expression level of β -actin did increase in expression on the third day of the culture and also appeared to decrease by day 5 of the culture (spot number 14). However, this may have been as a result of the protein spot being more diffuse than on the other days of the culture. As a result at day 7, β -actin appeared to be induced further on spot number 14, although the level of expression appeared to be similar on both of the β -actin protein spots.

5.3.5.14 GAPDH

Glyceraldehyde 3-phosphate dehydrogenase (GAPDH) (Figure 5.12, number 15 and 16) is a key glycolytic enzyme (Dastoor and Dreyer, 2001). Throughout the batch culture, the expression of the two GAPDH polypeptide spots differed from each other and also between the protein gels. Both sets of results for GAPDH on the autoradiographs

contrasted with the results obtained for the protein gels. This may reflect the need for different isoforms of GAPDH or conversely, may reflect changes in post-translational modifications (e.g. phosphorylation), which modulate activity. The level of protein expression on spot number 15 indicated that GAPDH reached its maximum level of expression by day 3, and reduced steadily after this time to the end of the culture. GAPDH expression on spot number 16 exhibited a similar pattern of expression to spot number 15, and reached the maximum level of expression by the third day of the culture and reduced steadily to day 7 (chapter 4, section 4.3.4.14 and 15). However, as discussed in chapter 4, the spot volumes for GAPDH on the protein gels could not be relied upon as the protein spots were highly abundant and in some cases the protein spots were saturated resulting in the volumes being underestimated.

Furthermore, the visual pattern of GAPDH expression indicated that the relative volumes on the autoradiographs were not accurate for either of the polypeptide spots. Therefore, the differences in the pattern of polypeptide expression may be as a result of the polypeptides being of high abundance and also the high background values on the autoradiographs. The GAPDH polypeptide spots are also highly diffuse and therefore in common with most of the polypeptide spots discussed in this chapter, resulted in unreliable spot volumes being obtained.

5.3.5.15 PPIase A

Peptidyl-prolyl *cis-trans* isomerase A (PPIase A) (Figure 5.12, number 17) is an important cellular folding catalyst (Schiene-Fischer and Yu, 2001). The expression of PPIase A was expressed at high levels at the start of the culture and decreased to below detectable levels throughout the rest of the culture. This occurred in contrast with the expression of PPIase A on the protein gels, which appeared to be expressed at similar levels throughout the culture (chapter 4, section 4.3.4.15). However, once again the visual pattern of PPIase A matched the observations on the protein gels more closely. The expression of PPIase A throughout the culture confirms that it must be involved in key cellular processes. As PPIase A was expressed at high levels at the end of the culture, it may be involved with modulating apoptotic pathways in common with the Hsp90 proteins, which are known to interact with PPIase A, although the functional consequence of this interaction is not known (Jacob and Buchner, 1994).

The results reported in both this and the previous chapter (chapter 4) have revealed that many alterations in protein and polypeptide expression occurred throughout the batch

culture of NS0 cells. The polypeptide and protein data follow the same general trend although it is apparent that there is a delay between observing an increase in nascent polypeptide synthesis and the concomitant increase in protein abundance. However, it is also apparent that the pattern of protein and polypeptide profiles was difficult to compare (Figure 5.7). Approximately half the number of polypeptide spots was observed on autoradiographs compared to the number observed on protein gels, and of these less than half of the polypeptide spots could be matched to the corresponding protein gel. The differences observed in the expression patterns can be explained by the different principles used to visualise the proteins and polypeptides, which detect constitutively and metabolically expressed proteins respectively. As a result dissimilar spot profiles have been reported to occur even without the influence of run-to-run variations (Westbrook et al., 2001), and the expression and relative abundance of polypeptides did not correlate with the visual level of expression in many cases. This shows the limitations of the technology currently available for this type of analysis, particularly the bioinformatic software capabilities. Ideally more than one autoradiograph should also have been prepared for each sample point so that statistical analysis may have been carried out. However due to sample availability and equipment requirements this was not possible.

Therefore, the technology utilised for generating the autoradiograph images results in very diffused spot patterns, which in turn proves difficult for the software programme to identify where the spot boundaries were positioned. This problem could be overcome by drawing the boundaries in manually. However, this increases the errors further and is not ideal. The autoradiograph images also suffered from very high background values, and as a result, when the background was subtracted from the autoradiograph images, the polypeptide spot volumes were very low. In some cases where the protein spots were already of high abundance the programme underestimated the values because the protein spots were saturated. As many of the protein spots were already of high abundance the software was also incapable of accurately determining small changes in protein expression and therefore although the expression levels could be seen to change visually, the software was not always sensitive enough to detect the changes.

Although many problems were encountered with the comparison of the autoradiograph and protein gel images, it was clearly shown that most of the changes in expression of the 17 proteins identified in the previous chapter were induced or up-regulated during exponential growth phase in agreement with the protein gels. At this point in the growth curve the cells had reached maximum cell density and IgG was being

produced at high levels. The increased cell numbers and productivity of the cell line also coincided with maximum glucose consumption. Although there were differences in the quantification of changes in polypeptide expression throughout the batch culture it was still apparent, when comparing the visual changes in nascent polypeptide synthesis to the protein gels, that most of the global changes in the proteome occurred during late exponential growth. Many of the proteins that were investigated here have been reported to be involved with general 'housekeeping' functions in the cell and are regulated throughout the growth curve as well as being induced as a result of the stress response, and therefore it is difficult to pinpoint **exactly** when cells in culture perceive stress. However, the relative expression levels as determined by the image analysis software clearly show that NS0 cells in culture appear to perceive stress earlier than predicted by protein analysis alone, which suggests late exponential phase (day 5). The autoradiograph polypeptide profiles suggest the cells begin to perceive stress much earlier (day 3) by initiating nascent polypeptide synthesis, but this is only detected at the protein level at day 5 of culture. We therefore suggest that cells begin to perceive 'stress' even at early to mid-exponential growth phase.

5.3.6 Implications for rIgG Production

The data resulting from the previous two chapters imply it is likely that NS0 cells in culture perceive stress at an earlier stage in culture than initially expected; as early as the start of exponential growth phase (day 3). The results also indicate that NS0 cells modulate their cellular machinery throughout batch culture to respond to their particular requirements at any given time point. This has been shown to involve in particular the modulation of 3 particular protein groups; chaperones, glycolytic proteins and structural proteins.

The data presented here shows that NS0 cells up-regulate proteins involved in energy transduction (i.e. glycolytic proteins) from early exponential growth phase and throughout exponential growth in order to provide the energy required for growth and proliferation. However, as the cells grow and divide, environmental 'pressures' (such as nutrient depletion, shear stresses and reduced culture space) result in the perception of stress (from approximately day 3 of culture), which the cells respond to by up-regulating chaperones and stress proteins. At the same time the relative expression levels of structural proteins is also modulated.

The effect of these observations on rIgG production mean that it is difficult to determine the differences between cellular responses to general growth stresses and any changes which may be as a direct result rIgG production. However, regardless, the changes observed in the previous two chapters correlate with rIgG production, all of which most likely facilitate rIgG production. The changes observed in NS0 cells during batch culture also correlate with a previous report by van Anken *et al.* who investigated the proteins that are expressed when B cells prepare for antibody production (van Anken *et al.*, 2003). Throughout B cell culture cytoskeletal proteins, chaperones and metabolic proteins were investigated. The cytoskeletal proteins investigated included β -actin and α -tubulin, and were shown to follow the same general trend in expression as NS0 cells, decreasing towards the end of culture. ER resident chaperones studied in the investigation included calreticulin, and in agreement with the results highlighted in these two chapters, calreticulin was observed to increase in expression throughout culture. Furthermore, glycolytic proteins including GAPDH and α -enolase were also investigated and once again, correlated with the observations reported here. However, it appears from our data that the majority of changes in expression levels are 'normal' responses (i.e. they would occur whether a cell is expressing recombinant protein or not) and are a consequence of environmental changes, including nutrient depletion and shear stresses and therefore only a minor component of the changes in protein expression levels can be attributed to rIgG production specifically. Regardless, the changes in protein expression that occur as a result of stress perception (e.g. molecular chaperones) and increased growth and proliferation (e.g. increased metabolic capability, by inducing expression of glycolytic proteins) appear to have a functional role in facilitating rIgG production and secretion as culture progresses.

5.3.7 General Discussion

The results highlighted in this chapter and chapter 4 have shown that the NS0 cell proteome is a dynamic system, in which protein expression levels fluctuate throughout batch culture in order to respond to the ever-changing demands and pressures the cells find themselves under. Many changes in the expression profiles occurred throughout the culture with proteins becoming up- and down-regulated as the culture progressed. The assessment of the 2-D autoradiographs generated from the batch culture experiment visualised less protein spots as expected. However, as the two methodologies are different

but complementary, it was difficult to match the autoradiograph images to the corresponding protein gel. The spot patterns also differed substantially from each other as a result of the two methodologies (which visualise metabolically or constitutively expressed proteins). Many of the 17 protein spots that were identified and located on both the protein and polypeptide gels exhibited different patterns of expression throughout the batch culture. It was expected that the nascent polypeptides would follow the same general trend in relative expression as the protein gels. This was apparent for a few of the polypeptide spots, even though the visual pattern of polypeptide expression in many cases did follow the same general expression profile observed on the protein gels. However, it may be that a change in protein spot abundance does not always necessary confer activity of the protein. Furthermore, an observed delay was clearly seen as described in this chapter.

It has clearly been shown in this and the previous chapter that there are many changes which occur in both protein expression and nascent polypeptide synthesis throughout the batch culture of NS0 cells. Many of the changes observed occurred mainly in correlation with the maximum viable cell density, IgG titre or glucose concentration. However, ideally more than one 2-D autoradiograph should have been prepared for each time point during the batch culture experiment to enable the statistical assessment of the changes observed in the NS0 cell proteome during batch culture. This data could then have been used to more accurately pinpoint when NS0 cells under culture conditions perceive stress.

In order to assess the NS0 cell proteome further, a series of transfectants differing in specific productivities derived from the same parental NS0 cell line were kindly donated by LONZA Biologics (Slough, U.K.) and investigated. As most of the changes in the global NS0 cell proteome were observed during exponential growth phase, the transfectants including the parental (and a blank transfectant, which was transfected with the GS vector but lacked the heavy and light chain genes for the antibody) were cultured under controlled conditions. The cells were extracted during exponential phase of growth and subjected to 2-D PAGE to identify the cellular processes, in order to try and determine the cellular make-up, which governs whether a given cell line will be 'productive'. The results are discussed in the next chapter.

Chapter 6 A Comparative Proteome Based Analysis of GS-NS0 Cell Lines Differing in Specific Productivities

6.1 Introduction

As previously discussed, mammalian cell lines are utilised routinely for the production of recombinant proteins and antibodies in industry (Jung et al., 2002; Meents et al., 2002). However, currently the cellular processes, which differentiate between a productive and non-productive cell line, are not well understood. Many different strategies have been implemented with a view to increasing the productive capacity of mammalian cell lines, including the delaying of apoptosis through the incorporation of anti-apoptotic genes including *bcl-2* (Bailey et al., 1996; Laken and Leonard, 2001; Tey et al., 2000) and *bcl-x_L* (Jung et al., 2002; Meents et al., 2002); however, these strategies have to date yielded mixed and disappointing results. p21 (a cyclin dependent kinase inhibitor, induced to cause G1-phase growth arrest) (Watanabe et al., 2002) was also engineered into NS0 cell lines and was reported to result in an increase in the productivity of a chimeric antibody by 4-fold. However, conventional one-gene over-expression of p21 has not been able to result in cell-cycle arrest at G1 phase in CHO cells (Fussenegger et al., 1998a).

With the inception of inducible expression systems involving cytostatic genes to arrest cell proliferation once a crucial cell density has been attained, it was believed by many that it should be possible for cell specific productivity to be optimised to avoid the problems associated with high cell densities such as oxygen and nutrient depletion and accumulation of toxic metabolites (Watanabe et al., 2002). Although incorporating anti-apoptotic genes (e.g. *bcl-2*) into mammalian cells has been shown to extend cell lifetime, delaying apoptosis and resulting in higher cell densities, this did not significantly increase productivity (Laken and Leonard, 2001; Tey et al., 2000) and in fact had detrimental effects on genomic stability, preventing cell death of mutated cells by p53 (Jung et al., 2002). In turn, this could result in the accumulation of variant hybridomas, leading to adverse effects on monoclonal antibody product (Jung et al., 2002). It is therefore unlikely that strategies involving the engineering of one or two proteins alone into mammalian cell lines will significantly improve a cells 'productive' lifetime or the 'amount' of protein a cell can produce at any one time.

In order to investigate the similarities and differences in the proteome of NS0 cell lines with a range of specific productivities, a series of GS-NS0 cell transfectants

6 A Comparative Proteome Based Analysis of GS-NS0 Cell Lines Differing in Specific Productivities

(engineered to produce a chimeric antibody IgG₄ (B72.3)) were derived from the same parental NS0 cell host. Each of the transfectants was weaned off serum-containing medium and cultured under controlled conditions in 4 L bioreactors. The transfectants under investigation included the parental NS0 host cell line, a blank transfectant (which was transfected with the GS vector, but without the heavy and light chain genes for the antibody), together with a series of transfectants with a range of productivities. Cells were extracted at mid-exponential growth phase for comparative global proteome analysis.

6.2 Results

6.2.1 Cell Growth

NS0 cell transfectants derived from the same NS0 parental host cell line were engineered to produce an IgG₄ raised against B72.3 (chapter 2, section 2.2.2.2 and 2.2.3) and were cultured and maintained in DMEM-F12 medium supplemented with 10% dFCS for initial growth and productivity studies. Seeding stocks and inocula were prepared in shaker flasks up to 100 mL volume, agitated at 100 rpm on a shaker platform, maintained at 37°C. Typically, cultures were inoculated at 2.5×10^5 cells mL⁻¹ into fresh medium, followed by sparging with 5% CO₂ for approximately 30 seconds. Cells were then left to grow until they reached mid-exponential growth phase (approximately 1×10^6 cells mL⁻¹) prior to passage.

The growth characteristics and productivity of 12 transfectants were assessed, although for clarity only the 6 transfectants carried onto fermentation culture are shown (Figure 6.1). The 12 transfectants were then sequentially weaned off serum-containing medium onto protein-free medium supplemented with 1% dFCS (chapter 2, section 2.2.7 for weaning procedure). After sequential weaning the growth characteristics were determined again in the new medium, together with the productivities to assess the effect of the weaning process (Figure 6.1, batch culture 2). Due to the time frame involved it was decided to only wean the transfectants to 1% dFCS and not to reduce the serum content further. Attempts to 'quickly' wean the transfectants onto serum-free medium were not successful and the cells died. Previously it has been reported that in order to wean cells off low serum concentrations involves a time consuming weaning process (Keen and Hale, 1996).

Figure 6.1 below shows the growth curves and changes in metabolite concentration throughout culture, together with the rIgG titre of the transfectants cultured in DMEM-F12 supplemented with 10% dFCS (Figure 6.1, batch culture 1) and in protein-free medium supplemented with 1% dFCS (Figure 6.1, batch culture 2). When the cells were weaned off serum onto protein-free medium supplemented with 1% dFCS, the viable cell density increased relative to 10% DMEM-F12 medium and rIgG titre were observed to reduce dramatically (Figure 6.1A and B), probably as a result of the increase in viable cell density.

6 A Comparative Proteome Based Analysis of GS-NS0 Cell Lines Differing in Specific Productivities

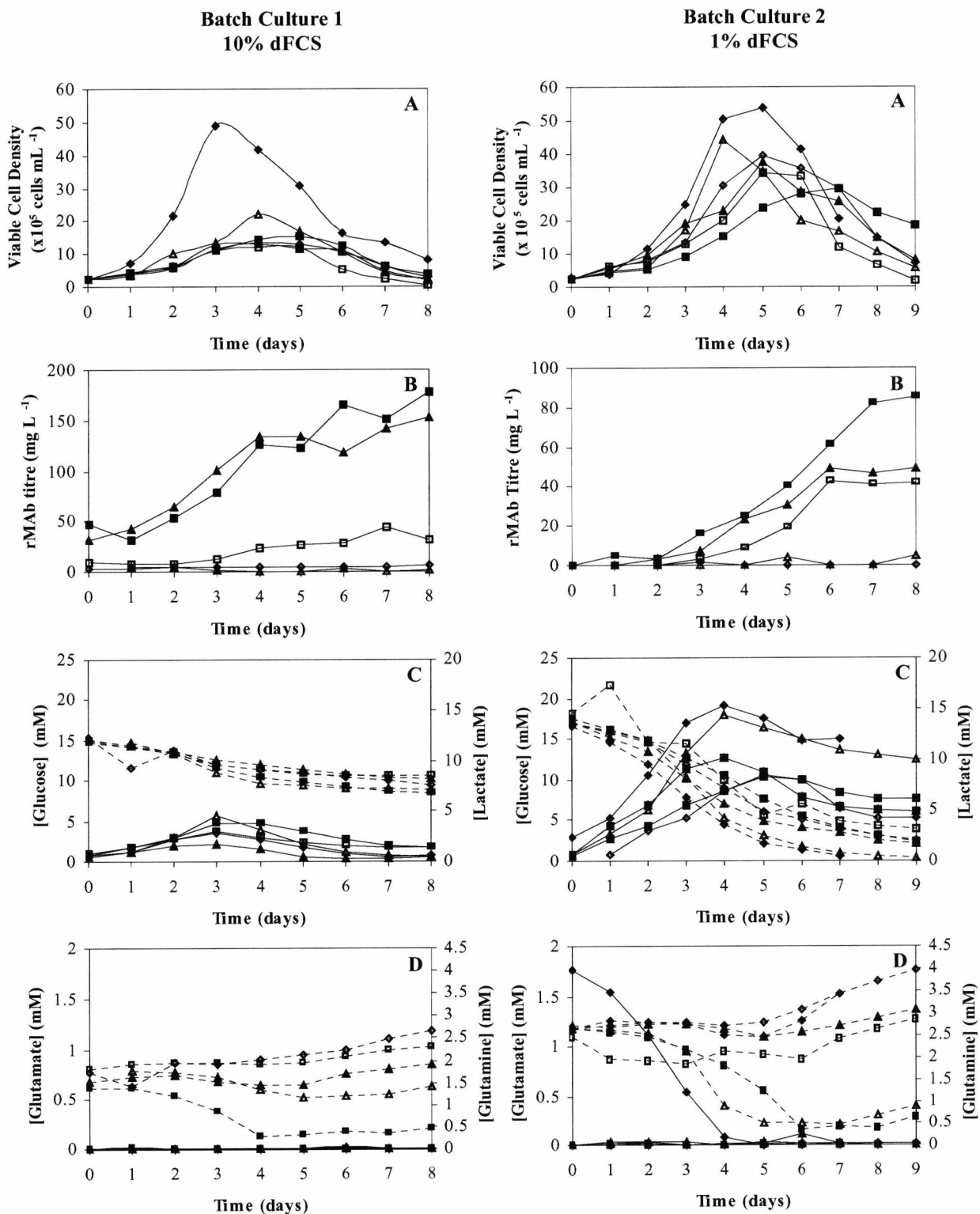


Figure 6.1 Batch culture growth of NS0 cell transfectants expressing rIgG₄ in DMEM-F12 supplemented with 10% dFCS (Batch culture 1), and protein-free media supplemented with 1% dFCS (Batch culture 2) in 100 mL shaker flasks. Typical NS0 cell growth of the transfectants was observed in both media types. Figure A, Viable Cell Density, Figure B, rMAb titre, Figure C, (----) Glucose and (—) Lactate, and Figure D, (----) Glutamate and (—) Glutamine concentration throughout batch culture. (◆) parental; (△) blank transfectant; high producers (■) 2X and (▲) 2P; mid producer, (□) 4R; and low producer (◇) 4O.

6.2.1.1 Cell Growth in DMEM-F12 Medium Supplemented with 10% dFCS

Figure 6.1A shows a typical growth curve for the NS0 cell transfectants cultured in 10% dFCS. The parental cell line, which was not glutamine limited grew much faster and reached much higher cell densities than any of the transfected cell lines. GS-NS0 cells had a maximum specific growth rate during exponential growth phase and the highest producer (2X) had a maximum specific growth rate (μ) of 0.017 h^{-1} between 24 and 96 h of culture. The doubling time for 2X was calculated as 39.1 h, which is similar to the values obtained for the NS0 cells cultured in serum-free medium in the previous chapter (chapter 4, Figure 4.1, Table 4.1). As previously reported in chapter 4 for the culture of NS0 cells in serum-free medium, the cell viability and viable cell density declined rapidly after 120 hrs, although the rIgG titre increased further after this time in all producing transfectants, reaching the maximum concentration towards the end of culture. The cell specific productivity (qMAb) was calculated as $1.41 \text{ pg cell}^{-1} \text{ h}^{-1}$ (during exponential growth) for the highest producing cell line (2X), which reached a maximum rIgG titre of 177.4 mg L^{-1} (Table 6.1).

Table 6.1 Maximum viable cell density, growth rate (μ), doubling time (Td), and maximum rIgG concentration (qMAb) in 100 mL shaker flasks in DMEM supplemented with 10% dFCS during period of maximum growth

Cell Line	$\mu \text{ (h}^{-1}\text{)}$	Td (h)	Generation Number	Max V.C.D. ($\times 10^5 \text{ Cells mL}^{-1}$)	Max rIgG Titre (mg L^{-1})	qMAb ($\text{pg Cell}^{-1} \text{ h}^{-1}$)
2X	0.017	39.10	1.84	15.30	177.40	1.41
2P	0.011	27.30	2.64	12.90	152.00	1.09
4R	0.010	34.20	2.11	12.20	43.80	0.31
4O	0.017	40.67	1.77	13.30	6.20	0.03
Blank	0.011	26.50	2.71	22.30	-	-
Parental	0.018	16.80	2.86	48.80	-	-

Glucose levels decreased rapidly throughout the batch culture of all cell lines (see chapter 2, section 2.2.9.2 for glucose and lactate determination). Maximum glucose utilisation occurred during exponential growth phase (Figure 6.1C, batch culture 1). However, as with the NS0 cells cultured in serum-free medium (chapter 4, Figure 4.1B), glucose was not completely exhausted by any of the cell lines during culture (Figure 6.1C). The lactate levels increased as the culture progressed in all transfectants, although lactate was consumed (or at least degraded) after the cells had reached exponential growth phase for most of the transfectants. As discussed in previous chapters it has been reported that lactate may be converted to pyruvate, which can enter the TCA cycle and/or be partially

converted to alanine via the transamination pathway (Zhou et al., 1997). It has also been reported that once lactate consumption occurs cells begin to die rapidly (deZengotita et al., 2000; Zhou et al., 1996). This was observed with many of the transfectants after day 4/5 of the batch cultures (Figure 6.1A and C).

The levels of glutamate utilisation and glutamine accumulation were also monitored throughout culture (see chapter 2, section 2.2.9.2 for glutamate and glutamine determination) (Figure 6.1D). Glutamate depletion, as with glucose levels, was not complete, and in many cases the level of glutamate increased towards the end of the culture, which has previously been reported in NS0 cells (Zhou et al., 1997) (Figure 6.1D). Glutamine levels, as expected for GS transfected cell lines remained below detectable levels (Figure 6.1D). Levels of ammonia were not assessed or measured throughout the batch culture of the transfectants as GS cell lines transfected with the GS system utilise ammonia and glutamate for the synthesis of glutamine (Zhou et al., 1997).

6.2.1.2 Growth Characteristics in Protein-Free Medium Supplemented with 1% dFCS

After the growth characteristics of the transfectants were investigated in DMEM-F12 medium supplemented with 10% dFCS, the transfectants were weaned off serum and DMEM medium into GSK protein-free medium supplemented with 1% dFCS (chapter 2, section 2.2.7 for weaning procedure). After the transfectants were successfully weaned to 1% dFCS, the serum content was not reduced further as the cells did not respond well to further decreases and complete weaning would have prolonged this study. Figure 6.1A, C and D (batch culture 2), show the resultant growth curves and changes in metabolite concentration throughout culture of cells grown in protein-free, 1% dFCS medium and Table 6.2 summarises the resulting growth characteristics.

Table 6.2 Maximum viable cell density, growth rate (μ), doubling time (Td), and maximum rIgG concentration (qMAb) in 100 mL shaker flasks of various NS0 cell lines in protein-free medium supplemented with 1% dFCS

Cell Line	μ (h^{-1})	Td (h)	Generation Number	Max V.C.D. ($\times 10^5$ Cells mL^{-1})	Max rIgG Titre (mg L^{-1})	qMAb ($\text{pg Cell}^{-1} \text{h}^{-1}$)
2X	0.018	38.40	2.50	29.60	85.50	0.36
2P	0.020	34.50	2.78	37.76	49.35	0.25
4R	0.018	38.90	2.47	34.16	42.70	0.24
4O	0.020	33.80	2.83	39.54	0.00	0.00
Blank	0.031	22.30	3.22	44.26	-	-
Parental	0.036	19.40	3.70	53.76	-	-

Throughout culture the viable cell densities obtained by each cell line were roughly twice that observed in the DMEM medium, and the rIgG titres were dramatically reduced (Figure 6.1B). Figure 6.1A (batch culture 2) above shows the growth characteristics of each of the 6 transfectants after the weaning process. The main difference observed between the transfectants cultured in protein-free medium supplemented with 1% dFCS and in DMEM with 10% dFCS was that the cells reached much higher viable cell densities which were similar to those that the parental cell line attained in both mediums (Figure 6.1A). This was not observed when the cells were cultured in 10% DMEM-F12 medium. In contrast with the transfectants cultured in DMEM supplemented with 10% dFCS, the maximum specific growth rates and generation numbers increased and doubling times reduced in the producing cell lines cultured in protein-free medium, coinciding with a reduction in rIgG titre (Figure 6.1B, batch culture 2 and Table 6.2).

The doubling time for the highest producing transfectant (2X) was calculated as 38.4 h, which is similar to this cell line cultured in serum-containing medium (Table 6.1 and 6.2), and during this time the generation number was 2.5 (Table 6.2). The cell viability reduced after exponential phase (day 4), although in agreement with others, the rIgG titre increased further in all producing transfectants to the end of culture. The highest producer yielded 85.5 mg L⁻¹ at the end of culture. The highest cell specific productivity (qMAb) was calculated as 0.36 pg cell⁻¹ h⁻¹ (between 48 and 120 h of culture), which was approximately half the titre observed for the transfectants cultured in DMEM (10% dFCS) shaker flask cultures (Table 6.1 and 6.2).

Glucose levels were monitored throughout batch culture for each of the transfectants, and as expected decreased with the maximum depletion in glucose concentration occurring during mid-exponential growth phase (Figure 6.1C, batch culture 2). In contrast with the transfectants cultured in DMEM-F12, 10% dFCS, the glucose consumption for each of the transfectants appeared to be almost complete. The level of lactate accumulation increased greatly as the batch cultures progressed, and reached maximum levels at mid-exponential growth phase, except for the parental cell line, in which the lactate concentration continued to increase (Figure 6.1C, batch culture 2). As observed with the transfectants in 10% serum, the consumption of lactate occurred concurrently with a reduction in viable cell density (Figure 6.1A and C). Glutamate and glutamine levels, in most cases, correlated with the observations of the transfectants in DMEM-F12 supplemented with 10% dFCS (Figure 6.1D).

6.2.2 Bioreactor Culture

In order to accurately assess the cellular proteome of all NS0 cell transfectants under the same conditions, each transfectant was cultured in a controlled environment in identically configured 4 L bioreactor vessels. In this culture environment, on-line controls for pH and D.O were monitored and adjusted throughout culture to maintain the cells in similar environments. Each of the 6 transfectants was cultured in duplicate in 4 L bioreactor vessels (chapter 2 section 2.2.2.2, 2.2.8.3 and 2.2.8.4 for maintenance and culture of NS0 cell lines). The cell growth characteristics were monitored from daily samples (Figure 6.2A) and the fluxes of glucose, lactate, glutamate and glutamine metabolite concentrations were monitored in cell-free supernatant samples as described in chapter 2, section 2.2.9.2 (Figure 6.2C and D).

6.2.2.1 Assessment of GS-NS0 Cell Transfectant Growth during Bioreactor Culture

Throughout the bioreactor cultures daily samples were taken to assess changes in metabolite concentrations of glucose, lactate, glutamate and glutamine (chapter 2, section 2.2.9.2). Samples of cell-free supernatant were also stored for the determination of rIgG product titre at the end of the experiment. The GS-NS0 cell transfectants had similar maximum specific growth rates during exponential growth, and also had similar doubling times and generation numbers for each of the duplicate runs (Table 6.3 and 6.4). The growth kinetics were also similar to the values obtained in 100 mL shaker flask cultures (Figure 6.1, batch culture 2).

The specific productivities and maximum rIgG titre observed for the transfectants cultured in bioreactor vessels was dramatically reduced between that observed in the 100 mL shaker flask experiments (Tables 6.1, 6.2, 6.3 and 6.4). The highest producing transfectant (2X) obtained an average maximum rIgG titre at the end of the culture of 27.23 mg L⁻¹ (compared to 85.5 mg L⁻¹ in 100 mL shake flasks), and had an average qMAB of 0.15 pg cell⁻¹ h⁻¹ which is less than half the value observed in the shaker flasks and is less than a quarter of the original rIgG titre observed in DMEM medium supplemented with 10% dFCS (Table 6.1).

As observed in the 100 mL shaker flask batch cultures, the cell lines all reached maximum viable cell densities between days 4 and 5 of culture (Figure 6.2A). After this time the cell viability and viable cell density rapidly reduced, although the level of rIgG titre did increase after this time (Figure 6.2B). The rate of glucose utilisation and lactate accumulation was similar to that observed in the shaker flask cultures. However, unlike

6 *A Comparative Proteome Based Analysis of GS-NS0 Cell Lines Differing in Specific Productivities*

the pattern in DMEM (10% dFCS) medium, glucose was completely exhausted when the transfectants were cultured in protein-free medium supplemented with 1% dFCS. Lactate initially accumulated in the culture medium and as observed in the shaker flasks, was consumed again after exponential growth phase coinciding with the rapid decline in cell viability (Figure 6.1C and 6.2C).

As in other experiments, the levels of glutamate and glutamine were monitored throughout batch culture. As observed in the 100 mL shaker flasks, glutamate was not totally consumed by all of the cell lines (4O, 2P and the parental NS0 cell line did not utilise glutamate present in the growth medium, and levels increased after mid-exponential growth phase) (Figure 6.2D). However, 2X, 4R and the blank 'mock transfected' cell line did fully utilise the glutamate present in the medium, which was exhausted by the end of exponential growth. Unexpectedly, transfectant 4R accumulated a small amount of glutamine over the period of the batch culture (Figure 6.2D).

Table 6.3 Growth kinetics for the 4 L fermentation of GS-NS0 cell transfectants in protein-free medium supplemented with 1% dFCS

Cell Line	μ (h ⁻¹)	Td (h)	Generation Number	Max V.C.D. (x 10 ⁵ Cells mL ⁻¹)	Max rIgG Titre (mg L ⁻¹)	qMAb (pg Cell ⁻¹ h ⁻¹)
2X	0.024	29.50	1.63	30.56	31.74	0.21
2P	0.023	30.80	1.56	31.54	22.12	0.17
4R	0.024	28.97	2.49	48.28	-	-
4O	0.024	28.80	2.50	36.98	-	-
Blank	0.034	20.20	2.38	39.76	-	-
Parental	0.039	17.70	4.06	56.34	-	-

Table 6.4 Growth kinetics for the duplicate 4 L fermentation culture of GS-NS0 cell transfectants in protein-free medium supplemented with 1% dFCS

Cell Line	μ (h ⁻¹)	Td (h)	Generation Number	Max V.C.D. (x 10 ⁵ Cells mL ⁻¹)	Max rIgG Titre (mg L ⁻¹)	qMAb (pg Cell ⁻¹ h ⁻¹)
2X	0.026	26.75	2.69	29.34	22.72	0.09
2P	0.022	32.20	1.49	34.96	17.28	0.08
4R	0.024	29.40	2.45	46.04	-	-
4O	0.024	28.67	2.51	42.66	-	-
Blank	0.032	21.90	2.19	38.80	-	-
Parental	0.039	17.80	4.05	52.34	-	-

6 A Comparative Proteome Based Analysis of GS-NS0 Cell Lines Differing in Specific Productivities

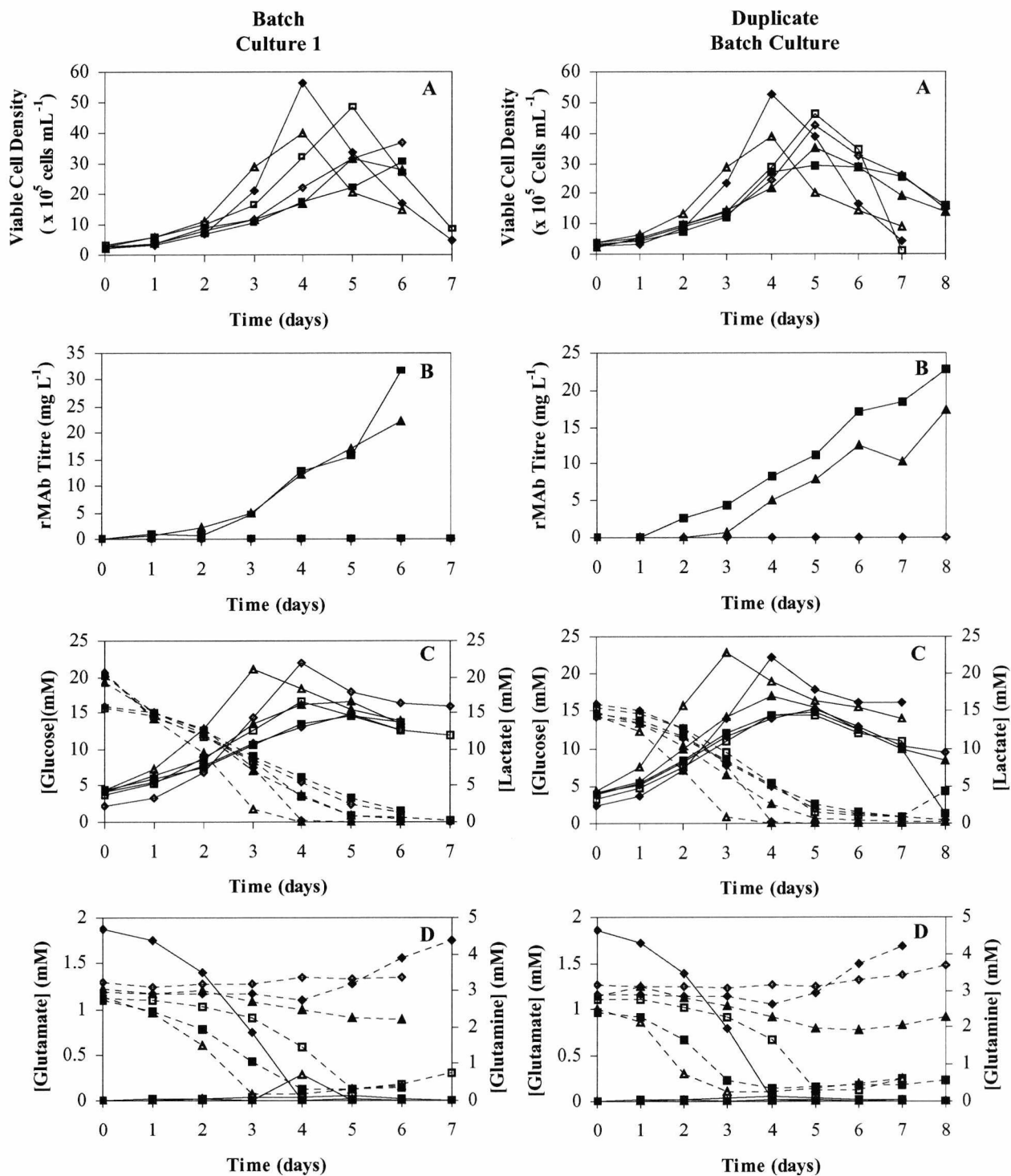


Figure 6.2 Batch culture growth of NS0 cell transfectants expressing rIgG₄ in protein-free medium supplemented with 1% dFCS in 4 L working volume fermenters. Each fermenter batch culture was carried out in duplicate. For clarity all of the cell lines have been grouped into duplicate runs. Figure A, Viable Cell Density, Figure B, rMAB titre, Figure C, (---) Glucose and (—) Lactate, and Figure D, (---) Glutamate and (—) Glutamine concentration throughout batch culture. (♦) parental NS0 host cell line; (Δ) blank transfectant; high producers (■) 2X and (▲) 2P; mid producer, (□) 4R; and low producer (◇) 4O.

Table 6.3 and 6.4 above show the growth kinetics of each of the duplicate fermentation runs. The Tables clearly show that the NS0 cell transfectants reached much higher densities during fermentation culture than in the shaker flask cultures in DMEM-F12 medium supplemented with 10% dFCS (Table 6.1, 6.3 and 6.4). Although the final cell densities increased during fermenter culture, we did not expect this to dramatically reduce the final antibody titre. However, this was not the case and at the completion of the fermentations it was apparent that the rIgG titre was reduced to less than a quarter of the original rIgG titre observed when the transfectants were cultured in the DMEM-serum-containing medium.

The relative levels of rIgG titre (comparison of one cell line versus another) are the same as those observed in the DMEM-serum supplemented medium, with the transfectant 2X remaining the highest producer followed by 2P and 4R. As a result of the loss of productivity and cell line instability the transfectants could no longer be utilised to accurately investigate the NS0 cell proteome of transfectants differing in the level of cell specific productivity. An alternative experimental strategy was therefore implemented, whereby the transfectants (all exhibiting no or very low productivity) were assessed to investigate cell line variation and genetic stability. A proteomic strategy was utilised to assess how quantitatively similar or different the protein profiles of each NS0 cell transfectant were at mid-exponential phase.

6.2.3 Proteome Analysis of NS0 Cell Transfectants at Mid-exponential Growth Phase

To assess the differences in clonal variation in the transfectants previously described and derived from the same parental NS0 host cell line, the cells extracted from the 4 L fermentations were analysed by 2-D PAGE. Once the cells had reached mid-exponential growth phase, 10 extracts of 1×10^7 cells were prepared from each of the transfectants as outlined in chapter 3, scheme 3.1. The same volume of cells was removed from each of the fermenters so that the environmental conditions for each of the transfectants remained comparable. Duplicate large format 2-D PAGE of whole NS0 cell proteins was carried out on one of the extracts chosen at random using the optimised protocol detailed in chapter 3, scheme 3.2. All 2-D gels were visualised using silver staining methodology (chapter 2, Table 2.11) and the resultant digital images captured using an ImageScanner (chapter 2, section 2.7.4) and were analysed in the same way as detailed in previous chapters (see

6 A Comparative Proteome Based Analysis of GS-NS0 Cell Lines Differing in Specific Productivities

chapter 2, section 2.7.4 and 2.7.4.2 for details). Figure 6.3 below shows an example of the 2-D gels resulting from the fermentation experiment.

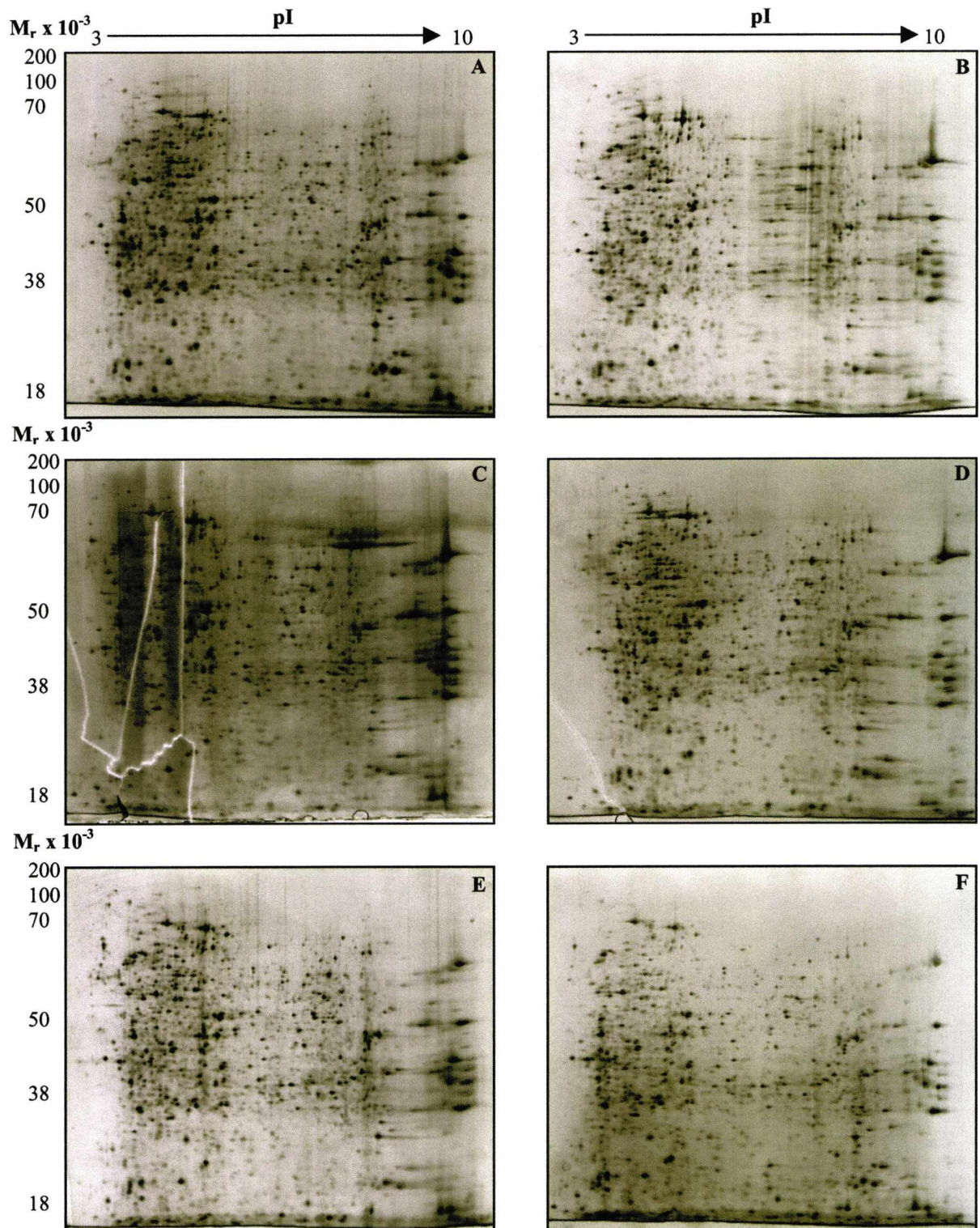


Figure 6.3 Large format 2-D PAGE (24 cm, pI 3-10 non-linear resolving range) of whole NS0 cell transfectants extracted at mid-exponential phase (1 gel of each duplicate). Figure A, parental NS0 host cell line; Figure B, blank transfectant; Figure C and D, 2X and 2P respectively; Figure E, 4R; and Figure F, 4O. All extracts were run in duplicate and visualised using silver staining methodology.

6.2.3.1 Analysis of NS0 Transfectants at Mid-exponential Growth Phase

For each of the duplicate 2-D gels run, the total number of protein spots was determined and used to form an average composite image, which was then compared against the reference gel (blank transfectant) to assess clonal variation. The total number of protein spots determined for each of the transfectants at mid-exponential growth phase is shown below in Table 6.5. The transfectants were not compared against the parental host NS0 cell line as these cells had not undergone the transfection process and were also cultured in glutamine-containing medium.

Table 6.5 Total number of protein spots detected on 24 cm 2-D gels of cell lines derived from the same parental NS0 host cell line at mid-exponential growth phase during controlled bioreactor culture

Transfectant	Number of Protein Spots Detected*
Blank	1487
2X	1146
2P	1461
4R	1447
4O	1505

* Note: The number of protein spots detected was derived from composite gel images produced from 2 gels

Table 6.5 above shows that a similar number of protein spots were detected for each of the transfectants apart from 2X, which numbered approximately 300 fewer protein spots. However, low spot numbers were observed for each of the 2D gels run for 2X, and therefore this is probably a true representation of the proteome of the cell line.

6.2.3.2 Assessment of Protein Regulation between Transfectants at Mid-exponential Growth Phase

The average images produced for the duplicate gels run for each of the transfectants at mid-exponential growth phase (Figure 6.3) were analysed using ImageMaster™ 2-D software to examine the differences between NS0 cell transfectants (chapter 2, section 2.7.4). The averaged gel images were compared against the blank transfectant (reference gel), which had undergone the transfection process, but was not transfected with the heavy and light chain genes for the antibody B72.3. The proteome maps showing the proteins, which exhibited at least a 2-fold change in expression between the different transfectants are shown below in Figure 6.4 and clearly shows that the transfectants exhibited differences in the global proteome at mid-exponential growth phase of batch culture. Table 6.6 shows the resulting global statistics for each of the transfectants.

6 A Comparative Proteome Based Analysis of GS-NS0 Cell Lines Differing in Specific Productivities

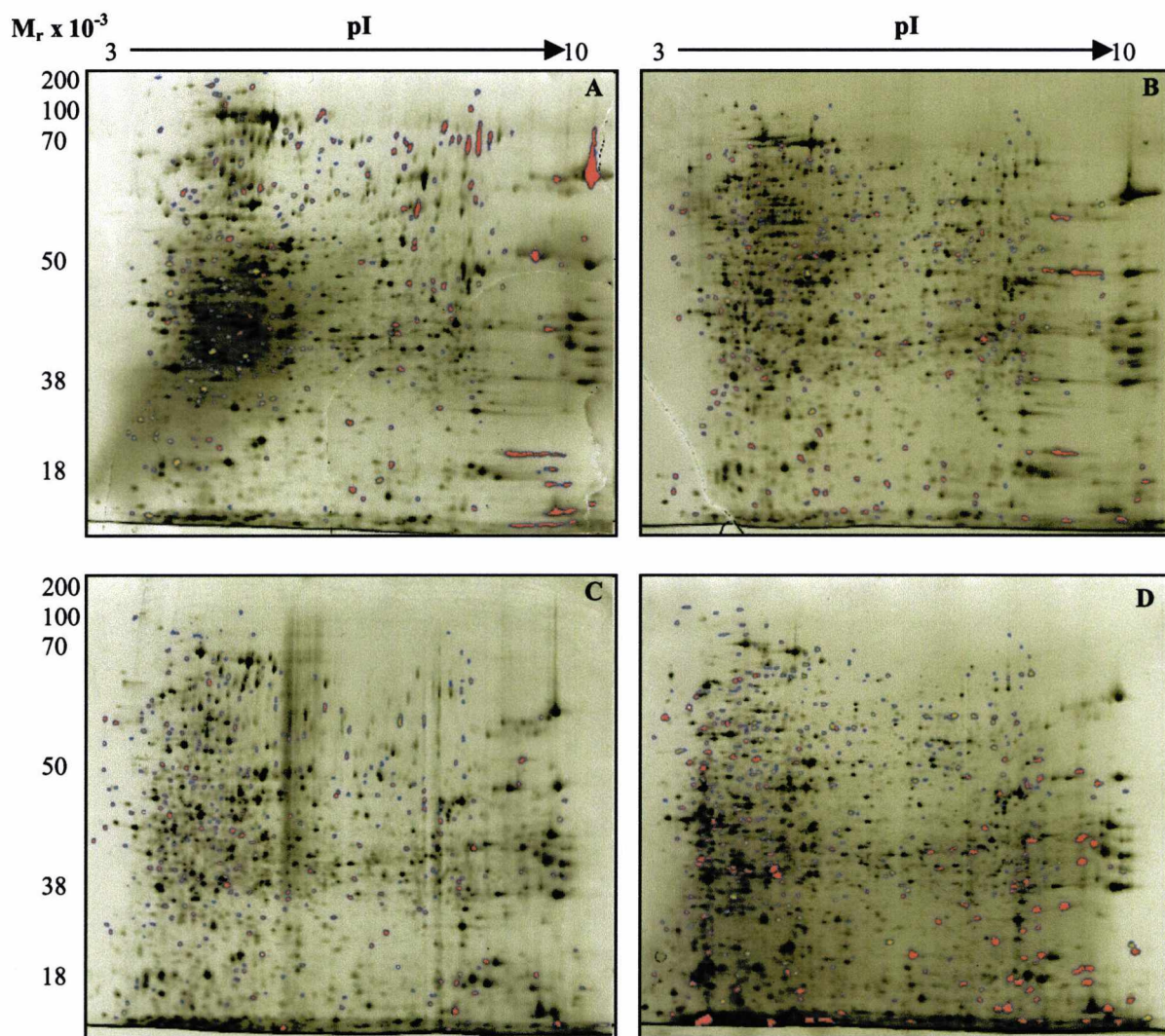


Figure 6.4 Difference maps derived from the analysis of NS0 cell lines at mid-exponential growth phase during bioreactor culture. Proteins exhibiting at least a 2-fold change in the level of expression are shown. Only the proteins matched between samples for each average gel are shown. Figure A, transfectant 2X, Figure B, 2P, Figure C, 4R and Figure D, 4O. All transfectants were compared against the average gel produced for the blank transfectant. (●) Matched proteins exhibiting at least a 2-fold increase in expression and (●) matched protein spots exhibiting at least a 2-fold decrease in expression when compared against the blank transfectant.

6.2.3.3 Changes in the Pattern of Protein Expression between Cell Lines Derived from the Same Parental NS0 Cell Host

Many differences in the proteome of the various GS-NS0 cell transfectants were apparent at mid-exponential growth phase (Table 6.6). In agreement with the data provided in chapter 4 and 5, the sum of all variables except those no longer expressed was equal to the total number of protein spots detected on each of the average gels (Table 6.6). For each of the transfectants, the number of proteins exhibiting no change was investigated. A similar pattern to the number of unchanged proteins was observed throughout batch culture

(chapter 4 and 5, Table 4.3 and 5.2) with approximately half the total number of protein spots remaining unchanged at mid-exponential growth phase when compared against the blank transfectant.

For each of the transfectants the number of proteins no longer expressed or newly expressed relative to the control was also investigated (Table 6.6). Each of the transfectants exhibited a similar pattern of expression when the number of proteins no longer expressed was investigated. Transfectants 2X, 2P and 4R had a greater number of proteins no longer expressed (i.e. a loss of expression) than were newly expressed. The exception to this observation was transfectant 4O, which exhibited slightly different characteristics, with the number of newly expressed proteins outnumbering the number no longer expressed. However, for transfectant 4O the difference between the numbers of proteins newly expressed and no longer expressed only numbered 16; therefore this difference cannot be judged as significant.

Although the number of newly synthesised or no longer expressed proteins provides global statistics, the data does not yield any information as to the extent of the change. Therefore the transfectants were assessed as in previous chapters using the difference map tool to investigate the number of proteins up- and down-regulated when compared against the blank transfectant. Transfectants 2X and 4O displayed similar characteristics, with the number of down-regulated proteins outnumbering the number that were up-regulated when compared against the blank transfectant. Conversely, transfectant 2P and 4R exhibited a greater number of proteins up-regulated than down-regulated. In total 2X exhibited 327 (29%) proteins that were newly expressed or up-regulated. For transfectant 2P 468 (32%) of the proteins detected were newly expressed or up-regulated by at least 2-fold. Transfectant 4R exhibited 560 (39%) proteins up-regulated or newly expressed. Finally, 605 (40%) of proteins detected in transfectant 4O were either up-regulated or newly expressed. The greatest number of up-regulated and newly expressed proteins was observed for what were the lowest producing cell lines (4R and 4O).

The total number of proteins exhibiting at least a 2-fold down-regulation in expression together with those no longer present at detectable levels was also investigated (Table 6.6). Unexpectedly, a large range of between 30-60% of proteins exhibiting a 2-fold or greater decrease in expression or those no longer expressed was observed. This suggests dramatic down-regulation and/or large genetic stability issues within these cell lines in the protein-free medium.

6 A Comparative Proteome Based Analysis of GS-NS0 Cell Lines Differing in Specific Productivities

Table 6.6 Number of proteins observed that were unchanged, newly synthesised and up- or down-regulated by at least 2-fold when compared against the blank transfectant at mid-exponential phase of growth

Transfectant	Total Number of Protein Spots	Unchanged*	Up-Regulated*	Down-Regulated*	Newly Expressed*	No Longer Expressed*
Blank	1487	-	-	-	-	-
2X	1146	664	109	155	218	559
2P	1461	877	138	116	330	356
4R	1447	754	173	131	387	429
4O	1505	696	163	202	442	426

* Indicates the number of proteins exhibiting alterations in the level of protein expression from averaged gel images relative to the level of expression on the blank transfectant gel

6.2.4 The Quantitative Assessment of NS0 Cell Transfectants at Mid-exponential Growth Phase

The image analysis software was utilised to identify those proteins, which exhibited at least a 2-fold change in expression. It is important to investigate the relative changes in expression levels of the 17 proteins previously studied in what are essentially non-producing cell lines. As a result any observed changes between these cell lines in the expression of these proteins are likely to be cell line specific and not productivity related. Figure 6.5 and 6.6 below show the expression profiles of the 17 proteins that were identified and observed to alter in the level of expression in chapter 4 (Table 4.5). The image analysis software normalises the spot volumes. However, for ease of comparison the spot volumes were normalised further as outlined in the methods section (chapter 2, section 2.7.4). Limited statistical analysis was carried out on the duplicate gel images shown by the error bars, which represent the standard deviations (chapter 2, section 2.7.4.2) for the normalised spot volumes for each of the 17 protein spots investigated.

6 A Comparative Proteome Based Analysis of GS-NS0 Cell Lines Differing in Specific Productivities

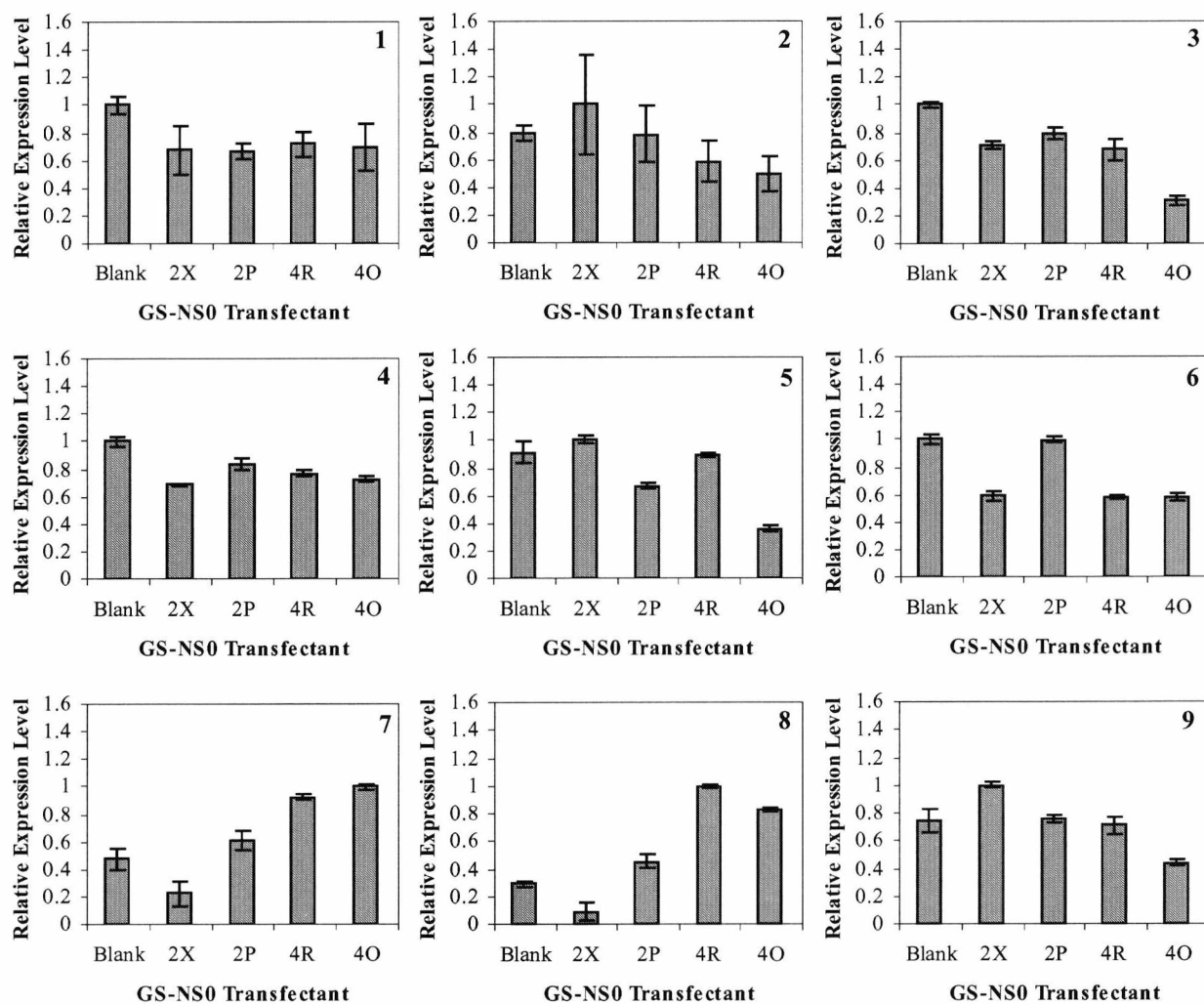


Figure 6.5 The semi-quantitative analysis of proteins 1-9 expression of NS0 cell transfectants identified in chapter 4, Table 4.5 at mid-exponential growth phase in controlled bioreactor culture. The graphs show the semi-quantitative information of proteins identified from NS0 cell sample extracts detailed in chapter 4. The data shown is the average value from two gels run for each of the samples. Error bars represent the standard deviations in relative normalised spot volume for each of the 17 protein spots on duplicate 2-D gel images. Protein 1= BiP; 2= Hsc71; 3= Mitochondrial stress-70 protein (Grp75); 4= Calreticulin precursor; 5= Hsp60; 6= PDI; 7= Endoplasmic (Grp94); 8= α -tubulin; 9= ERp60.

6 A Comparative Proteome Based Analysis of GS-NS0 Cell Lines Differing in Specific Productivities

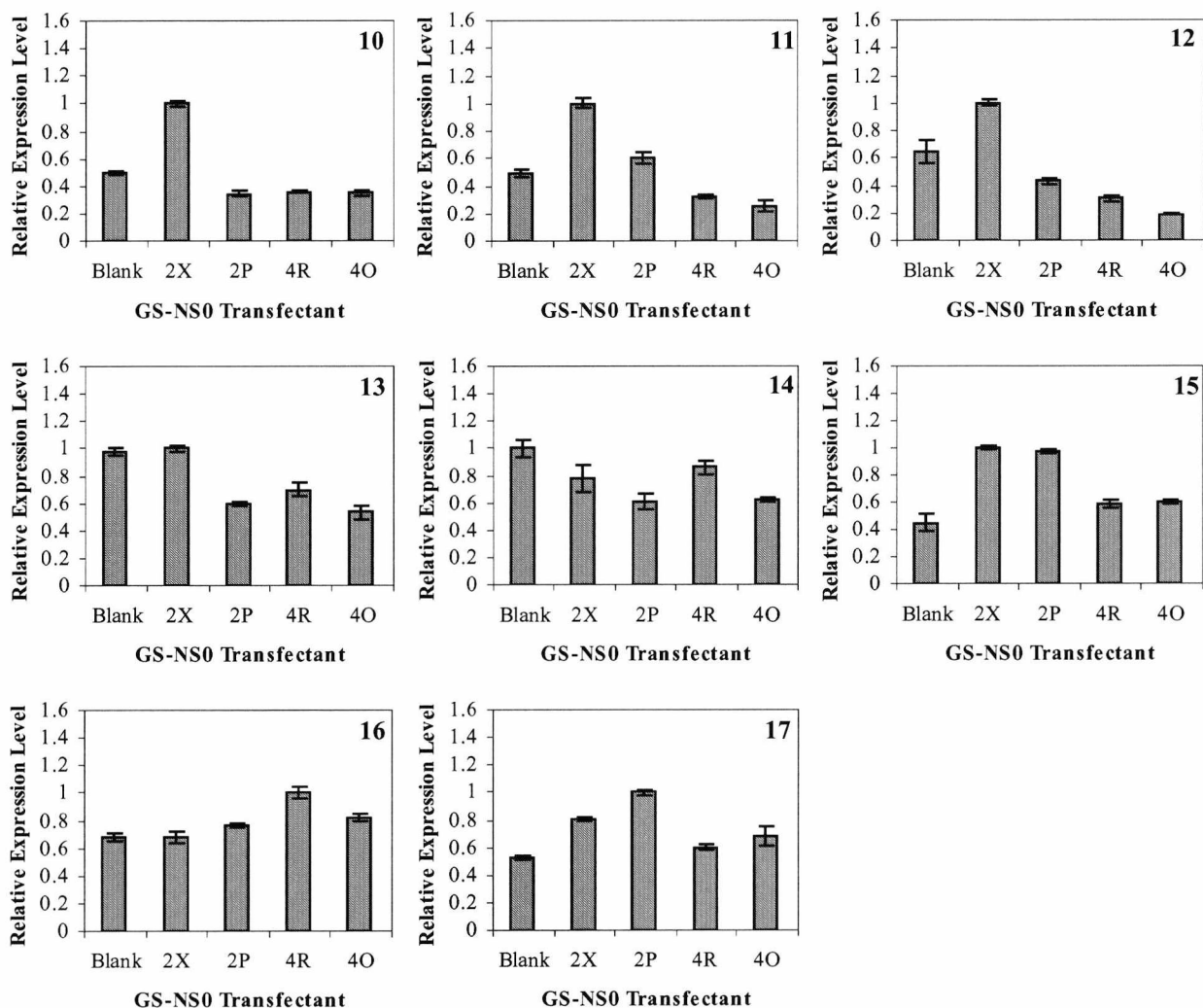


Figure 6.6 The quantitative analysis of proteins 10-17 expression (identified in chapter 4, Figure 4.5, Table 4.5) from NS0 cell transfectants at mid-exponential growth phase. The graphs show the semi-quantitative assessment of proteins identified from NS0 cell sample extracts detailed in chapter 4, Table 4.5. Each value is derived from the average of duplicate gels run for each cell sample. The error bars represent the standard deviations for each of the 17 protein spots represented on two replicate 2-D gel images. Protein 10= Pyruvate kinase; 11= Elongation factor 1-alpha-1 (eEF1A-1); 12= α -enolase; 13= β -actin; 14= β -actin; 15= Glyceraldehyde 3-phosphate dehydrogenase (GAPDH); 16= GAPDH; 17= Peptidyl-prolyl *cis-trans* isomerase A (PPIase A).

6.3 Discussion

6.3.1 Cell Growth

6.3.1.1 GS-NS0 Transfectant Growth in DMEM, 10% dFCS

Batch culture of the 6 NS0 cell transfectants was initially carried out in 100 mL shaker flasks in DMEM-F12 medium supplemented with 10% dFCS. The pattern of glucose utilisation in the cell lines was similar to the observations of the NS0 cell line in chapter 4. Glucose was not exhausted by any of the transfectants and the concentration of glucose in the medium reduced from 2.7 g L⁻¹ to approximately 1.7 g L⁻¹ for all transfectants. The halt in glucose utilisation by the transfectants coincided with a reduction in viable cell density after 5 days of culture (Figure 6.1A and C). After this time the rIgG titre was observed to increase further in each of the producing cell lines to the end of the culture (Figure 6.1B). The highest producing cell line (2X) reached a final rIgG titre of 177.4 mg L⁻¹. The level of lactate accumulation in the growth medium increased minimally as the cultures progressed to a maximum level of 0.4 g L⁻¹ in the blank transfectant. The level of lactate accumulation in each of the cultures was observed to reach maximum levels after the third day of the cultures, and was consumed again after this time in most of the transfectants apart from 2X and 4R, in which the level continued to increase until the end of culture reaching approximately 0.1 g L⁻¹. The consumption of lactate has been reported previously (deZengotita et al., 2000) and is discussed in previous chapters.

The levels of glutamate and glutamine were also assessed throughout the culture for each of the transfectants (Figure 6.1D). Glutamine was not supplemented in the culture medium (except for the parental host cell line) as the cells were transfected with the GS system. The levels of glutamate remained unchanged for most of the culture, increasing slightly towards the end of culture. It is likely that 2X, which showed a different profile, utilised glutamate together with ammonia to form glutamine at exponential phase. It has been previously reported that when NS0 cells utilise glutamate, less glucose is utilised (Zhou et al., 1997), although this was not observed here. It has also been reported that after cells have reached exponential phase the level of glutamate increases (Zhou et al., 1997), as was observed in this study.

6.3.1.2 GS-NS0 Cell Growth in Protein-Free Medium

Following the batch culture of the transfectants in serum-supplemented medium, the cells were weaned off serum and onto protein-free medium supplemented with 1% dFCS as described in the methods section. A direct weaning approach was unsuccessful therefore the cells were sequentially weaned by reducing the serum content after 2 passages at each concentration (cells were first weaned onto protein-free media containing 10% dFCS, then onto 5% dFCS and finally onto 1% dFCS).

Following weaning, the transfectants were subjected to another batch culture experiment in 100 mL shaker flasks to investigate the growth characteristics and rIgG titre under the different growth conditions. In agreement with the transfectants cultured in DMEM medium supplemented with 10% dFCS, the transfectants exhibited similar growth characteristics (Figure 6.1A, batch culture 2). However, each of the transfectants obtained higher cell densities than was observed in the DMEM medium supplemented with 10% dFCS (Figure 6.1A). The highest producer remained as 2X, which also attained the lowest viable cell density, in agreement with other reports which suggest that higher producing cell lines do not grow to such high densities as a result of utilising energy available to the cell for the production of the rIgG product at the expense of proliferation (Jung et al., 2002). As a result of the higher viable cell densities it was expected that the rIgG titre would be slightly reduced. This observation was confirmed when the rIgG titre was assessed by ELISA. The highest producer (2X) reduced by approximately half to 85.5 mg L⁻¹ by the end of the culture (Figure 6.1B, Table 6.2). However, the transfectants still produced rIgG in the same relative levels with 2X remaining the highest producer followed by the mid-producers 2P, 4R and the low producer 4O.

The pattern of glucose utilisation contrasted with the observations in the DMEM medium (Figure 6.1C). Most of the glucose that was available to the cells was utilised by the time the cells had reached their maximum densities, although it was not fully depleted (between day 4 to 6), (Figure 6.2C, batch culture 2). In agreement with the transfectants cultured in 10% serum supplemented medium, the level of lactate accumulated and reached maximum levels (approximately 0.8 g L⁻¹) once the cells reached their maximum viable cell densities (between day 4 to 6). Once the cells had reached maximum density, lactate was consumed in all of the transfectants, although the parental NS0 cell line did not consume as much lactate as the other cell lines (Figure 6.2C, batch culture 2). As discussed previously, the consumption of lactate occurred concomitantly with a reduction in the viable cell densities in all of the NS0 cell transfectants.

The levels of glutamate and glutamine were also assessed in cell-free supernatants for each of the transfectants, including the parental cell line throughout batch culture (Figure 6.1D, batch culture 2). As expected, in the parental host cell line the level of glutamine supplemented in the culture medium reduced dramatically as the culture progressed (from 4 mM to 0.18 mM) and was utilised once the cells had reached the maximum viable cell density by the fourth day of culture (Figure 6.1A and D, batch culture 2). For the rest of the transfectants the level of glutamine also agreed with previous observations, remaining at low levels throughout culture. As observed with the transfectants cultured in DMEM/10% dFCS, the glutamate levels remained almost constant for the transfectants (except for 2X and the blank transfectant), and only increased slightly towards the end of the culture after the maximum viable cell density was reached (Figure 6.1D).

6.3.1.3 GS-NS0 Transfectant Growth in 4 L Bioreactor Culture

Following the batch culture of the transfectants in 100 mL shaker flasks, the transfectants were grown under controlled conditions in bioreactors (4L culture volume). The growth characteristics observed in the bioreactors were similar to the cell growth in the 100 mL shaker flasks (Figure 6.1A, batch culture 2 and 6.2A). All transfectants reached maximum cell density after 4 or 5 days of culture. The rate of glucose consumption and lactate accumulation also agreed with that observed in the 100 mL shaker flask experiments (Figure 6.1C, and 6.2C).

The levels of glutamate and glutamine were also assessed and as observed in the 100 mL shaker flask cultures, the levels of glutamate decreased dramatically in the highest producer 2X and the blank transfectant. Unexpectedly, this was also observed for transfectant 4R suggesting once again that the cells were utilising glutamate as well as ammonia to form glutamine (Zhou et al., 1997) (Figure 6.2D). The levels of glutamine remained low for most of the transfectants apart from the parental cell line, as expected. Unexpectedly, however, transfectant 4R also appeared to secrete glutamine into the culture medium (albeit at low levels) (Figure 6.2D). The reasons for transfectant 4R having glutamine present in the culture medium are unclear, although it has been reported that GS-NS0 cells can accumulate glutamine in the culture medium particularly after exponential phase (Zhou et al., 1997).

Throughout each of the fermentation runs, the cell-free supernatant was stored to determine the level of rIgG produced. It was apparent once the fermentations were

complete that the level of IgG produced by each of the transfectants was dramatically reduced in the bioreactors relative to that observed in the 100 mL shaker flasks. The reasons for the reduction in product titre are unclear. However the media changes and reduction in serum concentration may have been contributing factors (Marino et al., 1997). Genetic instability was considered possible although this was unlikely to be the main contributing factor for loss of productivity in all cell lines over such a short period of time and the small number of generations. Furthermore, the same cell lines cultured in DMEM, 10% dFCS did not show reduced cell specific productivity after prolonged culture.

As a result of the loss of productivity by all of the transfectants, the system could no longer be considered robust enough to investigate the NS0 cell proteome (of a series of transfectants differing in the level of productivity) for productivity related changes in protein expression. Therefore the cell lines were utilised to investigate clonal variation and cell specific changes. In effect the non-producing cell lines could be utilised to identify the variations in the NS0 cell proteome at mid-exponential phase between cell lines derived from the same parental NS0 host cell line. 2-D PAGE was utilised to identify how quantitatively similar or different each transfectant was at mid-exponential growth phase, to identify proteins that were constitutively expressed and those that were variable.

6.3.2 Proteome Analysis of NS0 Cell Transfectants at Mid-exponential Phase during Bioreactor Culture

In this chapter the differences and similarities in NS0 cell transfectants derived from the same parental host cell line were investigated to assess clonal variation at mid-exponential growth phase. From the results highlighted in the previous chapters most of the changes in the NS0 cell proteome occurred at mid-exponential phase, when the cells were growing and proliferating at a maximum rate and the maximum levels of glucose and lactate consumption and accumulation also occurred. At this stage in the growth curve the cells were also producing maximum levels of rIgG, although as already stated the GS-NS0 cell transfectants had more or less lost productivity between being weaned off serum and cultured in the bioreactors.

The global results presented here for the average gel images show that the total number of protein spots detected at mid-exponential phase was similar for all of the transfectants except for transfectant 2X, which numbered approximately 300 less protein spots (Table 6.5). However, this was likely to be as a result of the one of the IPG strips not focussing as well as the other samples in the neutral and basic regions of the gels.

Interestingly, the gels with the highest number of spots were the blank transfectant and what was the lowest producing transfectant, 4O (1487 and 1505 protein spots respectively). Conversely, the highest producing cell line had the fewest number of protein spots detected (1146), followed by the two mid-producing transfectants 2P and 4R (with 1461 and 1447 protein spots detected respectively). This suggests a loss of functionality or ability to express certain proteins and may explain the resulting loss in ability to produce recombinant IgG (i.e. genetic instability). Furthermore, one would assume it is much easier to lose functionality than to gain, and therefore any changes would be expected to result in the expression of fewer proteins as observed here.

Although it can be seen that the spot numbers detected correlate with the relative production levels of rIgG, in reality there is no significant difference in spot numbers, with only 44 protein spots separating the 'lowest' producing transfectant and one of the highest producing cell lines, 2P. As a result of the loss in productive functionality with regard to recombinant protein production, it was expected that all the transfectants would have similar patterns of protein expression to the blank transfectant, since the cells were now in essence only required to grow and divide. The only differences expected in the proteome maps for each of the cell lines would therefore be attributable to clonal and cell specific differences and the different growth characteristics during culture.

6.3.3 Analysis of Proteins Exhibiting at Least a 2-Fold Change in the Level of Expression at Mid-exponential Growth Phase

The image analysis software was utilised further to assess the differences and similarities in protein expression between the transfectants and the blank transfectant. As in the observations of the silver stained gels in chapter 4, the duplicate 2-D gels undertaken for the NS0 cell transfectants stained with different levels of intensity. The image analysis software compensated for this by normalisation, which meant that each individual spot could then be accurately compared between gels. Approximately 750 (43%) of all proteins expressed by each of the transfectants remained unchanged when compared to the blank transfectant (Table 6.6). This value is similar to that observed for the 'throughout culture' experiment whereby 700 (40%) of all proteins remained unchanged throughout culture (chapter 4, Table 4.3). These proteins were therefore constitutively expressed between transfectants and were likely to be general 'housekeeping' proteins, essential to the functioning and survival of the cells at mid-exponential growth phase. One could therefore suggest that these proteins are absolutely essential for cell growth, survival and

proliferation and as such, large changes in their relative expression levels could not be tolerated without a detrimental effect upon the cells.

Proteins, which were newly expressed, no longer present at detectable levels together with those that exhibited at least a 2-fold (100%) change in expression, were investigated (Table 6.6). The results obtained from the comparison of each of the transfectants against the blank transfectant showed that many proteins altered at mid-exponential phase in the level of expression, including those which exhibited at least a 2-fold change (Table 6.6). Between the average gels created from transfectant 2X and the blank transfectant, at mid-exponential phase, 29% of all the proteins detected and matched to the reference gel exhibited a 2-fold increase in gene expression or were newly expressed, and approximately 62% showed a 2-fold or greater decrease in expression or were no longer expressed at detectable levels (Table 6.6).

The statistics show that many differences between the transfectants are apparent, and that the expression of many proteins was modulated, with more proteins being down-regulated than up-regulated. It is possible that the large differences in protein expression observed between the blank transfectant and the other transfectants were as a result of the cells still expressing the necessary cellular machinery required for rIgG synthesis, and that although the cells were seen to no longer be secreting IgG, the apparent 'loss' of production may have been a result of a blockage in the cell itself, within the ER and the secretory pathway (Lambert and Merten, 1997). It has been reported previously that CHO and NS0 cells can lose expression of the heavy chain of the antibody as a result of retention to the ER by chaperones. In recombinant antibody production there is a tight balance required between the transcription of the two genes (heavy and light chain) and the assembly of four polypeptide chains (Strutzenberger et al., 1999). This process has been identified as one of the major rate limiting steps in antibody synthesis in mouse hybridoma cell lines (Strutzenberger et al., 1999).

Furthermore, the 'loss' of antibody secretion has been reported to be due to a loss of the light chain in CHO cells (Strutzenberger et al., 1999). The light chain of IgG is required for the heavy chain to be secreted by the cell; therefore if the light chain is lost a build-up of heavy chain will occur in the secretory pathway (ER) (Strutzenberger et al., 1999). The build-up of heavy chain in the ER results in the overburdening of the post-translational pathway and the already translated heavy chain product will be degraded in proteasomes (Ho et al., 2000; Strutzenberger et al., 1999). However, investigation of a secretory pathway blockage in the NS0 cell transfectants was not undertaken during this

study. If a blockage in the secretory pathway was the cause of the apparent loss of productivity, we would have expected to see the intracellular rIgG represented on the 2D gel maps at 25 kDa and 50 kDa as a series of post-translationally modified protein spots (Lee, 2001; Manabe, 2003). However, this was not observed.

Alternatively the differences in the proteome maps of the transfectants could be as a result of genetic drift (Barnes et al., 2001). The transfection process may itself have been a source of variation between transfectants, and although the transfectants were not producing antibody, they may still appear to have differences in the global proteome. Barnes *et al.* reported that the utilisation of clonal cell lines is an ideal but unrealistic aim. They report that during periods of continued growth a rapid phenotypic drift can occur, so that what was originally a cell line derived from a single cell, can within a short time frame become a heterogeneous/mixed population (Barnes et al., 2001). This may also be observed in high producing cell lines, resulting in a population of producing and non-producing cells, which have a growth advantage over the producing cell lines resulting in a loss of productivity. This may have occurred in the GS-NS0 cell transfectants utilised in this study. The cell lines utilised in this study were unstable to some degree as they lost productivity early in their culture history, which may also have contributed to the variations observed in the global NS0 cell proteome. This observation has been reported previously, whereby GS-NS0 cells exhibited unstable recombinant protein production (Barnes et al., 2003). Therefore it is important to carefully select transfectants to increase the chance of having a stable cell line, which will continually produce recombinant protein over long-term culture (Barnes et al., 2003).

It is also possible that the differences in protein expression occurred as a result of differences in growth characteristics and cellular metabolism. As already discussed, each of the transfectants exhibited similar growth characteristics, reaching similar viable cell densities, and exhibiting similar characteristics of glucose and lactate consumption and accumulation respectively. The main differences in growth characteristics of the transfectants were observed in the glutamate and glutamine levels, although differences in glucose metabolism were also apparent when compared against the cell lines cultured in serum containing medium. All of the transfectants showed very small changes in the level of glutamate and none of the transfectants had glutamine present in the culture medium except for the parental cell line as expected. The exception to this was observed with transfectant 4R, which unexpectedly had glutamine detected in the growth medium throughout culture, particularly after the transition from exponential to stationary phase.

However, this has been reported before in GS-transfected NS0 cell lines (Zhou et al., 1997) (Figure 6.2D), although it is unlikely this was a major source of cell line specific variation.

Regardless of the reason for these cell line specific differences, it is clear that while the expression level of approximately half the NS0 cell proteins appears to be constant, these cell lines can tolerate large changes in the expression levels of the rest of the cellular protein machinery. This suggests that while the protein machinery required for some cellular tasks and makeup is relatively 'set', it is possible to have multiple variations in the remainder of the protein cellular makeup without adversely affecting the cells ability to survive, grow and proliferate. As a direct result of this large cell line specific variability, it will remain difficult to improve the productivity of NS0 cells by traditional cell engineering approaches whereby one or two proteins of interest are over-expressed.

6.3.4 Quantitative Analysis of Specific NS0 Cell Protein Expression

For each of the transfectants limited statistical analysis (in the form of standard deviation) was carried out on each of the 17 protein spots from the duplicate 2-D gel images. In correlation with the errors obtained for the replicate 18 cm 2-D gel images in chapter 4 (Figure 4.10 and 4.11) discussed previously, small variations in the normalised spot volumes were observed for the highly abundant protein spots investigated (Figure 6.5 and 6.6). However, for some protein spots (for example protein spot number 1 and 2) larger errors were observed in some of the transfectants. Although these protein spots were amongst the most abundant, they were also saturated in one of the duplicate gel images. This lead to high variations in normalised spot volumes (and therefore the standard deviation) for these protein spots being achieved.

For each transfectant, limited statistical analysis (in the form of standard deviation) was carried out for each of the 17 protein spots as each 2-D gel was carried out in duplicate (chapter 2, section 2.7.4.2). In correlation with the errors obtained for the replicate 2-D gel images in chapter 4 (Figure 4.10 and 4.11) discussed previously, small variations in the normalised spot volumes were observed for most of the highly abundant protein spots investigated (Figure 6.5 and 6.6). However, for some protein spots (especially for protein spot number 1 and 2) larger errors were observed for some transfectants. Although these protein spots were amongst the most abundant on the 2-D gels, they were also saturated in one of the duplicate gel images, which lead to high variations in normalised spot volume and standard deviation being achieved.

As previously discussed, many differences in the pattern of protein expression (by at least 2-fold) were observed between the NS0 cell transfectants at mid-exponential growth phase (Figure 6.4). Therefore, in order to accurately assess the global differences and similarities in protein expression further between the GS-NS0 cell transfectants at mid-exponential phase, the 17 proteins identified in chapter 4 were quantitatively assessed using the average composite gel images performed by the image analysis software in the same way as in previous chapters. As previously discussed in chapter 4 in greater detail, the proteins were separated into three main groups (chaperones, glycolytic proteins and structural proteins) based on the individual protein properties/functions. If we assume that any observed differences are not related to recombinant protein production we should be able to further group these proteins into those which do not change (and presumably the cell lines cannot tolerate significant changes in the expression levels of these proteins), and those proteins in which NS0 cells can tolerate a large change in expression levels without compromising growth and proliferation.

With respect to these 17 proteins, there was some variation between all cell lines (Figure 6.5 and 6.6), which is indicative of this type of investigation and therefore is to be expected. Bearing this in mind, it is clear that BiP, calreticulin, PDI, ERp60, β -actin (protein spot 14), glyceraldehyde 3-phosphate dehydrogenase (GAPDH) (protein spot 16) and peptidyl-prolyl *cis-trans* isomerase A (PPIase A) (protein spot 17), (Figure 6.5 and 6.6) exhibited little cell line specific variation outside of that expected in this type of study. The functions of these proteins have been discussed extensively in previous chapters. Presumably the expression levels of these proteins is relatively 'set' and not prone to change implying that these components of 'cellular machinery' do not differ significantly between NS0 cell lines, and are required for 'normal' cellular processes (for providing energy to the cell (glycolytic proteins), structural stability to the cell cytoskeleton and for preventing protein aggregation (structural proteins) and to mediate protein transport through the secretory pathway (chaperones)), and are essential for cell growth, survival and proliferation. Meanwhile the expression levels of Hsc71, pyruvate kinase, Hsp60 and Grp75 showed some cell line specific variation (Figure 6.5 and 6.6), although once again the change was not significant in most cases. However, the expression levels of elongation factor 1-alpha-1, α -enolase, Grp94, α -tubulin and glyceraldehyde 3-phosphate dehydrogenase (protein spot 15) did show significant cell line specific changes.

The visual inspection of Grp94 expression as observed in previous chapters, revealed conflicting results to that observed on the relative abundance graphs (Figure 6.5, number 7). Cell line 2X, 2P and 4R were observed to exhibit the highest levels of Grp94 expression with the blank transfectant and 4O expressing Grp94 to much lower levels. This is almost in direct opposition to the relative expression levels seen on the relative expression graph. Although conflicting results were observed between the visual and quantified expression levels the data clearly demonstrates that the expression of Grp94 was significantly altered, suggesting cell line specific changes in Grp94 expression. The NS0 cells could therefore tolerate large differences in the level of Grp94 protein expression without any detrimental effect upon the cell (i.e. cell death).

The relative level of α -tubulin expression revealed significant differences in the level of expression for each of the transfectants (Figure 6.5, number 8). This data again suggests that there are cell line specific changes in α -tubulin expression. The high-level of α -tubulin expression by cell line 4O and 4R is in agreement with the results observed previously, at mid-exponential phase suggesting cells require α -tubulin expression in absence of rIgG. The differences observed in α -tubulin expression again suggest that the cell can tolerate large fluctuations in α -tubulin expression.

GAPDH (Figure 6.6, number 15) showed a change in the level of expression between cell lines, with GAPDH either being expressed at high levels in 2X and 2P, and at significantly lower levels for the remaining cell lines. The visual pattern confirmed that each of the cell lines expressed GAPDH at varying levels, further confirming cell line specific expression of GAPDH. However, GAPDH expression in spot number 16, exhibited a similar pattern of expression for each of the cell lines (Figure 6.6, number 16). This demonstrates that the cell lines have differing requirements for each isoform of GAPDH and can accept large or only small differences in the relative level of GAPDH expression depending on the isoform (or post-translationally modified form) of GAPDH.

The two β -actin protein spots (Figure 6.6, number 13 and 14) exhibited the same general trend of relative expression and the visual pattern of expression was seen to closely correlate between each of the protein spots. In the β -actin spot (number 13) the protein was expressed at slightly varying levels by the cell lines, with 2X and the blank cell line expressing β -actin to similar levels, with the other transfectants (2P, 4R and 4O) expressing β -actin to lower levels. β -actin (protein spot number 14) suggested similar results to spot number 13, with the blank transfectant, 2X and 4R exhibiting high levels of

expression, and the remaining cell lines 4O and 2P exhibited lower levels of β -actin expression. However, the visual pattern of β -actin expression suggested that β -actin expression was similar for each of the cell lines demonstrating that β -actin was constitutively expressed between cell lines and the cell can only tolerate small alterations in β -actin expression.

α -enolase (Figure 6.6, number 12) as previously discussed in chapters 4 and 5 is a key glycolytic enzyme. The relative expression levels of α -enolase indicate the protein is differentially expressed by each of the cell lines with α -enolase showing significant variations in expression. 2X was observed to express α -enolase at the highest relative levels, with the other cell lines expressing decreasingly lower levels of α -enolase. This data suggests again that NS0 cell lines can tolerate large fluctuations in the expression of α -enolase without having negative effects upon cell growth, proliferation and survival.

A similar pattern of relative expression to α -enolase was observed for elongation factor 1-alpha-1 (eEF1A-1) (Figure 6.6, number 11) and pyruvate kinase (PK) although to a lesser extent (Figure 6.6, number 10). eEF1A-1 is an important protein required for mRNA translation elongation (Browne and Proud, 2002). In correlation with PK, the relative expression of eEF1A-1 closely correlated with the visual pattern of protein expression. 2X clearly exhibited the highest level of expression and the other cell lines expressed eEF1A-1 to varying levels. This again clearly shows the cell line specific differences in protein expression, and that the cell can tolerate large differences in the pattern of expression in eEF1A-1 without having a negative effect upon the cell.

Pyruvate kinase (PK) exhibited a similar expression profile to eEF1A-1, although to a lesser extent, with small fluctuations in the expression pattern. The visual pattern of expression closely followed the relative expression pattern (Figure 6.6, number 10). Again, 2X expressed the highest level of PK, with the blank expressing lower levels of PK. The other cell lines (2P, 4R and 4O) exhibited much lower levels of PK expression. This data further confirms the cell line specific expression of PK, suggesting PK can be expressed at varying levels without detrimental effects being felt by the various NS0 cell lines.

Grp75 (Figure 6.5, number 3), Hsc71 (Figure 6.5, number 2) and Hsp60 (Figure 6.5, number 5) exhibited small fluctuations in the pattern of protein expression. Grp75 expression was observed to be highest for the blank transfectant, followed by 2X, 2P and 4R, and 4O exhibited the lowest levels of Grp75 expression. Hsc71 exhibited a similar

pattern of expression with 2X exhibiting the highest level of expression followed by the blank transfectant and 2P, 4R and 4O expressed the lowest levels of Hsc71 expression. Finally, Hsp60 was highly expressed in the blank transfectant, 2X and 4R, followed by 2P and 4O expressed the lowest levels of Hsp60. Although the expression profiles for each of these proteins were observed to fluctuate for each of the cell lines, suggesting the cell could tolerate some cell line specific alterations in the level of expression, the extent of the 'tolerance' was not as significant as for other proteins discussed previously. This suggests only relatively small fluctuations in the level of protein expression can be accepted by each of the cell lines before a negative effect on cell growth, proliferation or survival would result.

The remaining proteins investigated, BiP (Figure 6.5, number 1), calreticulin (Figure 6.5, number 4), PDI (Figure 6.5, number 6), ERp60 (Figure 6.5, number 9) and PPIase A (Figure 6.6, number 17) did not exhibit any significant changes in the relative level of expression between cell lines, with each of the proteins being expressed at similar levels. In particular with BiP, calreticulin and ERp60, only very slight fluctuations in protein expression could be tolerated by the cell lines. PDI and PPIase A exhibited slightly more fluctuations in protein expression between cell lines, although the differences were not judged to be significant. The data suggests these proteins are constitutively expressed and are essential for each of the NS0 cell lines, being expressed at similar levels even in the absence of rIgG. Therefore the cell cannot tolerate any significant changes in the level of expression of these particular proteins, without having severe effects upon the cell and its growth and survival.

The possible reasons for the differences observed in protein expression between cell lines, which can or cannot tolerate changes in the level of protein expression, are threefold. Firstly, those proteins which exhibit no change and those which can tolerate changes in expression are required to carry out specific cellular tasks, although we can suggest that in those proteins which can tolerate a change can carry out the specific function at a lower expression level, or other protein/s can take over the function of the down-regulated proteins. Whereas those proteins that do not change between cell lines cannot carry out the specific function at lower levels or cannot have other proteins take over the specific function. Secondly, those proteins, which do not exhibit a change in the level of expression, may be less prone to cellular changes and are essential to the cell. Finally it is possible that the changes observed between each of the cell lines may be totally random events, although this is unlikely.

6.3.5 General Discussion

From the results obtained in this chapter despite only carrying out limited statistical analysis it is clear that there are many alterations in protein expression observed between the GS-NS0 cell lines at mid-exponential phase. A similar number of proteins in each cell line were observed to exhibit up- or down-regulation. At the same time approximately 50% of all the proteins observed showed no variation in the expression levels between cell lines. This suggests that within NS0 cells there are a set of proteins which are absolutely essential to cell survival, growth and proliferation and are therefore less prone to variation. However, changes in the expression levels of approximately 50% of all proteins can be 'tolerated' by the cell and do not adversely effect cell survival and growth. As a result individual cell lines may achieve the same 'result' in a large number of ways due to the different cellular makeup of a particular cell line.

It is likely that most of the differences in protein expression observed in the transfectants occurred as a result of clonal variation. Firstly, each of the cell lines was subjected to a transfection process, which may cause variations to be observed in global protein expression. Although the transfectants appeared to have lost the ability to produce rIgG upon growth in different media, the cell lines did originally produce varying levels of antibody. It is therefore possible that some cells may have retained the machinery required to produce the antibody, but not utilised it for reasons which are unclear, resulting in some of the differences observed. As described above, it is possible for cell lines to become heterogeneous (Barnes et al., 2003), and non-producing cells, that have a growth advantage over the producing cells can out number them resulting in a loss of productivity. It is also unlikely that the cell lines utilised in this study were truly 'clonal' populations (Barnes et al., 2001). As a result we would expect many differences to be observed in the global NS0 cell line proteome maps.

Unfortunately, this study has not provided any information on whether a high producing cell line contains more of the cellular machinery required by a high producing cell line (including ER resident chaperones) or alternatively whether an increase in recombinant protein expressed results in an increase in ER protein expression (Downham et al., 1996). However, on-going work at the University of Kent has shown that both CHO and NS0 cell lines that differ in cellular rMAb productivity exhibit a small number of discrete changes in protein machinery that correlate with productivity (data not shown). Furthermore, there are a large number of cell line specific changes in all of these cell lines

suggesting that it is the over-all cellular bias of machinery which determines the ability of a cell line to synthesise and secrete recombinant protein.

In summary, the study described in this chapter has clearly shown that the NS0 cell proteome of cell lines derived from the same NS0 parental host exhibit many differences in the pattern of protein expression. The protein spot patterns observed for each of the transfectants were similar, although the expression of many proteins was cell line specific, with few proteins exhibiting the same pattern or level of expression. It was initially expected that as the transfectants had all lost productivity, global protein expression pattern would be similar, although this did not appear to be the case. The differences appeared to be mostly due to clonal variation.

Although it was apparent that the relative abundance of the 17 proteins identified previously (chapter 4 and 5) was often not accurate, it was also apparent from the visual inspection of individual protein spots that many were expressed at varying levels for each of the transfectants. The differences observed in protein expression between transfectants correlated with changes in nutrient concentration (the maximum utilisation of glucose and glutamate (in some cases) together with lactate accumulation), cell growth, and possibly as a result of the induction of the stress response (chapter 4 and 5). At mid-exponential phase the cells were dividing at the maximum rate and therefore it was expected that proteins involved in providing energy through glycolysis to be up-regulated along with those proteins involved with protein synthesis (as discussed in previous chapters). Therefore, it is clear that the differential protein expression by each of the transfectants reflects the different needs of each cell line at this stage of growth. These differences between each of the cell lines occur in the global proteome as a result of clonal variation and different growth characteristics more-or-less without the influence of rIgG production.

The intended use of the GS-NS0 cell lines utilised in this study was to assess the global NS0 cell proteome at mid-exponential phase between cell lines differing in specific productivities. Unfortunately, between being cultured in DMEM-F12 medium supplemented with serum and weaning off serum for culture in controlled bioreactor culture, the cell lines lost the ability to secrete antibody. The loss of productivity may have been a result of many contributing factors including those highlighted above. Regardless, the results highlighted in this chapter indicate that even in non-producing NS0 cell lines the proteome is a dynamic system, in which protein expression profiles fluctuate according to 'normal' cell growth and environmental stresses/changes.

Chapter 7 General Discussion and Conclusions

7.1 Final Summary

Mammalian cells remain the host system of choice for the large-scale expression and production of therapeutic proteins in industry. The advantages of using mammalian cell lines include their ability to perform a wide variety of post-translational modifications, and that they usually fold the expressed recombinant protein in the functionally correct manner to form the appropriate tertiary structures, which are found in the equivalent human protein (Barnes et al., 2003; Schroder et al., 2002). Furthermore, other expression systems including yeast and bacteria are currently incapable of producing proteins with the required post-translational modifications to prevent an immune response in the human patient.

Despite the fact that animal cells are able to produce recombinant proteins of such high quality, little is currently known about the cellular processes, which define a productive cell line. Due to the increasing demand of biotherapeutics, the high-yield production of recombinant proteins by mammalian cell lines is becoming increasingly important to industrial companies (Barnes et al., 2003). To date a variety of different strategies to improve productivity and productive cell lifetime have been investigated. These include the incorporation of anti-apoptotic genes (*bcl-2* and *bcl-xL*) (Andersen and Krummen, 2002; Jung et al., 2002; Laken and Leonard, 2001; Meents et al., 2002; Tey et al., 2000), the use of caspase activation inhibitors (Andersen and Krummen, 2002; Sauerwald et al., 2003) and modulation of the cell-cycle to cause arrest at G1-phase through inducing the expression of regulatory proteins (cyclin dependent kinase inhibitors) p27 and p21 or treating cells with drugs such as rapamycin (Balcarcel and Stephanopoulos, 2001; Fussenegger et al., 1998a; Ibarra et al., 2003; Laken and Leonard, 2001; Watanabe et al., 2002), although, to date these attempts to manipulate the 'productivity' of cells have met with limited success, with results that were often contradictory or ambiguous. Increased productivity as a result of empirical optimisation of the cell culture environment (including media constituents, pH and osmolarity) has also been used to improve cellular productivity. However, these systems have now been optimised and further scope for improvement in this area is limited (Birch and Froud, 1994a; Dempsey et al., 2003; Hayter et al., 1992; Osman et al., 2002).

Furthermore, for many proteins the mRNA level often does not correlate to the amount of protein synthesised (Gabor Miklos and Maleszka, 2001; Smolke and Keasling, 2002), and as a result it may be more relevant in many cases to assess changes in protein

expression levels. The work presented in this thesis aimed to; (1) carry out the comparative analysis of the NS0 cellular proteome in culture to identify the specific cellular protein(s) involved with facilitating high-level productivity *in vitro* and (2) to use this information in order to derive new 'knowledge-based' strategies for the identification of potential engineering targets for the rational re-design of GS-NS0 cell lines with optimised functional phenotypes.

The initial goal was therefore to optimise a proteome analysis platform (chapter 3) for the accurate analysis of the global NS0 cell proteome throughout culture and between GS-NS0 cell lines. An optimised lysis buffer solution was developed which provided the most reproducible and accurate 2-D gel pattern (chapter 3, section 3.3.2.1). The number of cells to be extracted in a set volume of lysis buffer was also optimised so that 1×10^7 cells were extracted in a 400 μ L volume (chapter 3, section 3.3.3). Through employing this system the NS0 cell proteome could be accurately and reproducibly assessed (chapter 3, scheme 3.1 and 3.2).

The isoelectric point first dimensional resolving range was also optimised to allow the greatest visualisation of NS0 cell proteins. Linear and non-linear pI 3-10 resolving ranges were assessed (chapter 3, section 3.3.5). The non-linear range allowed the visualisation of more proteins in the acidic region of the 2-D gels, (which is the region where most chaperones were observed), and was therefore routinely utilised to separate whole NS0 cell proteins. Whole GS-NS0 cell proteins were visualised by silver staining methodology to enable high sensitivity of staining with low background staining and, through omission of glutaraldehyde in the staining methodology, the gels could be used for protein identification by MALDI-ToF-ms.

The optimised proteomic platform (chapter 3, scheme 3.2) was then applied to investigate the changes in protein expression throughout a controlled 1.5 L batch culture of GS-NS0 cells. Supernatant samples were taken daily to assess the changes in metabolite concentration (glucose and lactate) and to assess rIgG production titre throughout the culture. Samples of 1×10^7 cells were extracted in lysis buffer 2 throughout the culture at key time-points (lag phase, day 1; exponential phase, days 3 and 5; death phase, day 7). Large format 2-D PAGE (26 x 20 cm) was carried out for each of the samples, and ImageMaster 2-D Elite™ utilised to analyse the resultant digital images. Analysis based on total spot numbers indicated that the number of protein spots detected increased as the culture progressed. The above data was based on the analysis of individual gel images for

each time point. However, triplicate 18 cm 2-D gel images prepared for the comparison against the 2-D autoradiographs in chapter 5 confirmed these results, although spot numbers were observed to decrease at the end of the culture as expected.

The quantitative analysis of the NS0 cell proteome throughout batch culture indicated that the GS-NS0 cell proteome is a dynamic system, and many changes in protein expression were associated with growth, stress perception and possibly the production of rIgG. Many proteins (approximately 700, 40%) were constitutively expressed throughout culture, appearing to be unaffected by cellular stresses and nutrient depletion. These proteins were likely to be essential to the cell and were 'set' in terms of the required cellular machinery and the cell could not tolerate any fluctuations in their expression. The remaining 60% of the proteins detected may fluctuate during batch culture without causing detrimental effects upon the cell. Most of the changes in protein expression were observed at exponential phase of the culture (chapter 4, section 4.2.3.3).

When the levels of proteins exhibiting at least a 2-fold change in protein expression were investigated, approximately 400 proteins were observed to change as the culture progressed. These changes were presumably to enable the cell to adapt to the specific requirements at each stage of the growth curve. During exponential phase (between days 3 and 5), approximately 47% of all proteins were newly expressed or exhibited at least a 2-fold increase in expression (chapter 4, section 4.2.3.3 and Table 4.3). The number of proteins at the same time point exhibiting a decrease in expression by 2-fold or more represented 28% of the total protein spots. This suggests that many new proteins were required at this time-point in the growth curve and can be explained as the cells were reaching maximum cell densities, nutrients were being depleted and the cells were producing maximum levels of rIgG at this time. Previous reports also suggest the cells would be under stress as a result of the increase in rIgG at this point in the growth curve resulting in an increase in the expression levels of proteins involved with the general stress response and induction of the UPR (Patil and Walter, 2001). Recombinant IgG was not expressed at very high levels by the cell (maximum titre $109 \mu\text{g mL}^{-1}$) (chapter 4, Figure 4.1A) and it is unlikely that rIgG accumulation on its own would induce a stress response and the UPR as a result of the increased load upon the ER.

However, there is some precedent for this type of cellular response pattern. A recently reported proteomic investigation into the changes in cellular protein expression of B cells during culture showed that, not unexpectedly, B cells respond in a similar manner,

up-regulating stress proteins late in culture and during times of maximum Ig production (van Anken et al., 2003). In the report the identified proteins were separated into different groups according to temporal expression patterns (including metabolic, cytosolic and ER resident chaperones, cytoskeletal, metabolic and redox balance proteins). The group revealed that upon transformation of a dormant B cell to a professional secreting plasma cell, the B cells anticipate their new secretory role in a multi-step process involving sequential waves of coordinated protein expression (van Anken et al., 2003). On the first day after activation, mitochondrial and cytosolic chaperones were expressed at high levels, followed by a peak in metabolic enzymes after the third day. ER resident proteins were observed to increase in a linear fashion during the culture, accompanied by proteins involved in redox balance. The production of IgM by the plasma cells increased sharply only after the second day of culture. Therefore the B cell first ensured that metabolic capacity and the secretory machinery had expanded before launching the high-level production of Ig (van Anken et al., 2003), and clearly reflects the different needs of the cell at particular time points during culture. With this in mind we further investigated 17 specific proteins belonging to different functional groups to determine if a similar response was elicited in NS0 cells secreting rIgG.

Seventeen proteins were identified from the NS0 proteome maps by MALDI-ToF-ms and peptide mass fingerprinting. The proteins were grouped according to their function/properties: (1) chaperones, (2) glycolytic proteins and (3) structural proteins. Many of the proteins that were identified (for example Hsc71 and Grp75) have been reported to be required by cells for general 'housekeeping' functions as well as having stress properties (Agashe and Hartl, 2000; Kiang and Tsokos, 1998; Takano et al., 2001). Therefore any differences in the pattern of expression of these proteins cannot be directly attributed to a stress response. This makes identification or pinpointing exactly when cells perceive stress during culture very difficult as many of the proteins fluctuate during 'normal' growth to provide the necessary machinery to enable maximum cell growth and proliferation, and to provide the energy required by the cell.

However, of the 17 proteins that were identified for further investigation (chapter 4, section 4.2.5, Table 4.5), most were up-regulated at late exponential phase of the culture (day 5), which coincided with the end of the maximum rate of growth and proliferation, maximum glucose utilisation and lactate accumulation, but also with the maximum production of rIgG (chapter 4, Figure 4.1). These results were also confirmed by the analysis of the 17 protein spots on triplicate 18 cm 2-D gels run from the same samples

extracted during the batch culture experiment albeit on a different format. The up-regulation of proteins at this stage of the growth curve suggests that the cells perceived a large amount of stress at this time in the culture, although whether the increase in stress perceived by NS0 cells was as a result of the accumulation of rIgG within the ER and the induction of the UPR was not confirmed in this study. However, the regulation of many of these proteins at exponential phase was also observed for the duplicate 2-D gel images prepared for the non-producing cell lines (chapter 6, Figure 6.4 to 6.6) suggesting the proteins involved with the UPR are present at high levels in the absence of accumulating rIgG. For example, BiP is induced as a result of the UPR and facilitates IgG folding (Mayer et al., 2000), although BiP is also required for normal cellular processes (Agashe and Hartl, 2000; Patil and Walter, 2001). Taken together these results all indicate that cells respond to environmental stresses during *in vitro* culture that result in the up-regulation of proteins involved in generally combating stress and the UPR. The induction of these proteins is likely to facilitate the production of recombinant protein by providing more of the cellular machinery required for successful folding and secretion of complex recombinant glycoproteins, but may not be as a direct result of accumulation of the rIgG produced.

Proteome analysis by 2-D PAGE enables the interrogation of proteins showing a change in abundance, although a change in protein abundance does not always infer activity. That is, a change in the level of abundance does not necessarily indicate a protein has increased or decreased in the level of activity. To identify the polypeptides being actively synthesised by NS0 cells during the batch culture metabolic labelling of nascent polypeptides was carried out using [³⁵S] methionine (chapter 5).

Metabolic labelling with L-[³⁵S] methionine was utilised to measure nascent polypeptide synthesis throughout batch culture. The maximum incorporation of [³⁵S] methionine into nascent polypeptides, and therefore the maximum level of cell activity and protein synthesis, was observed early in culture (day 3). This agrees with the growth data and corresponds to the period in the culture where the cells were preparing for exponential growth and therefore presumably required the greatest amount of protein synthesis (chapter 5, Figure 5.1). The maximum level of [³⁵S] methionine secretion was observed during exponential growth as expected (days 3 and 5), and reduced after this time, correlating with the growth data in chapter 4 and the maximum levels of rIgG production.

The pattern of polypeptide synthesis assessed by individual 2-D PAGE and autoradiography was different to that observed on the protein gels. The

protein/polypeptide maps were also difficult to match and compare due to the different principles underlying each technique, which visualise constitutively expressed or metabolically labelled nascently produced proteins (Westbrook et al., 2001). Approximately half the number of newly synthesised proteins were observed when compared against the protein gels from the same time points (chapter 5, Table 5.1 and 5.3), with only half the number of polypeptide spots matched to the protein gels (chapter 5, Table 5.5). However, the same general trend of polypeptide numbers detected was observed as seen in the protein gels, confirming the greatest increase in spot numbers at late exponential phase, and reducing to death phase when most of the cells were dead or dying (chapter 5, Figure 5.3). At this stage in the growth curve cells would no longer synthesise proteins involved with general housekeeping functions or proliferation. However, this could have been offset by the cells up-regulating pro-apoptotic and stress related proteins. This again correlated with the growth data (cell density, glucose utilisation) and the level of secreted [³⁵S] methionine, which decreased after exponential phase (chapter 5, Figure 5.1), suggesting the cells were at their most active synthesising polypeptides during exponential phase of culture.

In agreement with the pattern of proteins exhibiting a 2-fold change in expression, the 2-D autoradiographs showed that there were many differences in the pattern of polypeptide synthesis throughout batch culture (chapter 5, Table 5.2). As previously observed in the protein gels, there were many time-specific changes in expression. The number of polypeptides throughout batch culture exhibiting no change in expression numbered approximately 200 (25%), which is less than observed on the protein gels. Again, these polypeptides were unaffected by cellular stresses and were required by the cells throughout the growth curve, with cells actively synthesising these proteins at a constant rate throughout. The greatest increase in protein expression was observed at exponential phase, although the number of polypeptides exhibiting a 2-fold increase in expression fluctuated. However, the results discussed in chapter 5 only utilised single 2-D autoradiographs for analysis. Therefore confirmation of the results discussed would be required by performing either a duplicate experiment and/or carrying out a greater number of replicates for the experiment so that the results could be statistically verified.

The relative expression levels of the 17 proteins identified in chapter 4 were compared to the polypeptide expression profiles and were observed to follow the same general trend (chapter 5, Figure 5.9-5.12). However, there appeared to be a delay between changes observed in polypeptide synthesis and the concurrent increase in protein

abundance. It was expected that an increase in polypeptide synthesis would result in an increase in protein expression at the same time point, but clearly this was not the case. This data suggests that NS0 cells perceive stress earlier in culture than previously thought, as early as day 3 of batch culture, as determined by increased polypeptide synthesis but that it takes much longer to observe an actual increase in protein abundance. To some extent this will be protein dependent being related to the time taken to translate, fold and traffic the protein to the required cellular compartment and also on the individual proteins half-life. However, as discussed above the results require confirmation.

The GS-NS0 cell transfectants discussed in chapter 6, were to be utilised to assess the differences and similarities in protein expression between producing and non-producing cell lines to identify the proteins specifically involved with productivity. The cells were successfully weaned off serum onto protein-free medium supplemented with 1% dFCS. However, upon culturing in bioreactors, all of the transfectants lost productivity (chapter 6, Figure 6.2B). The reasons for this are unclear, although the reduction in serum concentration and genetic drift may have contributed. The transfectants were therefore utilised to assess clonal variation and differences in protein expression between what were essentially non-producing NS0 cell transfectants derived from the same NS0 host cell line at mid-exponential growth phase.

Throughout the batch cultures cell growth was assessed and fermenters were monitored daily for changes in metabolite concentration of glucose, lactate, glutamate and glutamine (chapter 6, Figure 6.2C and D). The NS0 cell transfectants all reached similar viable cell densities, and glucose was utilised by all of the transfectants by the time the cells reached maximum viable cell density at day 4 or 5 of culture. The level of lactate accumulation was observed to reach maximum levels at the same time as glucose was utilised. However, the lactate was consumed again by all of the transfectants after maximum cell growth concomitant with a reduction in cell density.

The GS-NS0 cell lines were extracted at mid-exponential phase, and 2-D PAGE was carried out in duplicate and the averaged images assessed for differences between each sample when compared against a blank transfectant (chapter 6). Similar average spot numbers were observed for each of the samples subjected to 2-D PAGE, apart from 2X, which numbered approximately 300 fewer protein spots (chapter 6, Table 6.5). The quantitative analyses revealed a similar number of proteins exhibited a 2-fold change in the level of expression (chapter 6, Table 6.6). However, when the difference maps were

assessed, the expression patterns were different suggesting many cell line specific changes occurred in the global NS0 transfectant proteome at mid-exponential phase.

Initially it was expected that analysis of the GS-NS0 cell proteome throughout batch culture and between NS0 cell transfectants would show great changes in proteins involved in the UPR, although this was not the case. It has been reported previously that proteins involved with the stress response and the UPR (including BiP, Grp94 and PPIase A identified here) were present at high levels in NS0 cells during 'normal' growth (chapter 4 and 5) and that many have housekeeping functions as well as key roles in the stress response (Agashe and Hartl, 2000; Downham et al., 1996; Patil and Walter, 2001). Many of the proteins identified here and subjected to in depth image analysis have been reported to have roles in the processing and/or secretion of IgG (chapter 4, section 4.3.4), therefore they would be expected to become up-regulated concomitant with the increase in rIgG titre. This study has shown that typical UPR proteins are expressed at relatively high concentrations (relative to non UPR proteins) by NS0 cells throughout culture. While the levels of some of these proteins were increased as culture progressed it is not possible to associate this directly with rIgG production. It appears more likely that the levels of these proteins are increased as part of a general stress response mechanism, which may be of benefit in terms of recombinant protein production and is not elicited in response to recombinant protein production *per se*.

Despite the limitations inherent to proteome research discussed in chapter 4, section 4.3.5, the results reported in the previous chapters clearly suggest that many of the changes observed in the global NS0 cell proteome are cell line and time-specific and appear to be as a result of changes to the local culture environment, although the changes during culture were observed to correlate with the production of IgG. However, the level of rIgG secreted by the NS0 cell lines in this study were relatively low, and it is therefore unlikely that the cells would perceive much 'stress' as a result of rIgG accumulation within the ER alone. Furthermore, a similar pattern of protein expression of these proteins was observed in the panel of GS-NS0 cell transfectants, including the blank transfectant, which could not be responding to the accumulation of recombinant protein in the ER/Golgi complex. The blank transfectant was not engineered to produce rIgG, which provides further confirmation that different NS0 cell lines require the proteins identified here as part of normal growth and that these changes are not productivity related. Therefore, it is likely to prove difficult to identify specific proteins involved with productivity alone.

7.2 **Implications for Future Engineering Strategies**

Research to understand the cellular processes, which enable mammalian cells to continue to stably produce high-levels of recombinant protein will continue to be of increasing economic concern (Barnes et al., 2003). This study has used a proteomics approach to provide the platform with which to further our understanding of NS0 cell behaviour and requirements throughout batch culture. This study is ongoing and a more complete understanding of these requirements continues to develop. The proteome maps produced in this thesis may also be analysed retrospectively if required in the future. Therefore, any further protein identifications from other NS0 cell maps can be assigned to the maps produced from these experiments and interrogated. Future work will therefore concentrate on further annotating and fully characterising the whole NS0 cell proteome.

The identification of NS0 cell proteins is ongoing in order to understand in greater detail the changes in the NS0 cell proteome throughout batch culture. These identifications may also be utilised to further dissect clonal variation. More than 250 individual protein spots have now been identified by others at the University of Kent. As a result of the GS-NS0 cell transfectants 'losing' productivity during bioreactor culture (chapter 6), future work will also involve proteome analysis of the original GS-NS0 transfectants (pre-weaning). The transfectants have been subjected to batch culture in 100 mL shaker flasks but will require culture under controlled conditions in similar bioreactor culture to chapter 6. The transfectants, which vary in the levels of productivity ($0-180 \text{ mg L}^{-1}$), shall be utilised to investigate the specific cellular alterations in functional gene expression, which enable a cell line to become 'productive'. The results from chapter 6 can then be utilised as a control with which the producing cell lines can be compared in order to identify specific proteins directly related to productivity. This investigation has formed part of an on-going project.

The data reported in the results sections of this thesis was largely based on a small number of 2-D gel replicates produced to assess the NS0 cell proteome at specific time points or between NS0 cell transfectants (chapter 2, section 2.7.4.2). Ideally a larger number of 2-D gel replicates should have been produced for each experiment so that the results could have been statistically verified. This work is now underway and others have now carried out substantial statistical validation experiments at the University of Kent. Furthermore, confirmation of the level of individual protein expression levels could have been performed utilising an alternative technique. For example, Western blotting could have been utilised to probe for the 17 specific proteins in the samples extracted during the

bioreactor culture and to assess the differences in the level of protein expression between transfectants at mid-exponential growth phase. The above work has also been carried out by others at Kent and has confirmed the results discussed here for BiP, PDI, Hsc71 and Grp94, although the data was not reported in this thesis.

In conclusion, there are many cell specific changes in the global GS-NS0 cell proteome during batch culture and between GS-NS0 cell transfectants derived from the same parental host cell line. GS-NS0 cells modulate their cellular machinery in order to respond to their particular needs at any given time point. This involves the specific up-regulation of stress proteins (chaperones), glycolytic proteins and structural proteins. Although many of these proteins are reported to be constitutively expressed and regulated as part of 'normal' cell growth, together with the reduction in nutrients, shear stresses, pH changes and other changes in the culture environment (Agashe and Hartl, 2000; Downham et al., 1996), the changes correlated with rIgG production. The results suggest it is difficult to determine differences between cellular responses to environmental stresses and the up-regulation of proteins caused by the accumulation of rIgG. This confirms that many of the changes in expression level observed throughout batch culture are part of a 'normal' response to changes in the culture environment, and only a small part of the change in protein expression can therefore be attributed to rIgG production.

The data presented in this thesis, therefore, has direct implications for cell engineering strategies. This analysis has shown that very large changes in the relative abundance of discrete proteins are comparatively rare and that there are many cell line specific changes in protein abundance. This suggests that a 'productive' cell will have a 'bias' in its range of integrated cellular functions (e.g. growth/division, energy partitioning) that facilitates recombinant protein production and secretion. This bias may combine differential gene expression, metabolic shifts and regulatory processes such as phosphorylation. These conclusions imply that current genetic engineering strategies to improve cell specific productivity that manipulate one or two components of the cellular machinery are unlikely to be successful.

References

- Aaronson, R.M., Graven, K.K., Tucci, M., McDonald, R.J. and Farber, H.W. (1995) Non-neuronal enolase is an endothelial hypoxic stress protein. *Journal of Biological Chemistry*, **270**, 27752-27757.
- Agashe, V.R. and Hartl, F.-U. (2000) Roles of molecular chaperones in cytoplasmic protein folding. *Seminars in Cell & Developmental Biology*, **11**, 15-25.
- Andersen, D.C. and Krummen, L. (2002) Recombinant protein expression for therapeutic applications. *Current Opinion in Biotechnology*, **13**, 117-123.
- Argon, Y. and Simen, B.B. (1999) GRP94, an ER chaperone with protein and peptide binding properties. *Seminars in Cell & Developmental Biology*, **10**, 495-505.
- Babu, J.S., Sun, T., Xu, L. and Datta, S.K. (2002) B cell stimulatory effects of α -enolase that is differentially expressed in NZB mouse B cells. *Clinical Immunology*, **104**, 293-304.
- Bailey, J.E. (1991) Towards a science of metabolic engineering. *Science*, **252**, 1668-1675.
- Bailey, J.E., Prati, E., Jean-Mairet, J., Sburlati, A. and Umana, P. (1998) *Engineering glycosylation in animal cells*. Kluwer academic publishers, Netherlands.
- Bailey, J.E., Sburlati, A., Hatzimanikatis, V., Lee, K., Renner, W., A. and Tsai, P.S. (1996) Inverse metabolic engineering: A strategy for directed genetic engineering of useful phenotypes. *Biotechnology and Bioengineering*, **52**, 109-121.
- Balcarcel, R.R. and Stephanopoulos, G. (2001) Rapamycin reduces hybridoma cell death and enhances monoclonal antibody production. *Biotechnology and Bioengineering*, **76**, 1-10.
- Barnes, L.M., Bentley, C.M. and Dickson, A.J. (2000) Advances in animal cell recombinant protein production: GS-NS0 expression system. *Cytotechnology*, **32**, 109-123.
- Barnes, L.M., Bentley, C.M. and Dickson, A.J. (2001) Characterisation of the stability of recombinant protein production in the GS-NS0 expression system. *Biotechnology and Bioengineering*, **73**, 261-270.
- Barnes, L.M., Bentley, C.M. and Dickson, A.J. (2003a) Stability of protein production from recombinant mammalian cells. *Biotechnology and Bioengineering*, **81**, 631-639.
- Barnes, L.M., Bentley, C.M. and Dickson, A.J. (2003b) Stability of recombinant protein production in the GS-NS0 expression system is unaffected by cryopreservation. *Biotechnology Progress*, **19**, 233-237.

- Bebbington, C. and Hentschel, C. (1985) The expression of recombinant DNA products in mammalian cells. *Trends in Biotechnology*, **3**, 314-317.
- Bebbington, C.R., Renner, G., Thomson, S., King, D., Abrams, D. and Yarranton, G.T. (1992) High-level expression of a recombinant antibody from myeloma cells using a glutamine synthetase gene as an amplifiable selectable marker. *Bio/Technology*, **10**, 169-175.
- Berggren, K., Chernokalskaya, E., Steinberg, T.H., Kemper, C., Lopez, M.F., Diwu, Z., Haugland, R.P. and Patton, W.F. (2000) Background-free, high sensitivity staining of proteins in one- and two-dimensional sodium dodecyl sulfate-polyacrylamide gels using a luminescent ruthinium complex. *Electrophoresis*, **21**, 2509-2512.
- Berkelman, T. and Stenstedt, T. (1998) *2D Electrophoresis. Using immobilised pH gradients. Principles and methods*. Amersham Pharmacia Biotech Limited, Buckinghamshire.
- Binz, P.A., Muller, M., Walther, D., Bienvenut, W.V., Gras, R., Hoogland, C., Bouchet, G., Gasteiger, E., Fabbretti, R., Gay, S., Palagi, P., Wilkins, M.R., Rouge, V., Tonella, L., Paesano, S., Rossellat, G., Karmime, A., Bairoch, A., Sanchez, J.C., Appel, R.D. and Hochstrasser, D.F. (1999) A molecular scanner to automate proteomic research and to display proteome images. *Analytical Chemistry*, **71**, 4981-4988.
- Birch, J., Boraston, R.C., Metcalfe, H., Brown, M.E., Bebbington, C.R. and Field, P.R. (1994b) Selecting and designing cell lines for improved physiological characteristics. *Cytotechnology*, **15**, 11-16.
- Birch, J.R. and Froud, S.J. (1994a) Mammalian cell culture systems for recombinant protein production. *Biologicals*, **22**, 127-133.
- Bjellqvist, B., Pasquali, C., Ravier, F., Sanchez, J.C. and Hochstrasser, D.F. (1993) A nonlinear wide-range immobilised pH gradient for two-dimensional electrophoresis and its definition in a relevant pH scale. *Electrophoresis*, **14**, 1357-1365.
- Blackstock, W.P. and Wier, M.P. (1999) Proteomics: Quantitative and physical mapping of cellular proteins. *Trends in Biotechnology*, **17**, 121-134.
- Bradford, N.M. (1976) A rapid and sensitive method for the quantitation of microgram quantities of protein utilizing the principle of protein dye binding. *Analytical Biochemistry*, **72**, 248-254.
- Brewer, J.W., Cleveland, J.L. and Hendershot, L.M. (1997) A pathway distinct from the mammalian unfolded response regulates expression of endoplasmic chaperones in non-stressed cells. *EMBO Journal*, **16**, 7207-7216.
- Brown, M.E., Renner, G., Field, R.P. and Hassell, T. (1992) Process development for the production of recombinant antibodies using the glutamine synthetase (GS) system. *Cytotechnology*, **9**, 231-236.

- Browne, G.J. and Proud, C.G. (2002) Regulation of peptide-chain elongation in mammalian cells. *European Journal of Biochemistry*, **269**, 5360-5368.
- Bukau, B. and Horwich, A.L. (1998) The Hsp70 and Hsp60 chaperone machines. *Cell*, **92**, 351-366.
- Butt, A., Davison, M.D., Smith, G.J., Young, J.A., Gaskell, S.J., Oliver, S.G. and Beynon, R.J. (2001) Chromatographic separations as a prelude to two-dimensional electrophoresis in proteomics analysis. *Proteomics*, **1**, 42-53.
- Caraglia, M., Budillon, A., Vitale, G., Lupoli, G., Tagliaferri, P. and Abbruzzese, A. (2000) Modulation of molecular mechanisms involved in protein synthesis machinery as a new tool for the control of cell proliferation. *European Journal of Biochemistry*, **267**, 3919-3936.
- Celis, J.E. (1998a) Proteomics: Key technology in drug discovery. *Drug Discovery Today*, **3**, 193-195.
- Celis, J.E., Ostergaard, M., Jensen, N.A., Gromova, I., Rasmussen, H.H. and Gromov, P. (1998b) Human and mouse proteomic databases: Novel resources in the protein universe. *FEBS Letters*, **430**, 64-72.
- Champion, K.M., Arnott, D., Henzel, D., Hermes, S., Weikert, S., Stults, J., Vanderlaan, M. and Krummen, L. (1999) A two-dimensional protein map of Chinese hamster ovary cells. *Electrophoresis*, **20**, 994-1000.
- Chu, L. and Robinson, D.K. (2001) Industrial choices for protein production by large-scale cell culture. *Current Opinion in Biotechnology*, **12**, 180-187.
- Corbett, J.M., Dunn, M.J., Posch, A. and Gorg, A. (1994) Positional reproducibility of protein spots in two-dimensional polyacrylamide gel electrophoresis using immobilised pH gradient isoelectric focussing in the first dimension: An interlaboratory comparison. *Electrophoresis*, **15**, 1205-1211.
- Cudna, R.E. and Dickson, A.J. (2003) Endoplasmic reticulum signalling as a determinant of recombinant protein expression. *Biotechnology and Bioengineering*, **81**, 56-65.
- Dastoor, Z. and Dreyer, J.-L. (2001) Potential role of nuclear translocation of glyceraldehyde-3-phosphate dehydrogenase in apoptosis and oxidative stress. *Journal of Cell Science*, **114**, 1643-1653.
- Davidsson, P., Westman, A., Puchades, M., Nilsson, C.L. and Biennow, K. (1999) Characterisation of proteins from human cerebrospinal fluid by a combination of preparative two-dimensional liquid-phase electrophoresis and matrix-assisted laser desorption/ionisation time-of-flight mass spectrometry. *Analytical Chemistry*, **71**, 642-647.
- Dempsey, J., Ruddock, S., Osborne, M., Ridley, A., Sturt, S. and Field, R. (2003) Improved fermentation processes for NS0 cell lines expressing human antibodies and glutamine synthetase. *Biotechnology Progress*, **19**, 175-178.

- deZengotita, V.M., Miller, W.M., Aunin, J.G. and Zhou, W. (2000) Phosphate feeding improves high-cell-concentration NS0 myeloma culture performance for monoclonal antibody production. *Biotechnology and Bioengineering*, **69**, 566-576.
- Dickson, A.J. (1998) Apoptosis regulation and its applications to biotechnology. *Trends in Biotechnology*, **16**, 339-342.
- DiStefano, D.J., Mark, G.E. and Robinson, D.K. (1996) Feeding of nutrient delays apoptotic death in fed-batch cultures of recombinant NS0 myeloma cells. *Biotechnology Letters*, **18**, 1067-1072.
- Dove, A. (1999) Proteomics: Translating Genomics into Products? *Nature Biotechnology*, **17**, 233-236.
- Downham, M.R., Farrell, W.E. and Jenkins, H.A. (1996) Endoplasmic reticulum protein expression in recombinant NS0 myelomas grown in batch culture. *Biotechnology and Bioengineering*, **51**, 691-696.
- Dufner, A. and Thomas, G. (1999) Ribosomal S6 kinase signalling and the control of translation. *Experimental Cell Research*, **253**, 100-109.
- Dunn, M.J. (1997) Quantitative two-dimensional gel electrophoresis: From proteins to proteomes. *Biochemical Society Transactions*, **25**, 248-254.
- Edgington, S.M. (1992) Rites of passage: Moving biotech proteins through the ER. *Bio/Technology*, **10**, 1413-1420.
- Ellgaard, L. and Helelius, A. (2001) ER quality control: Towards an understanding at the molecular level. *Current Opinion in Cell Biology*, **13**, 431-437.
- Ferrari, D.M. and Soling, H.-D. (1999) The protein disulphide-isomerase family: Unravelling a string of folds. *Biochemical Journal*, **339**, 1-10.
- Fey, S.J. and Larsen, P.M. (2001) 2D or no 2D. *Current Opinion in Chemical Biology*, **5**, 26-33.
- Fields, S., Kohara, Y. and Lockhart, D.J. (1999) Functional Genomics. *Proceedings of the National Academy of Sciences of the USA*, **96**, 8825-8826.
- Fink, A.L. (1999) Chaperone-mediated protein folding. *Physiological Reviews*, **79**, 425-449.
- Forster, J., Gombert, A.K. and Nielsen, J. (2002) A functional genomics approach using metabolomics and *in silico* pathway analysis. *Biotechnology and Bioengineering*, **79**, 703-712.
- Frand, A.R., Cuozzo, J.W. and Kaiser, C.A. (2000) Pathways for protein disulphide bond formation. *Trends in Cell Biology*, **10**, 203-210.

- Freedman, R.B., Hirst, T.R. and Tuite, M.F. (1994) Protein disulphide isomerase: Building bridges in protein folding. *Trends in Biochemical Sciences*, **19**, 331-336.
- Friso, G., Kaiser, L., Raud, J. and Wikstrom, L. (2001) Differential protein expression in rat trigeminal ganglia during inflammation. *Proteomics*, **1**, 397-408.
- Fussenegger, M., Bailey, J.E., Hauser, H. and Mueller, P.P. (1999) Genetic optimization of recombinant glycoprotein production by mammalian cells. *Trends in Biotechnology*, **17**, 35-42.
- Fussenegger, M. and Betenbaugh, M.J. (2002) Metabolic Engineering II. Eukaryotic Systems. *Biotechnology and Bioengineering*, **79**, 509-531.
- Fussenegger, M., Fassnacht, D., Schwartz, R., Zanghi, J.A., Graf, M., Bailey, J.E. and Portner, R. (2000) Regulated overexpression of the survival factor *bcl-2* in CHO cells increases viable cell density in batch culture and increases DNA release in extended fixed-bed cultivation. *Cytotechnology*, **32**, 45-61.
- Fussenegger, M., Mazur, X. and Bailey, J.E. (1997) A novel cytostatic process enhances the productivity of Chinese hamster ovary cells. *Biotechnology and Bioengineering*, **55**, 927-939.
- Fussenegger, M., Moser, S. and Bailey, J.E. (1998b) Regulated multicistronic expression technology for mammalian metabolic engineering. *Cytotechnology*, **28**, 111-125.
- Fussenegger, M., Schlatter, S., Datwyler, D., Mazur, X. and Bailey, J.E. (1998a) Controlled proliferation by multigene metabolic engineering enhances the productivity of Chinese hamster ovary cells. *Nature Biotechnology*, **16**, 468-472.
- Gabor Miklos, G.L. and Maleszka, R. (2001) Protein functions and biological contexts. *Proteomics*, **1**, 169-178.
- Galeva, N. and Altermann, M. (2002) Comparison of one-dimensional and two-dimensional gel electrophoresis as a separation tool for proteomic analysis of rat liver microsomes: Cytochromes P450 and other membrane proteins. *Proteomics*, **2**, 713-722.
- Galfre, G. and Milstein, C. (1981) Preparation of monoclonal antibodies: Strategies and procedures. *Methods in Enzymology*, **73**, 3-46.
- Gething, M.-J. (1999) Role and regulation of the ER chaperone BiP. *Seminars in Cell & Developmental Biology*, **10**, 465-472.
- Gevaert, K. and Vandekerckhove, J. (2000) Protein identification methods in proteomics. *Electrophoresis*, **21**, 1145-1154.
- Gharahdaghi, F., Weinberg, C.R., Meagher, D.A., Imai, B.S. and Mische, S.M. (1999) Mass spectrometric identification of proteins from silver-stained polyacrylamide gel: A method for the removal of silver ions to enhance sensitivity. *Electrophoresis*, **20**, 601-605.

- Godovac-Zimmermann, J., Soskic, V., Poznanovic, S. and Brianza, F. (1999) Functional proteomics of signal transduction by membrane receptors. *Electrophoresis*, **20**, 952-961.
- Gorfien, S., Paul, B., Walowitz, J., Keem, R., Biddle, W. and Jayme, D. (2000) Growth of NS0 cells in protein-free, chemically defined medium. *Biotechnology Progress*, **16**, 682-687.
- Gorg, A. (1998) 2-D Electrophoresis. Using Immobilised pH Gradients. Principles and Methods. Amersham Pharmacia Biotech.
- Gorg, A. (2000a) Advances in 2D gel techniques. *Proteomics: A Trends Guide 2000*, 3-6.
- Gorg, A., Obermaier, C., Boguth, G., Harder, A., Scheibe, B., Wildgruber, R. and Weiss, W. (2000b) The current state of two-dimensional electrophoresis with immobilised pH gradients. *Electrophoresis*, **21**, 1037-1053.
- Goshe, M.B. and Smith, R.D. (2003) Stable isotope-coded proteomic mass spectrometry. *Current Opinion in Biotechnology*, **14**, 101-109.
- Gygi, S.P. and Aebersold, R. (2000) Mass Spectrometry and proteomics. *Current Opinion in Chemical Biology*, **4**, 489-494.
- Han, D.K., Eng, J., Zhou, H. and Aebersold, R. (2001) Quantitative profiling of differentiation-induced microsomal proteins using isotope-coded affinity tags and mass spectrometry. *Nature Biotechnology*, **19**, 946-951.
- Hanson, B.J., Schulenberg, B., Patton, W.F. and Capaldi, R.A. (2001) A novel subfractionation approach for mitochondrial proteins: A three-dimensional mitochondrial proteome map. *Electrophoresis*, **22**, 950-959.
- Harding, H.P., Calton, M., Urano, F., Novoa, I. and Ron, D. (2002) Transcriptional and translational control in the mammalian unfolded protein response. *Annual Reviews in Cell and Developmental Biology*, **18**, 575-599.
- Harry, J.L., Wilkins, M.R., Herbert, B.R., Packer, N.H., Gooley, A.A. and Williams, K.L. (2000) Proteomics: Capacity versus utility. *Electrophoresis*, **21**, 1071-1081.
- Hartl, F.-U. (1996) Molecular chaperones in cellular protein folding. *Nature*, **381**, 571-579.
- Hartl, F.-U. and Hayer-Hartl, M. (2002) Molecular chaperones in the cytosol: From nascent chain to folded protein. *Science*, **295**, 1852-1858.
- Haynes, P.A., Gygi, S.P., Figeys, D. and Aebersold, R. (1998) Proteome analysis: Biological assay or data archive? *Electrophoresis*, **19**, 1862-1871.

- Hayter, P.M., Curling, E.M.A., Baines, A.J., Jenkins, N., Salmon, I., Strange, P.G., Tong, J.M. and Bull, A.T. (1992) Glucose-limited chemostat culture of Chinese hamster ovary cells producing recombinant human Interferon-gamma. *Biotechnology and Bioengineering*, **39**, 327-335.
- Herbert, B.R., Sanchez, J.C. and Bini, L. (1997) *State of the art of two-dimensional electrophoresis*. Springer, Berlin.
- Hesse, F. and Wagner, R. (2000) Developments and improvements in the manufacturing of human therapeutics with mammalian cell cultures. *Trends in Biotechnology*, **18**, 173-180.
- Heukeshoven, J. and Dernick, R. (1988) Improved silver staining procedure for fast staining in Phastsystem development unit I. Staining of sodium dodecyl sulphate gels. *Electrophoresis*, **9**, 28-32.
- High, S., Lecomte, F.J.L., Russell, S.J., Abell, B.M. and Oliver, J.D. (2000) Glycoprotein folding in the endoplasmic reticulum: A tale of three chaperones? *FEBS Letters*, **476**, 38-41.
- Hills, A.E., Patel, A., Boyd, P. and James, D.C. (2001) Metabolic control of recombinant monoclonal antibody *N*-glycosylation in GS-NS0 cells. *Biotechnology and Bioengineering*, **75**, 239-251.
- Ho, S.C., Chaudhuri, S., Bachhawat, A., McDonald, K. and Pillai, S. (2000) Accelerated proteasomal degradation of membrane Ig heavy chains. *Journal of Immunology*, **164**, 4713-4719.
- Hochstrasser, D.F. (1998) Proteome in perspective. *Clinical Chemistry and Laboratory Medicine*, **36**, 825-836.
- Hoogland, C., Sanchez, J.C., Walther, D., Baujard, V., Baujard, O., Tonella, L., Hochstrasser, D.F. and Appel, R.D. (1999) Two-dimensional electrophoresis resources available from ExPASy. *Electrophoresis*, **20**, 358-3571.
- Hoving, S., Voshol, H. and van Oostrum, J. (2000) Towards high performance two-dimensional gel electrophoresis using ultrazoom gels. *Electrophoresis*, **21**, 2617-2621.
- Huang, P. and Oliff, A. (2001) Signalling pathways in apoptosis as potential targets for cancer therapy. *Trends in Cell Biology*, **11**, 343-348.
- Humphrey-Smith, I. and Blackstock, W.P. (1997a) Proteome analysis: Genomics via the output rather than the input code. *Journal of Protein Chemistry*, **16**, 537-544.
- Humphrey-Smith, I., Cordwell, S.J. and Blackstock, W.P. (1997b) Proteome research: Complementarity and limitations with respect to the RNA and DNA worlds. *Electrophoresis*, **18**, 1217-1242.

- Ibarra, N., Watanabe, S., Bi, J.-X., Shuttleworth, J. and Al-Rubeai, M. (2003) Modulation of cell cycle for enhancement of antibody productivity in perfusion culture of NS0 cells. *Biotechnology Progress*, **19**, 224-228.
- Iscove, N.N., Guilbert, L.J. and Weyman, C. (1980) Complete replacement of serum in primary cultures of erythropoietin-dependent red cell precursors [CFU-E] by albumin, transferrin, iron, unsaturated fatty acid, lecithin and cholesterol. *Experimental Cell Research*, **126**, 121-126.
- Iscove, N.N. and Melchers, F. (1978) Complete replacement of serum by albumin, transferrin and soybean lipid in cultures of lipopolysaccharide-reactive B lymphocytes. *Journal of Experimental Medicine*, **147**, 923-933.
- Jaattela, M., Wissing, D., Kokholm, K., Kallunki, T. and Egeblad, M. (1998) Hsp70 exerts its anti-apoptotic function downstream of caspase-3-like proteases. *EMBO Journal*, **17**, 6124-6134.
- Jacob, U. and Buchner, J. (1994) Assisting spontaneity: The role of Hsp90 and small Hsps as molecular chaperones. *Trends in Biochemical Sciences*, **19**, 205-211.
- James, P. (1997a) Breakthroughs and views of genomes and proteomes. *Biochemical and Biophysical Research Communications*, **231**, 1-6.
- James, P. (1997b) Protein identification in the post-genome era: The rapid rise of proteomics. *Quarterly Review of Biophysics*, **30**, 279-331.
- Johnson, S., Michalak, M., Opas, M. and Eggleton, P. (2001) The ins and outs of calreticulin: From the ER lumen to the extracellular space. *Trends in Cell Biology*, **11**, 122-129.
- Jung, D., Cote, S., Drouin, M., Simard, C. and Lemieux, R. (2002) Inducible expression of Bcl-X_L restricts apoptosis resistance to the antibody secretion phase in hybridoma cultures. *Biotechnology and Bioengineering*, **79**, 180-187.
- Kaufman, R.J. (1990) Selection and coamplification of heterologous genes in mammalian cells. *Methods in Enzymology*, **185**, 537-566.
- Kaul, S.C., Taira, K., Pereira-Smith, O.M. and Wadhwa, R. (2002) Mortalin: Present and Prospective. *Experimental Gerontology*, **37**, 1157-1164.
- Keen, M.J. and Hale, C. (1996) The use of serum-free medium for the production of functionally active humanised monoclonal antibody from NS0 mouse myeloma cells engineered using glutamine synthetase as a selectable marker. *Cytotechnology*, **18**, 207-217.
- Kelly, B.D. (2001) Bioprocessing of therapeutic proteins. *Current Opinion in Biotechnology*, **12**, 173-174.

- Kemper, C., Berggren, K., Diwu, Z. and Patton, W.F. (2001) An improved, chemoluminescent europium-based stain for detection of electroblotted proteins on nitrocellulose or polyvinylidene difluoride membranes. *Electrophoresis*, **22**, 881-889.
- Kettman, J.R., Coleclough, C., Frey, J.R. and Lefkovits, I. (2002) Clonal proteomics: One gene-family of proteins. *Proteomics*, **2**, 624-631.
- Kiang, J.G. and Tsokos, G.C. (1998) heat shock protein 70 kDa: Molecular biology, biochemistry, and physiology. *Pharmacology and Therapeutics*, **80**, 183-201.
- Klose, J. (1975) Protein mapping by combined isoelectric focussing and electrophoresis of mouse tissues. A novel approach to testing for induced point mutation in mammals. *Humangenetik*, **26**, 231-243.
- Klose, J. (1999) Genotypes and phenotypes. *Electrophoresis*, **20**, 643-652.
- Klose, J. and Kobalz, U. (1995) Two-dimensional electrophoresis of proteins: An updated protocol and implications for a functional analysis of the genome. *Electrophoresis*, **16**, 1034-1059.
- Kohno, K., Normington, K., Sambrook, J., Gething, M.-J. and Mori, K. (1993) The promoter region of the yeast KAR2 (BiP) gene contains a regulatory domain that responds to the presence of unfolded proteins in the endoplasmic reticulum. *Molecular and Cellular Biology*, **13**, 877-890.
- Kovarova, H., Hajduch, M., Livingstone, M., Dzubak, P. and Lefkovits, I. (2003) Analysis of state-specific phosphorylation of proteins by two-dimensional gel electrophoresis approach. *Journal of Chromatography B*, **787**, 53-61.
- Laemmli, U.K. (1970) Cleavage of structural proteins during the assembly of the head of bacteriophage T4. *Nature*, **227**, 680-685.
- Laken, H.A. and Leonard, M.W. (2001) Understanding and modulating apoptosis in industrial cell culture. *Current Opinion in Biotechnology*, **12**, 175-179.
- Lambert, N. and Merten, O.-W. (1997) Effect of serum-free and serum-containing medium on cellular levels of ER-based proteins in various mouse hybridoma cell lines. *Biotechnology and Bioengineering*, **54**, 165-180.
- Lasunskaja, E.B., Fridlianskaia, I.I., Darieva, Z.A., da Silva, M.S.R., Kanashiro, M.M. and Margulis, B.A. (2002) Transfection of NS0 myeloma fusion partner cells with hsp70 gene results in higher hybridoma yield by improving cellular resistance to apoptosis. *Biotechnology and Bioengineering*, **81**, 496-504.
- Lauber, W.M., Carroll, J.A., Dufield, D.R., Kiesel, J.R., Radabaugh, M.R. and Malone, J.P. (2001) Mass spectrometry compatibility of two-dimensional gel protein stains. *Electrophoresis*, **22**, 906-918.

- Lee, K.H. (2001) Proteomics: A technology-driven and technology-limited discovery science. *Trends in Biotechnology*, **19**, 217-222.
- Lee, K.H., Harrington, M.G. and Bailey, J.E. (1996) Two-dimensional electrophoresis of proteins as a tool in the metabolic engineering of cell cycle regulation. *Biotechnology and Bioengineering*, **50**, 336-340.
- Lee, Y.K., Brewer, J.W., Hellman, R. and Hendershot, L.M. (1999) BiP and immunoglobulin light chain cooperate to control the folding of heavy chain and ensure the fidelity of immunoglobulin assembly. *Molecular Biology of the Cell*, **10**, 2209-2219.
- Lefkovits, I. (2003) Functional and structural proteomics: A critical appraisal. *Journal of Chromatography B*, **787**, 1-10.
- Lengwehasatit, I. and Dickson, A.J. (2002) Analysis of the role of GADD153 in the control of apoptosis in NS0 myeloma cells. *Biotechnology and Bioengineering*, **80**, 719-730.
- Lilley, K.S., Razzaq, A. and Dupree, P. (2001) Two-dimensional gel electrophoresis: Recent advances in sample preparation, detection and quantitation. *Current Opinion in Chemical Biology*, **6**, 46-50.
- Llewellyn, D.H., Johnson, S. and Eggleton, P. (2000) Calreticulin comes of age. *Trends in Cell Biology*, **10**, 399-402.
- Lopez, M.F. (2000) Better approaches to finding the needle in a haystack: Optimizing proteome analysis through automation. *Electrophoresis*, **21**, 1082-1093.
- Lopez, M.F. and Pluskal, M.G. (2003) Protein micro- and macro-arrays: Digitizing the proteome. *Journal of Chromatography B*, **787**, 19-27.
- Lubiniecki, A.S. (1998) Historical reflections on cell culture engineering. *Cytotechnology*, **28**, 139-145.
- Lui, M., Tempst, P. and Erdjument-Bromage, H. (1996) Methodical analysis of protein-nitrocellulose interactions to design a refined digestion protocol. *Analytical Biochemistry*, **241**, 156-166.
- Malone, J.P., Radabaugh, M.R., Leimgruber, R.M. and Gerstenecker, G.S. (2001) Practical aspects of fluorescent staining for proteomic applications. *Electrophoresis*, **22**, 919-932.
- Manabe, T. (2003) Analysis of complex protein-polypeptide systems for proteomic studies. *Journal of Chromatography B*, **787**, 29-41.
- Mann, M. and Jensen, O.N. (2003) Proteomic analysis of post-translational modifications. *Nature Biotechnology*, **21**, 255-261.

- Marino, M., Corti, A., Ippolito, A., Cassani, G. and Fassina, G. (1997) Effect of bench-scale culture conditions on murine IgG heterogeneity. *Biotechnology and Bioengineering*, **54**, 17-25.
- Mastrangelo, A.J., Hardwick, J.M., Zou, S. and Betenbaugh, M.J. (2000) Part II. Overexpression of Bcl-2 family members enhances survival of mammalian cells in response to various culture insults. *Biotechnology and Bioengineering*, **67**, 555-564.
- Mayer, M., Kies, U., Kammermeier, R. and Buchner, J. (2000) BiP and PDI cooperate in the oxidative folding of antibodies *in vitro*. *Journal of Biological Chemistry*, **275**, 29421-29425.
- McDonough, J.L., Neverova, I. and Van Eyk, J.E. (2002) Proteomic analysis of human biopsy samples by single two-dimensional electrophoresis: Coomassie, silver, mass spectrometry, and western blotting. *Proteomics*, **2**, 978-987.
- Meents, H., Enenkel, B., Eppenberger, H.M., Werner, R.G. and Fussenegger, M. (2002) Impact of coexpression and coamplification of sICAM and antiapoptosis determinants bcl-2/ bcl-x_L on productivity, cell survival, and mitochondria number in CHO-DG44 grown in suspension and serum-free media. *Biotechnology and Bioengineering*, **80**, 706-716.
- Melnick, J., Dul, J.L. and Argon, Y. (1994) Sequential interaction of the chaperones BiP and GRP94 with immunoglobulin chains in the endoplasmic reticulum. *Nature*, **370**, 373-375.
- Merril, C.R., Dunau, M.L. and Goldman, D. (1981) A rapid sensitive silver stain for polypeptides in polyacrylamide gels. *Analytical Biochemistry*, **110**, 201-207.
- Michalak, M., Corbett, E.F., Mesaeli, N., Nakamura, K. and Opas, M. (1999) Calreticulin: One protein, one gene, many functions. *Biochemical Journal*, **344**, 281-292.
- Michalski, W. and Shiell, B.J. (1999) Strategies for analysis of electrophoretically separated proteins and peptides. *Analytica Chimica Acta*, **383**, 27-46.
- Miller Jr, M.D., Acey, R.A., Yu-Tzu Lee, L. and Edwards, A.J. (2001) Digital imaging considerations for gel electrophoresis analysis systems. *Electrophoresis*, **22**, 791-800.
- Minch, S.L., Kallio, P.T. and Bailey, J.E. (1997) Tissue plasminogen activator co-expressed in Chinese hamster ovary cells with $\alpha(2,6)$ -sialtransferase contains NeuAc $\alpha(2,6)$ Gal $\beta(1,4)$ Glc-N-AcR linkages. *Biotechnology Progress*, **11**, 348-351.
- Mitchell, P. (2003) In the pursuit of industrial proteomics. *Nature*, **21**, 233-237.
- Mo, W. and Karger, B.L. (2002) Analytical aspects of mass spectrometry and proteomics. *Current Opinion in Chemical Biology*, **6**, 666-675.

- Moller, A., Malerczyk, C., Volker, U., Stoppler, H. and Maser, E. (2002) Monitoring daunorubicin-induced alterations in protein expression in pancreas carcinoma cells by two-dimensional gel electrophoresis. *Proteomics*, **2**, 697-705.
- Molloy, M.P. (2000) Two-dimensional electrophoresis of membrane proteins using immobilised pH gradients. *Analytical Biochemistry*, **280**, 1-10.
- Murray, K., Ang, C.E., Gull, K., Hickman, J.A. and Dickson, A.J. (1996) NSO myeloma cell death: Influence of *bcl-2* overexpression. *Biotechnology and Bioengineering*, **51**, 298-304.
- Noiva, R. (1999) Protein disulfide isomerase: The multifunctional redox chaperone of the endoplasmic reticulum. *Seminars in Cell & Developmental Biology*, **10**, 481-493.
- O'Farrell, P.H. (1975) High resolution two-dimensional electrophoresis of proteins. *Journal of Biological Chemistry*, **250**, 4007-4021.
- Oguri, T., Takahata, I., Katsuta, K., Nomura, E., Hidaka, M. and Inagaki, N. (2002) Proteome analysis of rat hippocampal neurons by multiple large gel two-dimensional electrophoresis. *Proteomics*, **2**, 666-672.
- Oh-Ishi, M. and Maeda, T. (2002) Separation techniques for high-molecular-mass proteins. *Journal of Chromatography B*, **771**, 49-66.
- Ohlmeier, S., Scharf, C. and Hecker, M. (2000) Alkaline proteins of *Bacillus subtilis*: First steps towards a two-dimensional alkaline master gel. *Electrophoresis*, **21**, 3701-3709.
- Osman, J.O., Birch, J. and Varley, J. (2002) The response of GS-NS0 myeloma cells to single and multiple pH perturbations. *Biotechnology and Bioengineering*, **79**, 398-407.
- Papoutsakis, E.T. (1998) Express together and conquer. *Nature Biotechnology*, **16**, 416-417.
- Parcellier, A., Gurbuxani, S., Schmitt, E., Solary, E. and Garrido, C. (2003) Heat shock proteins, cellular chaperones that modulate mitochondrial cell death pathways. *Biochemical and Biophysical Research Communications*, **304**, 505-512.
- Patil, C. and Walter, P. (2001) Intracellular signalling from the endoplasmic reticulum to the nucleus: The unfolded protein response in yeast and mammals. *Current Opinion in Cell Biology*, **13**, 349-356.
- Patton, W.F. (1999) Proteome analysis II. Protein subcellular redistribution: Linking physiology to genomics via the proteome and separation technologies involved. *Journal of Chromatography B*, **722**, 203-223.
- Patton, W.F. (2002) Detection technologies in proteome analysis. *Journal of Chromatography B*, **771**, 3-31.

- Pennington, S.R., Wilkins, M.R., Hochstrasser, D.F. and Dunn, M.J. (1997) Proteome analysis: From protein characterization to biological function. *Trends in Cell Biology*, **7**, 168-173.
- Perkins, D.N., Pappin, D.J.C., Creasy, D.M. and Cottrell, J.S. (1999) Probability-based protein identification by searching sequence databases using mass spectrometry data. *Electrophoresis*, **20**, 3551-3567.
- Potter, M. and Boyce, C.R. (1962) Induction of plasma cell neoplasma in strain BALB/c mice with mineral oil and mineral oil adjuvants. *Nature*, **193**, 1086-1087.
- Proud, C.G. (2002) Regulation of mammalian translation factors by nutrients. *European Journal of Biochemistry*, **269**, 5338-5349.
- Quadroni, M. and James, P. (1999) Proteomics and automation. *Electrophoresis*, **20**, 664-677.
- Rabilloud, T. (1999) *Solubilisation of proteins in 2-D electrophoresis*. Humana Press, New Jersey.
- Rabilloud, T., Adessi, C., Giraudel, A. and Lunardi, J. (1997) Improvement of the solubilisation of proteins in two-dimensional electrophoresis with immobilised pH gradients. *Electrophoresis*, **18**, 307-316.
- Ramagli, L.S. (1999) *Quantifying protein in 2-D PAGE solubilising buffers*. Humana Press, New Jersey.
- Reichert, J.M. (2000) New biopharmaceuticals in the USA: Trends in development and marketing approvals 1995-1999. *Trends in Biotechnology*, **18**, 364-369.
- Renner, G., Lee, K.H., Hatzimanikatis, V., Bailey, J.E. and Eppenberger, H.M. (1995) Recombinant cyclin E expression activates proliferation and obviates surface attachment of Chinese hamster ovary (CHO) cells in protein-free media. *Biotechnology and Bioengineering*, **47**, 476-482.
- Rhoads, R.E. (1999) Signal transduction pathways that regulate eukaryotic protein synthesis. *Journal of Biological Chemistry*, **274**, 30337-30340.
- Richarme, G. (1998) Protein-disulphide isomerase activity of elongation factor EF-Tu. *Biochemical and Biophysical Research Communications*, **252**, 156-161.
- Robinson, D.K., Chan, C.P., Ip, C.Y., Tsai, P.K., Tung, J., Seamans, T.C., Lenny, A.B., Lee, D.K., Irwin, J. and Silberklang, M. (1994) Characterisation of a recombinant antibody produced in the course of a high yield fed-batch process. *Biotechnology and Bioengineering*, **44**, 727-735.
- Sabounchi-Schutt, F., Astrom, J., Olsson, I., Eklund, A., Grunewald, J. and Bjellqvist, B. (2000) An immobilised DryStrip application method enabling high-capacity two-dimensional gel electrophoresis. *Electrophoresis*, **21**, 3649-3656.

- Samali, A., Cai, J., Zhivotovsky, B., Jones, D.P. and Orrenius, S. (1999) Presence of a pro-apoptotic complex of pre-caspase-3, Hsp60 and Hsp10 in the mitochondrial fraction of Jurkat cells. *EMBO Journal*, **18**, 2040-2048.
- Samali, A. and Cotter, T.G. (1996) Heat shock proteins increase resistance to apoptosis. *Experimental Cell Research*, **223**, 163-170.
- Santoni, V., Molloy, M.P. and Rabilloud, T. (2000) Membrane proteins and proteomics: Un amour impossible? *Electrophoresis*, **21**, 1054-1070.
- Sauer, P.W., Burky, J.E., Wesson, M.C., Sternard, H.D. and Qu, L. (2000) A high-yielding, generic fed-batch cell culture process for production of recombinant antibodies. *Biotechnology and Bioengineering*, **67**, 585-597.
- Sauerwald, T.M., Oyler, G.A. and Betenbaugh, M.J. (2003) Study of caspase inhibitors for limiting death in mammalian cell culture. *Biotechnology and Bioengineering*, **81**, 329-340.
- Schiene-Fischer, C. and Yu, C. (2001) Receptor accessory folding helper enzymes: The functional role of peptidyl prolyl *cis-trans* isomerases. *FEBS Letters*, **495**, 1-6.
- Schroder, M., Schafer, R. and Friedl, P. (2002) Induction of protein aggregation in an early secretory compartment by elevation of expression level. *Biotechnology and Bioengineering*, **78**, 131-140.
- Schuler, H. (2001) ATPase activity and conformational changes in the regulation of actin. *Biochimica et Biophysica Acta*, **1549**, 137-147.
- Scrivener, E., Barry, R., Platt, A., Caivert, R., Masih, G., Hextall, P., Soloviev, M. and Terrett, J. (2003) Peptidomics: A new approach to affinity protein microarrays. *Proteomics*, **3**, 122-128.
- Sehgal, S.N. (1998) Rapamune (RAPA, rapamycin, sirolimus): Mechanism of action immunosuppressive effects results from blockade of signal transduction and inhibition of cell cycle progression. *Clinical Biochemistry*, **31**, 335-340.
- Shevchenko, A., Wilm, M., Vorm, O. and Mann, M. (1996) Mass spectrometric sequencing of proteins from silver-stained polyacrylamide gels. *Analytical Chemistry*, **68**, 850-858.
- Smales, C.M., Birch, J.R., Racher, A.J., Marshall, C.T. and James, D.C. (2003) Evaluation of individual protein errors in silver-stained two-dimensional gels. *Biochemical and Biophysical Research Communications*, **306**, 1050-1055.
- Smolke, C.D. and Keasling, J.D. (2002) Effect of copy number and mRNA processing and stabilisation on transcript and protein levels from an engineered dual-gene operon. *Biotechnology and Bioengineering*, **78**, 412-424.
- Sorger, P.K. and Pelham, R.B. (1987) Cloning and expression of a gene encoding hsc73, the major hsp70-like protein in unstressed rat cells. *EMBO Journal*, **6**, 993-998.

- Soskic, V., Gorlach, M., Poznanovic, S., Boehmer, F.D. and Godovac-Zimmermann, J. (1999) Functional proteomic analysis of signal transduction pathways of the platelet-derived growth factor Beta receptor. *Biochemistry*, **38**, 1757-1764.
- Spibey, C.A., Jackson, P. and Herick, K. (2001) A unique charge-coupled device/xenon arc lamp based imaging system for the accurate detection and quantitation of multicolour fluorescence. *Electrophoresis*, **22**, 829-836.
- Steinberg, T.H., Haugland, R.P. and Singer, V.L. (1996) Applications of SYPRO orange and SYPRO red protein stains. *Analytical Biochemistry*, **239**, 238-245.
- Strutzenberger, K., Borth, N., Kunert, R., Steinfeldner, W. and Katinger, H. (1999) Changes during subclone development and ageing of human antibody-producing recombinant CHO cells. *Journal of Biotechnology*, **69**, 215-226.
- Sugahara, T., Shimizu, S., Abiru, M., Matsuoka, S. and Sasaki, T. (1998) A novel function of enolase from rabbit muscle: An immunoglobulin production stimulating factor. *Biochimica et Biophysica Acta*, **1380**, 163-176.
- Takano, S., Wadhwa, R., Mitsui, Y. and Kaul, S.C. (2001) Identification and characterisation of molecular interactions between glucose-regulated proteins (GRPs) mortalin/GRP75/peptide-binding protein 74 (PBP74) and GRP94. *Biochemical Journal*, **357**, 393-398.
- Tao, W.A. and Aebersold, R. (2003) Advances in quantitative proteomics via stable isotope tagging and mass spectrometry. *Current Opinion in Biotechnology*, **14**, 110-118.
- Taylor, S.W., Fahy, E., Zhang, B., Glenn, G.M., Warnock, D.E., Wiley, S., Murphy, A.N., Gaucher, S.P., Capaldi, R.A., Gibson, B.W. and Ghosh, S.S. (2003) Characterisation of the human heart mitochondrial proteome. *Nature Biotechnology*, **21**, 281-286.
- Tey, B.T., Singh, R.P., Piredda, L., Piacentini, M. and Al-Rubeai, M. (2000) Bcl-2 mediated suppression of apoptosis in myeloma NS0 cultures. *Journal of Biotechnology*, **79**, 147-159.
- Thyberg, J. and Moskalewski, S. (1999) Role of microtubules in the organisation of the Golgi Complex. *Experimental Cell Research*, **246**, 263-279.
- Tonge, R., Shaw, J., Middleton, B., Rowlinson, R., Rayner, S., Young, J., Pognan, F., Hawkins, E., Currie, I. and Davison, M. (2001) Validation and development of fluorescence two-dimensional differential gel electrophoresis proteomics technology. *Proteomics*, **1**, 377-396.
- Unlu, M. (1999) Difference gel electrophoresis. *Biochemical Society Transactions*, **27**, 547-559.

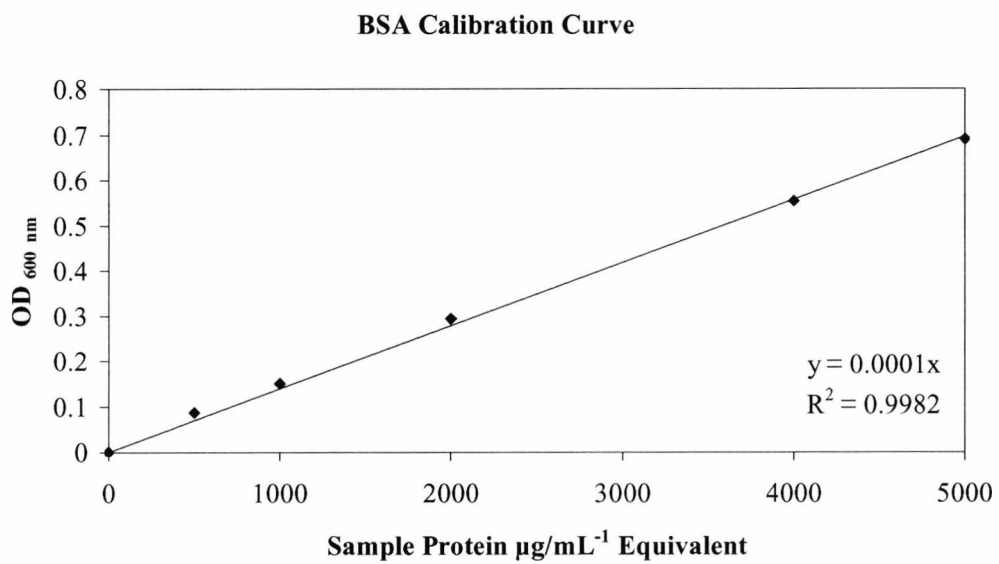
- Urquhart, B.L., Cordwell, S.J. and Humphery-Smith, I. (1998) Comparison of predicted and observed properties of proteins encoded in the genome of *Mycobacterium Tuberculosis* H37Rv. *Biochemical and Biophysical Research Communications*, **253**, 70-79.
- van Anken, E., Romijn, E.P., Maggioni, C., Mezghrani, A., Sitia, R., Braakman, I. and Heck, A.J.R. (2003) Sequential waves of functionally related proteins are expressed when B cells prepare for antibody secretion. *Immunity*, **18**, 243-253.
- Van Dyk, D.D., Misztal, D.R., Wilkins, M.R., Mackintosh, J.A., Poljak, A., Varnai, J.C., Teber, E., Walsh, B.J. and Gray, P.P. (2003) Identification of cellular changes associated with increased production of human growth hormone in a recombinant Chinese hamster ovary cell line. *Proteomics*, **3**, 147-156.
- Verhaert, P., Uttenweiler-Joseph, S., de Vries, M., Loboda, A., Ens, W. and Standing, K.G. (2001) Matrix-assisted laser desorption/ionisation quadrupole time-of-flight mass spectrometry: An elegant tool for peptidomics. *Proteomics*, **1**, 118-131.
- Voisard, D., Meuwly, F., Ruffieux, P.-A., Baer, G. and Kadouri, A. (2003) Potential of cell retention techniques for large-scale high density perfusion culture of suspended mammalian cells. *Biotechnology and Bioengineering*, **82**, 751-765.
- Wang, C.-C. (2002) Protein disulphide isomerase as an enzyme and a chaperone in protein folding. *Methods in Enzymology*, **348**, 66-75.
- Washburn, M.P. and Yates, J.R.I. (2000) New methods of proteome analysis: Multidimensional chromatography and mass spectrometry. *Trends in Biotechnology (supplement)*, **7**, 27-30.
- Wasinger, V.C., Cordwell, S.J., Cerpa-Poljak, A., Yan, J.X., Gooley, A.A., Wilkins, M.R., Duncan, M.W., Harris, R., Williams, K.L. and Humphrey-Smith, I. (1995) Progress with gene-product mapping of the mollicutes: *Mycoplasma genitalium*. *Electrophoresis*, **16**, 1090-1094.
- Wasinger, V.C. and Corthals, G.L. (2002) Proteomic tools for biomedicine. *Journal of Chromatography B*, **771**, 33-48.
- Watanabe, S., Shuttleworth, J. and Al-Rubeai, M. (2002) Regulation of cell cycle and productivity in NS0 cells by the overexpression of p21^{cip1}. *Biotechnology and Bioengineering*, **77**, 1-7.
- Westbrook, J.A., Yan, J.X., Wait, R. and Dunn, M.J. (2001) A combined radiolabelling and silver staining technique for improved visualisation, localisation, and identification of proteins separated by two-dimensional gel electrophoresis. *Proteomics*, **1**, 370-376.
- Wilkins, M.R., Sanchez, J.C., Williams, K.L. and Hochstrasser, D.F. (1996) Current challenges and future applications for protein maps and post-translational vector maps in proteome projects. *Electrophoresis*, **17**, 830-838.

- Williams, K.L. (1999) Genomes and Proteomes: Towards a multidimensional view of biology. *Electrophoresis*, **20**, 678-688.
- Wingren, C., Ingvarsson, J., Lindstedt, M. and Borrebaeck, C.A.K. (2003) Recombinant antibody microarrays- a viable option? *Nature Biotechnology*, **21**, 223.
- Wu, C.C. and Yates, J.R.I. (2003) The application of mass spectrometry to membrane proteomics. *Nature*, **21**, 262-267.
- Wu, C.C., Yates, J.R.I., Neville, M.C. and Howell, K.E. (2000) Proteomic analysis of two functional states of the Golgi complex in mammary epithelial cells. *Traffic*, **1**, 769-782.
- Xanthoudakis, S., Roy, S., Rasper, D., Hennessey, T., Aubin, Y., Cassady, R., Tawa, P., Ruel, R., Rosen, A. and Nicholson, D.W. (1999) Hsp60 accelerates the maturation of pro-caspase-3 by upstream activator proteases during apoptosis. *EMBO Journal*, **18**, 2049-2056.
- Yamada, K. and Noguchi, T. (1999) Nutrient and hormonal regulation of pyruvate kinase gene expression. *Biochemical Journal*, **337**, 1-11.
- Yanagida, M. (2002) Functional proteomics: Current achievements. *Journal of Chromatography B*, **771**, 89-106.
- Yoon, S.K., Song, J.Y. and Lee, G.M. (2003) Effect of low culture temperature on specific productivity, transcription level, and heterogeneity of erythropoietin in Chinese hamster ovary cells. *Biotechnology and Bioengineering*, **82**, 289-298.
- Zhou, H., Roy, S., Schulman, H. and Natan, M.J. (2001) Solution and chip arrays in protein profiling. *Trends in Biotechnology (supplement)*, **19**, S35-S39.
- Zhou, W., Biliba, T.B., Glazomitsky, K., Montalvo, J., Chan, C.P., Distefano, D.J., Munshi, S., Robinson, D.K., Buckland, B.C. and Aunins, J.G. (1996) Large scale production of recombinant mouse and rat growth hormone by fed-batch GS-NS0 cell cultures. *Cytotechnology*, **22**, 239-250.
- Zhou, W., Chen, C.-C., Buckland, B. and Aunins, J. (1997) Fed-batch culture of recombinant NS0 myeloma cells with high monoclonal antibody production. *Biotechnology and Bioengineering*, **55**, 783-792.
- Zong, Q., Schummer, M., Hood, L. and Morris, D.R. (1999) Messenger RNA translation state: The second dimension of high-throughput expression Screening. *Proceedings of the National Academy of Sciences of the USA*, **96**, 10632-10636.
- Zuo, Z., Echan, L., Hembach, P., Tang, H.Y., Speicher, K.D., Santoli, D. and Speicher, D.W. (2001) Towards global analysis of mammalian proteomes using sample prefractionation prior to narrow pH range two-dimensional gels and using one-dimensional gels for insoluble large proteins. *Electrophoresis*, **22**, 1603-1615.

Appendix I

Determination of Protein Content

The protein content from whole NS0 cell extracts was determined using a Modified Bradford assay calibrated against a BSA standard, followed by interpolation:



Appendix II

Determination of Power Input for 1.8 L Applikon Bioreactor

The power input by agitation into the Applikon bioreactor was calculated by the following equation:

$$P = P_o \rho N^3 D^5$$

P = Power (Watts)

P_o = Power number

ρ = Fluid density (kg m⁻³)

N = Impellor speed (min⁻¹)

D = Impellor diameter (m)

P_o for the Applikon axial impellor was 3.0, fluid density is approximately 1000 kg m⁻³ (assumed to be the same as water), impellor diameter is 4.5 cm (0.045 m). Therefore, at an agitation rate of 150 r.p.m (2.5 s⁻¹) in a 1.8 L volume, the power input is:

$$0.005 \text{ W L}^{-1}$$

Appendix III

Determination of Specific Growth Rates and Productivity

Specific growth rates (μ), during exponential growth phase in culture, were calculated using the following equation:

$$\mu = (\ln N - \ln N_0)/t$$

Specific consumption of glucose, production of lactate were calculated as follows:

$$K = C - C_0/T (\ln N - \ln N_0/N - N_0)$$

Specific productivity of rIgG was calculated using the following equation:

$$q_{\text{MAb}} = (P - P_0/N + N_0) 2/\text{Number of days}$$

The generation number was calculated as follows:

$$X = (\log N - \log N_0)/\log 2$$

The doubling time was calculated thus:

$$td = T/X$$

μ = Specific growth rate (h^{-1})

K = Specific consumption or production rate ($\mu\text{mol } 10^6 \text{ cells}^{-1} \text{ h}^{-1}$)

N = Final cell number ($\times 10^6 \text{ cell mL}^{-1}$)

N_0 = Initial cell number ($\times 10^6 \text{ cell mL}^{-1}$)

t = Time (h)

C = Final concentration (mM)

C_0 = Initial concentration (mM)

T = Elapsed time (h)

X = Generation number

td = Doubling time

q_{MAb} = Specific productivity ($\text{pg cell}^{-1} \text{ h}^{-1}$)

P = Final product concentration ($\mu\text{g mL}^{-1}$)

P_0 = Initial product concentration ($\mu\text{g mL}^{-1}$)

Appendix IV

Media Composition of DMEM/F12

COMPONENT	Molecular Weight	Conc. (mg L⁻¹)	Molarity (mM)
INORGANIC SALTS			
Calcium chloride (CaCl ₂)	111	116.6	1.05
Cupric sulfate (CuSO ₄ ·5H ₂ O)	250	0.0013	0.0000052
Ferric nitrate (Fe(NO ₃) ₃ ·9H ₂ O)	404	0.05	0.00012
Ferrous sulfate (FeSO ₄ ·7H ₂ O)	278	0.417	0.0015
Potassium chloride (KCl)	75	311.8	4.157
Magnesium chloride (MgCl ₂ ·6H ₂ O)	203	61	0.3
Magnesium sulfate (MgSO ₄ ·7H ₂ O)	246	100	0.407
Sodium chloride (NaCl)	58	6995	120.6
Sodium bicarbonate (NaHCO ₃)	84	2438	29.02
Sodium phosphate, monobasic (NaH ₂ PO ₄ ·H ₂ O)	138	62.5	0.453
Sodium phosphate, (Na ₂ HPO ₄ ·7H ₂ O)	264	134	0.508
Zinc sulfate (ZnSO ₄ ·7H ₂ O)	288	0.432	0.0015
OTHER COMPOUNDS			
D-Glucose	180	3151	17.51
Hypoxanthine-Na	159	2.39	0.015
Linoleic Acid	280	0.042	0.00015
DL-68-Thioctic Acid	208.3	0.105	0.0005
Phenol Red	398	8.1	0.020
Sodium Putrescine-2HCl	161	0.081	0.0005
Sodium Pyruvate	110	55	0.500
AMINO ACIDS			
L-Alanine	89	4.45	0.050
L-Arginine hydrochloride	211	147.5	0.699
L-Asparagine-H ₂ O	150	7.5	0.050
L-Aspartic acid	133	6.65	0.050
L-Cysteine-HCl-H ₂ O	176	17.56	0.100
L-Cysteine-2HCl	194	31.29	0.160
L-Glutamic acid	147	7.35	0.050
Glycine	75	18.75	0.250
L-Histidine-HCl-H ₂ O	210	31.48	0.150
L-Isoleucine	131	54.47	0.416
L-Leucine	131	59.05	0.451
L-Lysine hydrochloride	183	91.25	0.499
L-Methionine	149	17.24	0.116
L-Phenylalanine	165	35.48	0.215
L-Proline	115	17.25	0.150
L-Serine	105	26.25	0.250
L-Threonine	119	53.45	0.449
L-Tryptophan	204	9.02	0.044
L-Tyrosine-2Na-2H ₂ O	261	55.79	0.214
L-Valine	117	25.85	0.221
VITAMINS			
Biotin	244	0.0035	0.0000143
D-Calcium pantothenate	477	2.24	0.0046
Choline chloride	140	8.98	0.0641
Folic acid	441	2.65	0.006
i-Inositol	180	12.6	0.07
Nicotinamide	122	2.02	0.0165
Pyridoxine hydrochloride	206	2.031	0.00986
Riboflavin	376	0.219	0.00058
Thiamine hydrochloride	337	2.17	0.0064
Thymidine	242	0.365	0.0015
Vitamin B12	1355	0.68	0.000005

Appendix V

Media Composition of IMEM

COMPONENT	Molecular Weight	Conc. (mg L⁻¹)	Molarity (mM)
INORGANIC SALTS			
Calcium chloride (CaCl ₂ ·2H ₂ O)	147	219	1.500
Potassium chloride (KCl)	75	330	4.400
Potassium Nitrate (KNO ₃)	101	0.076	0.00075
Magnesium sulfate (MgSO ₄)	120	97.67	0.800
Sodium chloride (NaCl)	58	4505	77.700
Sodium bicarbonate (NaHCO ₃)	84	3024	36.000
Sodium phosphate, monobasic (NaH ₂ PO ₄)	138	109	0.800
Sodium Selenite (Na ₂ SeO ₃ ·5H ₂ O)	263	0.017	0.000065
OTHER COMPOUNDS			
D-Glucose	180	4500	25.000
HEPES	238	5958	25.000
Phenol Red	398	16	0.040
Sodium Pyruvate	110	110	1.000
AMINO ACIDS			
L-Alanine	89	25	0.300
L-Arginine hydrochloride	211	84	0.400
L-Asparagine-H ₂ O	150	28.4	0.190
L-Aspartic acid	133	30	0.222
L-Cysteine-2HCl	194	91.24	0.470
L-Glutamic acid	147	75	0.500
Glycine	75	30	0.400
L-Histidine-HCl-H ₂ O	210	42	0.200
L-Isoleucine	131	105	0.800
L-Leucine	131	105	0.800
L-Lysine hydrochloride	183	146	0.800
L-Methionine	149	30	0.200
L-Phenylalanine	165	66	0.400
L-Proline	115	40	0.350
L-Serine	105	42	0.400
L-Threonine	119	95	0.800
L-Tryptophan	204	16	0.078
L-Tyrosine-2Na-2H ₂ O	261	104	0.400
L-Valine	117	94	0.800
VITAMINS			
Biotin	244	0.013	0.0000533
Choline chloride	140	4	0.029
Folic acid	441	4	0.009
i-Inositol	180	7.2	0.040
Niacinamide	122	4	0.033
D-Ca Pantothenate	477	4	0.008
Pyridoxal hydrochloride	203.6	4	0.002
Riboflavin	376	0.4	0.0011
Thiamine hydrochloride	337	4	0.012
Vitamin B12	1355	0.013	0.00000959

Appendix VII

Proteins Successfully Identified by others at Kent since the Completion of this Project

Spot	Protein Identity	ExPASy Accession No.	MOWSE Score	PMF ¹	Sequence Coverage	Sequence Tag ²	Mr/pI ³
Cell signalling							
143Ea	14-3-3 protein epsilon (PKC inhibitor-1)	P42655	6.66 x 10 ³	11/50	34%	ASSDIATELPPTHPIR(37) YLAEFATGNDR(59)	29.2/4.6
143Eb	14-3-3 protein epsilon (PKC inhibitor-1)	P42655	2.60 x 10 ⁶	13/50	31%	-	29.2/4.6
143G	14-3-3 protein gamma (PKC inhibitor-1)	P35214	4.31 x 10 ⁴	13/31	40%	NVTELNEPLSNEER(96)	28.2/4.8
143Z	14-3-3 protein zeta/delta (PKC inhibitor-1)	P35215	4.25 x 10 ⁶	17/40	50%	-	27.8/4.7
143T	14-3-3 protein tau	P35216	1.30 x 10 ⁶	15/40	36%	AVTEQGAELSNEER(62)	27.8/4.7
HNT1	HINT protein (Protein kinase C-inhibitor 1)	P70349	4.50 x 10 ⁴	7/50	55%	-	13.6/6.4
Chaperones/foldases							
BiPa	GRP78 (Glucose regulated protein-78)	P20029	8.21 x 10 ¹¹	23/43	52%	-	72.4/5.1
BiPb	GRP78 (Glucose regulated protein-78)	P20029	6.57 x 10 ⁷	19/50	38%	-	72.4/5.1
BiPc	GRP78 (Glucose regulated protein-78)	P20029	9.01 x 10 ⁵	16/50	30%	-	72.4/5.1
BiPd	GRP78 (Glucose regulated protein-78)	P20029	1.87 x 10 ⁴	11/50	22%	-	72.4/5.1
BiPe	GRP78 (Glucose regulated protein-78)	P20029	3.79 x 10 ³	9/50	17%	-	72.4/5.1
BiPf	GRP78 (Glucose regulated protein-78)	P20029	1.30 x 10 ⁴	10/42	16%	VTHAVVTVPAYFNDAQR(74) HNEPTAAAAIYGLDKR(38) ITPSYVAFTPEGER(46)	72.4/5.1
BiPg	GRP78 (Glucose regulated protein-78)	P20029	1.50 x 10 ⁵	11/49	21%	-	72.4/5.1
BiPh	GRP78 (Glucose regulated protein-78)	P20029	8.05 x 10 ³	10/50	18%	ITPSYVAFTPEGER(40)	72.4/5.1
BiPi	GRP78 (Glucose regulated protein-78)	P20029	1.15 x 10 ³	6/25	24%	-	72.4/5.1
CRTC	Calreticulin precursor	P14211	7.59 x 10 ⁴	11/42	28%	EQFLDGDWWTNR(38) HEQNDICGGGYVK(52)	50.0/4.3
CYPHa	Peptidyl-prolyl cis-trans isomerase (PPIase)	P17742	1.78 x 10 ⁴	9/50	47%	TVTNAVTVPAYFNDSQR(35)	17.8/7.9
CYPHb	Peptidyl-prolyl cis-trans isomerase (PPIase)	P17742	8.62 x 10 ⁴	9/20	59%	-	17.8/7.9
ENPLa	Endoplasmin precursor	P08113	2.71 x 10 ⁹	20/50	28%	-	92.5/4.7
ENPLb	Endoplasmin precursor	P08113	5.79 x 10 ⁶	19/32	29%	SILFVPTSAPR(66) FAFQAEVNR(43) GVVDSDLPLNVSQR(44) EEEEAIQLDGLNASQIR(58)	92.5/4.7
ENPLc	Endoplasmin precursor	P08113	4.41 x 10 ³	7/39	10%	-	92.5/4.7
ENPLd	Endoplasmin precursor	P08113	-	-	-	SILFVPTSAPR(46)	92.5/4.7
GR75	GRP75 (Glucose regulated protein-75)	P38647	1.40 x 10 ⁵	14/50	22%	LLGQFTLIGIPPAPR(27) SQIHDIIVLGGSTR(65)	73.5/5.9
HS7Ca	Heat shock cognate 71kD protein	P08109	2.19 x 10 ⁸	13/23	32%	STAGDTHLGGEDFDNR(66) TTPSYVAFTDTER(51)	70.9/5.4
HS7Cb	Heat shock cognate 71kD protein	P08109	4.39 x 10 ⁶	14/50	31%	TVTNAVTVPAYFNDSQR(45) TTPSYVAFTDTER(31) TTPSYVAFTDTER(33)	70.9/5.4
HS7Cc	Heat shock cognate 71kD protein	P08109	7.12 x 10 ⁶	11/22	26%	SQIHDIIVLGGSTR(54) STAGDTHLGGEDFDNR(60)	70.9/5.4
HS7Cd	Heat shock cognate 71kD protein	P08109	5.45 x 10 ⁸	16/40	35%	-	70.9/5.4
HS7Ce	Heat shock cognate 71kD protein	P08109	2.24 x 10 ⁴	10/50	18%	STAGDTHLGGEDFDNR(69) FEELNADLFR(40) FEELNADLFR(50)	70.9/5.4
HS7Cf	Heat shock cognate 71kD protein	P08109	2.29 x 10 ⁶	13/50	22%	SQIHDIIVLGGSTR(46)	70.9/5.4
HS7Cg	Heat shock cognate 71kD protein	P08109	-	-	-	SQIHDIIVLGGSTR(72)	70.9/5.4
HS7Ch	Heat shock cognate 71kD protein	P08109	-	-	-	NQTAEKEEFEHQK(53)	70.9/5.4
HS7Ci	Heat shock cognate 71kD protein	P08109	8.31 x 10 ⁵	14/50	28%	-	70.9/5.4
HS7Cj	Heat shock cognate 71kD protein	P08109	1.20 x 10 ⁸	15/33	37%	-	70.9/5.4
HS7Ck	Heat shock cognate 71kD protein	P08109	-	-	-	NQTAEKEEFEHQK(64)	70.9/5.4
HS7Cl	Heat shock cognate 71kD protein	P08109	-	-	-	SQIHDIIVLGGSTR(42)	70.9/5.4
HS7Cm	Heat shock cognate 71kD protein	P08109	1.30 x 10 ⁷	17/50	31%	SQIHDIIVLGGSTR(41)	70.9/5.4
HS7Cn	Heat shock cognate 71kD protein	P08109	1.47 x 10 ⁸	21/33	34%	SQIHDIIVLGGSTR(41) STAGDTHLGGEDFDNR(55)	70.9/5.4
HS7Co	Heat shock cognate 71kD protein	P08109	1.27 x 10 ⁵	9/50	19%	-	70.9/5.4
HS7Cp	Heat shock cognate 71kD protein	P08109	1.48 x 10 ⁵	11/36	20%	TTPSYVAFTDTER(57) STAGDTHLGGEDFDNR(80)	70.9/5.4
HS9A	Heat shock protein 90-alpha	P07901	-	-	-	HFSVEGQLEFR(54) HSQFIGYPITLFVEK(34)	84.7/4.9
HS9Ba	Heat shock protein 90-beta	P11499	-	-	-	HLEINPDHPIVETLR(39)	83.2/5.0

HS9Bb	Heat shock protein 90-beta	P11499	-	-	-	HLEINPDHPIVE ^{TLR} (44)	83.2/5.0
HSP60a	60 kDa Heat shock protein	P19226	7.73 x 10 ⁵	10/50	25%	-	61.0/5.9
HSP60b	60 kDa Heat shock protein	P19226	2.26 x 10 ⁴	10/50	18%	-	61.0/5.9
HSP60c	60 kDa Heat shock protein	P19226	-	-	-	AAVEEGIVLGGGVALLR(62)	61.0/5.9
HSP60d	60 kDa Heat shock protein	P19226	1.14 x 10 ⁵	12/50	25%	ISSVQSIVPALEIANHR(93)	61.0/5.9
PDA3a	Protein disulfide isomerase A3 (precursor)	P27773	1.00 x 10 ⁵	11/50	20%	-	56.6/6.0
PDA3b	Protein disulfide isomerase A3 (precursor)	P27773	2.47 x 10 ⁵	11/30	23%	-	56.6/6.0
PDA3c	Protein disulfide isomerase A3 (precursor)	P27773	1.05 x 10 ⁸	18/50	41%	-	56.6/6.0
PD1a	Protein disulfide isomerase (precursor)	P09103	8.28 x 10 ⁴	9/27	20%	-	57.1/4.8
PD1b	Protein disulfide isomerase (precursor)	P09103	2.35 x 10 ⁵	14/50	27%	VDATEESDLAQQYGVR(59) ILFIFIDSDHTDNQR(48)	57.1/4.8
TRAL	Heat shock protein 75kDa,mitochondrial (Precursor)	Q9CQN1	-	-	-	GVVDESDIPLNLSR(52)	80.2/6.3
Cytoskeletal							
ACTBa	Actin, cytoplasmic 1	P02570	1.34 x 10 ⁶	11/50	31%	QEYDESGPIVHR(45) SYELPDGQVITIGNER(74)	41.7/5.3
ACTBb	Actin, cytoplasmic 1	P02570	7.64 x 10 ⁴	10/50	31%	-	41.7/5.3
ACTBc	Actin, cytoplasmic 1	P02570	3.96 x 10 ⁴	8/50	25%	SYELPDGQVITIGNER(90) QEYDESGPSIVHR(33)	41.7/5.3
ACTBd	Actin, cytoplasmic 1	P02570	1.79 x 10 ⁵	10/27	22%	SYELPDGQVITIGNER(71) QEYDESGPSIVHR(48)	41.7/5.3
ACTBe	Actin, cytoplasmic 1	P02570	4.89 x 10 ³	8/50	28%	SYELPDGQVITIGNER(71) QEYDESGPSIVHR(48)	41.7/5.3
ACTBf	Actin, cytoplasmic 1	P02570	1.35 x 10 ⁴	6/50	15%	-	41.7/5.3
ACTBg	Actin, cytoplasmic 1	P02570	5.43 x 10 ³	6/50	17%	-	41.7/5.3
ACTBh	Actin, cytoplasmic 1	P02570	4.39 x 10 ⁵	9/27	28%	VTHAVVTVPAYFNDAQR(74) ITPSYVAFTEPGER(46) HNEPTAAAIAYGLDKR(38)	41.7/5.3
ACTBi	Actin, cytoplasmic 1	P02570	1.97 x 10 ⁶	10/23	41%	-	41.7/5.3
LAM1a	Lamin B1	P14733	1.09 x 10 ⁶	16/50	23%	-	66.8/5.1
LAM1b	Lamin B1	P14733	3.44 x 10 ⁶	19/50	25%	-	66.8/5.1
TBA1a	Tubulin alpha-1 chain	P02551	2.07 x 10 ⁴	7/50	19%	LISQIVSSITASLR(35) AVFVDLEPTVIDEVR(47) NLDIERPTYTNLNR(37)	50.2/4.9
TBA1b	Tubulin alpha-1 chain	P02551	-	-	-	AVFVDLEPTVIDEVR(56) LISQIVSSITALR(56)	50.2/4.9
TBA2a	Tubulin alpha-2 chain	P05213	2.86 x 10 ⁶	11/50	33%	-	50.2/4.9
TBA8	Tubulin alpha-8 chain	Q9JJZ2	-	-	-	LISQIVSSITALR(47) NLDIERPTYTNLNR(21)	50.0/4.9
TBB5a	Tubulin beta-5 chain	P05218	4.16 x 10 ⁵	10/27	27%	-	49.7/4.8
TBB5b	Tubulin beta-5 chain	P05218	5.49 x 10 ⁵	9/18	30%	-	49.7/4.8
TBB5c	Tubulin beta-5 chain	P05218	2.88 x 10 ⁷	14/40	38%	-	49.7/4.8
TBB5d	Tubulin beta-5 chain	P05218	2.63 x 10 ⁶	10/50	26%	-	49.7/4.8
TPM3	Tropomyosin alpha 3 chain	P21107	-	-	-	IQVLQQQADDAEER(41)	32.8/4.7
Metabolic – glycolysis/TCA							
ALFA	Fructose-bisphosphate aldolase	P05064	3.80 x 10 ⁴	7/50	31%	-	39.2/8.4
ENOAa	Alpha-enolase	P17182	9.87 x 10 ⁶	11/36	24%	-	47.0/6.4
ENOAb	Alpha-enolase	P17182	8.88 x 10 ⁹	12/19	47%	AAVPSGASTGIYEALRLR(77)	47.0/6.4
ENOAc	Alpha-enolase	P17182	8.16 x 10 ⁶	12/32	26%	VNQIGSVTESLQACK(53) YITPDQLADLYK(46)	47.0/6.4
ENOAd	Alpha-enolase	P17182	3.15 x 10 ⁸	12/39	30%	-	47.0/6.4
ENOAe	Alpha-enolase	P17182	1.82 x 10 ⁶	9/48	23%	-	47.0/6.4
G3Pa	Glyceraldehyde-3-phosphate dehydrogenase	P16858	-	-	-	LISWYDNEYGYSNR(34) VPTPNVSVVDLTCR(48)	35.7/8.5
G3Pb	Glyceraldehyde-3-phosphate dehydrogenase	P16858	2.86 x 10 ⁶	15/50	42%	LISWYDNEYGYSNR(29) VPTPNVSVVDLTCR(30) LVINGKPITIFQER(33)	35.7/8.5
G3Pc	Glyceraldehyde-3-phosphate dehydrogenase	P16858	1.13 x 10 ³	7/50	19%	-	35.7/8.5
G3Pd	Glyceraldehyde-3-phosphate dehydrogenase	P16858	7.91 x 10 ²	5/9	15%	VPTPNVSVVDLTCR(71)	35.7/8.5
G3Pe	Glyceraldehyde-3-phosphate dehydrogenase	P16858	3.86 x 10 ⁶	10/28	30%	-	35.7/8.5
G3Pf	Glyceraldehyde-3-phosphate dehydrogenase	P16858	2.83 x 10 ³	5/8	21%	LVINGKPITIFQER(25) VPTPNVSVVDLTCR(39)	35.7/8.5
G3Pg	Glyceraldehyde-3-phosphate dehydrogenase	P16858	5.68 x 10 ⁴	7/50	14%	-	35.7/8.5
G3Ph	Glyceraldehyde-3-phosphate dehydrogenase	P16858	1.06 x 10 ⁴	9/50	32%	LISWYDNEYGYSNR(32) LVINGKPITIFQER(40) VPTPNVSVVDLTCR(55)	35.7/8.5
G3Pi	Glyceraldehyde-3-phosphate dehydrogenase	P16858	-	-	-	LISWYDNEYGYSNR(65) VPTPNVSVVDLTCR(36)	35.7/8.5
G3Pj	Glyceraldehyde-3-phosphate dehydrogenase	P16858	-	-	-	VPTPNVSVVDLTCR(79)	35.7/8.5
MDHC	Malate dehydrogenase	P14152	-	-	-	FVEGLPINDRSR(36)	36.3/6.1
PMG2	Phosphoglycerate mutase 2	O70250	-	-	-	HGESLWNQENR(52) VLIAAHGNSLR(69)	28.6/8.6

KPY2a	Pyruvate kinase, M2 isozyme	P52480	2.24 x 10 ⁴	9/50	23%	-	57.8/7.4
KPY2b	Pyruvate kinase, M2 isozyme	P52480	1.95 x 10 ¹³	26/50	50%	-	57.8/7.4
KPY2c	Pyruvate kinase, M2 isozyme	P52480	3.46 x 10 ³	11/50	23%	-	57.8/7.4
KPY2d	Pyruvate kinase, M2 isozyme	P52480	2.27 x 10 ⁶	15/50	32%	LNFSHGTHEYHAETIK(65) NTGIICTIGPASR(42)	57.8/7.4
KPY2e	Pyruvate kinase, M2 isozyme	P52480	5.05 x 10 ⁶	16/50	29%	-	57.8/7.4
KPY2f	Pyruvate kinase, M2 isozyme	P52480	1.19 x 10 ¹²	23/50	46%	-	57.8/7.4
KPY2g	Pyruvate kinase, M2 isozyme	P52480	2.04 x 10 ⁸	17/50	37%	-	57.8/7.4
KPY2h	Pyruvate kinase, M2 isozyme	P52480	7.83 x 10 ³	10/50	20%	-	57.8/7.4
KPY2i	Pyruvate kinase, M2 isozyme	P52480	7.01 x 10 ⁴	11/50	23%	-	57.8/7.4
KPY2j	Pyruvate kinase, M2 isozyme	P52480	3.33 x 10 ⁷	18/50	32%	-	57.8/7.4
KPY2k	Pyruvate kinase, M2 isozyme	P52480	-	-	-	LNFSHGTHEYHAETIK(63)	57.8/7.4
PGK1a	Phosphoglycerate kinase 1	P09411	7.59 x 10 ⁴	7/50	23%	-	44.4/7.5
PGK1b	Phosphoglycerate kinase 1	P09411	5.95 x 10 ⁴	8/50	27%	ALESPERPFLAILGGAK(30) LGDVYVNDAFGTAHR(40)	44.4/7.5
PGK1c	Phosphoglycerate kinase 1	P09411	3.32 x 10 ⁶	9/12	37%	-	44.4/7.5
TPIS	Triosephosphate Isomerase	P17751	6.41 x 10 ³	6/50	28%	-	26.6/7.1
Metabolic – mitochondrial and redox							
PDX1a	Thioredoxin peroxidase 2	P35700	1.31 x 10 ⁸	12/42	60%	-	22.2/8.3
PDX1b	Thioredoxin peroxidase 2	P35700	1.02 x 10 ⁷	10/50	55%	-	22.2/8.3
PDX4	Antioxidant enzyme AOE372	O08807	1.31 x 10 ⁸	14/24	51%	IPLLSDLNHQISK(22) DYGVYLED SGHTLR(58)	31.1/6.7
ATPBa	ATP synthase beta chain	P56480	4.86 x 10 ⁷	14/50	44%	-	56.4/5.1
ATPBb	ATP synthase beta chain	P56480	6.25 x 10 ⁴	12/50	24%	AHGGYSVFAGVGER(83) LVLEVAQHLGESTVR(68)	56.4/5.1
ATPBc	ATP synthase beta chain	P56480	-	-	-	AHGGYSVFAGVGER(78) FTQAGSEVSALLGR(80) VALTGLTVAEYFR(28)	56.4/5.1
Protein synthesis							
EF1D	Elongation factor 1-delta	P57776	-	-	-	ITSLEVENQNL(47)	31.3/4.7
EF11a	Elongation factor 1-alpha	P10126	-	-	-	YYVTIIDAPGHR(40)	50.2/9.1
EF11b	Elongation factor 1-alpha	P10126	-	-	-	EHALLAYTLGVK(35) THINIVVIGHVDSGK(38)	50.2/9.1
EF11c	Elongation factor 1-alpha	P10126	2.45 x 10 ⁴	12/50	31%	-	50.2/9.1
EF11d	Elongation factor 1-alpha	P10126	2.02 x 10 ³	7/22	16%	-	50.2/9.1
IF5A	Eukaryotic translation initiation factor 5A	P10159	-	-	-	VHLVGIDIFTGK(73)	16.7/5.1
RSP4a	40S ribosomal protein SA	P14206	3.62 x 10 ²	5/50	37%	-	32.7/4.7
RSP4b	40S ribosomal protein SA	P14206	-	-	-	FTPGTFTNQIAAFR(39)	32.7/4.7
SYS	Seryl-TRNA synthetase	P26638	2.46 x 10 ⁴	10/50	35%	-	32.0/5.1
Miscellaneous							
ADA	Adenosine deaminase	P03958	2.69 x 10 ⁷	20/50	67%	-	40.0/5.5
ALBU	Serum albumin (precursor)	P07724	-	-	-	LGEYGFQNAILVR(50)	68.7/5.8
ALDR	Aldose reductase	P45376	9.89 x 10 ⁵	9/50	29%	-	35.6/6.8
PEBP	Phosphatidylethanolamine-binding protein	P70296	-	-	-	LYTLVLTDPDAPSR(57)	20.6/3.8
PHB	Prohibitin (B-cell receptor associated protein)	P24142	1.30 x 10 ⁷	15/49	74%	-	29.8/5.6
RAN	GTP-nuclear binding protein RAN	P28746	1.84 x 10 ⁶	12/50	57%	-	24.4/7.0
ROA3	Heterogenous nuclear ribonucleoprotein A3	Q8BG05	-	-	-	GFAFVTFDDHDTV(42) IFVGGIKEDTEEYNLR(43)	39.6/9.1
ROAAa	Heterogenous nuclear ribonucleoprotein A/B	Q99020	-	-	-	EVYQQQQYSGGGR(57) GFVFITFKEEDPVK(51)	30.8/7.7
ROAAb	Heterogenous nuclear ribonucleoprotein A/B	Q99020	2.70 x 10 ³	8/50	26%	-	30.8/7.7
SAD1	Interferon-gamma inducible protein	Q60710	1.80 x 10 ³	11/50	14%	-	68.8/7.3
TCTP	Translationally controlled tumour protein	P14701	5.12 x 10 ³	8/37	33%	-	19.5/4.8
Recombinant proteins							
GC4	Ig gamma-4 chain C region	P01861	-	-	-	TPPPVLSDSGSFFKYSR(67) SGTASVVCLLNFFYPR(79)	35.9/7.2
KACa	Human/Mouse Ig kappa chain C region	P01834/ P01635	4.46 x 10 ³	4/15	12%	FSGSGSTQYSLK(65) VYACEVTHQGLSSPVTK(50) TVAAPSVFIFPPSDEQLK(47)	11.6/8.5 12.6/8.5
KACb	Human/Mouse Ig kappa chain C region	P01834/ P01635	-	-	-	SGTASVVCLLNFFYPR(92) FSGSGSTQYSLK(100)	11.6/8.5 12.6/8.5
KACc	Human Ig kappa chain C region	P01834	-	-	-	SGTASVVCLLNFFYPR(46)	11.6/8.5

Notes:

¹PMF = peptide mass fingerprint. Column shows number of peptides matched/number submitted to search.

²Sequence tag generated by ms/ms (Mascot Ion Score)

³Theoretical molecular weight and pI.